Quantitative Characterisation of Root Tip Regeneration and Tropism in External Electric Field

Nicolas Kral

Department of Life Sciences

Faculty of Natural Sciences

Imperial College London

Submitted for the degree of Doctor of Philosophy

January 2018

Abstract

We studied two phenomena specific to the root of the *Arabidopsis*, the effect of weak external electric field on root tip regeneration and root growth. We constructed and validated three experimental tools V-tank, V-box and V-slide that allowed us to subject roots to electric fields, with various imaging capabilities.

We observed an increase in root regeneration frequency caused by application of 2.5V/cm weak external electric field. In addition, we observed change in the distribution of auxin and a decreased number of cell divisions in the remaining root stump shortly after electric field treatment.

In addition to regenerating roots, we also studied the perturbation caused by electric field in the growing roots of *Arabidopsis*. *Arabidopsis* root tip showed electrotropic bend towards cathode in response to external electric field, which we described quantitatively. After testing six different media, our data suggests 0.1-1mA conductance of the media leads to the most dramatic root electrotropism. The data showed asymmetric cell expansion during root electrotropism, suggesting cellular mechanism of root turn. We found out gravitropism and electrotropism does not share the same molecular mechanism. Our data confirmed that functional *glr3.4* gene coding for a Ca^2 ion channel is necessary for wild type electrotropism, in addition further seven ion channel genes were identified to be potentially necessary for root electrotropism. Membrane depolarisations in root cells were attempted to be observed with fluorescent Voltage Sensitive Dyes. The data showed that membrane depolarisations prior electric field exposure inhibited growing root from responding with electrotropic turn, suggesting the role of membrane voltage maintenance in electrotropism.

The observations showed electric field can perturb root regeneration and root growth. The mechanism behind increase in root regeneration frequency is unknown. The mechanism of root electrotropism seen in a growing root is separate to that of gravitropism and it involves Ca^{2+} channel GLR3.4 and membrane depolarisations.

Contents

Declaration of Originality

I, Nicolas Kral, declare that this thesis is an original piece of work written entirely by myself. All described results arise from my own research unless otherwise stated. Any information and conclusions derived from other works has been referenced properly.

Copyright Declaration

Acknowledgements

First and foremost I owe many thanks to my supervisor Dr Giovanni Sena, who has been a great mentor for the past four years of my life. It is thanks to his continuous support and guidance that I have been able to grow my scientific abilities and complete the work presented in this thesis. I was very lucky to have been part of his laboratory.

In addition, I would want to thank my co-supervisors Dr Colin Turnbull and Dr Chris Dunsby, who have provided me with tips and assistance whenever necessary.

All members of Dr Sena's lab, past and present, have played their part in the shaping of this PhD project. I thank Alexandra Hanna, for obtaining the preliminary results that provided confidence for the direction of this PhD. I am also indebted to Dr Paolo Baesso, who have introduced me to the world of tinkering, coding and supported me throughout many technical parts of this PhD. I also have to thank Alex Guyon, a keen intern, who followed me everywhere and provided the much needed extra pair of hands. I also owe many thanks to students Nick Oliver, Mara Sgroi, Shayna Lin, Philip Li and Alex Hunt who all contributed to the work presented in this thesis. In addition, I am thankful for the many times I relied on the expertise and help of Dr Rico Randall and Dr Todd Fallesen. I am also grateful for practical help from Deniz Tiknaz and Olaf Kranse.

I owe big thanks to members of Dr Turnbull's lab, particularly William Pelton for his help solving many different technical problems.

Special thanks goes to my partner Despoina Paschou, my brother Daniel Kral and my parents who supported me endlessly during these four years.

Finally, I am indebted to the BBSRC for funding this PhD work and my research studies at Imperial College.

Thesis Summary

This thesis sheds light on how external electric fields affect root development. External electric fields are found in many environments including soil, yet the effect of these on root morphogenesis and growth are largely unknown. The goal of this study was to learn more about root regeneration and tissue repair, as well as root growth and plant root behaviour in the presence of electric fields. To enable the pursuit of these aims, it was needed to develop tools that allow for study of root development in presence of external electric fields. These may be used, modified and improved by researchers who wish to take the study of root development and interaction with electric fields further. An added aim was to begin examining the emerging role of bioelectricity in plant development, with focus on tools enabling observation of root bioelectricity.

The thesis starts with the introduction to *Arabidopsis* as a model organ and summarises current knowledge on cell types (Introduction, 1.1.1) and genetic regulatory networks underlying cell specifications in root meristem (Introduction, 1.1.2). Further on, up-to-date description of the action of hormone auxin (Introduction, 1.1.3), cytokinin as well as other hormones (Introduction, 1.1.4) is presented in cell division and cell differentiation. The control of meristem size (Introduction, 1.1.5) and specification of the elongation zone (Introduction, 1.1.6) is also reviewed. The role of ion channels in the root tip (Introduction 1.1.7) is introduced with respect to root tip homeostasis. Specific attention is placed on Glutamate-like Receptors (Introduction 1.1.8), unique cation channels that have high homology to neuron localised iGLURs that contribute to memory and learning in animals. GLRs have been focus of plant ion channel research in recent years due to their implications in electrophysiology and a number of root developmental processes.

The introduction continues with a short review on root tropisms (Introduction, 1.2.1), what is known on the cellular causes of tropic growth and how different tropisms may or may not share the same molecular mechanisms of perception, signalling and action. Signal transduction of root gravitropism from perception of gravity change to the physiological response is described in

Introduction 1.2.2. The understanding of molecular mechanism in gravitropism may allow its comparison to electrotrotropism. Further on, a number of examples of animal electrotaxis (Introduction, 1.2.3) are listed, the movement of animals in response to external the electric fields. The next part summarises all the previous findings of electrotropism (Introduction, 1.2.4), guided plant root growth in the presence of external electric fields, the phenomenon that is studied at length in this thesis.

The last introductory section reviews root tip regeneration (Introduction, 1.3.1) a unique example of whole organ post-embryonic development in plants. It describes molecular mechanisms that are part of the root tip regeneration process, with particular focus on hormones auxin and cytokinin. In addition, examples of cell polarisation as well as tissue regeneration driven by external or internal electric field in animals and few cases of external electric field perturbing plant regeneration (Introduction, 1.3.2) are mentioned. This sets the background for the new results of root tip regeneration perturbed by an external electric field.

The thesis continues with the description of materials and methods used to study the thesis topic. General material and methods can be found in Methods 2.1, while chapter specific methods can be found in further three sections (Methods, 2.2, Methods 2.3 and Methods 2.4).

The first of the result chapters presents specific assay tools that were developed to be able to study the perturbation of root tip regeneration in electric field and perturbation of root growth in electric field. The background (Results I, 3.1.1) on previous tools is mentioned as well as expectations from ideal assays for root exposure to electric field. Further on, aims (Results I, 3.1.2) are listed for individual tools named V-tank, V-box and V-slide.

V-tank results (Results I, 3.2.1) show a conversion of existing gel electrophoresis tank into a complex experimental set up, which allows us to study the perturbation of root regeneration by external electric fields. Second set of results show the construction and validation of V-box (Results I, 3.2.2) a novel set-up that for the first time provides a tool to observe *Arabidopsis* root

electrotropism. Low cost tools and materials were used to construct V-box including tissue culture box, perfusion system and raspberry Pi microcomputer with a camera. The last set of results in the chapter 3 presents the construction and validation of V-slide (Results I, 3.2.3). This is a novel set-up that allows individual *Arabidopsis* roots to be timelapse imaged by a camera attached to inverted light microscope or confocal microscope. This lets us observe root electrotropism at micro resolution, allowing the observer to leverage the many fluorescent reporters found in *Arabidopsis* lines. The V-slide set up consists of perfusion and 3D printed unique microscope slide. After results are presented, the application (Results I, 3.3.1) of external electric field to roots is discussed.

The fourth chapter includes the published results (Kral *et al.* 2016) that present the effects of electric field on regenerating root tips. The background to the results explains developmental control of root regeneration (Results II, 4.1.1) and the motivation behind exposure of regenerating root tips to the electric field (Results II, 4.1.2). The aims (Results II, 4.1.3) list a number of objectives that were wanted from the perturbation of roots with external electric field. These include root regeneration frequency phenotype, observation of hormonal distribution in the remaining root stump shortly after perturbation, measurement of cell division rates and observation of spatial distribution of cell fates after electric field perturbation.

The first results (Results II, 4.2.1) show that the decrease in the frequency root tip regeneration is connected to the remaining size of root meristem after cutting of the root tip. In addition, the exposure of cut root tips to mock treatment in V-tank without electric field does not further affect frequency of root tip regeneration. It was also shown (Results II, 4.2.2) that 5V/cm electric field treatment significantly decreases frequency of root tip regeneration.

After decreasing the strength of the electric field to 2.5V/cm to avoid the previously observed root regeneration frequency decrease, it is shown with systematic exploration of 9 different spatial and temporal conditions (Results II, 4.2.3) that electric field perturbation increases frequency of root tip regeneration. In addition, it was observed (Results II, 4.2.4) that spatial

localisation of Scarecrow (SCR) transcription factor does not change with electric field perturbation of regenerating root tips. It was also observed (Results II, 4.2.5) that the electric field perturbation has significantly decreased cell divisions in the first hour of the regeneration process. Lastly (Results II, 4.2.6) the distribution of auxin, but not cytokinin, was observed to change in when regenerating root tips were perturbed with electric field.

Discussion of this chapter analyses the interaction between external electric field and tissue reorganisation (Results II, 4.3.1), and interaction between auxin and cytokinin (Results II, 4.3.2) that may be perturbed by the application of the electric field. The last section (Results II, 4.3.3) discusses the role of cell division in regeneration, considering the observed results and compares these to cell division patterns during regeneration in animal tissues.

The fifth chapter enquires the effect of electric field on growing roots. The background introduces electrotropism (Results III, 5.1.1), and provides further information (Results III, 5.1.2) for the question whether electrotropism is driven by the same molecular mechanism as gravitropism. Further in the background (Results III, 5.1.3), the potential necessity of ion signals during root electrotropism is mentioned and the potential candidate genes necessary for electrotropism are shown. In the aims (Results III, 5.1.4) the objectives are listed which include the observation of wild type electrotropism, the observation of auxin action in electrotropism, search for non-electrotropic mutant and observation of calcium dynamics in the electrotropic root.

The V-box was used to conduct first experiment of growing *Arabidopsis* root in 1V/cm electric field (Results III, 5.2.1), which showed electrotropic bend towards cathode. The effect was quantified and wild type roots are seen to have a root tip deflection of an average of $34^{o}\pm15^{o}$ in two hours. The results (Results III, 5.2.2) further continue with a test of how media with different conductance affect electrotropism. The results show that differences in media composition are not as relevant as media concentration, with the strongest electrotropic effects observed in media with conductance between 0.1-1mA. Asymmetric cell expansion (Results III, 5.2.3) in the transition and

distal elongation zone during root electrotropism causes the bend in the root. Also presented (Results III, 5.2.4) are the side effects caused by exposure to 1V/cm for longer than 2 hours and the damage caused by 2.5V/cm electric field at a cellular and molecular level.

To test the similarity of the molecular mechanism of gravitropism and electrotropism a number of agravitropic mutants have been exposed to electric field. It was observed (Results III, 5.2.5) that agravitropic roots of *pin2* and *aux1* mutants are electrotropic. Further, *pin2* roots showed significantly increased electrotropism in comparison with wild type, while *aux1* roots have shown a significant decrease of electrotropism compared with wild type only after 2 hours.

To further enquire if electrotropic molecular mechanism is different to that of gravitropism, PIN2 protein distribution was measured in root meristem after root was subjected to electric field (Results III, 5.2.6). The pixel intensities in the images of roots expressing PIN2:GFP protein in the meristem were counted with a custom MATLAB script, and it was observed that PIN2:GFP does not asymmetrically distribute. This is in contrast to previously published asymmetric distribution of PIN2:GFP observed during gravitropism. Auxin distribution in meristem is known to be asymmetrically distributed during gravitropism. Auxin distribution was also observed in root meristems after exposure to external electric field (Results III, 5.2.7). The pixel intensities in the images of roots expressing R2D2 auxin reporter were counted and it was observed that auxin does not asymmetrically distribute. From the results it was concluded that gravitropism and electrotropism do not share the same molecular mechanism.

The search for a non-electrotropic mutant is found in the section Results III, 5.2.8. Finding a gene necessary for wild type electrotropism could provide information on the mechanism behind electrotropism. The average root tip deflections of 24 ion channel mutants during two hours of root exposure to electric field were measured. Roots with missing functional genes *glr1.2* and *glr3.4* were observed to have decreased electrotropic deflection in comparison with wild type throughout the whole two hours. Further roots with non-functional genes *glr2.4*, *clc-D*, *kat1*, *skor*, *gork* and *tpc1* had

decreased electrotropic deflections only in some instances of the two hours. These genes were suggested to be necessary for wild type electrotropism. In addition, the genetic screen identified missing *pin1*, *pin3* and *ost2-1D* genes led to increased root tip deflection in presence of electric field in comparison with wild type.

The effect of missing *glr3.4* gene in *Arabidopsis* during root electrotropism is further studied in Results III, 5.2.9. Roots missing functional *glr3.4* gene were seen capable of gravitropic turn while having decreased deflection during electrotropic turn in comparison to roots containing functional *glr3.4* gene segregated from the same population. The rescue mutants (Results III, 5.2.10) expressing a *proGLR3.4::GLR3.4:GFP* transgene while being homozygous recessive for *glr3.4* were observed to have statistically same electrotropic root deflection as wild type roots. The results confirm that *glr3.4* gene is necessary for wild type *Arabidopsis* electrotropism. Since GLR3.4 is a Ca^{2+} channel, Ca^{2+} dynamics in the electrotropic root were observed (Results III, 5.2.11). It is possible there is a change in Ca^{2+} distribution in the root meristem in response to the application of the electric field.

The discussion (Results III, 5.3.1) of the electrotropism results starts with comparison of the observed results to previously published findings. Simple outline of possible osmotically driven mechanism for asymmetric cell expansion is presented. The role of auxin and the difference in molecular mechanism between electrotropism and gravitropism is discussed in section Results III, 5.3.2. The necessity of a functional *glr3.4* gene and the likely role of calcium in root electrotropism are discussed in section Results III, 5.3.3. The last section (Results III, 5.3.4) proposes a hypothesis for the molecular mechanism and speculates how the effect of electric field could be translated on the molecular and cellular level causing root to bend.

The last results chapter presents preliminary results of studying cell membrane potentials in *Arabidopsis* root. The background (Results IV, 6.1.1) presents information on what is known about endogenous electric signals in *Arabidopsis* and specifically the root. Further on, the use of potassium as depolarising agent (Results IV, 6.1.2) and the use of voltage sensitive dyes to monitor membrane

potentials is introduced (Results IV, 6.1.3). The aims (Results IV, 6.1.4) list the objectives for the results, which consist of the optimisation of protocols for the use of voltage sensitive dyes in the root and testing the connection between membrane potential and electrotropism.

The results (Results IV, 6.2.1) show the use of three voltage sensitive fluorescent dyes, DiBAC4(3), Rhodamine 6G and completely novel dye SS44-DC (Akita Innovations, personal communication) to report membrane depolarisations in *Arabidopsis* root. After treatment of roots with 100mM potassium chloride and 100mM potassium gluconate, the fluorescence of DiBAC4(3) increased in the root, while fluorescence of Rhodamine 6G decreased in the root and spatial localisation of SS44 fluorescence in the root changed. Time course observations (Results IV, 6.2.2) of roots stained with DiBAC4(3) and Rhodamine 6G have identified discrepancies in Rhodamine 6G reporting in comparison to results in previous section. DiBAC4(3) reliably reported repolarisation of membranes in root meristem with decrease in fluorescence. The result suggests that DiBAC4(3) is a promising VSD that could be used to report membrane potentials in root cells, but needs an independent validation. The last result (Result IV, 6.2.3) of this chapter shows that the application of the depolarising buffer to the root before the exposure to transverse external electric field inhibits electrotropism. It is possible that membrane depolarisations may be needed for root electrotropism.

The discussion in the sixth chapter (Results IV, 6.3.1) talks about the microscopic observation of plant membrane potentials and compares the observed results to previously published plant cell membrane potential observations. Methods for independent validation of the voltage sensitive dyes are also suggested. The last section (Results IV, 6.3.2) discusses connection between electrotropism and cell membrane potential and the role of membrane depolarisation in electrotropic turn.

The thesis ends with concluding remarks on new experimental tools (Concluding Remarks, 7.1), multiple ways with which external electric field affects root development and growth (Concluding Remarks, 7.2) and mention of cell membrane potentials and role of bioelectricity in root development (Concluding Remarks, 7.3).

1 Introduction

1.1 Arabidopsis root

1.1.1 Anatomy – cell types

Arabidopsis thaliana root is a good model organ for a range of developmental and physiological phenomena. It is a simple and almost transparent organ that contains a root apical meristem (Figure 1), which is responsible for cell division and growth. The meristem is formed during embryonic development from hypophysis and neighbouring embryo cells (Dolan *et al.* 1993). Once root cells in the meristem are organised in the mature embryo, they maintain their organisation and do not change during growth of the primary root.

The cell files of root meristem in a growing root originate from a small but variable number of quiescent centre cells that divide asymmetrically to maintain quiescent centre and to form columella initials, cortex/endodermis initials, epidermis/lateral root cap initials and stele initials (Figure 1). Together these cells are considered to be the stem cell niche (Dolan *et al.* 1993). The stem cell initials further asymmetrically divide into multiple cell files leading to radial pattern of *Arabidopsis* root meristem. When cells in the stem cell niche divide, generally a stem cell initial, which is a stem cell that was in contact with quiescent centre cell remains a stem cell initial, while the other dividing cell gives rise certain types of mitotically active cell types (Scheres 2007).

The outer layers of the meristem (Figure 1) are the lateral root cap and epidermis layers, moving inwards are the cortex and endodermis. The innermost layers are the pericycle and the stele. Within the meristem, the cells continue to divide, with less differentiated cells being closer to stem cell niche and more differentiated cells moving upward in their cell files, forming transit amplifying cells at the proximal boundary of root meristem. It is at this point that the cells enter transition zone, their proliferative capacity start to decrease and the cell fate starts to be fully defined in mature cell files of epidermis, cortex, endodermis, pericycle and vasculature (Perilli *et al.* 2012). At the distal part of the root meristem, there are columella initials as well as lateral root cap

initials, which do not progress upwards as they mature. Instead they form a cap that surrounds the stem cell niche that protects the root during growth as well as detects changes in gravity and receives signals from soil (Arnaud *et al.* 2010).

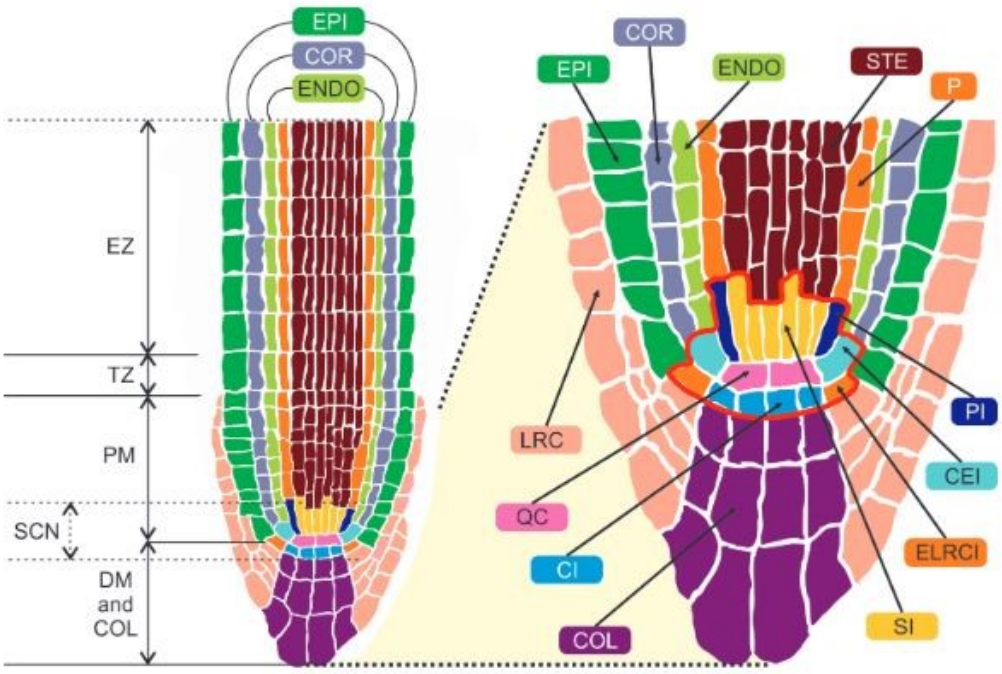

Figure 1: Description of Arabidopsis root meristem. On the left whole root meristem is shown, SCN stem cell niche, DM & COL distal meristem & columella, PM proximal meristem, TZ transition zone, EZ elongation zone. Cell types described on the right, QC quiescent centre, CI columella initials, ELRCI epidermis/lateral root cap initials, CEI cortex/endodermis initials, PI pericycle initials, SI stele initials, LRC lateral root cap, COL columella, EPI epidermis, COR cortex, ENDO endodermis, P pericycle, STE stele. Used with permission from (Lee *et al.* 2013), copyright by the Oxford University Press.

1.1.2 Genetic Regulatory Networks in meristem organisation

The specification of each of the cell fates to result with a specific cell in a defined tissue relies on an intricate interplay between transcription factors, positional information and their genetic expression output. The maintenance and specification of the stem cell niche is the result of convergent activities of hormone auxin, transcription factor action and other signalling events. Hormone auxin induces activity of PLETHORA (PLT1-4) transcription factors (Aida *et al.* 2004), which are kept at the high concentration in the stem cell niche (Figure 2), specifying the cell identity of the stem cells, but the PLT concentrations in the differentiating cells are decreased (Galinha *et al.* 2007). In addition, further regulation to maintain PLT concentration highest in the QC is done by transcriptional and post-translational modification by secreted signal peptides known as Root Meristem Growth Factors (Matsuzaki *et al.* 2010).

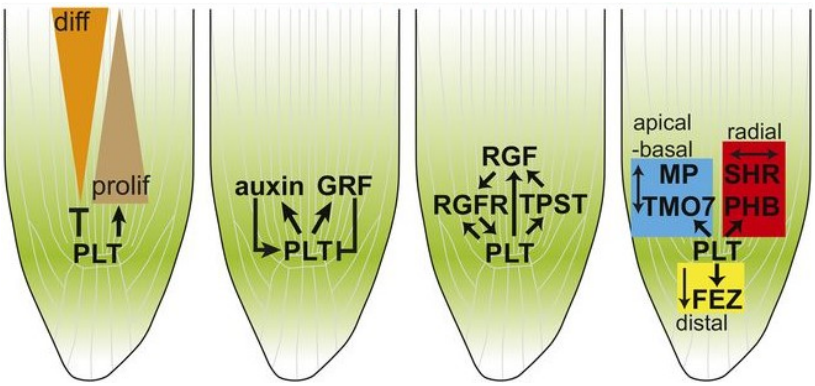

Figure 2: Diagram of PLETHORA (PLT) transcription action in the stem cell niche of the root meristem. Abbreviations: GRF GROWTH RECEPTOR FACTOR, RGF ROOT GROWTH FACTOR, RGFR ROOT GROWTH FACTOR RECEPTOR, TPST TYROSYL PROTEIN SULFOTRANSFERASE, MP MONOPTEROS, TMO7 bHLH transcription factor, PHB PHABULOSA transcription factor, SHR SHORTROOT transcription factor, FEZ NAC transcription factor. Adapted with permission from (Santuari *et al.* 2016), copyright by the American Society of Plant Biologists.

A separate action of another group of transcription factors based on interaction of SHORTROOT (SHR), SCARECROW (SCR) and the genes they target also helps maintain stem cell niche (Figure 3), establishment of radial symmetry and further specifies cell types as it aids the differentiation process (Helariutta *et al.* 2000), (Sabatini *et al.* 2003), (Welch *et al.* 2007). The SHR is transcribed and expressed in the stele cells, but it cannot enter nucleus there, instead through regulated transport (Gallagher *et al.* 2004), (Cui *et al.* 2007) it is moved one layer outwards through plasmodesmata, 40 – 60nm wide channels that connect symplastic space of cells, into the endodermis, cortex/endodermis initials and QC where it activates the expression of SCR, controls the asymmetric divisions of cortex/endodermis cells and keeps QC identity (Nakajima *et al.* 2001).

On the other hand, SCR maintains the QC functions and identity of stem cells by cell-autonomous action (Sabatini *et al.* 2003). Both SHR and SCR also control asymteric cell division in stem cell niche by affecting the expression of genes involved in cell cycle such as CYCD6 (Sozzani *et al.* 2010). Both SCR and SHR activity is influenced by the product transcription factors whos expression they enhance. Downstream gene JACKDAW (JKD) together with SCR and SHR is needed to maintain QC, but four transcription factors MAGPIE (MGP), JKD, SHR and SCR impact the fate of cortex/endodermis initials (Welch *et al.* 2007). In addition, maintenance of the QC is kept by SCR

transcription factor repressing action of another plant hormone cytokinin, on which cell differentiation is dependent.

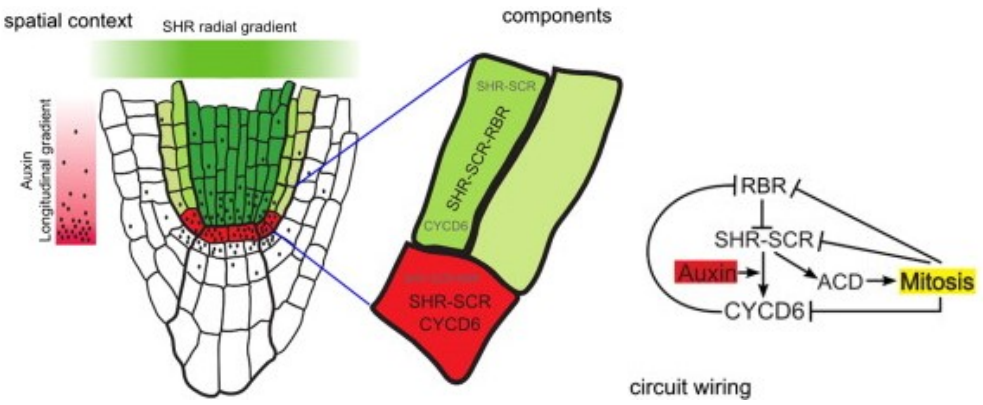

Figure 3: The action of SHORTROOT (SHR) and SCARECROW (SCR) transcription factors in the specification of stem cell niche and endodermal cell types with asymmetric cell division. Spatial restriction is imposed by the interaction of SHR/SCR complex with Retinoblastoma related (RBR) protein. CYCLIN D6 – CYCLIN DEPENDENT KINASE complex can interact with RBR to block activity of SHR-SCR, auxin can provide bias into the regulation by promoting transcription of CYCD6. SHR-SCR itself promotes transcription of CYCD6. The mechanism provides bi-stable switch for asymmetric cell division (ACD) depending on high or low SHR-SCR activity. Adapted with permission from (Cruz-Ramirez *et al.* 2012), copyright by Elsevier Inc.

In addition to the PLT and SHR/SCR maintenance of the QC also short range signal that originates in the QC was proposed (van den Berg *et al.* 1997). WOX5 is a transcription regulator that shows highest expression in the QC and helps regulate slow rate of cell divisions in the quiescent centre by supressing expression of cyclin D genes involved in cell cycle progression (Forzani *et al.* 2014). Homeodomain WOX5 protein is also able to move from quiescent centre cells into columella initials where it is able to manage differentiation state of the cells by suppresing a differentiation factor CDF4, essentially forming an opposing gradient of the WOX5 and CDF4 resulting in less to more differentiated columella cells (Pi *et al.* 2015). Roots that miss functional *wox5* gene have the differentiation process of columella cells only affected (Sarkar *et al.* 2007), highlighting the level of redundancy and alternate mechanisms such as PLT and SHR/SCR in place to maintain the stem cell niche and differentiation process of the cells in the meristem.

1.1.3 A brief introduction to Auxin

Plant hormones are relevant factors that contribute to the balance of cell division and cell differentiation. One of the most important hormones maintaining the growth of the root is the auxin, which is synthesised in the shoot tip and is transported downwards to the root. The local maximum of auxin in the root meristem is found at the location of the Quiescent Centre (Figure 4) and columella initials (Friml *et al.* 2003). It is set up by the PINs transporters, which are auxin efflux carriers and are expressed in distinct spatial zones of the root meristem (Blilou *et al.* 2005). Together with PIN proteins, the AUX1/LAX influx carriers contribute towards specific auxin sinks and result in the acropetal, toward root tip and basipetal, away from the root tip, auxin transport system. This is sometimes known as the 'reverse fountain' (Grieneisen *et al.* 2007).

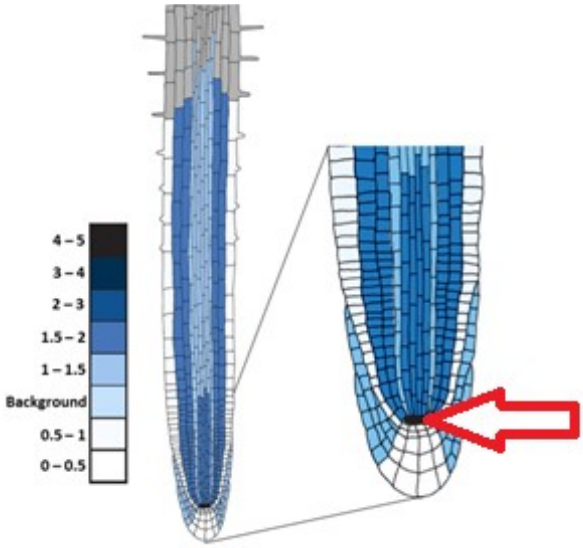

Figure 4: Concentration of hormone auxin in *Arabidopsis* root meristem. Auxin maximum is found in the Quiescent Centre (red arrow). Adapted with permission from (Petersson *et al.* 2009), copyright by the American Society of Plant Biologists.

The way PIN proteins are able to form a specific transport system for auxin is because their localisation in the cell is polarised to one end, forming a series of cells with auxin transporters localised only at one end of the cell. PIN localisation in the cell and spatially defined expression of individual PIN proteins helps directs auxin (Figure 5) around the root meristem (Wiśniewska *et al.* 2006). Specifically, PIN1 protein transports auxin downwards through the vasculature cells (Galweiler *et al.* 1998), while PIN4 in particular mediates the auxin sink leading to auxin maximum at

the QC (Friml *et al.* 2002a). PIN3 and PIN7 redistribute the auxin hormone away from the maximum at the QC towards outer layers of the root meristem (Friml *et al.* 2002b), (Blilou *et al.* 2005). PIN2 expressed in the outer layers of the meristem, cortex and epidermis, moves the auxin towards the shoot away from the quiescent centre (Luschnig *et al.* 1998). At the transition zone auxin moves back to the vasculature cells and the reverse fountain is maintained. In addition to the efflux PIN system, the AUX1 permease like influx auxin transporter has similar expression pattern to PIN2, mainly in the lateral root cap and epidermis, however the transporter is not localised in polar manner in cell and allows for further mobilisation of auxin around the root meristem (Bennett *et al.* 1996), (Marchant *et al.* 1999).

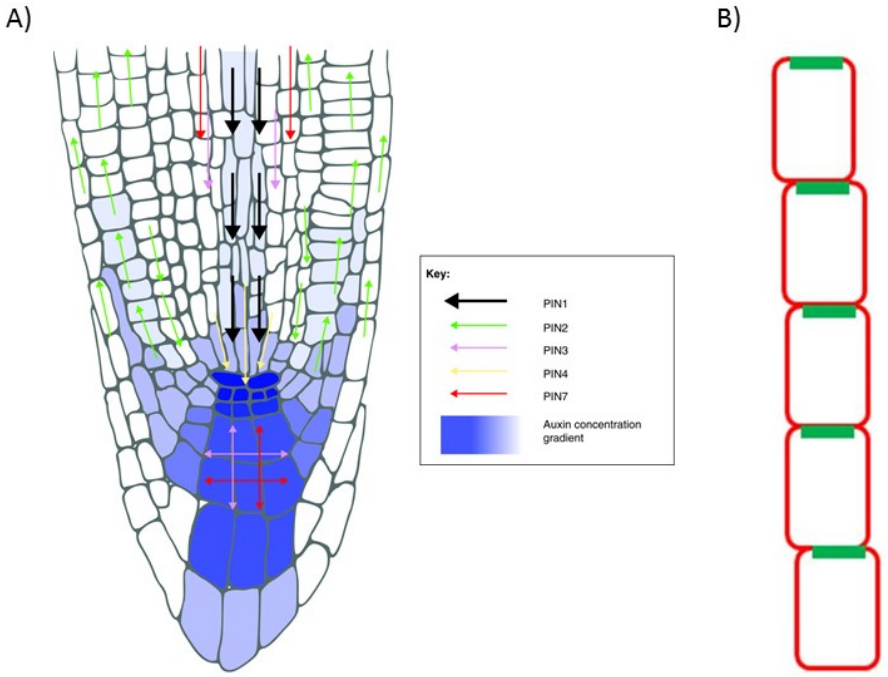

Figure 5: A) Direction of auxin flow by PIN proteins expressed in different root tissues. Adapted from (Křeček *et al.* 2009), under Creative Commons Attribution (CC-BY). B) Schematic of polar PIN localisation within cells.

Once in cell, auxin interacts with TRANSPORT INHIBITOR RESPONSE 1 / AUXIN-SIGNALING F-BOX PROTEINs (TIR1/AFBs) to direct for proteasome-based degradation of repressors of auxin response Aux/IAA. In the absence of auxin, Aux/IAA interacts with auxin response factors (ARFs), which are unable to trigger gene expression of target genes. In the presence of auxin, Aux/IAA are degraded, ARFs can activate the downstream genes (Figure 6).

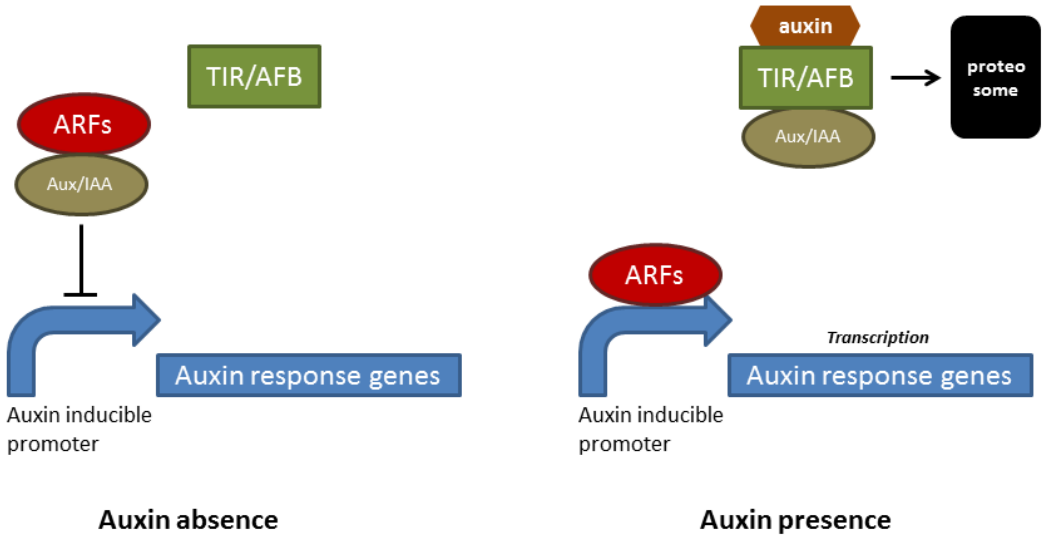

Figure 6: Auxin hormone activity in the cell. In the absence of auxin, ARF activity is blocked by Aux/IAA. In the presence of auxin, TIR/AFB complex is recruited to direct Aux/IAA complex for degradation, freeing ARFs to trigger transcription of auxin controlled genes.

In terms of maintenance of the stem cell niche and driving root development, the auxin maximum is found just at the QC and auxin drives the expression of PLTs transcription factors (Galinha *et al.* 2007) as well as ARFs that influence identity of the cells in the meristem (Aida *et al.* 2004) as well as PINOID (PID) protein kinase that regulates polarisation of PINs (Friml *et al.* 2004). On the other hand, PIN transcription is also maintained by PLT proteins to secure the position of stem cell niche through directional auxin flow (Grieneisen *et al.* 2007). There is an important feedback loop between auxin transport, auxin action and action of stem cell niche specifying transcription factors which results in stability of the stem cell niche. The interaction between auxin and SHR/SCR transcription factors is not as direct as it is for PLTs, but mutations in the *shr* gene led to decreased accumulation of PIN efflux carriers (Lucas *et al.* 2011). However PIN gene expression is not directly controlled by SHR/SCR pathway (Levesque *et al.* 2006), it is likely post-transcriptional control of PINs is influenced by SHR/SCR (Lucas *et al.* 2011).

Auxin is also an essential driver of cell division. Exogenous auxin applied to plant tissues as well as plant tissue culture has been seen to stimulate cell division. The observed increase in cyclin-dependent kinase A (CDKA), which is important for progression through cell cycle has been linked to

directly to auxin driven gene expression (Ferreira *et al.* 1994). CYCLIN B1 (CYCB) and CYCLIN A2 (CYCA) have auxin response elements (AuxRE) in their promoter sequences (Hu *et al.* 2003), and their transcript profile also revealed potential regulation by auxin (Hartig and Beck 2006). Auxin also turns down the expression of cyclin-dependent kinase inhibitors KRP1 and KRP2 (Himanen *et al.* 2002). KRP1 and KRP2 under normal conditions prevent pericycle cells from forming lateral roots, and *krp2* mutant has many more lateral roots than wild type (Sanz *et al.* 2011).

Auxin plays an important role in asymmetric divisions found in the stem cell niche. Specifically, the asymmetric cell divisions of CEI cells that give rise to ground tissue are controlled by SHR/SCR by driving CYCD6 expression (Sozzani *et al.* 2010). The promoter of CYCD6 contains an auxin Responsive Element (AuxRE) and the expression of CYCD6 is upregulated by auxin, but in the case of missing a functional *shr* gene, auxin treatment did not cause CYCD6 expression (Cruz-Ramirez *et al.* 2012). This shows auxin is likely an enhancer of asymmetric divisions, but not its trigger.

1.1.4 Cytokinin and other hormones

In addition to auxin, another hormone crucial for the overall control of cell proliferation and differentiation in the root meristem is a group of hormone molecules known as cytokinins. Cytokinins are split into groups as trans-zeatins and isopentenyl-adenines (Hirose *et al.* 2008). Different types of cytokinins have different distribution in the root, but the distinct functions of different cytokinin types in root development are not yet well described. Cytokinin signalling in the cell is relayed into the cell by a two-component system, with three transmembrane receptors Arabidopsis Histidine Kinases AHK2, AHK3 and AHK4 (Hwang and Sheen 2001), (Inoue *et al.* 2001). When cyokinin triggers the signal relay, AHKs turn on by phosphorylation the B-type Arabidopsis Response Regulators (ARRs) which drive the expression of cytokinin response genes (Hwang and Sheen 2001).

Cytokinin and auxin action in the root is long thought to be antagonistic when defining root meristem size with auxin promoting cell proliferation while cytokinin promoting cell differentiation.

Exogenously applied cytokinins led to decreased cell division in the root meristem (Beemster and Baskin 2000). Cell differentiation process is mainly controlled by cytokinins in the transition zone (Dello Ioio *et al.* 2007). Cytokinin largely self regulates its own levels, influencing the impact it has when controlling the root growth. Cytokinin synthesis is partly triggered by PHABULOSA (PHB) and PHAVULOTA (PHV) transcription factors, as they directly drive the expression of cytokinin biosynthesis gene IPT7 (Dello Ioio *et al.* 2012). However, PHB is repressed by ARR1 mediated action of cytokinins. In addition, cytokinin through ARR1 also supresses miRNA165 which when abundant can post-transcriptionally repress PHB (Dello Ioio *et al.* 2012). This complex regulation means robust control of cytokinin concentration and action in the growing root.

In addition to auxin and cytokinin also giberellins are type of hormones associated with the control of meristem size. In the endodermis, gibberellins cause the degradation of DELLA growth repressor and enhance mitotic activity (Ubeda-Tomas *et al.* 2009).

1.1.5 Control of meristem size

Hormonal control of the meristem dedicated to cell proliferation versus transition and elongation zone dedicated to differentiation is specified spatially and temporally by the process controlled by an Aux/IAA protein short hypocotyl2 (SHY2). SHY2 expression is highest when co-driven by two cytokinin triggered ARRs, ARR1 and ARR12 (Dello Ioio *et al.* 2008). When the root tip is younger than 5 days after germination, cytokinin levels are kept low and ARR12 triggers only basal expression of SHY2. This is possible, because ARR1 levels are controlled by giberrellins, blocking the optimal expression of SHY2. Low levels of SHY2 allow for PIN gene expression, auxin flow and higher rate of cell divisions than cell differentiation (Figure 7). Towards the end of meristem growth phase, when root meristem is setting its size, giberrellin levels decrease and cytokinin levels increase, triggering the action of ARR1. This increases SHY2 concentration which leads to repression of auxin flow, and increase in cell differentiation in the transition zone and overall balances cell division and cell differentiation (Dello Ioio *et al.* 2008), (Sozzani and Iyer-Pascuzzi 2014).

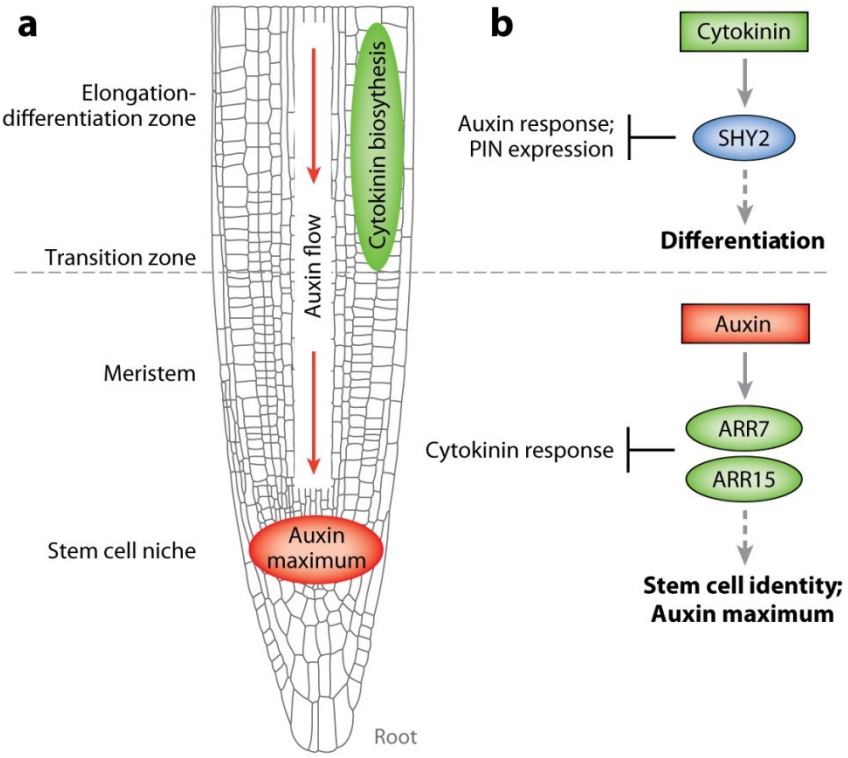

Figure 7: The role of auxin and cytokinin when specifying the meristem and the differentiation zone. a) Auxin maximum is found near the quiescent centre, whereas high concentration of cytokinins is found in the transition/elongation zone. b) High concentrations of cytokinins are able to supress auxin response using SHY2 (short hypocotyl 2); high concentration of auxin is able to supress cytokinin response using ARRs (Auxin Response Regulator). Taken with permission from (Chapman and Estelle 2009).

The coordination of the auxin driven cell division and maintenance of stem cell niche and the cytokinin driven cell differentiation in the transition zone is also influenced by the SCR. SCR controls the size of transition zone through ARR1 as well as controlling the auxin production in the quiescent centre, by controlling auxin biosynthetic gene ASB1 (Moubayidin *et al.* 2013). In addition, SCR activates miRNA 165 to decrease levels of PHB, which shows that SCR also controls the levels of cytokinin and leads to specification of cell types in the transition zone (Carlsbecker *et al.* 2010) (Figure 8).

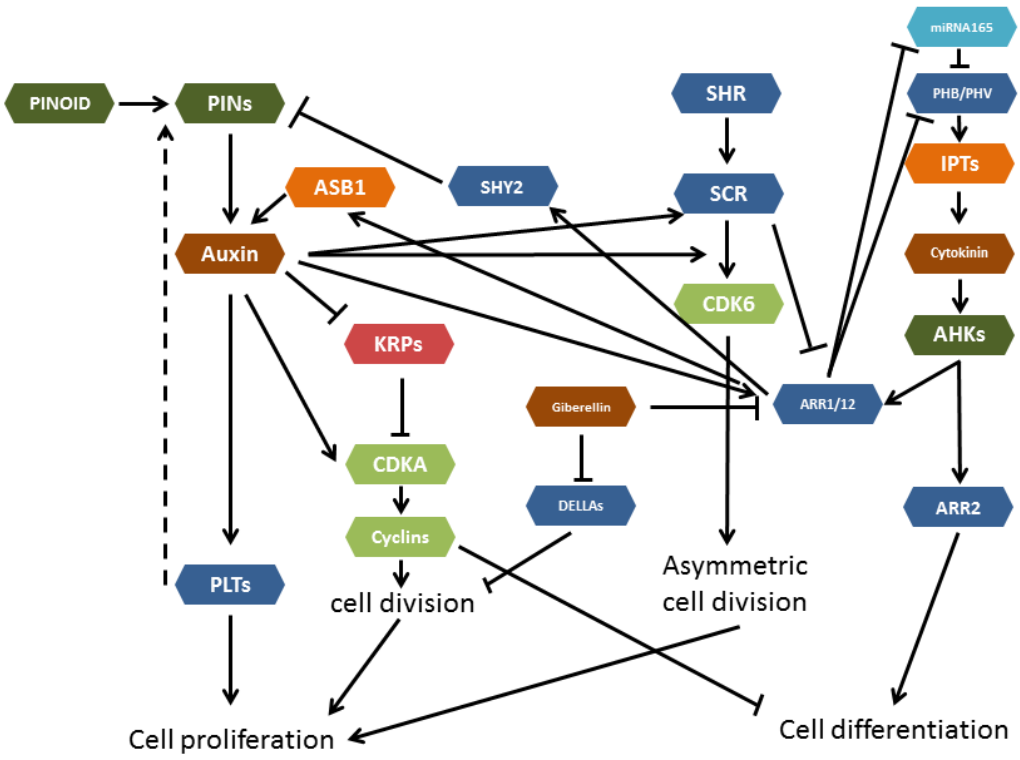

Figure 8: Summary of the interaction of molecular actors controlling cell proliferation and cell differentiation in the root tip. Colour coding aids to differentiate molecular types. Brown = hormones, blue = transcription factors, light blue = miRNA, dark green = regulatory units of hormone transport, light green = drivers of cell cycle, orange = biosynthesis enzymes, red = inhibitors.

Overall this level of hormonal specification defines the boundary between dividing cells in the proximal meristem and the endoreplication of the genomic DNA that occurs in cells of the transition zone (Joubes and Chevalier 2000). This also coincides with first elongated cells, which are part of the transition zone (Benfey *et al.* 1993). It is also assumed that cell differentiation is progressing through the transition zone and elongation zone, with endoreplication a clue marking cell differentiation process.

1.1.6 Specification of elongation zone

The elongation zone is found above the transition zone (Figure 7). This zone comprises of rapidly elongating cells, causing root size increase. Many factors are contributing towards the rapid cell elongation, such as water uptake into the vacuoles and irreversible extensions of cell wall (Dolan and Davies 2004). It has been shown that exogenously applied cytokinin decreases overall cell elongation, which may suggest that even though cytokinins are necessary for endoreplication, they

may negatively regulate cell expansion in the elongation zone (Beemster and Baskin 2000). In addition to already mentioned hormones, ethylene another hormone type, increases auxin biosynthesis and basipetal transport from the root tip, this results in higher concentrations of auxin in the elongation zone and leads to inhibition of cell elongation (Swarup *et al.* 2007). Ethylene was also observed to inhibit the accumulation of giberrellins in the endodermis of the elongation zone, where giberrellin is responsible for induction of cell elongation (Shani *et al.* 2013).

Lastly the relevance of the hormones interacting with other signalling components is also very crucial to maintain division and elongation of cells in balance. As an example, the hormone abscisic acid triggers the activation of calcium channels. The resulting change in the Ca^{2+} homeostasis leads to decreased cell elongation (Bai *et al.* 2009). The interaction of hormones with other components such as ions and ion based signalling pathways is necessary for a more complete understanding of the root cell divisions and cell elongations.

1.1.7 Role of ion channels in root homeostasis

In the root a number of different ion transporters are expressed to manage environmental conditions such as salinity changes, nutrient changes as well as heavy metal presence (Ward *et al.* 2009). In addition, the ion channels also contribute towards fluctuation and maintenance of cell membrane potential, the charge difference that is kept between symplast and apoplast, which is used to generate action potentials within plant tissues and may be necessary component of cellular signalling (Baluška and Mancuso 2013).

There are different types of ion channels present in plants and more specifically in roots and they often have redundant roles. There are types of symporters and antiporters, moving different ions such as Cl^-, K^+, Na^+, H^+ and Ca^{2+} in the same or opposite direction across membrane. There are also ligand gated as well as voltage gated channels that can be passive or active, using diffusion or using energy in form of ATP to force the movement of ions across the membrane (Ward *et al.* 2009). A unique category within the ion channel group are the glutamate receptor-like channels, calcium

transporters that appear to be triggered by a number of ligands such as glutamate, serine and even glycine (Michard *et al.* 2011).

1.1.8 Glutamate Receptor-like channels

Since Ca2+ is not only regulated to maintain balance with the external environment, but also it is an important signalling molecule, ion channels that control its presence and fluctuation are crucial to the development and growth of the root. Glutamate Receptor-like channels (GLRs) are a class of non-selective cation channels that have been observed to transport Ca^{2+} in plant cells across membranes (Lam *et al.* 1998). They are unique, because they share high degree of homology with animal ionotropic Glutamate receptors, which are triggered by glutamate and play a major role in synaptic transmission in neurons and have been implicated in memory and learning (Maren and Baudry 1995).

In *Arabidopsis* 20 GLRs have been observed to be triggered by a number of ligands and have been identified with various cellular and physiological roles. GLRs in *Arabidopsis* were observed to trigger Ca^{2+} fluxes and membrane depolarisations (Demidchik *et al.* 2004). A number of physiological effects can be attributed to GLRs. Root architecture is controlled by the action of GLR 3.2 and GLR 3.4, double mutant *glr3.2glr3.4* showed higher number of lateral root primordia (Vincill *et al.* 2013). In addition, mutations in the *glr3.1* gene found in rice were found to affect the whole root structure architecture (Li *et al.* 2006). GLRs have also been necessary for fine tuning of gravitropism response in roots, it was observed that mutants of the *glr3.3* gene had a delayed response to gravity by 5 to 10 hours compared to wild type (Miller *et al.* 2010).

GLRs were also observed to mediate wounding signals among leaves, caused by herbivore attack that results in complex hormonal response. The signals themselves were electric variable surface potentials that were measured on stems of the leaves attacked by herbivore and also on the adjacent leaves showing increased presence of plant hormone jasmonate. *Arabidopsis* double

mutants *glr3.3glr3.6* were unable to convey any surface potential signal and these plants did not show response to herbivore attack (Mousavi *et al.* 2013).

Overall action of glutamate receptor-like channels has been observed to be necessary in a number of different plant physiological processes such as plant development, tropism, stress signalling, plant immunity, stomatal movements connected to photosynthesis and carbon metabolism (Weiland *et al.* 2015) (Figure 9). There may be other physiological and developmental phenomena that need GLRs for their correct functioning that were not yet discovered.

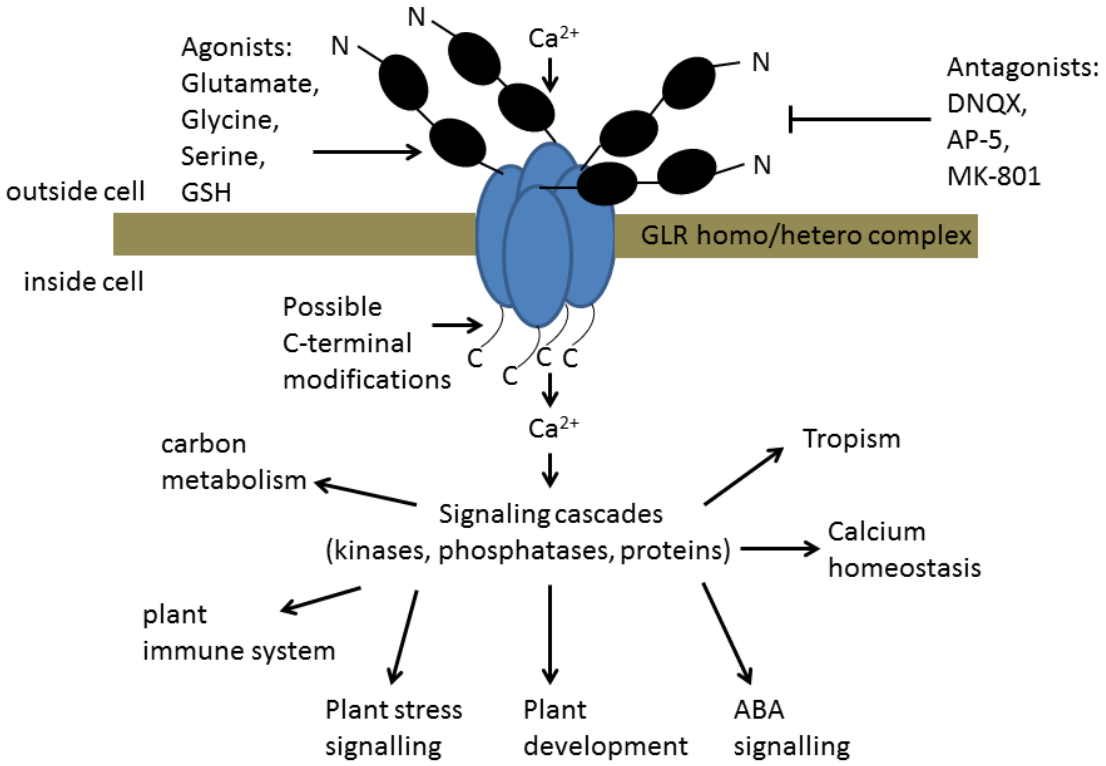

Figure 9: Actions of GLR proteins within cells and downstream physiological effects. Adapted and modified from (Weiland *et al.* 2015) under CC-BY license.

1.2 Root tropisms

1.2.1 Background

The soil environment in which the roots live is a very complex, heterogeneous mixture that contains both threats to avoid and opportunities for the root to exploit. The role of the root in the soil is to maximise water and nutrient uptake, while avoiding toxin or stress-inducing exposures of unwanted inputs, all the while minimising the growth expenditure. Since plants are sessile

organisms, they cannot physically upend their root to move it closer to a source of wanted nutrient, an example can be phosphate, instead roots are able perform 'guided growth' towards or away from the input that's been detected by the root. These responses, known as tropisms, have evolved in order for the root to adapt to highly heterogeneous and dynamic conditions in the soil (Figure 11). Tropisms rely on asymmetric cell elongation in the same part of the root (Figure 11), effectively re-orienting the root tip (Muday 2001).

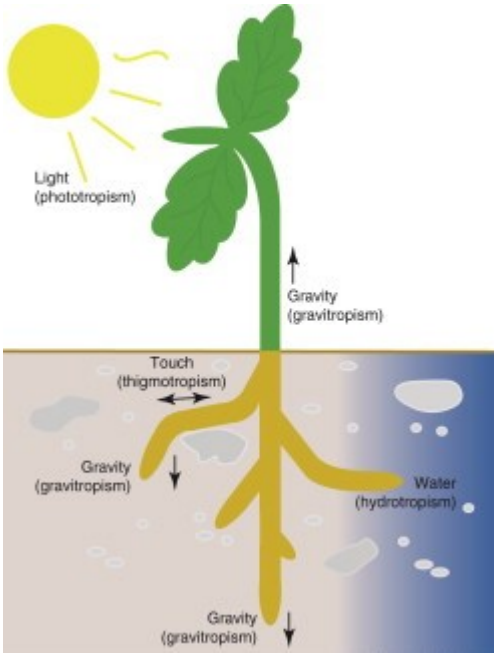

Figure 10: Examples of some of the tropisms. Adapted with permission from (Gilroy 2008), copyright by Elsevier.

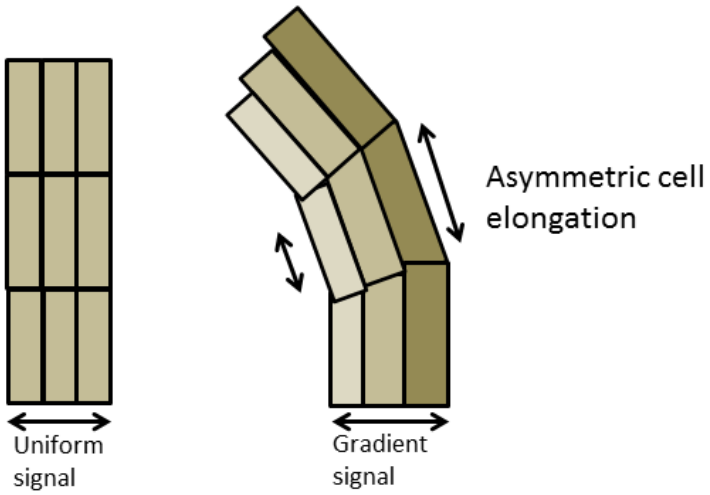

Figure 11: Description of cellular mechanism behind plant tropism. Asymmetrical cell elongation caused by signal gradient results in roots readjusting their direction of growth.

A number of tropisms have been identified, both for guided growth of root towards the source of stimulus as well as away from the stimulus. The most studied of tropisms is gravitropism, when primary root tip is reoriented towards earth's gravity field (Hangarter 1997) and lateral roots show graded growth towards the Earth's centre of gravity (Kiss *et al.* 2002). Another known tropism, more studied in the shoot, but also observed as behaviour by roots, is the phototropism, or in case of roots it's the escape response from blue light (Kiss *et al.* 2003). Other tropisms include halotropism, which is a response of the roots to avoid high salinity environment (Galvan-Ampudia *et al.* 2013) and hydrotropism when the direction of root growth is guided by increasingly moist environment (Eapen *et al.* 2005) as well as thigmotropism which is a change of root growth direction according to touch (Massa and Gilroy 2003). Another type of tropism, which is studied at length in this thesis is the electrotropism, the ability of roots to align with external electric fields (Stenz and Weisenseel 1993).

Since it is likely that roots will be responding in soil to more than one stimulant at a time, some tropic stimuli could in certain conditions affect the root more strongly than others. Overall not much is known about integration of different tropic stimuli. Roots respond to gravity continuously, because all the plants are constantly affected by the Earth's gravity field. When root is responding to different tropic stimuli, the tropic response of the root to these stimuli causes an offset of the root growth following the gravity vector. The competition between tropisms may translate into a competition at the molecular level, where some of the components of the two tropisms are shared.

One example of shared molecular components for two different tropic stimuli is the case of gravitropism and halotropism, where there is a same molecular component, PIN2 protein. The asymmetric accumulation of PIN2 protein necessary for auxin driven cell expansion is influenced by different upstream molecular components in the case of gravitropism and halotropism. Once reaching PIN2 component within the molecular mechanism, both gravitropic and halotropic signal uses the same mechanism to cause asymmetric cell expansion (Galvan-Ampudia *et al.* 2013).

There are also examples of two tropisms that do not share any molecular components resulting in asymmetric cell elongation driven completely separately to one another. One such example is gravitropism and hydrotropism, where cells in different tissues were observed to perform asymmetric cell expansion (Dietrich *et al.* 2017). In the case of gravitropism this is the epidermis, while in the case of hydrotropism it was observed to be the cortex cells. Additionally, agravitropic mutants were able to show hydrotropic movement, while hydrotropic mutants were able to show gravitropic movement (Dietrich *et al.* 2017). This suggests that the root is able to respond to both gravitropism and hydrotropism at once, without any competition in their respective molecular mechanisms.

It was previously observed that root tips respond to weak external electric field (Stenz and Weisenseel 1993). The soil contains many components that are charged and we can hypothesise that potentially these could provide cues to growing root on the basis of the electric field. It was also previously hypothesised that individual plant roots cause a formation of the weak external electric field in their vicinity to signal with other root tips nearby (Baluška *et al.* 2009). The molecular mechanism of root tropic responses is well described for gravitropism, but for electrotropic response the molecular mechanism is unknown. We aim to compare electrotropic response to that of gravitropic response of the roots and evaluate if there are any shared molecular components.

1.2.2 Gravitropism

Tropic response starts with perception of stimulus, which results in asymmetric cell expansion. Gravity stimulus is first detected by the columella cells. These cells contain amyloplast filled granules present only in columella cells (Kiss *et al.* 1989). The amyloplast granules order themselves within the cells differently depending on the orientation of the cell in relation to gravity vector. When the root tip is re-oriented, amyloplast granules redeposit (Figure 12), applying force to endoplasmic reticulum, which is thought to be a mediator of the physical trigger to mechano-sensitive ion channels converting physical into biochemical signal (Leitz *et al.* 2009).

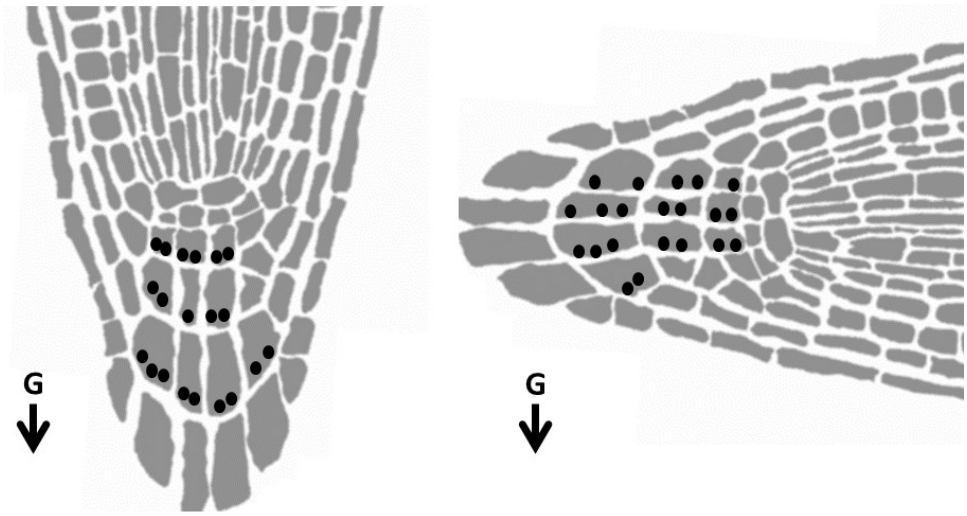

Figure 12: Starch statolith repositioning after change of root position to gravity vector.

Minutes after re-positioning of the statoliths, the cells in the root cap show change in the cytoplasmic and apoplastic pH (Fasano *et al.* 2001). This change seems to be necessary for the root's response to gravity since acidifying or alkalizing treatment can lead to altered gravitropic response (Hou *et al.* 2004). It is possible that actin cytoskeleton may also be involved in the perception and trigger of gravitropic response. Specifically a protein involved in cytoplasmic alkalisation is also able to bind cytoskeleton, so it is possible changes in the actin filaments are necessary for the initiation of gravitropic signal (Boonsirichai *et al.* 2003).

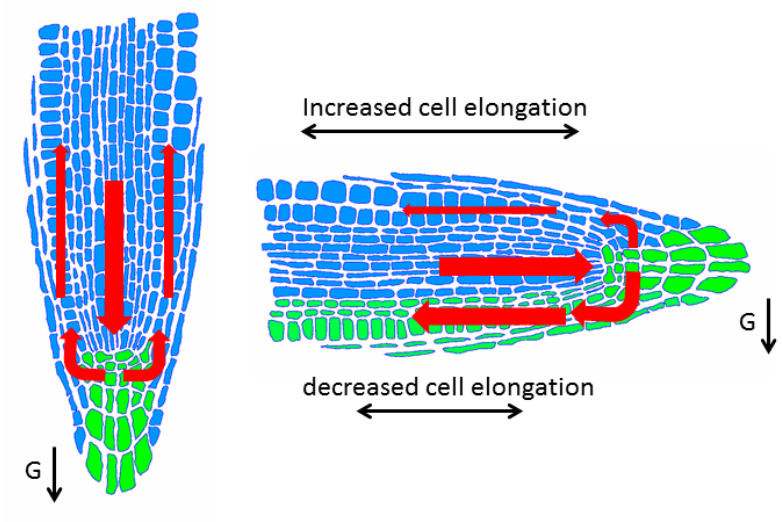

Figure 13: Distribution of auxin shown with red arrows at different positions of root in gravity field. Green cells represent cells with high auxin concentration. G stands for gravity. Cells with higher auxin concentration expand less, while cells with little auxin concentration expand more, causing a root to reorient.

The transduction of gravity signal is a crucial component of the gravity response, since the perception of gravity occurs in the root tip, but the asymmetric cell expansion that causes the root to reorient occurs in the elongation zone (Figure 13). Hormone auxin was identified as the signal that is present differentially in the two sides of the root and ultimately causes the cells to expand asymmetrically at the two sides of the root (Band *et al.* 2012). One of the auxin transporters that is necessary for gravitropism is the AUX1 influx transporter and Like-AUX1 proteins, inability to respond to gravity was observed in roots with mutated AUX1 (Bennett *et al.* 1996). AUX1 provides enough auxin into the tissues such as lateral root cap cells, and epidermis, so that auxin can be an effective signal for gravitropic response (Swarup *et al.* 2005).

Even thou AUX1 is necessary for gravitropic turn, it is the PIN auxin efflux transporters that asymmetrically arrange on the two sides of the root, leading to differential auxin distribution and asymmetric cell expansion. Of the PIN proteins in the root tip, it is mostly PIN2 and PIN3 and PIN7 that contribute towards gravitropism related redistribution of auxin (Luschnig *et al.* 1998), (Friml *et al.* 2002b). PIN2 is expressed in the epidermal and cortical cells, having polar localisation on the proximal side of the cells. PIN2 transports auxin away from the quiescent centre, and there is a difference in PIN2 concentrations on the membranes of cells localised at the 'top' compared to those at the 'bottom' when root is reoriented in the gravity field, caused by proteolysis and rapid recycling of the PIN2 protein from the membranes of cells (Abas *et al.* 2006), (Kleine-Vehn *et al.* 2008). The PIN2 recycling mechanism results in the asymmetry of PIN2 distribution, leading to the difference of the auxin flow, which further controls PIN2 turnover (Abas *et al.* 2006). The result is differential auxin flow along the whole of epidermis in the root meristem, resulting in asymmetric cell expansion (Band *et al.* 2012).

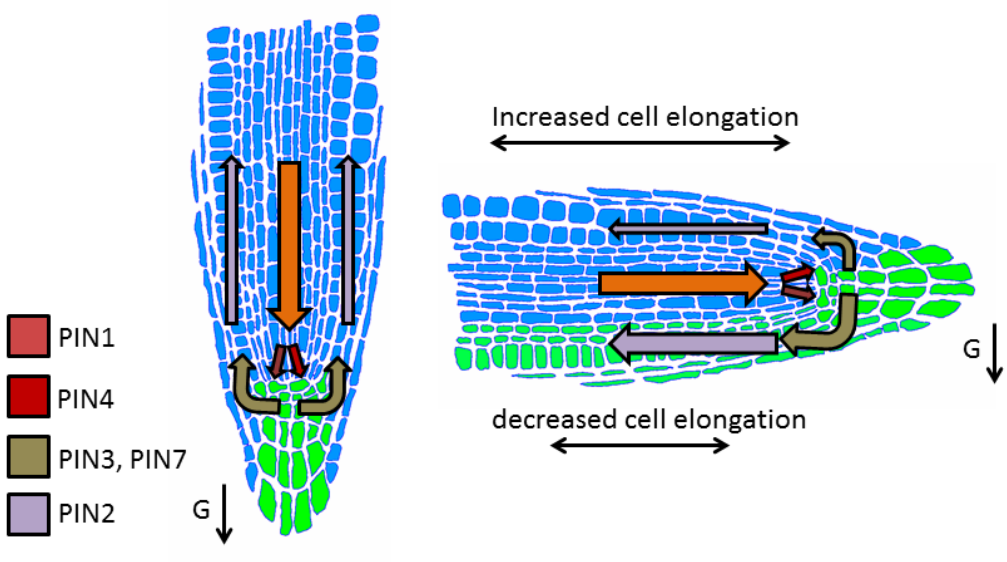

Figure 14: Differential auxin flow during gravitropism is caused by asymmetric accumulation of PINs in spatially distrinct zones on two sides of the root. Green cells have higher concentration of auxin than blue cells causing asymmetrical cell expansion.

PIN2 concentration asymmetry leads to differential auxin distribution along the whole length of the meristem, but it is the PIN3, found in columella, that initiates the change in the auxin distribution. Upon receiving gravitropic trigger, PIN3 proteins relocate within columella to provide a simple mechanism for the change of auxin flow. PIN3 protein is partially redundant for this role, since *pin3* mutants show only reduced gravitropism (Friml *et al.* 2002b). PIN7 which is also expressed in the columella cells, also undergoes differential localisation when gravity stimulus is perceived, most likely having a partially redundant role with PIN3 transporter. As a single mutant *pin7* roots are weakly gravitropic, while double mutant *pin3pin7* is significantly more agravitropic than the two single mutants (Kleine-Vehn *et al.* 2010). Overall it is clear that PIN-dependent differential auxin distribution is the mechanism with which the perception of gravitropic stimulus gets translated into a biochemical response that results asymmetric cell expansion (Figure 14).

The last step of gravitropic response is the translation of differential auxin concentration of two sides of the root meristem into asymmetric cell expansion. The mechanistic response of gravitropism is not very well understood, but there correlation between stimulating roots with change in gravity vector, the presence of cytosolic calcium waves in the cells of the root meristem

and differential accumulation in auxin concentration on the two sides of the meristem (Mullen *et al.* 1998). Auxin also controls changes in the apoplastic pH which result in the direct control of the cell expansion. With alkalinisation of the apoplastic space comes reduced cell elongation, while increased acidification allows for more elongated cells (Barbez *et al.* 2017). Changes in the root curvature can be observed as early as 10 minutes after changing the roots' position gravity vector. The described gravitropic mechanism offers a rapid way of translating a perceived environmental stimulus into a change of direction of root growth, without any initial need for changes in the expression pattern of the root (Monshausen *et al.* 2011).

1.2.3 Effects of external electric field in animals - electrotaxis

Soil is a very complex environment that needs to be navigated by the organisms that live in it. These organisms need to read and obtain as many spatial cues as possible. One of the directional cues that may be found in soil are the transient weak external electric fields that can be present as a result of heterogenous distribution of charged compunds (Jouniaux *et al.* 2009). This effect is present in the soil thanks to irregular surface shapes of soil particles and overall inability of soil to become completely homogenous for its charged molecule presence. This leads to irregular presence of charged minerals or even charged toxins that animals, microbes and even organs such as roots need to exploit or avoid (Hodge 2006).

There are many soil dwelling organisms that have been observed to perform electrotaxis, a single-cell or whole organism movement driven by a weak external electric field. Soil dwelling amoeba *Dictyostelium discoideum* lives part of its life as a single cell organism, but is able to form a multicellular fruiting body in certain occasions. The single cells are able to perform electrotactic movements and several genes underlying the behaviour have been identified (Gao *et al.* 2015). Nematode *Caenorhabditis elegans* is also a soil dwelling nematode, which is commonly used to study developmental and behavioural patterns in animals. *C. elegans* readily shows electrotactic behaviour in laboratory conditions, with scientists pinpointing a number of genes linked to neuronal differentiation as essential for wild-type electrotaxis behaviour (Chrisman *et al.* 2016). Many

phytopathogenic organisms have also displayed electrotactic behaviour towards plant roots, as a result of weak external electric field generated by the continuous release of charged molecules by the root into the rhizosphere (Judelson and Blanco 2005). Overall many soil organisms use presence of weak external electric field in their environment to guide their movement.

1.2.4 Effects of external electric field in plants - electrotropism

It is possible that plant roots also use weak external electric fields found in soil to avoid toxins or are attracted to unequally distributed sources of minerals. It is also possible that roots can use weak external electric fields generated by other roots, to avoid growing too close to one another or exploring the same patch of soil (Baluška *et al.* 2009).

In laboratory conditions roots from a number of different plant species such as *Lepidium*, *Synapsis*, *Raphanus*, *Zea mays* and *Vigna murgo* were subjected to transverse weak external electric field (Plowman, 1904), (Shrank, 1959), (Moore *et al.* 1987), (Ishikawa and Evans 1990), (Stenz and Weisenseel 1991), (Stenz and Weisenseel 1993), (Wolverton *et al.* 2000), (Wawrecki and Zagórska-Marek 2007). Due to different experimental set ups used, as well as different strengths of electric field applied, three main different observations were made. Either the root turned towards negative electrode, or it turned towards positive electrode or it showed damage. With more systematic observations it was established that the true electrotropic turn is towards negative electrode (cathode) (Stenz and Weisenseel 1993), with the asymmetry in cell elongation found in the distal elongation zone (Wolverton *et al.* 2000).

The mechanism underlying the electrotropic turn in plant roots is largely unexplored. Dated experiments have shown that applying auxin transport inhibitors pyrenoyl benzoic acid (PBA) and 2,3,5-triiodobenzoic acid (TIBA) have stopped roots from turning in electric field, but did not inhibit root growth (Moore *et al.* 1987), (Ishikawa and Evans 1990). How is auxin related to electrotropic turn remains to be seen. In addition, increased Ca^{2+} ion concentration was measured in the vicinity of one of the sides of the electrotropic root of Zea Mays (Moore *et al.* 1987). Changes in Ca^{2+}

concentrations have also been associated with gravitropic turn and the level of similarity between gravitropism and electrotropism can be compared.

1.3 Regeneration

1.3.1 Root tip regeneration

Root tip regeneration is a unique example of cellular self-organisation found in plants (Sena *et al.* 2009). The cells within the root tip are able to interact among each other and use positional cues to drive the rebuild process.

Growing primary root meristem relies on the Quiescent Centre and stem cell niche to maintain indeterminate growth. In cases of removing the very root tip including the stem cell niche or ablating the quiescent centre, the root is able to redevelop a new root tip in *Mays* (Feldman 1976), *Pisum* (Rost and Jones 1988) and in *Arabidopsis* within 5 days (Sena *et al.* 2009). This is a unique example of the post-embryonic development, with *de novo* plant organogenesis.

With the removal of quiescent centre, the most undifferentiated cells in the root are missing. It has been shown that the establishment of cell fates in roots and in plants in general is much more plastic than in animals, and even more mature, differentiated cells can guide the cell differentiation in newly formed cells, based on their position within the root (van den Berg *et al.* 1995). When *Arabidopsis* root tip is removed, within one day cells with specialised cell fates begin to re-emerge, eventually establishing a new stem cell niche and a new quiescent centre. Even more so, roots with genetic mutation in the genes *plt1plt2*, which are unable to maintain the stem cell niche due to missing PLT transcription factors, were still able to regenerate the primary root tip, even though it was not then able to continue in root tip growth (Sena *et al.* 2009).

Even though mutants with decreased pericycle activity and lateral root initiation have shown inhibition in some features of regeneration (Liu *et al.* 2014), it does not appear that an alternative stem-cell niche, possibly following lateral root formation is responsible for root regeneration (Efroni *et al.* 2016). Instead a whole range of cells within the root meristem, is able to

organise themselves to reform a root tip, not having to rely on stem cell niche. These cells have to rely on inclusion of cells at different maturity and different cell fates, effectively across tissues. It is likely that multiple signals of physical, chemical and possible even electric nature using membrane potentials could be used by the cells in the root stump when reorganising cells to form a new organized tip.

Once the root is regenerating it employs cells from all of the tissues and follows embryo-like patterning program when forming new root. This was observed particularly when triple mutants of *nww* (NO TRANSMITTING TRACT), which are unable to form embryonic root were also unable to regenerate a root (Efroni *et al.* 2016). Application of exogenous hormone auxin to the *nww* regenerating roots has managed to increase the regenerating frequency, suggesting necessity of the auxin presence in the regenerating root tip. This is similar to the embryonic root formation, where mutants of the stem cell niche maintenance such as *shr*, *plt1plt2* were still able to form embryonic root (Sabatini *et al.* 2003), (Aida *et al.* 2004). Regenerating root following similar pattern of root tip formation as the embryonic root has one major difference to tackle with. In the embryo, the root is formed from two cells in the hypophysis, whereas regenerating root forms from a whole group of cells still found in the root meristem. It appears that the genes normally upregulated during hypophysis of the embryonic root formation are also upregulated in the regenerating root (Wendrich *et al.* 2015), (Efroni *et al.* 2016).

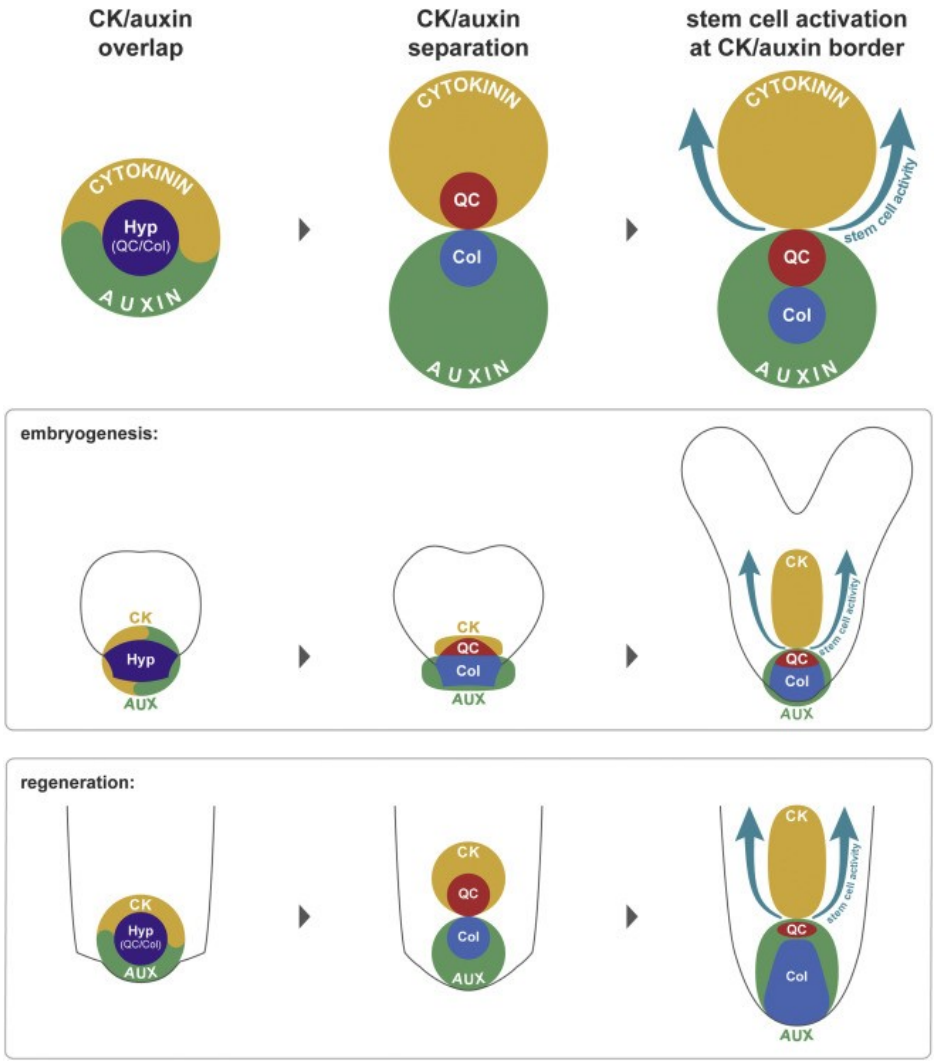

Figure 15: Embryonic root development and post-embryonic root regeneration are governed by a similar process involving auxin and cytokinin. Initial mix of cytokinin and auxin gets separated into cytokinin in the proximal part and auxin in the distal part, providing cues for the stem cell niche, the root cap and the proximal meristem. Col columella, QC quiescent centre, Hyp hypophysis. Adapted with permission from Efroni *et al.* 2016, copyright by Elsevier.

The hormonal concentration of auxin and cytokinin defines boundaries of the of the apical and basal cells in the embryo when forming a new root, and auxin and cytokinin were also reported to define proximal and distal ends of the new forming root tip in the regenerating root and outline tissue boundaries in the radial manner acting across a whole area of meristem left after root tip removal (Efroni *et al.* 2016) (Figure 15).

The root cells that are normally located in the proximal part of the meristem rapidly lose cell fate identities after the root tip removal. These cells then lead to the origin of new tissues, in the manner that cells that were cortex/endodermal cells, become epidermal cells, and pericycle cells

become new endodermal cells, suggesting there is an order with which cells transition their cell fate and its possible it is guided by their position in the remnant tissue (Efroni *et al.* 2016). Also within 24 hours new markers of QC such as WOX5 and WOX11 appear after being removed by the root tip cut (Efroni *et al.* 2016). It also is the case with other types of post-embryonic root organogenesis, such as induced root growth from leaf explants, that the WOX11 marks the first steps in the formation of new cell fates (Liu *et al.* 2014).

Root regeneration is not an all or nothing phenotype. Instead there is a frequency with which the root can regenerate. An obvious influence to the regeneration frequency is a presence of genetic mutations or exogenous supply of hormones, but it can also be influenced by the amount of root meristem left after the root tip removal. The more distal the position of the cut, the higher the likelihood for the root to regenerate, hence the position of the cut can influence regeneration frequency (Sena *et al.* 2009). There may be multiple reasons why this is the case, possibly related to mitotic activity of remaining cells in the stump, or the cell fate maturity of the remaining cells, since more mature cells are found in the further away from the root tip. It also may be possible to perturb the regeneration frequency with other means than just with genetic mutations or chemical treatment. This may help identifying the necessary components of root tip regeneration.

1.3.2 Electric field and regeneration in animals and plants

Root tip regeneration is a fascinating process of cellular self-organisation as cells use spatial cues to reform a new organ. It is interesting to learn how this dynamical system interacts with weak external electric fields. This allows us to understand more about the mechanisms of electric field perception and the maintenance of tissue organization.

Application of weak external electric field is a type of perturbation that was previously tested more on animal regeneration models than on plants and roots. It has been demonstrated that by placing electrodes and applying electric field on regenerating limbs of frogs, the rate of regeneration can be enhanced (Smith 1974). In addition, the external electric field was seen to aid

polarised migration of many cell types, such as neurons (Patel and Poo 1982), but also other cell types such as keratinocytes or epithelial cells (Nishimura *et al.* 1996), (Zhao *et al.* 2006), to increase growth, wound healing or overall regeneration process (Chang and Minc 2014). External electric field application was also observed to affect yeast cells (Minc and Chang 2010) causing change in cell polarity, affecting the overall shape of the single celled organism. In addition, even endogenously occuring electric fields present in the tissues of regenerating *Xenopus* tadpoles as well as other organisms such planaria *Schmidtea mediterranea* were necessary for correct regrowth of damaged organs (Adams *et al.* 2007), (Beane *et al.* 2012) and manipulation of these electric fields led to abnormally regenerated organs. It is clear that at least in animals internal electric field is a necessary component of cell development, migration and organ regeneration and external electric field is able to perturb phenotypes guided by the internal electric field (Figure 16).

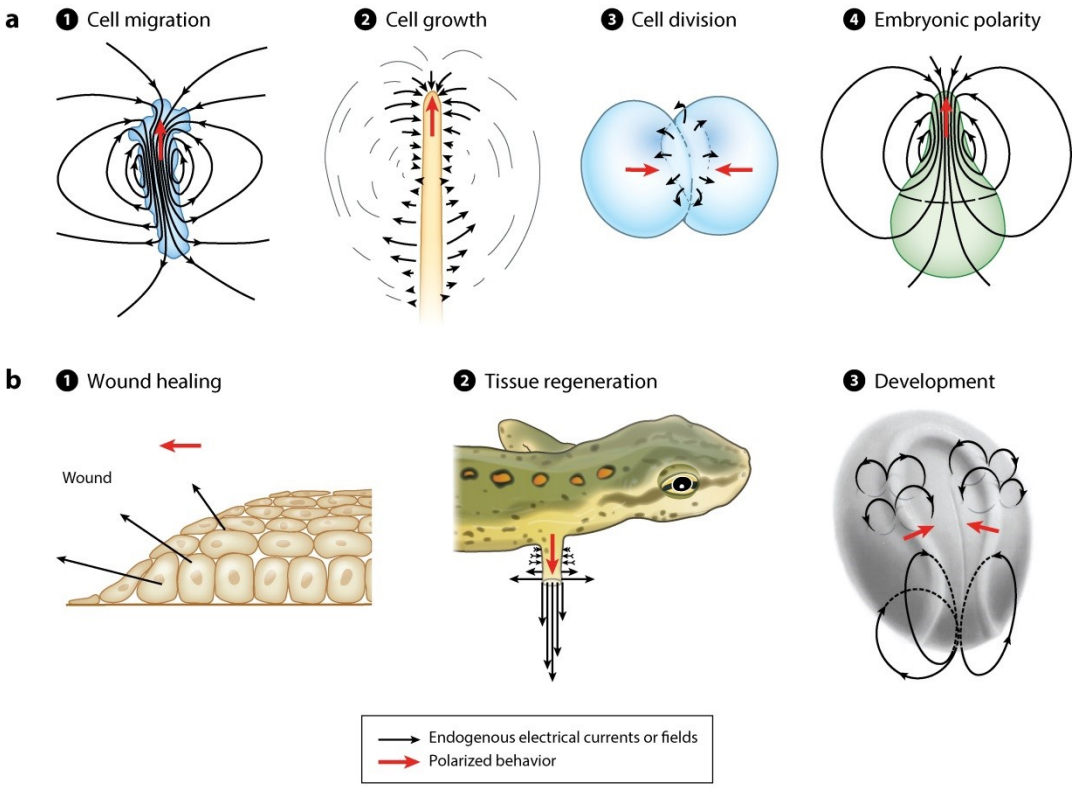

Figure 16: Internal electric fields guide a range of cellular, physiological and developmental processes in animals. A) Cellular effects of electric field include cell migration, growth, division and cell polarity. B) Tissue and organism effects of electric field include wound healing, tissue regeneration and development. Adapted with permission from Chang and Minc 2014, copyright by Annual Reviews.

In plants and algae, weak external electric field was observed to perturb polarity of *Fucus vesiculosus* seaweed egg embryos (Peng and Jaffe 1976) as well as shape and cell wall deposition of single cell green algae *Micrasterias denticulata* (Brower and McIntosh 1980). In higher plants there a few examples of regeneration being affected by the weak external electric field. Tobacco regeneration *in vitro* in shoot inducing medium was observed to be increased by the application of direct and alternating current (Rathore and Goldsworthy 1985), (Cogalniceanu *et al.* 1998). Plant cells cannot migrate like animal cells, so we assume that any parallel between animal regeneration and plant regeneration being influenced by electric field is superficial. However external electric field could influence positional information of the root cells in the regenerating root stump, possibly perturbing root regeneration frequency.

We aim to observe the effects of the external electric field on the regenerating root tips to further describe the perception of weak external electric field by the root and observe possible perturbations of the regeneration process.

2 Methods

2.1 General material and methods

2.1.1 Plant material

In Results II, chapter 4, to study root regeneration and electric field exposure these genotypes of the *Arabidopsis thaliana* were used: wild type Col-0 (Columbia) ecotype, reporters *pSCR::H2B:YFP* (Heidstra *et al.* 2004), *CYCB1;1::GFP* (Reddy *et al.* 2004), *TCSn::GFP* (Zürcher *et al.* 2013) all in Col-0 background. Reporter expressing *RPS5A::mDII:ntdTomato-RPS5A::DII:n3Venus*, known as *R2D2* (Liao *et al.* 2015) with the Col-utr ecotype was also used.

In Results III, chapter 5, *Arabidopsis thaliana* wild type Col-0 and wild type Ler (Landsberg) were used to study root electrotropism. In addition, a collection of published homozygous mutants was used (Table 1). We also used multiple unpublished mutant alleles for a number of functional genes, these were part of the SALK library of mutants (Alonso *et al.* 2003). In order to identify the individual alleles tested, the Nottingham Seed Stock Centre is listed (Table 2). We also used *Arabidopsis thaliana* with a rescue mutation for the non-functional *glr3.4*. This is *Arabidopsis* with *proGLR3.4::GLR3.4:GFP* transgene present in *glr3.4-1* background (Vincill *et al.* 2013). In addition we used *Arabidopsis* reporters expressing *PIN2::PIN2:GFP* (Abas *et al.* 2006), *UBQ10::YC3.6:NES* (Krebs *et al.* 2012) in Col-0 background and *pUBQ10::WAVE131:YFP* expressing in Col-0 background (Geldner *et al.* 2009) as well as *R2D2* reporter (Liao *et al.* 2015) in Col-utr background.

In Preliminary Results IV, chapter 6, we used wild type Col-0 plants and *pUBQ10::WAVE131:YFP* expressing roots in Col-0 background (Geldner *et al.* 2009).

Table 1: List of previously published genotypes used in Results III, 5.

Homozygous allele	Ecotype Background	Publication
pin1-1	En-2 (Enkheim-2)	(Galweiler *et al.* 1998)
eir1-1	Col-0	(Roman *et al.* 1995)
pin3-4	Col-0	(Friml *et al.* 2002b)
pin7-1	Ler (Landsberg)	(Friml *et al.* 2003)
aux1-7	Col-0	(Pickett *et al.* 1990)
aha1-6	Col-0	(Haruta *et al.* 2010)
aha2-5	Col-0	(Haruta *et al.* 2010)
ost2-1D	Ler	(Merlot *et al.* 2007)
akt1-1	Ws (Wassilewskija)	(Hirsch *et al.* 1998)
glr3.4-1	Col-0	(Stephens *et al.* 2008)

Table 2: List of previously unpublished genotypes used in Results III, 5.

Gene	NASC number used as allele label	Ecotype Background
clcB	N852518, N667718	Col-0, Col-2
clcD	N855430, N542895, N680982	Col-2, Col-0, Col-0
clcG	N686466	Col-0
kco4	N666058	Col-0
kat1	N681711, N678836	Col-0, Col-0
kat3	N667113, N664173, N633047	Col-0, Col-0, Col-0
skor	N655760, N658036	Col-0, Col-0
gork	N654279, N655190	Col-0, Col-0
tpc1	N645413	Col-0
vdac1	N653635	Col-0
vdac4	N656391	Col-0
glr1.1	N654208	Col-0
glr1.2	N664922, N664609	Col-0, Col-0
glr1.4	N663986, N665506	Col-0, Col-0
glr2.3	N613206	Col-0
glr2.4	N681712, N654061	Col-0, Col-0
glr3.2	N676991	Col-0
glr3.3	N672760, N663463	Col-0, Col-0
glr3.4	N853381	Col-2
glr3.6	N663316	Col-0

2.1.2 Plant growth

Standard protocols were used to germinate and grow *Arabidopsis* seedlings following previously published methods (Sena *et al.* 2009). All seeds were imbibed in H_2O and kept in the dark and 4°C for 2 days to synchronise germination. All seeds were surface sterilised using 50% Haychlor bleach (sodium hypochlorite) (Brenntag, UK) and 0.0005% Triton-X-100 (Sigma Aldrich, UK) for 3 minutes and then rinsed 6 times with sterilised deionised H_2O. Seeds were then moved under sterile conditions onto 0.8% agar solid medium (1X Murashige-Skoog basal medium (Sigma Aldrich, UK), 0.5% sucrose (Sigma Aldrich, UK), 0.05% MES, 2-MorpholinoEthaneSulfonic acid (Sigma Aldrich, UK) adjusted to pH 5.7 with KOH (Sigma Aldrich, UK)). The solid medium was present either in plates when plants were then allowed to germinate in vertical position or it was present in the cartridge of the V-box (see chapter 3) when plants were allowed to grow through the pods (see chapter 3) into liquid medium (1/4X Murashige-Skoog basal medium (Sigma Aldrich, UK), 0.5% sucrose (Sigma Aldrich, UK), 0.05% MES, 2-MorpholinoEthaneSulfonic acid (Sigma Aldrich, UK) adjusted to pH 5.7 with KOH (Sigma Aldrich, UK)). The germination and 3 day post-germination plant growth was allowed in a plant growth chamber with 120 µmol/m^2/s on a 16h/8h light/dark cycle.

2.2 Root Regeneration

2.2.1 Root meristem excision

All root tips were excised on plants grown for 3 days post germination in accordance with an existing protocol (Sena *et al.* 2009). Seedlings were moved onto the 5% agar solid medium (1X Murashige-Skoog basal medium (Sigma Aldrich, UK), 0.5% sucrose (Sigma Aldrich, UK), 0.05% MES, 2-MorpholinoEthaneSulfonic acid (Sigma Aldrich, UK) adjusted to pH 5.7 with KOH (Sigma Aldrich, UK)) which was used as a cutting surface. The root tips were dissected with 100 Sterican 27G needles (B Braun) under a stereo-microscope (Nikon SMZ1000 at 180x magnification). The excisions were performed at three positions 120µm, 160µm, 200µm with ±10µm variation.

2.2.2 Electric field in V-tank

Plantlets with excised root tips were placed into the V-tank set up (Results I, 3.2.1). Within the V-tank was a gel support with 'pillow-like' structures constructed from solid medium with 0.8% agar and 1X Murashige-Skoog basal medium (Sigma Aldrich, UK), 0.5% sucrose (Sigma Aldrich, UK), 0.05% MES, 2-MorpholinoEthaneSulfonic acid (Sigma Aldrich, UK) adjusted to pH 5.7 with KOH (Sigma Aldrich, UK). The gel was positioned horizontally in the V-tank (Results I, 3.2.1) with roots horizontally laying, facing negative or positive electrode. The tank was filled with 550ml of sterile liquid MS medium (1X Murashige-Skoog basal medium (Sigma Aldrich, UK), 0.5% sucrose (Sigma Aldrich, UK), 0.05% MES, 2-MorpholinoEthaneSulfonic acid (Sigma Aldrich, UK) adjusted to pH 5.7 with KOH (Sigma Aldrich, UK)). This way roots were submerged, but shoots were kept out of the liquid thanks to the 'pillow-like structure' (Results I, 3.2.1). The homogenous condition of the set up was kept thanks to 40ml/min peristaltic pump with tubing positioned at positive and negative electrode (Results I, 3.2.1). Part of the tubing was also placed in an LTD6/20 chiller (Grant Instruments, UK) to maintain 23^{o}C. The roots were exposed to electric field for 30 minutes. After electric field exposure, plantlets were moved onto previously unused sterile 0.8% agar solid medium plates.

2.2.3 Regeneration frequency assay

Vertically placed plates with plantlets that had their root tip removed and subjected to electric field were rotated by 90^{o} so that the roots were now placed 90^{o} to the gravity vector. Plantlets regenerated for 5 days and then were scored for gravitropic response, to assess if the root tip was regrown, in accordance with previously described method (Sena *et al.* 2009). Scoring for regeneration of root tips was done under blind conditions, when observer did not know the identity of the sample observed. Re-established positive gravitropism was used to indicate regenerated root tip and was further assessed by a morphological examination under a dissecting microscope (Nikon SMZ1000 at 22X magnification). The frequency of regeneration was estimated as the fraction of the

cut roots successfully regenerated after 5 days of post-cut recovery period out of the total number of roots.

2.2.4 Regeneration frequency statistics

Repeats for each condition ($n \geq 3$) were organised in a contingency table with categories regenerated and non-regenerated. A chi-square statistical test was performed within each condition, to examine the null hypothesis that there is no association between replicates and categories, to make sure that replicates are samples selected from the same population (Everitt 1992). If the null hypothesis was rejected, with $p<0.05$, a standard analysis of residuals was used to identify and remove any outlier replicate, one at a time (adjusted residual higher than 1.96 or below -1.96 considered critical value when $\alpha=0.05$ (Everitt 1992). Once the test to identify outliers was completed, the remaining replicates were pooled together to increase sample size while keeping biological variability. The frequency of regeneration was calculated as the fraction of cut roots that have regenerated, f, considered in the analysed sample out of the total number, N, of roots that were cut: $f = \frac{N_{reg}}{N_{cut}}$. Standard error of proportion was calculated as $\sqrt{\frac{f(1-f)}{N}}$ (Glantz 2005). When comparing two independent regeneration frequencies, one for mock and one for exposed to electric field treatment a contingency table was used and chi-square statistical test was deployed to test association between treatment (electric field or mock) and category of roots (non-regenerated or regenerated). The null hypothesis was rejected every time $p<0.01$, so that statistically significant difference was observed. In the instances mock sample was used for multiple tests such as when comparing to aligned and anti-aligned conditions, the value for significance was corrected from $p<0.01/2$, $p<0.005$ following standard Bonferroni inequality (Glantz 2005). The regeneration ratio can be also thought of as the risk ratio and was calculates as the ratio between regeneration frequency in exposed and mock conditions, with its 95% interval (Glantz 2005).

2.2.5 Confocal imaging

Single roots were imaged throughout the regeneration process at mentioned timepoints, using recognized methods (Sena *et al.* 2009). Each root present in the images stands for at least three observed roots.

After roots were exposed to the electric field, roots with constructs *CYCB1;1::GFP, TCSn::GFP* & *pSCR::H2B:YFP* were stained with 10µg/ml propidium iodide (Sigma Aldrich, UK) to mark cell walls allowing to observe developing morphology during regeneration process. Roots expressing *R2D2* construct were not stained, because both propidium iodide and *R2D2* fluoresces red. Roots were mounted on microscope slides (VWR, UK) with sterile deionised water and imaged using Leica SP5 laser scanning confocal microscope, with 63X water immersion objective, with total magnification at 630X.

The *R2D2* reporter was imaged using an already established protocol (Liao *et al.* 2015). In addition, roots expressing *pSCR::H2B:YFP*, *TCSn::GFP* and *CYCB1;1::GFP* were imaged using SP5 confocal microscope (Leica). The imaging settings are summarised in Table 3.

Table 3: Settings used for imaging of the listed reporters using Leica SP5 confocal microscope.

Reporter	Imaged	Fluorophore 1	Excitation	Emission	Fluorophore 2	Excitation	Emission
R2D2	in sequence	Venus	514nm, Argon laser	524-570nm HyD Leica	ntdTomato	543nm HeNe laser	524-570nm HyD Leica
pSCR::H2B:YFP	in parallel	YFP	514nm, Argon laser	524-570nm HyD Leica	Propidium Iodide	514nm, Argon laser	580-630nm HyD Leica
TCSn::GFP	in parallel	GFP	488nm, Argon laser	495-550nm HyD Leica	Propidium Iodide	488nm, Argon laser	580-630nm HyD Leica
CYCB1;1::GFP	in parallel z-stacks 3µm step	GFP	488nm, Argon laser	495-550nm PMT Leica	Propidium Iodide	488nm, Argon laser	580-630nm PMT Leica

Between daily imaging observations, the roots were moved from microscope slides onto 0.8% agar solid medium (1X Murashige-Skoog basal medium (Sigma Aldrich, UK), 0.5% sucrose

(Sigma Aldrich, UK), 0.05% MES, 2-MorpholinoEthaneSulfonic acid (Sigma Aldrich, UK) adjusted to pH 5.7 with KOH (Sigma Aldrich, UK)) and kept under standard growth conditions (23°C, 16/8h light/dark with 120µmol/m^2/s intensity of light).

2.2.6 R2D2 ratiometric analysis of images

The ratio of two channels collected for each image showing results of R2D2 fluorescence was calculated using script in MATLAB (The Mathworks Inc.) (Appendix, 9.1). The script worked as following: in both channels, the background mean and standard deviation is calculated from pixel intensity of 80x80 pixel square in the bottom right corner. This background mean is subtracted from every pixel both the control (red fluorescence) image and signal (yellow fluorescence) image. The control channel (red fluorescence) was subsequently subject of thresholds, where only pixels with value higher than background mean plus 25 times the standard deviation were considered for the next step. All the pixels that did not pass thresholds were assigned minimum value. Once pixels with high enough intensity to pass threshold were identified, a natural logarithm of division of pixels in the control (red fluorescence) image by pixels in the signal (yellow) fluorescence image ($\ln \frac{ctrl_{pixel_i}}{signal_{pixel_i}}$) was calculated and these values were used to render a new image displaying the ratiometric result, colour coded to show whole range of values (Figure 17).

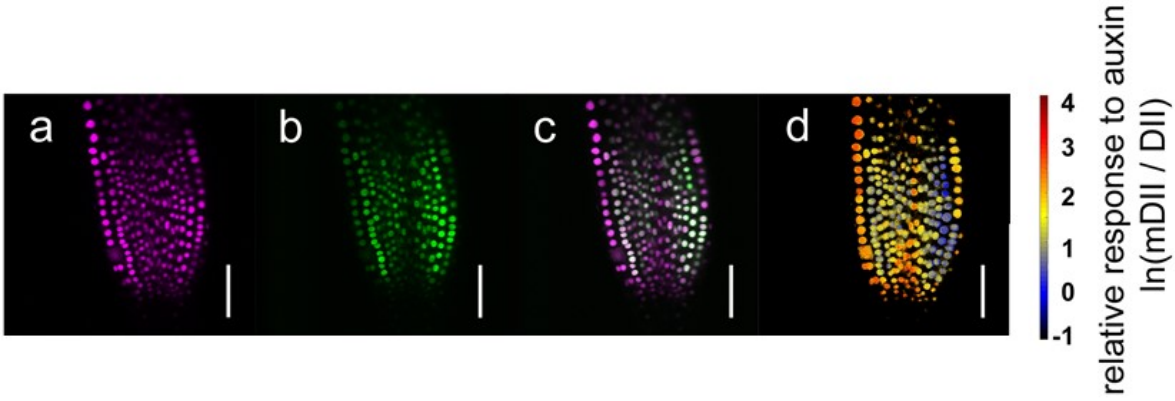

Figure 17: R2D2 two channel image collection and conversion into a ratiometric image. a) control channel fluorescence collected from *mDII::ntdTomato* which fluoresces in red spectrum. b) signal channel fluorescence collected from *DII:n3xVenus* which fluoresces in yellow spectrum. c) overlay image of the two channels. d) ratio image of the two channels, higher ratio indicates higher auxin. Values for the colours used in the ratio image are shown next to the colour bar, standing for relative response to auxin ln(mDII fluorescence/DII fluorescence). Scalebar 50µm.

2.2.7 Mitotic index calculation and statistics

Images of z-stacks of roots expressing *CYCB1,1::GFP* were analysed using FIJI (Schindelin *et al.* 2012b). The number of cells emitting green fluorescence, in the field of view, within the whole z-stack was counted while considering epidermis, cortex and endodermis only. The total number of cells was estimated by counting the number of cells seen in each tissue in median section of the z-stack and multiplying this by the stereotypical number of cells in the circumference of the tissues, 16 cells for epidermis, 8 for cortex and 8 for endodermis (Dolan *et al.* 1993). Mitotic index was calculated as the ratio between GFP fluorescing cells and total estimated number of cells ($\frac{N\ cells_{\ GFP+}}{N\ cells_{\ total}}$). The error was calculated as standard error of proportion. All biological replicates were organised in contingency tables *n x 2* with category for green fluorescing cells and non-green fluorescing cells. Analysis of residuals using chi-square test was used to identify and remove outliers, one at a time, similar to the frequency of regeneration statistics (Everitt 1992). Afterwards, the samples were combined and compared using 2x2 contigency table for treatment (electric field vs mock) and number of fluorescing cells (fluorescent cells vs non-fluorescent cells) and tested using chi-squared statistical test. Significant difference was defined for $p<0.01$.

2.3 Root Electrotropism

2.3.1 Electric field in V-box

In order to test for electrotropism, all roots were grown in a sterile box (Magenta, UK), which was adapted for growth of roots and subsequent exposure to electric field (Results I, 3.2.2). After 3 days post germination, liquid medium in the box was replaced to previously used (Stenz and Weisenseel 1993) liquid medium B (1 mM MES, 2-MorpholinoEthaneSulfonic acid (Sigma Aldrich, UK) adjusted to pH 5.7 with 1M Tris, 2-Amino-2-(hydroxymethyl)-1,3-propanediol (Sigma Aldrich, UK)), unless otherwise stated, when six different salts (Murashige and Skoog, DKW/Juglans, Hoagland's No.2, Gamborg's B-5, White's & Chu N6, all Sigma Aldrich UK) were added at stated g/L together with 1mM MES (2-MorpholinoEthaneSulfonic acid (Sigma Aldrich, UK)) and adjusted pH to 5.7 with 1M Tris (2-Amino-2-(hydroxymethyl)-1,3-propanediol (Sigma Aldrich, UK)) to make an

alternative liquid medium. An extra 2L of medium B (or other stated liquid medium) was connected to the box (Magenta, UK) with roots with tubing and 40ml/min speed pumps, tubing also passing through an LTD6/20 chiller (Grant Instruments, UK) to maintain 23°C (Results I, 3.2.2). The roots within the V-box were positioned directly in front of Raspberry Pi Camera controlled by *crontab* timer function with a custom script (Appendix, 9.2) within Raspberry Pi model B+ microcontroller (Raspberry Pi, UK) in order to be imaged (Results I, 3.2.2). The images were collected throughout the duration of the experiment, typically 2 hours unless otherwise stated, in 10 minute intervals. The electric field was applied to the roots by attaching two wires soldiered with 0.8cm x 5cm platinum/iridium foils (VWR, UK) to the PS-1302 D power supply (Voltcraft, UK) and inserting foils into the V-box (Results I, 3.2.2) and using a direct current at a constant voltage. After the exposure, roots were either discarded unless they were kept for genotyping. Boxes (Magenta, UK) with cartridges were cleaned and re-sterilised to be used again. The image data was further analysed to quantify electrotropic behaviour.

2.3.2 Electrotropic data analysis and statistics

After time lapse images of electrotropism were collected, the data was quantified using FIJI (Schindelin *et al.* 2012) calculating how many degrees the root tip turned from the start, referred to cumulative root tip deflection (Figure 18). Data from individual roots was combined to provide population distribution of cumulative root tip deflections. The population data was plotted as boxplots using R (R Core Team 2015). The normality of each distribution was tested by Shapiro-Wilk test. When distributions were considered normal, Welch t-test was applied to test the null hypothesis between two distributions such as mock vs treated with electric field or WT genotype vs mutant genotype. When the two distributions were non-normally distributed, non-parametric Mann-Whitney U test was used to determine whether two distributions at any given time point were the same. Null hypothesis was rejected with graded confidence *$p<0.05$, **$p<0.01$.

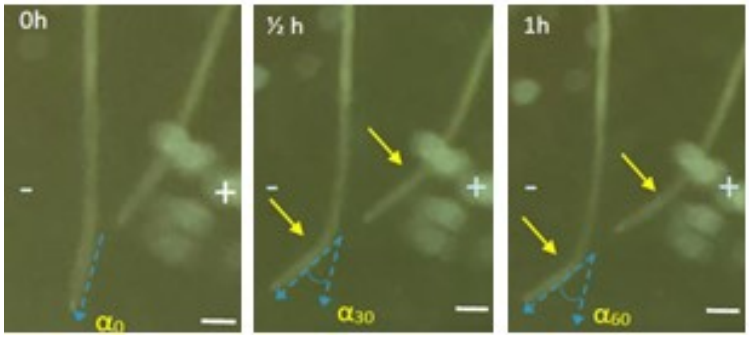

Figure 18: Measuring cumulative root tip deflection in FIJI (Schindelin *et al.* 2012).

2.3.3 Gravitropism tests

Arabidopsis roots of wildtype (Col-0) and mutants *eir1-1* and *aux1-7* as well as segregated *glr3.4-1* homozygous and segregated wildtype homozygous plants were subjected to simple gravitropic tests. Three days post-germination germination on 0.8% agar solid medium (1X Murashige-Skoog basal medium (Sigma Aldrich, UK), 0.5% sucrose (Sigma Aldrich, UK), 0.05% MES, 2-MorpholinoEthaneSulfonic acid (Sigma Aldrich, UK) adjusted to pH 5.7 with KOH (Sigma Aldrich, UK)), the plates at which seedlings were positioned were turned 90° for one day after which the plates with plants were imaged. In addition the roots with segregated *glr3.4-1* homozygous and segregated wildtype homozygous genotype were counted for gravitropism to obtain a quantitative measure of gravitropism. The gravitropic ratio was constructed as number of roots that turned in response to gravity divided by the total number of roots. Standard error of proportion was calculated as $\sqrt{\frac{f(1-f)}{N}}$ (Glantz 2005). The data from one biological repeat was then compared for two genotypes and two outcomes (*glr3.4-1* and wiltype)x(gravitropic and non-response) using *n x 2* contingency table. Chi-square statistical test was used to discard null hypothesis, which suggested that there is no difference between two genotypes in gravity response. The null hypothesis was discarded for $p<0.05$.

2.3.4 Imaging of roots after exposure to electric field in V-box

Roots expressing *RPS5A::mDII:ntdTomato-RPS5A::DII:n3Venus*, known as *R2D2* (Liao *et al.* 2015) and *PIN2::PIN2:GFP* (Abas *et al.* 2006) were exposed to electric field using V-box (Results I, 3.2.2) and electric field conditions described above in Methods, 2.3.1. After 40 minutes of exposure

to electric field or mock conditions in the V-box (Results I, 3.2.2) the roots were removed from the pods found in the cartridges of the V-box and placed on 0.8% agar solid medium (1X Murashige-Skoog basal medium (Sigma Aldrich, UK), 0.5% sucrose (Sigma Aldrich, UK), 0.05% MES, 2-MorpholinoEthaneSulfonic acid (Sigma Aldrich, UK)) adjusted to pH 5.7 with KOH (Sigma Aldrich, UK)) plates to transport and keep until the next step, with the transfer time less than 10 minutes.

Prior imaging, roots expressing *PIN2::PIN2:GFP* were stained with 10µg/ml propidium iodide (Sigma Aldrich, UK) to mark cell walls. Plantlets were mounted on glass slides (VWR, UK) with sterile deionised water and imaged using SP5 confocal microscope (Leica) with 63X water immersion objective, with total magnification at 630X. The roots expressing *PIN2::PIN2:GFP* and stained with PI had the excitation of fluorophores done at 488nm with Argon laser and emission was collected at 495-550nm using HyD (Leica) detectors for green GFP derived fluorescence and 580 -630nm for red PI derived fluorescence also collected with HyD (Leica) detectors. Roots expressing *R2D2* were unstained and mounted on the glass slides (VWR, UK) to be imaged by SP5 confocal microscope (Leica) with 63X water immersion objective, with total magnification at 630X. The *R2D2* reporter was excited with 514nm Argon laser and 543nm HeNe laser in sequence, using an already established protocol (Liao *et al.* 2015). Emission from R2D2 was collected in an emission window 524-570nm for yellow fluorescence and 580-630nm for red fluorescence using HyD (Leica) detectors. Result images were further analysed to extract data.

2.3.5 Analysis of PIN2 protein concentration in root exposed to electric field

We intended to set up a quantitative method of measurement of PIN2 proteins located on the membranes. PIN2 concentration on two sides of the root can change according to the tropic stimulus, but this effect is hard to observe measure and compare. We set up a semi-automatic analysis algorithm to calculate and combine pixel intensities at the operator chosen membranes of roots expressing *PIN2::PIN2:GFP*, to quantitatively compare an asymmetry in PIN2 concentration.

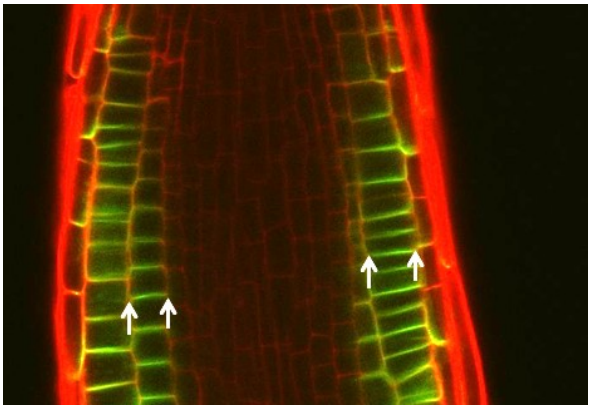

Figure 19: The start and end of each membrane in the epidermis and cortex was marked in FIJI (Schindelin *et al.* 2012) to point out start and end of visible green signal on the image.

After images were collected, the start and end of green signal in each cell in epidermis and cortex was marked in FIJI (Schindelin *et al.* 2012) to indicate the span of the membrane (Figure 19). The order of the markers describes the membrane orientation with respect to the cylindrical coordinate system found within the root and with respect to the applied electric field. The markers are also sorted into files depending on the cell file identity (epidermis or cortex). The markers provide spatial co-ordinates for MATLAB script to define boundaries of membranes for quantification analysis. A multi-step MATLAB script (Appendix, 9.3) is used to extract membranes and calculate membrane intensity. For each membrane the script initially extracts a rectangle of pixels with dimensions *L x 17*, where 17 pixels was chosen arbitrarily as it was guessed to be the best compromise to ensure all pixels potentially beloning to the same membrane included, while excluding neighbour membrane pixels and L is the length between two markers. Since the two markers are not at the same position on the perpendicular axis along the 17 pixel units, linear interpolation was performed using **interp2** function to reorient the membrane and determine intensity of the pixels who's coordinates were a fraction in the original image. After rectangle reorientation, the membrane with PIN2:GFP signal is identified and pixel intensity quantified. We used a hard cut-off of ±4 pixels so only 9 pixels including the central intensity pixel are included in the intensity calculation. The central intensity pixel is determined with a centre-of-mass algorithm described with the equation below and its action shown in Figure 20.

$$\forall x_j (1 \leq j \leq L): y_j^{CM} = \frac{\sum_{i=1}^{17} y_i \cdot I(x_j, y_i)}{\sum I(x_j, y_i)}$$

For each position X_j along the membrane, the algorithm estimates the centre of mass of the intensities *I* in the Y direction (y^{CM}). Afterwards an average of membrane intensity was calculated from the centre of mass values with ±4 pixels from each X_j point. The distribution of average membrane intensities was then plotted as a boxplot and identified to be a normal or non-normal distribution using Shapiro-Wilk test. The distributions of individual categories (root side facing positive electrode vs root side facing negative electrode vs mock not in electric field) were compared using Wilcoxon paired signed rank test, with null hypothesis rejected at p-value<0.05.

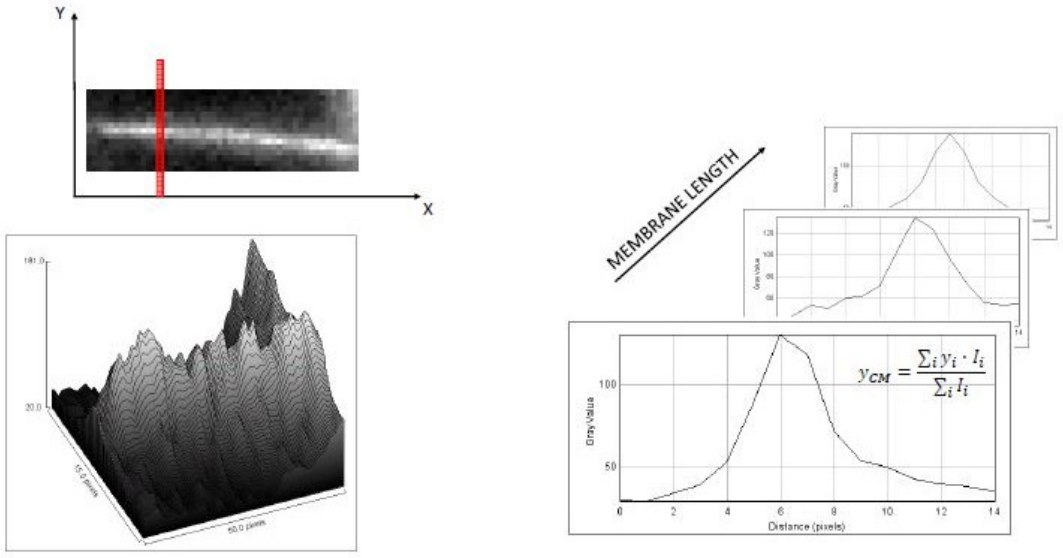

Figure 20: The position of the membrane is determined by moving along is length L, and estimating at each pixel position in X, the centre of mass of pixel intensity in Y.

2.3.6 Analysis of auxin concentration in root subjected to electric field

The conversion of raw images collected after imaging *R2D2* expressing roots into ratiometric images, which directly show auxin concentration has been done in the same way as already described in Methods, 2.2.6. In addition, the ratio of the pixel intensity control signal (mDII:ntdTomato) and pixel intensity auxin responsive signal (DII:nx3Venus) was calculated by manual segmentation of the epidermal and cortex nuclei using FIJI (Schindelin *et al.* 2012). The nuclei were selected in the control signal image and the average pixel intensity for that region of

interest (ROI) was extracted and the same ROI was then used on the auxin responsive signal image to extract pixel intensity.

The values from both control image and auxin responsive signal image were used to calculate $Ratio_{nucleus} = \frac{<x>_{control}}{<y>_{auxin\ responsive}}$, with <x> = average pixel intensity in ROI of control image and <y> = average pixel intensity in ROI of auxin responsive signal image, to obtain a value (Ratio) for each nucleus. The ratio values of individual cells were grouped into distributions depending on the side of the meristem the cells were found with respect to the position of the electric field. The three distributions established were “mock”, “facing negative electrode”, “facing positive electrode”. The average of each distribution with standard error of the mean was plotted using bar plots. The distributions were tested for normality using Shapiro-Wilk test. The null hypothesis, that the three distributions are the same was tested using Welch t-test, rejecting null hypothesis at p-value<0.05.

2.3.7 Imaging roots exposed to electric field in V-slide

Roots expressing *pUBQ10::WAVE131:YFP* (Geldner *et al.* 2009) and *pUBQ10::YC3.6:NES* (Krebs *et al.* 2012) were exposed to electric field using V-slide (Results I, 3.2.3) to monitor the effects of the electric field live using time-lapse microscopy with high temporal resolution. To mount roots onto V-slide, a small amount of medium B (1 mM MES, 2-MorpholinoEthaneSulfonic acid (Sigma Aldrich, UK) adjusted to pH 5.7 with 1M Tris, 2-Amino-2-(hydroxymethyl)-1,3-propanediol (Sigma Aldrich, UK)) was added onto the slide on which the roots were positioned and then kept in place using the weight associated with V-slide (Results I, 3.2.3). Afterwards the slide was mounted to be imaged with Leica SP5 laser scanning confocal microscope, with 63X water immersion objective, with total magnification at 630X or it was mounted to be imaged with Zeiss Axio Observer inverted wide-field microscope, with 20X air objective, with total magnification at 200X. Tubings were connected to the V-slide to allow perfusion using a peristaltic pump (Adafruit, UK) while the set-up was filled with medium B (Results I, 3.2.3). Platinum electrodes within the V-slide were connected to the PS-1302 D

power supply (Voltcraft, UK). The electric field was applied during the whole imaging session. The roots expressing *pUBQ10::WAVE131:YFP* were imaged solely using confocal microscope (Leica) and had the fluorophore excited with 514nm Argon laser and the emission collected with PMT detector (Leica) at 524-570nm. The imaging duration was 60 minutes with images taken at 2 minute intervals.

Post-imaging, time-lapse video was constructed using FIJI (Schindelin *et al.* 2012) for qualitative analysis. The roots expressing *pUBQ10::YC3.6:NES* were imaged using both confocal (Leica) and inverted light wide field (Zeiss) microscope for time-lapse FRET. When in confocal microscope set up the only the Cyan fluorophore of the YC3.6 protein was excited with 458nm Argon laser, and emission was collected with PMT detector (Leica) in two emission windows simultaneously, 465-495nm for the Cyan fluorophore and 520-570nm for the Yellow fluorophore. The imaging duration was 60 minutes with images taken at 2 minute intervals. The resulting images were post-processed in FIJI (Schindelin *et al.* 2012) to show ratiometrically the FRET reporting and resulting Ca^{2+} levels.

When using inverted light wide field microscope (Zeiss), the Cyan fluorophore of the YC3.6 protein was excited and the emitted wavelength filtered with LED lightsource, Lumencor Spectra X light engine (Lumencor, UK) with CFP filter cube with dichroic mirror with excitation 440/20nm and emission 483/32nm. The fluorescence from Yellow fluorophore of the YC3.6 protein was excited and the emitted wavelength filtered with LED lightsource, Lumencor Spectra X light engine (Lumencor, UK) with FRET filter cube with dichroic mirror with excitation 440/20nm and emission 542/27nm. The images were collected for duration of 30 minutes with 10 second time intervals between each image. After image collection images were further processed with MATLAB script to make ratiometric FRET images.

2.3.8 pUBQ10::YC3.6:NES ratiometric analysis of images

The two images with pixel intensity from cyan fluorophore and from yellow fluorophore when excited with cyan filter from roots expressing *pUBQ10::YC3.6:NES* construct, were divided by

each other using MATLAB script (Appendix, 9.4) to generate ratiometric FRET image. The script calculated in both images, the background mean and standard deviation from pixel intensity of 80x80 pixel square in the bottom right corner. These background means were subtracted from every pixel both the cyan fluorescence image (CFP portion of YC3.6) and FRET, the yellow fluorescence triggered by cyan excitation (YFP portion of YC3.6) image. The channel image with cyan fluorescence pixel intensity was subsequently subject of thresholds, where only pixels with value higher than background mean plus 25 times the standard deviation were considered for the next step. All the pixels that did not pass threshold were assigned minimum value. Once pixels with high enough intensity to pass threshold were identified, a natural logarithm of division of pixels in the FRET image by pixels in the cyan fluorescence image ($\ln \frac{FRET_{pixel_i}}{CFP_{pixel_i}}$) was calculated and these values were used to render a new image displaying the ratiometric result, colour coded to show increase and decrease of Calcium Ca^{2+} concentration in different parts of the root tip (Figure 21).

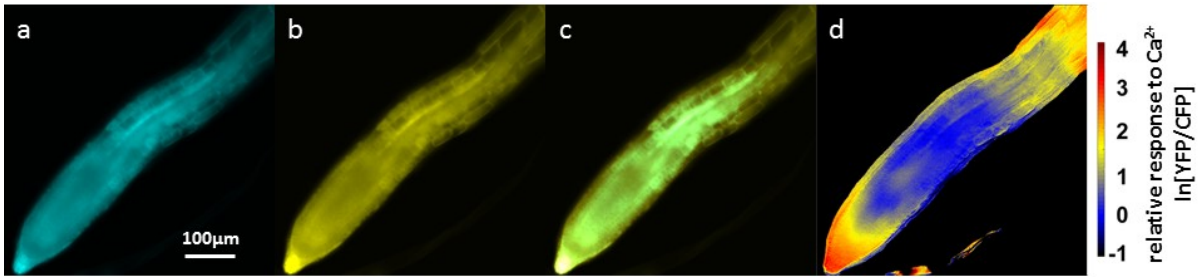

Figure 21: Two channel image collection and conversion into a ratiometric image of roots expressing YC3.6:NES Ca^{2+} FRET reporter protein. a) fluorescence collected from CFP portion of YC3.6:NES which fluoresces in cyan spectrum. b) fluorescence collected from YFP portion when excited with cyan excitation (440/20nm) of YC3.6:NES which fluoresces in yellow spectrum. c) overlay image of the two channels. d) ratio image of the two channels, higher ratio (shown by warmer colours) indicates higher Ca^{2+} presence. Values for the colours used in the ratio image are shown next to the colorbar, standing for relative response of YC3.6:NES to Ca^{2+} ln(FRET YFP/CFP). Scalebar 100µm.

2.3.9 DNA extraction and Genotyping

To further confirm that homozygous *glr3.4-1* allele (Stephens *et al.* 2008) presence in the *Arabidopsis* genome decreases the electrotropic behaviour of the root, we have genotyped plant material assumed to be homozygous wild type, heterozygous wild type and *glr3.4-1* mutant and homozygous for *glr3.4-1* allele all from Arabidopsis line segregating for *glr3.4-1*. We have obtained seeds heterozygous for *glr3.4-1* allele from Nottingham Arabidopsis Stock Centre (NASC, UK) with number N579842. The plants were grown to full maturity in soil at standard growing conditions (120

µmol/m^2/s on a 16h/8h light/dark cycle), 3 weeks into the growth process a small portion of the leaf material was used for DNA extraction and genotyping of heterozygous presence of *glr3.4-1* gene. Afterwards seeds were collected from the heterozygous parents, germinated and grown in the Magenta box (Results I, 3.2.2) and after 3 days post germination subjected to electric field using V-box set-up (Methods, 2.3.1).

Afterwards the plants were recovered from V-boxes and kept vertically for 7 days on 0.8% agar solid medium (1X Murashige-Skoog basal medium (Sigma Aldrich, UK), 0.5% sucrose (Sigma Aldrich, UK), 0.05% MES, 2-MorpholinoEthaneSulfonic acid (Sigma Aldrich, UK)) after 7 days the DNA was extracted. In addition DNA was also extracted from 7 day old seedlings of *Arabidopsis* expressing *pGLR3.4::GLR3.4:GFP* in the homozygous *glr3.4-1* background. The DNA extraction was done using PureLink Plant (Life Technologies, UK) Total DNA extraction kit following the protocol in the kit. Afterwards the DNA was quantified using NanoDrop ND-1000 spectrophotometer (ThermoFisher, UK).

Table 4: Primers used to genotype the presence of wild type *glr3.4* allele or mutated *glr3.4-1* allele.

Primer name	Primer sequence
LP GLR3.4	GGGTTAATCCGGCTTATGAAG
RP GLR3.4	GAAGTGAGACTGGCCGTGTAG
LBb1.3	ATTTTGCCGATTTCGGAAC

Genotypes of the plants in question were tested with a PCR using the extracted DNA, designed primers for the *glr3.4* (AT1G05200) gene as well as T-DNA detecting LBb1.3 primer using Signal SALK Primer Design tool (SALK, USA) and sourced from Life Technologies, UK (Table 4) and RedTaq 2X master mix (Sigma, UK). The PCR reaction was set up following standard PCR protocol, diluting individual components in a reaction to the desired concentration (0.5µM primer A, 0.5µM primer B, 1-10ng DNA template, 1X Redtaq master mix (Sigma, UK), volume matched to 20µl with

PCR grade ddH_2O) and running 35 cycle reaction (95°C for 30s, 53°C for 30s, 72°C for 75s with final extension 72°C for 10 minutes) using Veriti 96 Well Thermal Cycler (Applied Biosystems, UK).

After the PCR reaction, the sizes of the PCR products were assessed with gel electrophoresis. 1% Agarose (Sigma, UK) was used to make gel out of 1X TAE buffer (Sigma, UK) with 1X SybrSAFE (Life Technologies, UK) DNA dye added in. The gel was placed into the gel tank (Bio-Rad, UK) and flooded with 1X TAE buffer (Sigma, UK), the wells within the gel were loaded with the PCR product as well as 1kb plus DNA ladder (ThermoFisher, UK). The gel tank was supplied 90V for 50 minutes from PowerPac Basic power supply (Bio-Rad, UK). Afterwards the gel was imaged to observe size separation of PCR products and obtain an image of the gel using BioDoc-It Imaging system, UltraViolet Transilluminator (UVP, UK).

2.3.10 Imaging of roots expressing glr3.4 rescue gene

Roots expressing *pGLR3.4::GLR3.4:GFP* in the homozygous *glr3.4-1* background (Vincill *et al.* 2013) were grown using standard protocol on 0.8% solid medium plates (Methods, 2.1.2) for 7 days post germination. Afterwards the roots were stained with 10µg/ml propidium iodide (Sigma Aldrich, UK) for three minutes to mark cell walls and then briefly de-stained in ddH_2O. Roots were mounted on microscope slides (VWR, UK) with sterile deionised water and imaged using Leica SP5 laser scanning confocal microscope with resonant scanner for fast imaging using 63X objective with total magnification 630X. The excitation of the fluorophore was done at 488nm with Argon laser and emission was collected at 495-550nm for green fluorophore (GLR3.4:GFP) and 580-630nm for red fluorophore (PI) using PMT (Leica) detectors simultaneously. The images were qualitatively analysed in FIJI (Schindelin *et al.* 2012).

2.4 Root Bioelectricity

2.4.1 Imaging of roots when stained with voltage-sensitive dyes

Roots of Col-0 wild type as well as roots expressing *pUBQ10::WAVE131:YFP* (Geldner *et al.* 2009) were grown for three days post germination on 0.8% agar solid plates using described

protocol (Methods, 2.1.2). Afterwards the roots were either bathed in MS light buffer (1/4X Murashige-Skoog basal medium (Sigma Aldrich, UK), 0.05% MES, 2-MorpholinoEthaneSulfonic acid (Sigma Aldrich, UK) adjusted to pH 5.7 with 1M Tris (Sigma Aldrich, UK)) or in MS light buffer with depolarising agent added either 100mM KCl potassium chloride (Sigma Aldrich, UK) or 100mM $C_6H_{11}KO_7$ potassium gluconate (Sigma Aldrich, UK) for the stated length of time. Voltage sensitive dye 9.7µM DiBAC4(3) (Thermo Fischer, UK) or 1µM Rhodamine6G (Sigma Aldrich, UK) or 100nM SS44-DC, gift of Akita Innovations (Billerica MA, USA), was added into the buffer for the stated length of time (Preliminary Results IV, 6.2.1).

The roots were mounted on the microscope slides (VWR, UK) in the MS light buffer with or without depolarising salts, with the dye present in the solution and imaged Leica SP5 laser scanning confocal microscope, with 63X water immersion objective, with total magnification at 630X. Roots stained with DiBAC4(3) were illuminated with 488nm Argon laser using an already established protocol (Konrad and Hedrich 2008). Emission from DiBAC4(3) was collected in an emission window 500-550nm using HyD (Leica) detectors. Roots stained with Rhodamine6G were illuminated with 514nm Argon laser, emission from Rhodamine6G was collected in an emission window 524-570nm using HyD (Leica) detectors. Roots stained with SS44 were illuminated with 633nm HeNe laser and the reporter protein WAVE131:YFP was excited using 514nm Argon laser simultaneously, emission from SS44 was collected in an emission window 640-700nm for red fluorescence and emission from WAVE131:YFP was collected in a 524-570nm emission window using HyD (Leica) detectors. After image collection, images were qualitatively analysed using FIJI (Schindelin *et al.* 2012).

2.4.2 Root electric field exposure, data collection, data analysis and statistics

Col-0 wild type roots were grown in a sterile box (Magenta, UK), which was adapted for growth of roots and subsequent exposure to electric field (Results I, 3.2.2). After 3 days post germination depolarising buffer 100mM KCl, potassium chloride, was added into the liquid growth medium (1/4X Murashige-Skoog basal medium (Sigma Aldrich, UK), 0.5% sucrose (Sigma Aldrich, UK), 0.05% MES, 2-MorpholinoEthaneSulfonic acid (Sigma Aldrich, UK) adjusted to pH 5.7 with KOH

(Sigma Aldrich, UK)) for one hour. After the depolarisation treatment, the liquid medium in the box was replaced with the previously used (Stenz and Weisenseel 1993) liquid medium B (1 mM MES, 2-MorpholinoEthaneSulfonic acid (Sigma Aldrich, UK) adjusted to pH 5.7 with 1M Tris, 2-Amino-2-(hydroxymethyl)-1,3-propanediol (Sigma Aldrich, UK) and the roots were exposed to electric field using V-box set up just like described in Methods, 2.3.1. After data collection the quantitative data was extracted from the images and tested for statistical significance using the same procedure as already described in Methods, 2.3.2.

3 Results I: New tools for *Arabidopsis* root exposure to electric field

3.1 Background

3.1.1 Assays for exposure of roots to the electric field

Exposure of plant roots to electric field under laboratory conditions is not a very common assay. This fact presented us with both obstacles, since no standardised procedure was there to follow, but also opportunity that allowed us to build and tune the working set-ups exactly to our experimental needs.

There are a small number of reports showing effects of external electric field on the roots of *Mays*, *Arabidopsis* and other plant species (FONDREN and MOORE 1987), (Moore *et al.* 1987), (Ishikawa and Evans 1990), (Stenz and Weisenseel 1993), (Wolverton *et al.* 2000), (Wawrecki and Zagórska-Marek 2007). Some of the previous reports showed root tip in external electric field turning towards cathode while others show root tip turning towards anode (Moore *et al.* 1987), (Stenz and Weisenseel 1993). These contradictory results can be attributed to a lack of standardised laboratory set-ups, which were used to expose roots to an electric field. An ideal electric exposure tool takes into account the toxic by-products that form within the medium at the electrodes, and dilute or remove these. It also prevents chemical gradients from forming by electrophoresis, such as pH gradients that should be dispersed to maintain medium homogeneity (Stenz and Weisenseel 1993). In addition, the temperature of the medium within the exposure vessel should stay constant.

Table 5: Table of wanted conditions from the novel tools.

Desired specifications of electric field exposure tool
Dilution of toxic by-products
Prevention of chemical gradients
Keeping constant temperature
Timelapse imaging (optional)

Some of the previously used set-ups for electric field exposure did not contain any perfusion element and medium storage allowing for the build-up of harmful chemicals and pH gradients (Moore *et al.* 1987), (Wawrecki and Zagórska-Marek 2007). Other set-ups may have stirring or other mechanism for dispersal of harmful chemicals (Stenz and Weisenseel 1993), but none have validated the homogeneity of the medium and the stability of the temperature of the medium used for electric field exposure to show that the results observed are due to the electric field and not an artefact of the setup used to expose the roots to the electric field.

In addition to the un-validated electric field exposure set ups, previous experimental assays did not allow for time-lapse observation. Thanks to advances in micro-computers and cameras, as well as conventional time-lapse microscopy, we can use imaging to describe the physiological and molecular phenomena that are associated with root tip exposure to electric field. To achieve this, the observational tool, such as macro camera or an inverted fluorescence microscope, has to be accounted for in the overall design of the electric field exposure set-up, to allow all of the above mentioned requirements to be met and consolidated with the type of data that will be collected.

We aim to expose regenerating and growing roots to an electric field in order to observe the biological response. We measure root regeneration competence as the proportion of regenerated roots within a large population of cut roots, therefore to observe electric field effects on root regeneration competence, we need to be able to expose large numbers of regenerating roots to electric field. On the other hand, electric field-induced curvature of the growing root is best observed on individual roots, therefore a set-up that allows macro and micro imaging during exposure to an electric field is required to study this. To this end we developed three unique tools that allow the characterisation of regenerating and growing roots in presence of a weak external electric field.

3.1.2 Aims

- To develop V-tank, a tool that allows for a population of regenerating roots to be exposed to an electric field.

  V-tank must allow the exposure of regenerating roots, not the whole plants, to a short term (minutes) electric field, while maintaining homogeneity of the medium and a constant temperature. It is also necessary that the roots maintain sterility, since the regeneration competence is scored five days after the cutting tool is used, which is a long enough time for contamination to develop if the system is not sterile.

- To develop V-box, a tool that allows for macro time-lapse imaging of individual *Arabidopsis* roots more than one at a time, while exposed to an electric field.

  The V-box set-up must allow the exposure of roots, but not the whole plants to the electric field. It must maintain homogeneity of the medium and a constant temperature. In addition it has to be built such that continuous imaging of the roots is possible. The V-box also needs to be autoclavable and re-usable, so that it is possible to maintain sterility while staying inexpensive.

- To develop V-slide, a tool that allows for micro time-lapse imaging of single *Arabidopsis* roots while exposed to an electric field.

  The set-up must allow the exposure of roots, but not the whole plants to the electric field. It must maintain homogeneity of the medium and a constant temperature. It also has to allow for mounting on a microscope, so that continuous imaging of the roots is possible. This will allow us to leverage the many fluorescent reporters that are present in *Arabidopsis* and observe molecular dynamics when root is exposed to an electric field. The set-up does not have to be sterile, but it should be re-usable in order to be inexpensive.

3.2 Results

3.2.1 V-tank

To be able to observe the effect of an electric field on root regeneration competence, we needed to expose a large number of roots to the electric field to obtain population data. We used a tank commonly used for DNA electrophoresis, and converted it for exposure of plants to an electric field. For the V-tank to be fully functional, a number of technical objectives had to be met.

Technical objective 1

To minimise the difference between the growth medium and the exposure medium to ensure only roots are only exposed to an electric field.

Solution 1

We used a solid medium with MS salts and agar for support of the plants that was overlaid with a second liquid medium to provide electrical conductivity. To keep hypocotyl and leaves out of the liquid medium, 'pillows' made of solid medium were set up for shoot support (Figure 22A).

Technical objective 2

To maintain medium homogeneity in the presence of an electric field by preventing build-up of ions at electrodes as well as build-up of ion gradients within the medium. In addition the temperature of the conducting medium was also to be kept constant.

Solution 2

We used cooled perfusion, to constantly replace the medium from one electrode and move it to the second electrode at the other end of the set-up. We drilled holes into the lid of the tank to allow for the access of tubing, and then used peristaltic pump to move liquid constantly setting up a flow of the medium within the tank. The tubing was passed through a cooling device in order to cool the medium, which was then entering the customised electrophoresis tank, maintaining the temperature (Figure 22C). We have measured the temperature and the pH of the medium within the

tank to validate that our set-up buffers the unwanted effects of electric field in the medium. We set the cooling of the perfusion such that the temperature of the medium was maintained at 23°C (Table 6). We also measured the pH within the tank at the two electrodes after running the V-tank for 30 minutes and found that the change in the pH at the electrodes was still within the ideal range for *Arabidopsis* growth (Table 7).

The V-tank maintains homogeneity and temperature of the medium when an electric field in the range 0-5V/cm is applied for 30 minutes. The current measured when using 4.3g/L 1X liquid MS as a conducting liquid and an applied electric field of 2.5 V/cm was 100-150mA. The tank allows for up to 80 plants to be present at any one time, with a gel 'pillow' making sure that only the roots are submerged in the conducting liquid (Figure 22D).

Table 6: Temperature of the liquid medium measured in the V-tank after 30 minutes of 2.5V/cm electric field, 150mA current in 1X liquid MS medium. Two set-ups tested: without pump and cooling, with pump and cooling.

	Initial temperature	**Room temperature**	**Temperature after 30 minutes of V-tank operation**
Without perfusion	23°C	23°C	25°C
With cooled perfusion	23°C	23°C	23°C

Table 7: Acidity of the liquid medium was measured in the V-tank after 30 minutes of mock electric field or after 30 minutes of 2.5V/cm electric field, 150mA current in 1X liquid MS medium.

Position	**pH of 1X liquid MS medium**
No electric field, V-tank	5.7±0.05
Electric field, positive electrode	5.81±0.07
Electric field, negative electrode	5.57±0.08

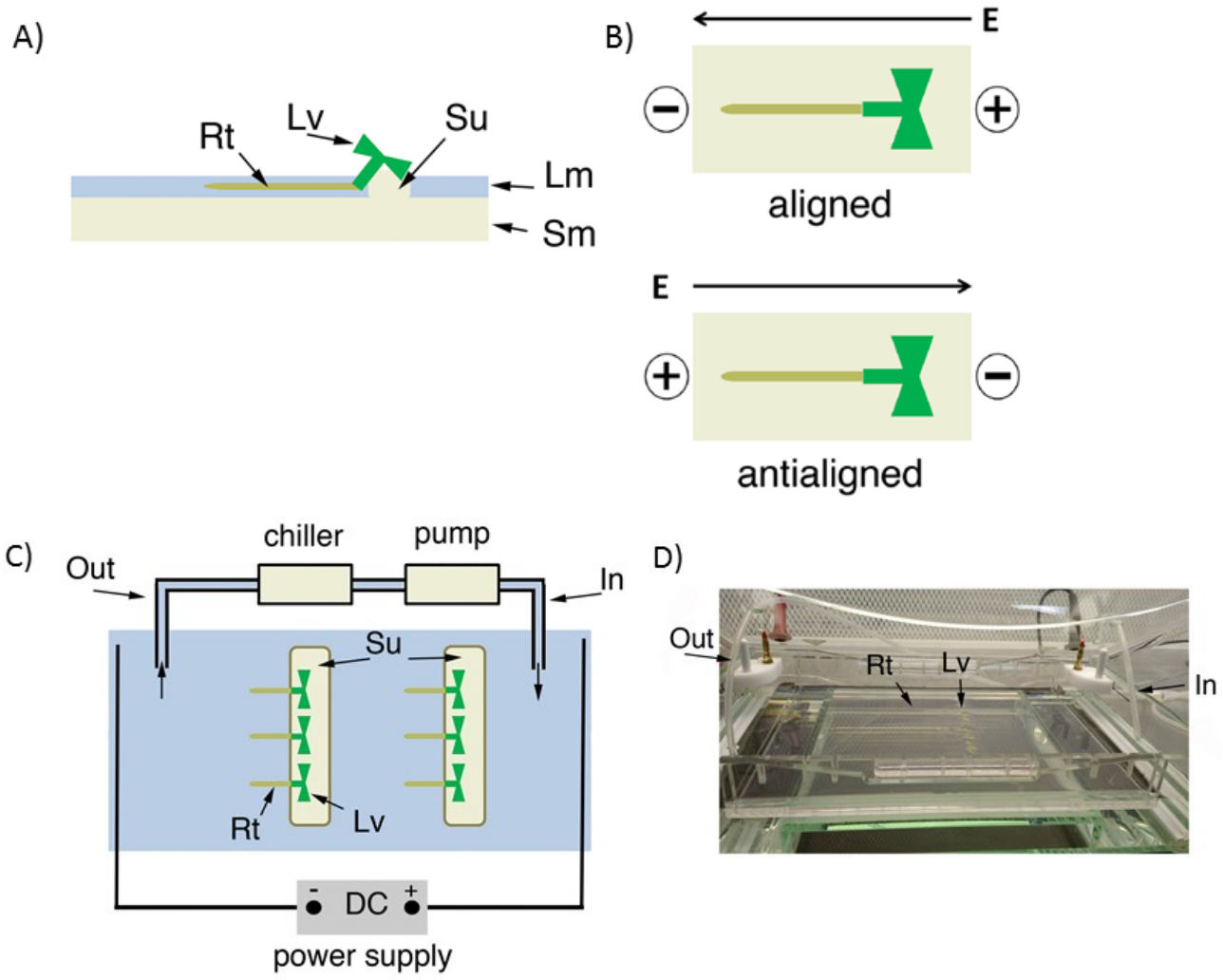

Figure 22: V-tank for electric exposure of population of roots. A) Agar gel and agar gel pillow as well as position of plant. Rt – root, Lv – Leaves, Su – Support, Lm – Liquid media, Sm- Solid media. B) Two orientations of electric field to which the roots can be subjected to in V-tank. C) Schema of the V-tank system. Direct Current power supply, peristaltic pump and chiller for cooled perfusion, solid media support with gel pillows where hypocotyl is placed, covered in liquid medium. D) Image of the V-tank with plants inside. Taken from (Kral *et al.* 2016), distributed under CC BY 4.0 open access license.

3.2.2 V-box

In order to monitor root electrotropism, we needed to image individual roots while exposed to an electric field. We decided to construct a completely novel tool, the V-box, and had to overcome a number of obstacles during its development.

Technical objective 1

To expose roots to a planar electric field in a compartment that allows for live imaging.

Solution 1

We chose transparent tissue culture Magenta™ boxes. These are autoclavable boxes that allow for air exchange while maintaining sterility due to the unique design of the lid.

Technical objective 2

To avoid damaging roots as well as avoiding contamination, roots should be grown, exposed to the electric field and imaged in the same tissue culture Magenta™ box. To this end we needed to develop a device that allows plant growth, root exposure to electric field and is transparent. The device also needed to be autoclavable and re-usable to maintain sterility and remain inexpensive.

Solution 2

We built a 'cartridge', a module to hold plants during imaging. This can be easily slotted into the Magenta™ box and satisfies all of the above requirements (Figure 23B). It is made of autoclavable nylon-6 plastic that is black, and serves well as a background for imaging of small almost transparent roots and glass that serves as a transparent wall at the front of the cartridge (Figure 23A). In addition, the cartridge at the top has modified PCR tubes that can also be autoclaved. In addition, these serve as pods for solid medium MS agar gel that allow for germination and growth of the seedlings. The roots naturally grow down through the gel into the medium liquid that is present in the *Magenta* box below the pods.

Technical objective 3

To expose roots to an electric field, while maintaining the medium homogeneity as well as temperature for at least two hours.

Solution 3

We used an external reservoir of medium as well as two peristaltic pumps and a cooler that can decrease the temperature of the medium passed by the pumps in silicone tubes. The tubes

connected the medium reservoir to the Magenta™ box and pumps continuously replaced the medium present in the box (Figure 24C), while a cooler maintained a constant temperature of the moving medium. After running the V-box with medium B for 2 hours at 1V/cm and 150µA current, we have observed very small change of pH at the two electrodes (Table 8). The temperature was also measured at 10 minute intervals during the two hours (Figure 26). The temperature was maintained at 23±0.5°C. In addition, the electric field was generated by two platinum electrodes positioned on the side of the cartridge (Figure 25B) and connected to the power supply with wires.

Technical objective 4

To maintain an electric field in the V-box for at least two hours. To avoid medium spilling and maintain a constant volume of medium in the Magenta™ box while keeping a constant exchange of the medium.

Solution 4

We used an external reservoir of fresh medium and adjusted the flow speed of the medium from the reservoir into the Magenta™ box such that the flow into the Magenta™ box is lower than flow of the medium out of the box. Thanks to longer tubing that passed through the chiller before it feeds liquid into the Magenta™ box, the liquid in the tubing supplying the Magenta™ box moves slower than the liquid in the tubing that removes the liquid from the box back into the reservoir. We positioned the tube that removes medium out of the Magenta™ box at the surface of liquid volume within the box, such that medium is removed out of the box only when enough of the medium is fed into the box with the inflow tube, otherwise the outflow tube removes air. This solution maintains the volume constant, while continuously exchanging medium (Figure 24B).

Technical objective 5

To perform time-lapse imaging of the effect of the electric field on the *Arabidopsis* root tips, we needed automatic control of the image acquisition. In addition, the roots that need to be imaged

are at most 1-2cm long and only 100µm across. This means that a specific camera for macro object imaging is needed.

Solution 5

Using micro-computer Raspberry Pi Model B+, we were able to control the timing of the repeated collection of the images (Figure 25C). For the camera itself, we were presented with an obstacle. One option we could use were web-cameras with a macro lens that could be controlled by Raspberry Pi micro-computer, but they were costly and not very easy to implement for the time-lapse image collection. Another option was to use Raspberry Pi's own camera Module. This is an inexpensive web-camera that is easy to set-up for time-lapse imaging with Raspberry Pi computer, but it is not suitable for macro images. We hacked the camera by unscrewing the lens, making the focal length between the lens and the detector longer. This allowed us to place light from smaller surface area onto a larger surface area of the detector resulting in a cheap and simple way to make 'macro' lens for imaging of small objects such as *Arabidopsis* root tip.

By fulfilling all of the technical objectives, we have constructed the V-box, a tool that allows us to grow roots and expose them to a weak external electric field, while maintaining all other variables resulting from electric field presence unchanged. In addition the V-box set-up has been built in such a way that allows for automatic continuous image collection of the *Arabidopsis* root tips.

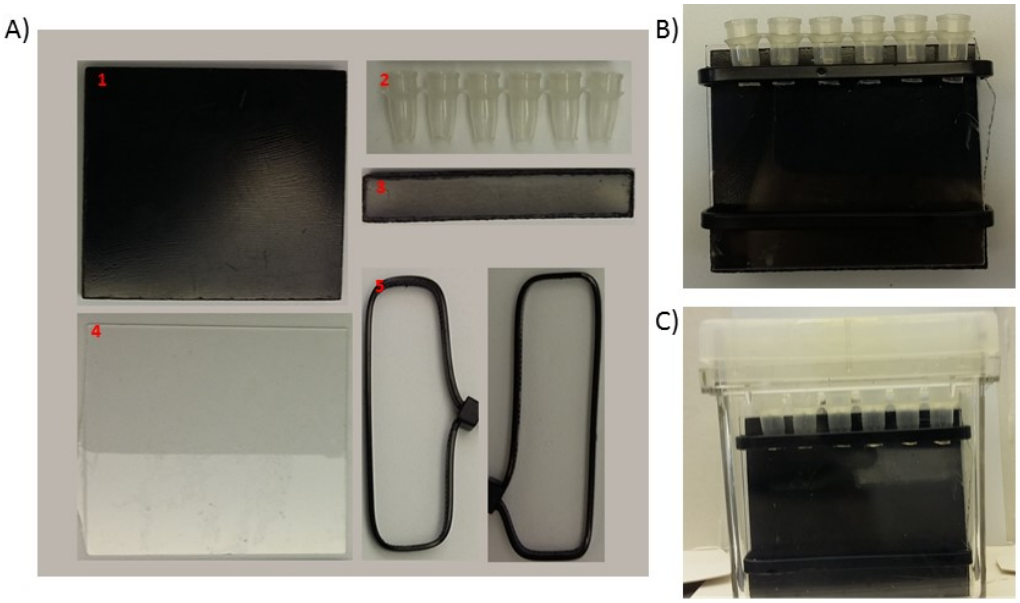

Figure 23: Components of the box that was used to grow and expose *Arabidopsis* roots to electric field. Part of the V-box set-up which allowed for the individual root macro observation. A) Components of the 'cartridge', a tool which allowed for growth for roots as well as easy slotting into a clear autoclavable Magenta™ box. 1) background - black nylon-6 rectangle 2) modified PCR tubes with no bottom 3) bottom cartridge support – black nylon-6 rectangle 4) front – clear glass rectangle 5) attachment belts – nylon-6 bands. B) constructed 'cartridge' C) cartridge within box.

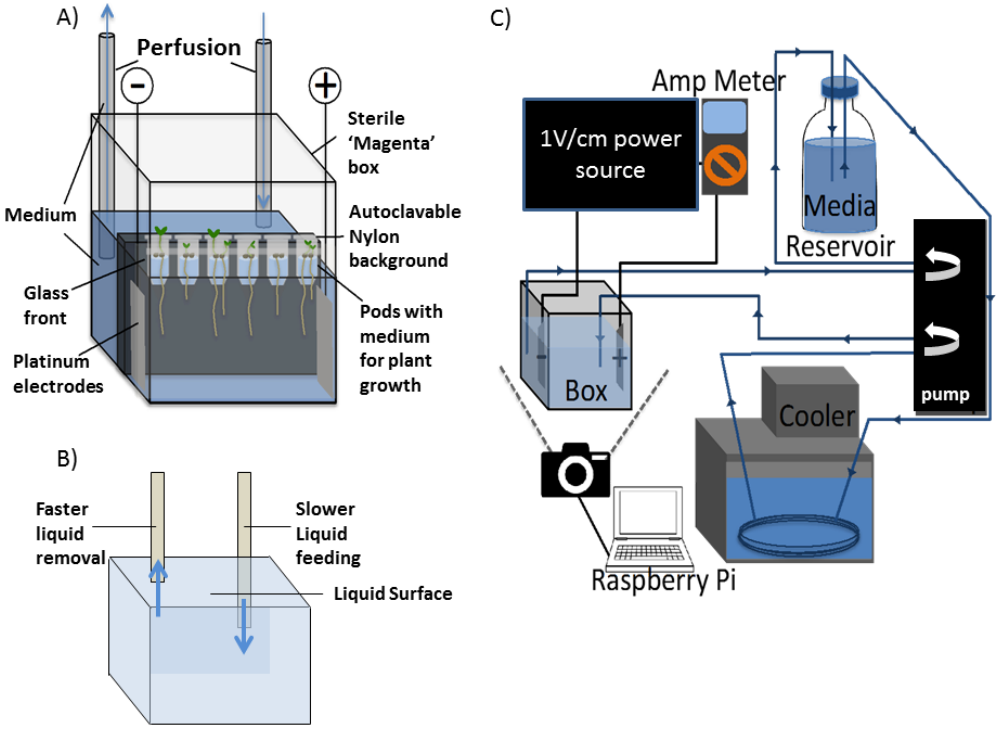

Figure 24: Schema of the V-box set-up that allows for exposure of *Arabidopsis* roots to electric field in perpendicular direction. A) Magenta™ box, with 'cartridge' containing roots submerged in liquid medium. Perfusion of the medium from and to the box is achieved with tubes connected to peristaltic pumps. Electric field is supplied by electrodes connected to DC power supply. B) Position of the perfusion tubes within the box. C) Schematic of the overall V-box set-up.

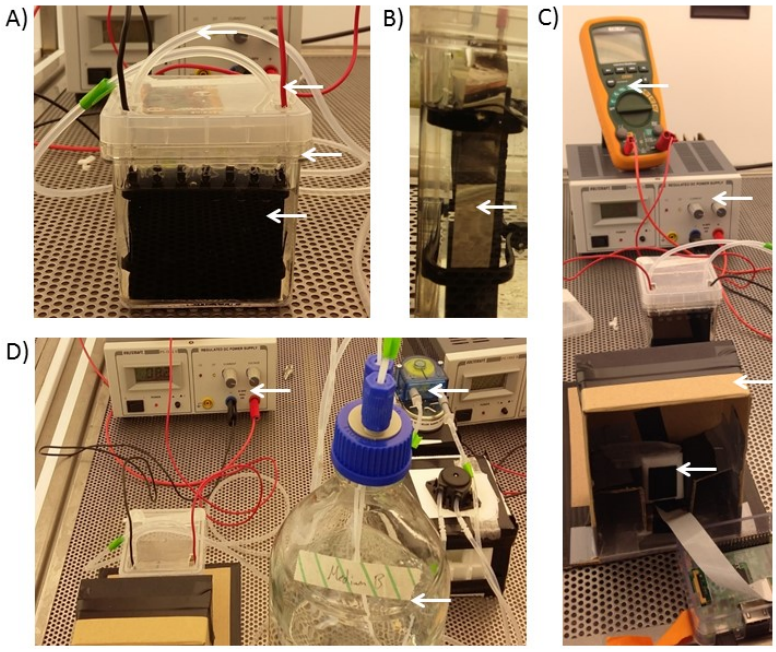

Figure 25: Images showing the V-box set-up. A) Magenta™ box, with cartridge and plants inside attached with tubes and electrodes. B) side image of a platinum electrode C) Imaging set-up using Raspberry Pi microcomputer and Raspberry Pi camera for image collection. Cardboard box is present for shading and Magenta™ box is in front of the camera. Current meter and power supply is also visible. D) Medium reservoir and peristaltic pumps are shown, which are attached to the Magenta™ box with tubes. DC power supply attached with cables to electrodes within the box is also on the image.

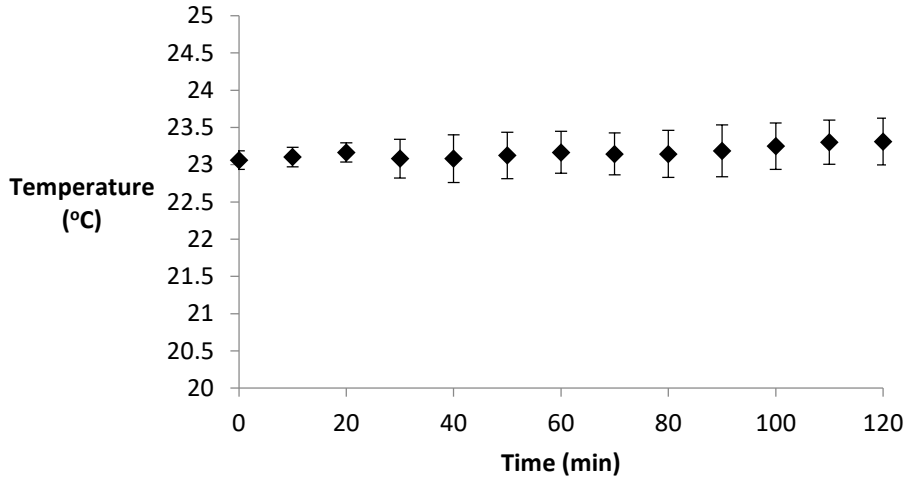

Figure 26: Temperature measured within V-box in 10 minute intervals when 1V/cm electric field with 150 µA was passed through for 2 hours in liquid medium B. The temperature was measured independently 3 times with data shown as average ± standard deviation.

Table 8: Acidity of the liquid medium was measured in the V-box after 2 hours of mock electric field or after 2 hours of 1V/cm electric field, 150µA current in medium B.

Position	pH of medium B
No electric field, V-box	5.7±0.06
Electric field, positive electrode	5.73±0.07
Electric field, negative electrode	5.68±0.06

3.2.3 V-slide

To image at cellular resolution fluorescent reporters that report the presence of different molecular components that may be influenced by the weak external electric field in the root tip of *Arabidopsis*, we needed a tool that allowed for the roots to be exposed to an external electric field and imaged using time-lapse confocal or wide-field microscopy. To achieve a constant temperature and consistency of the medium as well as exposure of roots to an electric field on a slide that can be mounted on a microscope, we constructed the V-slide.

Technical objective 1

To use high magnification lens on a confocal or wide-field microscope to image the roots.

Solution 1

Since the working distance of some of the higher magnification objectives (40x – 63x) is 100-220 µm, and the coverslip thickness is 100 µm, we realised that the roots have to be pressed against the coverslip to stay in focus. We had two options, either have a really thin channel, with a coverslip on top, or having coverslip as the lowest part of the slide and have some weight or a channel keeping roots in place on top of the coverslip. We chose to place the coverslip as the very lowest part of the slide so a number of types of inverted microscopes could be used for observation (Figure 27B).

Technical objective 2

To apply uniform electric field at a small distance in the slide so that roots maybe placed into the field.

Solution 2

We used two platinum wires embedded on the sides of the slide, which are submerged in the medium. The wires are attached to electrodes that are connected to the power supply with

wires. When the electrodes are submerged and at the same height, roots can be placed in between the two electrodes to allow application of electric field to the roots (Figure 27B).

Technical objective 3

To maintain continuous medium perfusion, in order to achieve a constant temperature and uniform concentration of the medium in the V-slide.

Solution 3

Medium exchange proved to be a difficult problem to solve. The first designs of the V-slide used a closed 100µm tall channel to keep roots in (not shown). This allowed for slow perfusion only, because the higher pressure required for fast perfusion would cause weak points in the slide to burst open. This is because the peristaltic pump used is not perfectly accurate when removing and feeding the liquid medium. This results in volume variation of the liquid in the channel, which resulted in pressure and slide damage. The reason why slow perfusion could not have been used was because once an electric field was established within the slide, slow perfusion did not manage to mitigate the side-effects of the electric field and we observed a changed pH at the positive and negative electrodes (not shown). Instead we opted for an open design of the slide (Figure 27A). This allows roots to be mounted on the banked edges while not constricting liquid to a fixed volume space, allowing for fast perfusion and liquid volume variation. We have measured the pH in the new system with medium B and electric field 1V/cm and 15µA current and observed no differences in the pH at the two electrodes (Table 9).

Technical objective 4

To prevent the roots from moving in the 3D space, even though the slide had only one solid surface, and was open from the other.

Solution 4

We needed to ensure the roots were able to move only in two dimensions, so they stayed in focus. To solve this, we developed weights (Figure 27C) with a handle and transparent glass. The metal weights, which can be removed from the handle, allow for mass adjustment. The glass allows for visible confirmation that roots are held down by the weights and also allow for imaging with transmitted light. The handle (also referred to as top cover) itself provides a support structure for the weights and glass.

By fulfilling all of the technical objectives we have managed to construct the V-slide, a tool that allows for the microscopic observation of effects of weak external electric field on the *Arabidopsis* root tip.

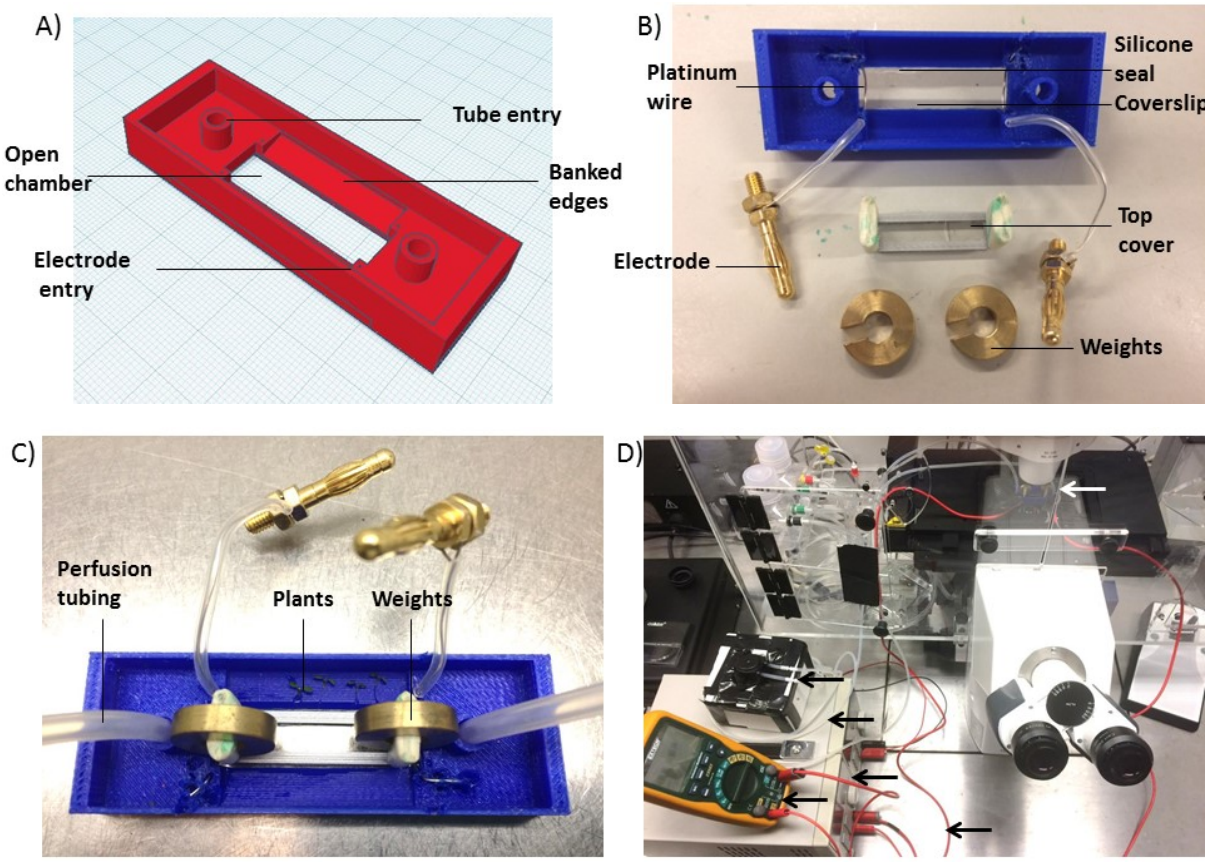

Figure 27: V-slide set-up, which allows for microscopic observation of roots while subjected to electric field. A) Computer Aided Design of the slide structure. B) Components of the V-slide. C) Tubes that allow cooled perfusion, electrodes that are connected to the power supply and weights that hold down the roots for observation are all part of the V-slide set up. D) Complete V-slide setup with power supply, current meter and peristaltic pump connected to the slide with wires and platinum electrodes and perfusion tubing. Microscope is used for time-lapse image collection.

Table 9: Acidity of the liquid medium was measured in the V-slide after 1 hour of mock electric field or after 1 hour of 1V/cm electric field, 15µA current in medium B.

Position	pH of medium B (measured with colour strip)
No electric field, V-slide	5.5-6.0
Electric field, positive electrode	5.5-6.0
Electric field, negative electrode	5.5-6.0

3.3 Discussion

3.3.1 External electric field application to roots

We have successfully constructed three different experimental set-ups that allow: a population of roots to be exposed to an electric field; individual exposure and imaging; and individual exposure and microscopic imaging. These tools have proven to be essential to study the physiological and developmental effects of the electric field in *Arabidopsis* roots (Results II, chapter 4; Results III, chapter 5; Preliminary Results IV, chapter 6).

While the observation of the external electric field's effect on plants remains a very unique topic that we examine, there were other tools developed that used application of current to plants to study a certain physiological or developmental trait. In particular, studies that do not study the effect of electric field, but instead try to simulate current spikes caused by changes in membrane voltage of plants, use set-ups based on insertion of an electrode directly into the plant to apply an electric field and to cause membrane depolarisation (Mousavi *et al.* 2013, (Mousavi *et al.* 2014).

In order to be able to observe new phenomena and explain unknown mechanisms caused by the external electric field in roots, new apparatuses had to be established. Our three tools, V-tank, V-box and V-slide have satisfied the necessary specifications of their designs and can be used when answering biological questions related to *Arabidopsis* root regeneration and growth in electric field.

4 Results II: Root regeneration in external electric field

4.1 Background

4.1.1 Developmental control of root regeneration

The regeneration of the *A. thaliana* roots and the post-embryonic development is a rather unique process that does not rely on the stem cell niche for the re-growth of the root following damage or complete removal of the root tip. Interestingly mutants that are unable to maintain stem cell niche (quiescent centre), are still able to regenerate the root tip after its complete excision (Sena *et al.* 2009) (Figure 28).

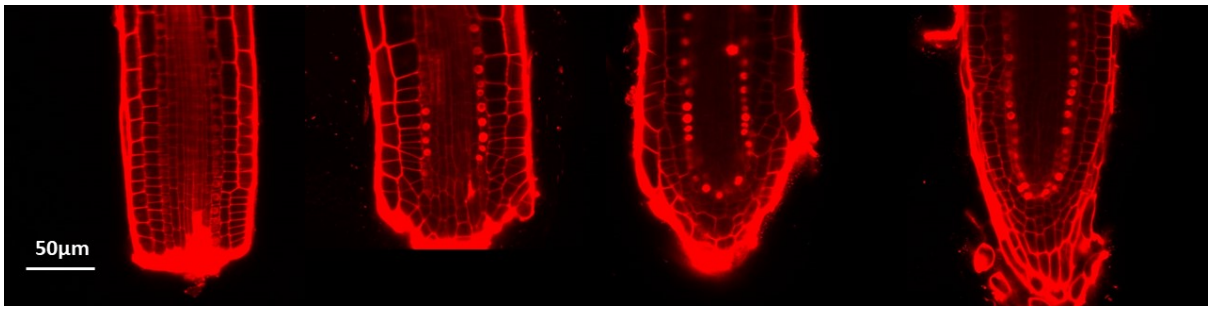

Figure 28: Example of root tip regeneration when QC was removed. Images were taken at the time of cut, one day post cut, two days post cut and four days post cut. Scalebar 50µm.

Post-embryonic development of a functional organ, such as root with somatic cells relies on a number of crucial aspects. It relies on the inclusion of cells with differing potencies to change cell fate, the action of signalling processes in a number of cells to act in sync and the positional information of all of the cells participating in the regenerative process (Birnbaum *et al.* 2003). In the root regeneration multiple signals, such as mechanical, chemical and potentially electrical might have a role on the underlying genetics on cells during regeneration. Therefore it is important to recognise that the presence and propagation of the aforementioned signals has a role during organ development.

The regenerative process starts with the wounding response that is triggered by the changes in the turgor pressure. Environmentally induced wounding is also thought to generate transmembrane potential changes, but these were not yet observed in wounding of *Arabidopsis* root

(Fromm and Lautner 2007). The steps following the initial wounding response lead to the redistribution of auxin and cytokinin hormones in the damaged tissue (Sena *et al.* 2009), (Efroni *et al.* 2016). The regenerative step in the root of *A. thaliana* is achieved with cell proliferation and recapitulation of embryogenic root developmental program (Efroni *et al.* 2016). The mutants in maintenance of the stem cell niche are still able to form embryonic root (Sabatini *et al.* 2003), (Aida *et al.* 2004) and the triple mutants in the genes known as *NO TRANSMITTING TRACT* family (*nww*), which are unable to form embryonic root unless supplied with exogenous auxin have also shown severe decrease in the frequency of root regeneration (Efroni *et al.* 2016).

The obvious difference between the regenerating root and a root growing from the embryo is that the root growing from the embryo has to originate from only two cells, whereas the regenerating root is originating from many different cells found in the root stump. It still appears that similarly to embryonic root formation, auxin and cytokinin, two crucial hormones driving cell division and growth, might be necessary for the post-embryonic root regeneration (Sena *et al.* 2009). In the case of root regeneration, both auxin and cytokinin define spatial regions of the root stump, which leads to the formation of new root, rather than specification of a single cell which happens in the initial steps of embryonic root growth (Efroni *et al.* 2016).

The cell files in the regenerating root have been observed to switch fates (Efroni *et al.* 2016) in the manner of 'old endodermal' cells becoming outer cell files such as epidermis, and the cells present at the very outer cell layer getting omitted from the root regeneration process. It appears that even though multiple cell files contribute cells towards cell fate switching and formation of root tip, there is a limit with which the cells can transition to a new cell type and their cell fate transition is guided by their position in the remnant tissue (Efroni *et al.* 2016). However different positions of the cells that are forming different tissues regenerating root tip also correlate with auxin and cytokinin concentration zones. This process is temporally sensitive, and it may aid the cells gain a cue for a new identity when switching cell fates (Efroni *et al.* 2016).

There are other examples of defining root tissue using auxin and cytokinin as cell specification agents, such as root vasculature (De Rybel *et al.* 2014), but the presence of auxin and cytokinin alone may not be enough to specify new cell fates during regeneration process. Indeed there is a complex hormonal cross-talk involving giberrelins, strigolactone, brassinosteroids and abscisic acid that guides the development of primary root (Pacifici *et al.* 2015) and may be also involved in the root regeneration process. It is possible that combination of cell to cell communication together with a hormonal specification may aid cells in establishing their new roles and forming a new root.

4.1.2 Perturbing root regeneration competence using electric field

The likelihood of root regenerating its root tip can be altered by many different approaches. The most obvious one is genetic, with the already mentioned example of embryogenetic mutant having also drastically decreased root regeneration competence. Another way of altering root tip regeneration frequency is to remove the root tip at different distance, in effect removing more or less of the root tip (Sena *et al.* 2009). It is possible that the ability of the cells to switch fates using underlying mechanisms such as cell to cell communication and auxin and cytokinin definition of new tissue boundaries depends on how many dividing cells in the meristem tissue are left.

The external electric field perturbations have a long history in changing the polarities of single cells as well as affecting regeneration of animal tissues (Smith 1974), (Peng and Jaffe 1976), (Chang and Minc 2014). In addition, endogenous electric field patterns constructed from membrane voltages found on surface of individual cells can act as a guiding morphogen for the regeneration observed in *Xenopus* and planaria (Adams *et al.* 2007), (Beane *et al.* 2012). There are only sparse accounts of perturbation of regeneration processes in plants using external electric field. Tobacco tissue regenerating *in vitro* in shoot inducing medium was observed to have increased efficiency of regeneration when both electric field with direct or alternating current was applied to the tissue (Rathore and Goldsworthy 1985), (Cogalniceanu *et al.* 1998).

We want to use electric field to perturb the molecular mechanism of root regeneration process. We aim to see if external electric field is able to alter the frequency of root tip regeneration. We also aim to see if any underlying components of root tip regeneration such as hormone concentrations, cell fate switching or rates of cell divisions are changed when the root regenerating root tip is subjected to electric field.

4.1.3 Aims

These are the aims that we hope to accomplish with the results presented in this chapter:

- Systematically explore the effect of external electric field on root regeneration.

  We use electric field exposure on regenerating roots in an attempt to observe perturbation in the regeneration competence at given spatial positions within the regenerating meristem. In addition to perturbing spatial competence of root regeneration with electric field, want to find out if perturbation of regeneration competence with electric field is time dependent.

- Observe the distribution of auxin and cytokinin in the regenerating root tip after it has been subjected to electric field.

  We know that the two hormones are crucial for re-patterning of the root stump and beginning of the new root tip formation. There are past reports that auxin distribution within the root may be affected by electric field (Moore *et al.* 1987), (Ishikawa and Evans 1990). We will use electric field in an attempt to perturb auxin and cytokinin ditribution in the regenerating root tip. We will observe the potential changes using timelapse imaging, in order to see spatial and temporal relevance of the hormonal distribution during root regeneration.

- Observe the rate of cell divisions in the regenerating root tips perturbed with electric field.

  One of the necessary components for successful root tip regeneration is the presence of proliferative tissue (Efroni *et al.* 2016). The entering of cell mitosis is a tightly regulated mechanism. We use electric field exposure on regenerating root tips, in order to

observe perturbation of cell division rate in regenerative tissue caused by electric field. It is possible that perturbation in regeneration competence may correlate with perturbations in proliferation.

- Observe cell fate identity in regenerating roots perturbed with electric field.

  We aim to use electric field to perturb regeneration competence and observe cell fate re-establishment, to assess whether cell fate re-establishment during root tip regeneration is perturbed with electric field.

4.2 Results

4.2.1 Root regeneration in the absence of the electric field

In order to compare the effect of external electric field on regenerating root tips, first we had to devise an assay for exposing regenerating *A. thaliana* roots to electric field with direct current with media that is maintained for homogeneity as much as possible. To achieve this we have used the V-tank where up to 80 roots with their root tips removed can be bathed in medium, which maintains ion and temperature homogeneity and be exposed to external electric field or to mock treatment (Results I, 3.2.1) (Figure 29).

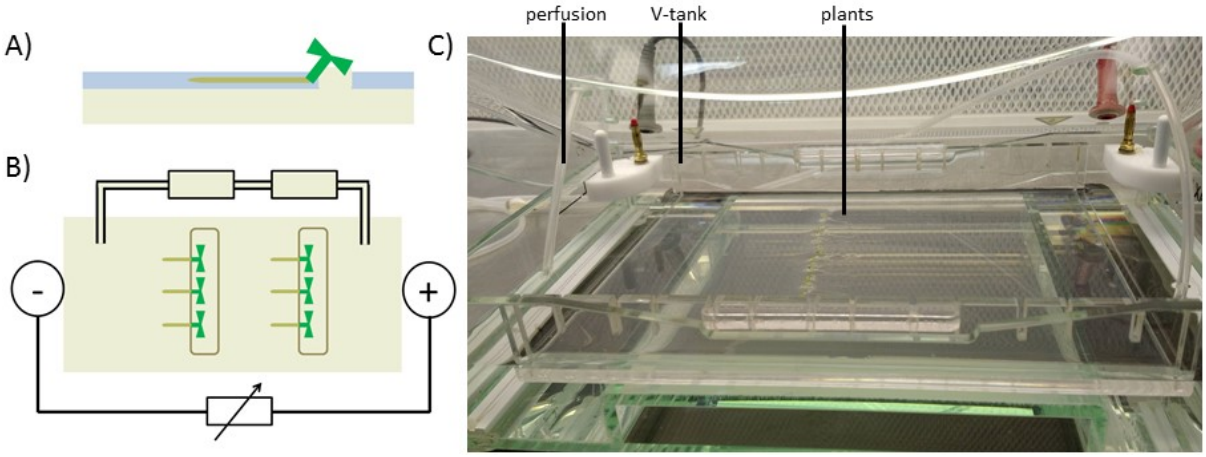

Figure 29: V-tank set up. A) *Arabidopsis* hypocotyl and cotyledons are placed on agar 'pillows' to avoid being submerged in the conductive liquid. B) schematic of the set up, with root orientation towards an electrode being interchangeable. C) Image of the V-tank set-up with plants inside. Taken from (Kral *et al.* 2016), distributed under CC BY 4.0 open access license.

To define how we will study the effect of electric perturbation on root tip regeneration, we first defined 3 zones in root meristem where the root tip will be removed. This is the distal, median and proximal cut with 120±10µm, 160±10µm and 200±10µm distances removed from the root tip meristem (Figure 30A). We first wanted to observe the already established result that spatial gradient causes different regeneration frequencies (Sena *et al.* 2009). The regeneration frequency was established as a number of roots that were regenerated on solid media 5 days after the cut and brief 30 minute placement into the V-tank, divided by the total number of roots that were cut and

passed through the 5 day process. The error for the root regeneration frequency was calculated as standard error of proportion.

It can be seen that roots exposed to mock conditions in the V-tank were cut at distal mark, their regeneration frequency is observed to be 0.82 – 0.89 (±0.02), while roots subjected to cut at the median mark were observed to regenerate with 0.56-0.59 (±0.03) frequency and roots cut at the proximal mark were seen to regenerate with 0.20-0.28 (±0.03) frequency (Figure 30B). The significant difference was observed between the frequencies using chi-square test with Bonferroni correction. We have also defined 3 different 'resting times', defined as the time between the moment a population of roots was cut, and when it was placed into the V-tank for brief exposure to mock treatment. From the results we can observe that 30, 80 or 160 minute resting time did not change significantly the regeneration frequency in the populations of root tips (Figure 30B).

The results show that position of the cut matter to the regeneration frequency, but short immersion into medium in V-tank at a varied time point has no effect on the regeneration frequency (Kral *et al.* 2016). These results were used as control measurements in further experiments.

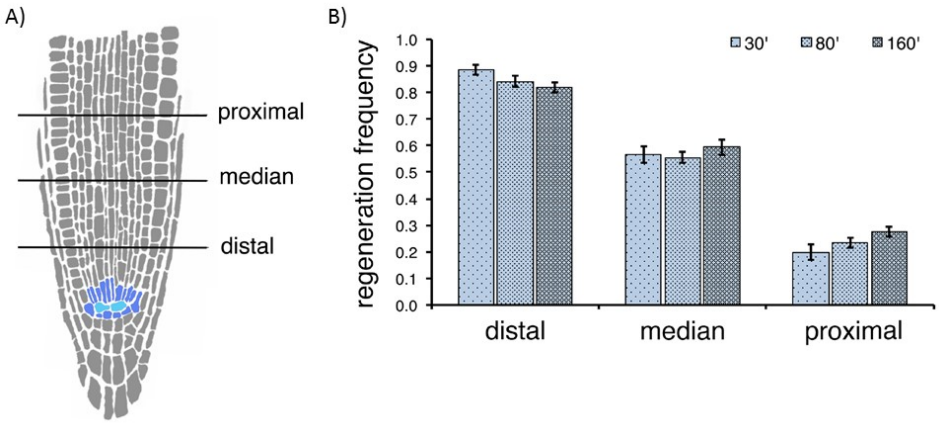

Figure 30: Three different root cut points for commencing regeneration process were used. A) Distal, median and proximal position of the cut in the root meristem at 120±10µm, 160±10µm, 200±10µm respectively. Quiescent centre was removed with each of the three distances used. B) Quantification of frequency of root tip regeneration without electric field stimulation. The frequency of regeneration is shown ± standard error of the proportion. 30', 80' and 160' stand for three different times between cut inducing regeneration and exposure to mock condition of electric field exposure. At least N≥175 roots were cut per spatial and temporal point. This data is later used as mock data in **Figure 32**. Taken from (Kral *et al.* 2016), distributed under CC BY 4.0 open access license.

4.2.2 Strong electric field inhibits root tip regeneration

There are few examples of the use of electric field on plant roots, so choosing strength of the electric field can be difficult. Number of reports show damage caused to the maize root meristem after 3 hours of exposure to 5, 3 and 1.5 V/cm (Ishikawa and Evans 1990), (Stenz and Weisenseel 1991), (Wawrecki and Zagórska-Marek 2007).

In the first attempt, assuming short electric field exposure, we have used 5.0V/cm (200-220mA) for 30 minute exposure of roots cut at the median region (160µm±10µm) after 80 minute resting time. We have observed significant decrease in the frequency of regeneration of the roots subjected to electric field as oppose to those exposed to mock condition. The effect was observed when the electric field applied to the roots faced negative (aligned) or positive (anti aligned) condition (Figure 31). The result shows that 30 minute 5.0 V/cm electric field exposure is enough to inhibit root regeneration (Kral *et al.* 2016).

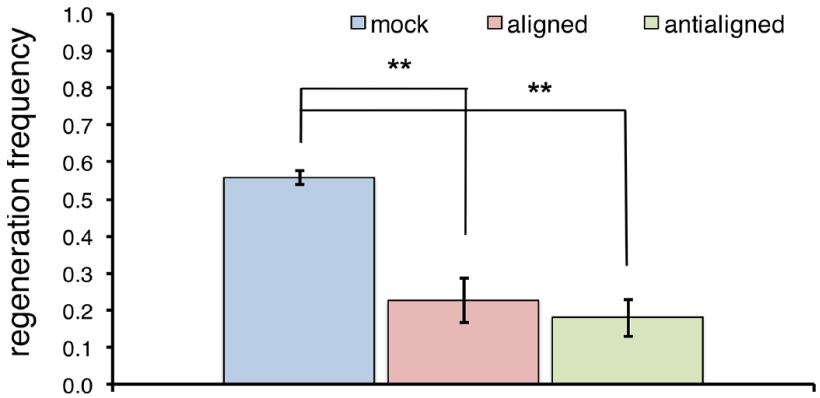

Figure 31: Root regeneration frequency of roots subjected to 5V/cm electric field was measured. Root tips cut in the median region of the meristem were exposed to aligned (facing negative electrode) or anti-aligned (facing positive electrode) electric field for 30 minutes, 80 minutes after the root tip was removed. The regeneration frequency is shown as a mean ± standard error of the proportion. At least N≥44 roots per exposure were cut to generate frequency of regeneration. Chi square test with Bonferroni correction was used to compare the proportions. p-value<0.005 is shown with **. Taken from (Kral *et al.* 2016), distributed under CC BY 4.0 open access license.

4.2.3 Weak external electric field enhances root tip regeneration

In order to examine any other effect of the electric field than just inhibitory effect on root regeneration, we decided we will use 2.5V/cm electric field to perturb root regeneration process. In an attempt to examine the effects of electric field more fully, we used two orientations of the

electric field, aligned (root facing negative electrode) and anti-aligned (root facing positive electrode) (Figure 32A).

In order to examine the possibility of the root tip affecting different regions of the regenerating root tip differently, we have examined root stumps with tips cut at 120µm±10µm, 160µm±10µm and 200µm±10µm. The quiescent centre was removed with all three types of cuts. Even thou the regeneration process starts the moment root tip is removed, it is yet unexplored at what point in time can the electric field affect the root regeneration process. Therefore, we explored three distinct resting times, 30 minute, 80 minutes and 160 minutes, which were times between root tip removal and exposure to 30 minute 2.5V/cm electric field treatment in V-tank. In effect we have systematically exposed to regenerating root tips to 18 different treatment types: three spatial root tip removal points, three temporal points and two orientations of electric field (distal, median, proximal)x(30, 80, 160 minutes resting time)x(aligned, antialigned). In addition to calculating regeneration frequency for each condition, we have also quantified the scale of the effect of the electric field. We have done this by calculating regeneration ratio (RR), done by dividing frequency of regeneration of exposed roots with frequency of regeneration of roots exposed to mock condition (f_e/f_m). We also calculate the limits of the ratio with 95% confidence interval.

The most intense outcome was observed at the proximal region of the meristem (200µm±10µm) when it was exposed to aligned 2.5V/cm electric field 30 minutes after root tip removal. At this point we can calculate 80% (confidence interval 31% -153%) increase in regeneration frequency due to electric field. At the same spatial and temporal condition, but using anti-aligned electric field orientation we can observe 65% (confidence interval 23% - 132%) increase in root tip regeneration due to electric field treatment (Figure 32B1). Interestingly this effect was not observed in further time points (80, 160 minutes) and the root regeneration frequency of roots exposed to electric field was statistically same as mock.

Roots with the root tip removed at the median region (160µm±10µm) and exposed to 2.5V/cm electric field 30 minutes after excision showed significantly higher root tip regeneration frequency than mock in both orientations. Aligned orientation of root tips showed 32% (confidence interval 19% - 55%) increase in root regeneration frequency and anti-aligned orientation showed 26% (confidence interval 17% - 58%) increase due to electric field (Figure 32B2). However, when roots with root tip removed at the median region were exposed to electric field 80 minutes after excision, only root stumps exposed to aligned orientation of electric field have shown significant 19% (confidence interval 8% - 30%) increase in regeneration frequency in comparison to mock. The effect was not observed in roots exposed to anti-aligned orientation of electric field. Interestingly, when root tips with excised root tip at the median region were exposed to electric field 160 minutes after root tip removal, only roots exposed to anti-aligned orientation of electric field have shown 25% (confidence interval 7% - 40%) increase in root tip regeneration in comparison to mock. The effect was not observed in roots exposed to aligned orientation of electric field. These results show that there may be polarities present within the unknown mechanism that regulates the temporal ability to respond to the field.

Finally, roots that were cut at the distal region did not have their root tip regeneration frequency altered with electric field at any of the spatial and temporal conditions tested (Figure 32B3). It is possible that due to the fact that a high number of roots regenerate when these roots have their tip removed at the distal position, there may be some roots that won't regenerate despite the influence of electric field on the underlying mechanism (Kral *et al.* 2016).

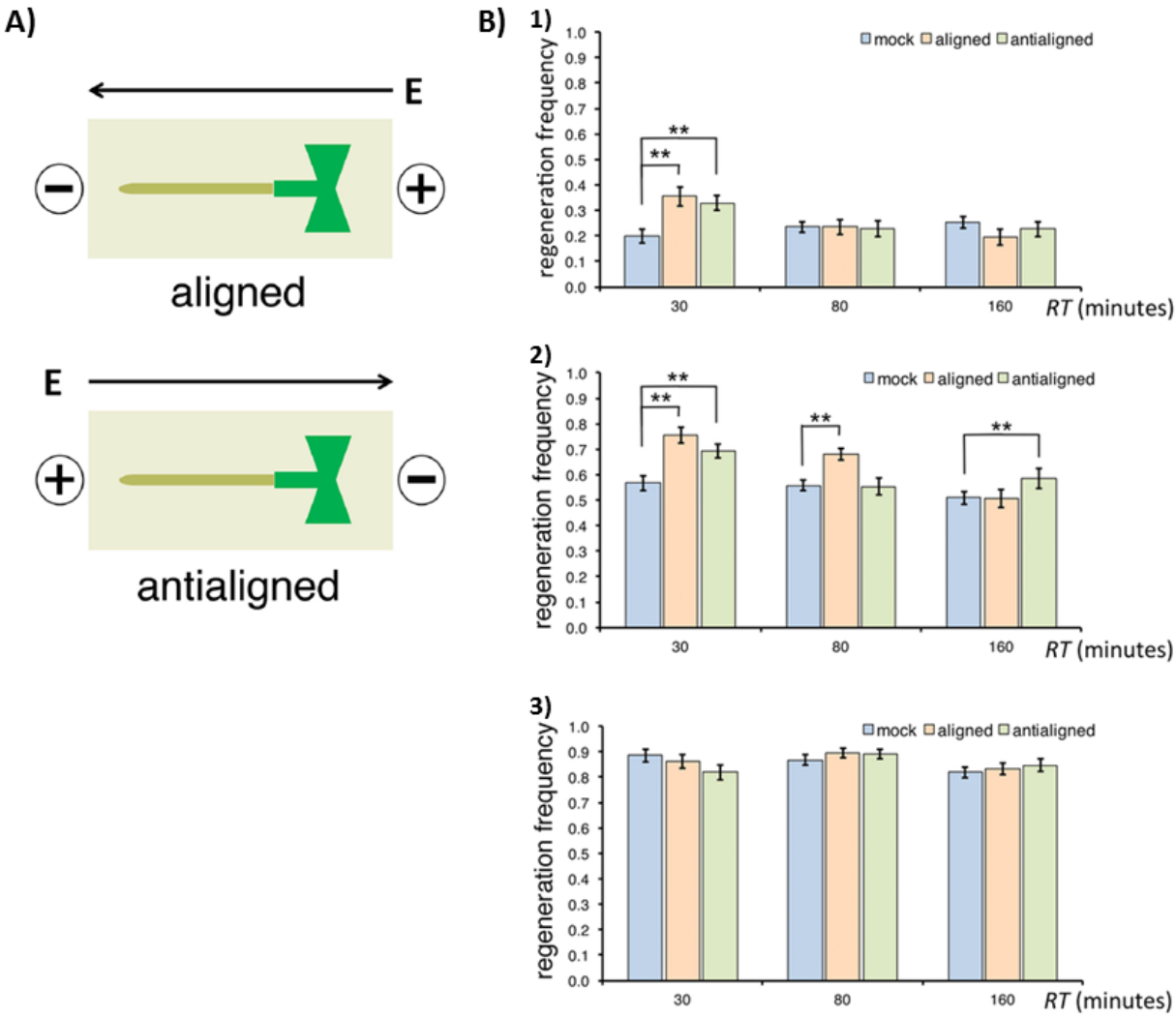

Figure 32: Root regeneration frequency of roots subjected to 2.5V/cm electric field was measured. Root tips were cut in the three regions of the meristem defined in **Figure 30A**, distal, median and proximal. A) Roots with removed root tips were exposed to aligned (facing negative electrode) or anti-aligned (facing positive electrode) electric field for 30 minutes. B) Roots with root tips removed were subjected to electric field 30, 80 or 160 minutes after the root tip was removed. Regeneration frequency is shown with or without electric field perturbation when root tips were cut at (1) distal position, (2) at median position, (3) at proximal position. All of the data sets are shown as regeneration frequency ± standard error of the proportion. At least N≥163 roots were used to construct the regeneration frequency proportion per temporal and spatial point tested. Chi square test with Bonferroni correction was used to compare the proportions. p-value<0.005 is shown with **. Taken from (Kral *et al.* 2016), distributed under CC BY 4.0 open access license.

4.2.4 Weak external electric field does not perturb tissue organisation during regeneration

In order to observe the progress of regenerating roots at cellular level we have imaged root tips of regenerating *A. thaliana* roots using scanning laser confocal microscope at different times, by already established methods (Sena *et al.* 2009). This gave us temporal series of median sections of the regenerating root, providing cues on cellular dynamics of regeneration process, for roots that

were subjected to 30-minute electric field treatment and for those that were exposed to mock treatment.

We first wanted to observe if the overall cell fate re-establishment is found to be different in the regenerating root tips that were subjected to a condition that determined a significant increase in the frequency of regeneration. For this we picked the condition when root tips were excised at median region (160µm±10µm) and exposed to aligned 2.5V/cm electric field 30 minutes after excision. The transcription factor SCARECROW (SCR) is an important controller of radial pattern formation as well as quiescent centre in *A. thaliana* root (Sabatini *et al.* 2003). We use SCR as a cell fate reporter for endodermis, to see if pattern of cell fate re-establishment is perturbed when regenerating roots are subjected to electric field. We can observe SCARECROW activity using transcriptional reporter *pSCR::H2B:YFP*, which expresses histone H2B attached to yellow fluorescent protein and is localised to the nucleus (Heidstra, Welch and Scheres 2004). We have exposed root with excised root tips that express *pSCR::H2B:YFP* to the chosen electric field treatment as well as mock treatment 30 minutes after excision. No qualitative differences were observed in the simple morphology as well as in the pattern of SCR expression between regenerating root tips exposed to electric field and those exposed to mock condition as can be seen in Figure 33 (Kral *et al.* 2016).

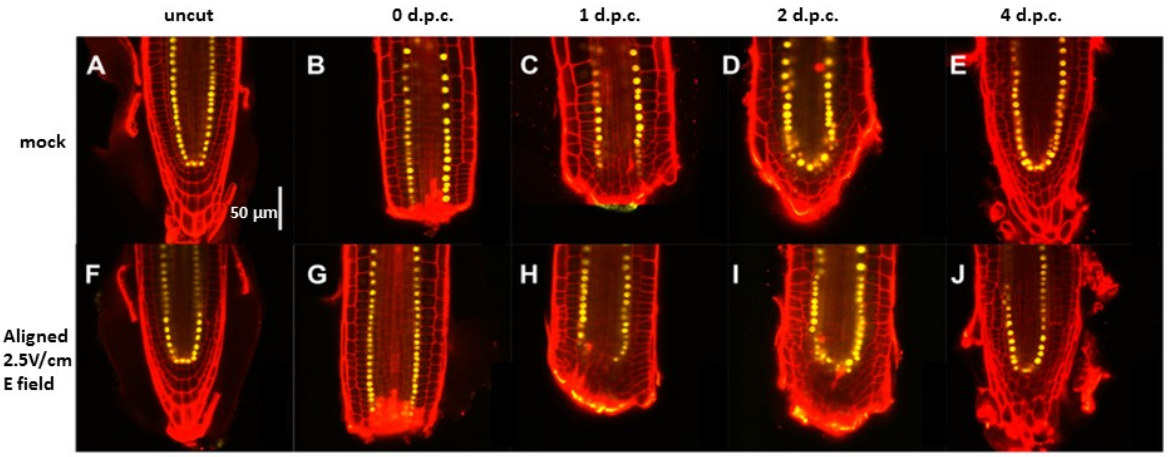

Figure 33: Roots expressing *pSCR::H2B:YFP* marker for SCARECROW expression pattern had their with root tip removed at median position and were exposed to mock treatment (A-E) or to aligned orientation 2.5V/cm electric field (F-J) for 30 minutes, 30 minutes after root tip removal. Root tips were stained with 10µg/ml propidium iodide to reveal morphology of the regenerating root tip. Root tips were imaged when uncut, 0 days post cut (d.p.c.), 1 d.p.c., 2 d.p.c. and 4 d.p.c. Each image represents at least 4 roots. Scale bar stands for 50µm. Taken from (Kral *et al.* 2016), distributed under CC BY 4.0 open access license.

4.2.5 Weak external electric field inhibits cell divisions early in the regeneration process

Cell proliferation is necessary component of root tip regeneration without which roots do not regenerate. In addition, extent to which cell proliferation occurs may influence root regeneration competence. We use external electric field to perturb the root regeneration process and we observe and quantitate the perturbation of cell divisions within the regenerating root. We have used the transgenic mitotic cyclin reporter *CYCB1;1::GFP*, which expresses CYCLINB-GFP chimera protein under the control of *pCYCB1;1* promoter, allowing to visualise individual cells about to enter mitosis (Colón-Carmona *et al.* 1999), (Reddy *et al.* 2004). We have subjected roots expressing *CYCB1;1::GFP* with root tips excised at 160µm±10µm to 2.5V/cm aligned electric field for 30 minutes, 30 minutes after the excision. We focused on the first hours of the root regeneration process, and we have 3D imaged the roots using confocal microscope and z-stack collection.

In order to generate temporal series, we have imaged the root stumps within 1 hour of exposure to mock or electric field and within 2 – 4 hours of exposure to mock or electric field condition. Qualitatively we have observed a decrease in cell divisions after the root tip has been excised (Figure 34A). We have also quantitatively analysed the effect of electric field on proliferation in regenerating root stumps. We have used mitotic index, which was a ratio calculated by the number of cells expressing *CYCB1;1::GFP* in the whole of z-stack divided by the total number of cells considered (Methods, 2.2.7).

We have observed that the short exposure to electric field significantly decreases cell divisions in the root tip 1 hour after electric field exposure in comparison with root stumps exposed to mock conditions. Furthermore, we have observed that regenerating root stumps of both electricity and mock treated roots have shown decreased cell divisions 4 hours after the exposure (Figure 34B). This appeared to be a temporary effect, because one day after root tip excision cell divisions in regenerating root tips appeared to be occurring at the same rate as those found in uncut root tips, regardless of electric field exposure (data not shown). This suggests that rate of cell

division temporarily decreases hours into the root regeneration process and 2.5V/cm aligned electric field causes this decrease in proliferation to occur faster (Kral *et al.* 2016).

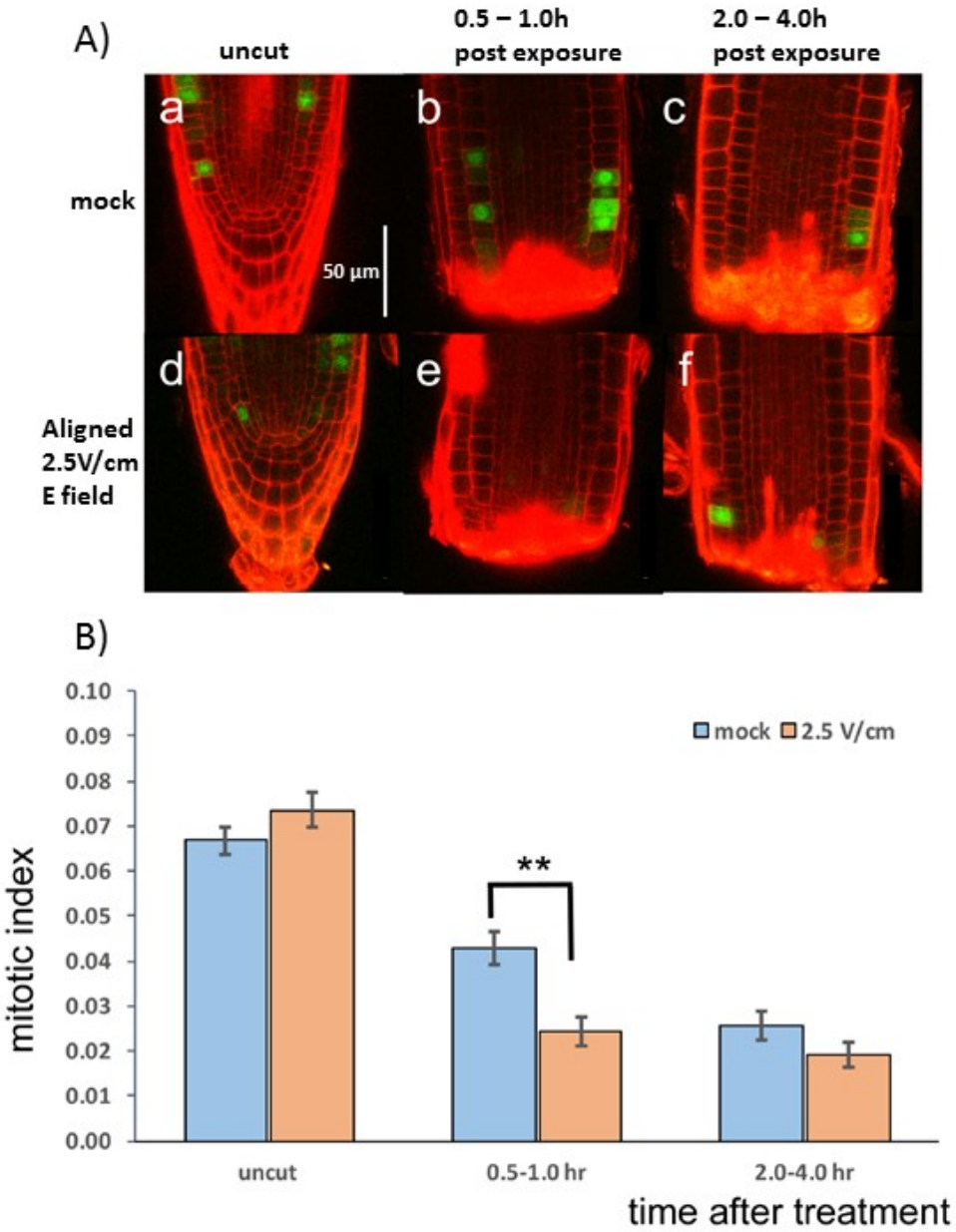

Figure 34: Roots expressing *CYCB1;1::GFP* marker of mitotic cyclin B had their with root tip removed at median position and were exposed to mock treatment or to aligned orientation 2.5V/cm electric field for 30 minutes, 30 minutes after root tip removal. A) Root tips were imaged when uncut within 1 hour of mock or E field exposure (a, d), imaged within 1 hour of removal the root tip and exposure to the the electric field or mock treatment (b, e) or within 4 hours of root tip removal and exposure to treatment (c, f). Roots were stained with 10µg/ml propidium iodide to reveal morphology of the root tip and full 3D z-stack image of each root was taken at every time point (not shown). Each image represents at least 7 roots. Scale bar stands for 50µm. B) Quantification of cell division rate in the observed roots was done by calculating mitotic index. Mitotic index is a proportion of dividing cells (observed green) in all cells observed. The data were compared between uncut, cut exposed to treatment and imaged within 1 hour and cut exposed to treatment and imaged within 4 hours. The graph shows the mitotic index as proportion ± standard error of proportion. The data has been tested for significant difference using Chi square test. p-value less than 0.01 is shown with **. Taken from (Kral *et al.* 2016), distributed under CC BY 4.0 open access license.

4.2.6 Weak external electric field changes auxin distribution but does not affect the distribution of cytokinin

The complex mechanism of molecular controllers of cell divisions in the *A. thaliana* root meristem is not yet completely unravelled, but it is known that a number of plant specific hormones play an important role maintaining balance between cell division and differentiation (Pacifici *et al.* 2015). Auxin and cytokinin are most well researched hormones managing the formation and upkeep of root apical meristem (Dello Ioio *et al.* 2007), (Schaller *et al.* 2015). In root tip regeneration both cytokinin and auxin are thought to play pivotal roles, defining boundaries for formation of new tissues, and aiding cells take on new cell fates (Efroni *et al.* 2016). In addition auxin movement was previously observed to be affected by the electric field (Morris 1980). We wanted to observe if exposure of regenerating roots to weak external electric field causes changes in the auxin or cytokinin distribution.

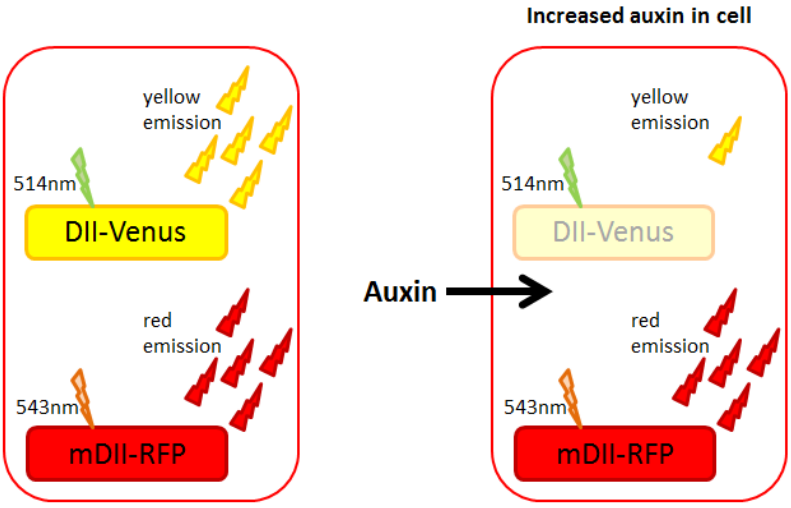

Figure 35: Diagram highlights the mechanism of R2D2 reporter action. The ratio between yellow and red fluorescence is used to inform of auxin concentration.

We have observed the auxin levels within root using semi-quantitative ratiometric reporter *R2D2*, which expresses auxin degradable and auxin non-degradable proteins from constructs *pRPS5A::DII:nx3Venus, pRPS5A::mDII:ntdTomato* (Liao *et al.* 2015) (Figure 35). We have excised root tips expressing *R2D2* reporter at the median region of root meristem (160µm±10µm) and exposed them for 30 minutes to 2.5V/cm aligned electric field, 30 minutes after excision. We have also exposed *R2D2* expressing regenerating root tips to mock conditions. We have also exposed uncut

R2D2 expressing root tips to the same conditions. We have observed auxin distribution in regenerating root tips using confocal microscope, imaging roots at a median section in temporal series in 1 hour of root being exposed to treatment and within 2 - 4 hours of root stumps being exposed to treatment.

We have generated fluorescence ratio for every pixel in the images which passed threshold to eliminate background (Methods, 2.2.6), by calculating natural log of mDII:Tomato fluorescence divided by DII:Venus fluorescence. We can observe from the ratiometric images in Figure 36 that electric field exposure has caused an increase in auxin concentration all across the root meristem in the uncut root tips not found in root tips exposed to mock conditions. The increased auxin concentration due to electric field treatment can also be observed in the regenerating root tips imaged 1 hour after the exposure to electric field, but less so in the root tips imaged 4 hours after the exposure to electric field. It appears that the exposure to an aligned electric field causes a temporary increase in auxin concentration in regenerating root stumps early on after root tip excision (Figure 36) (Kral *et al.* 2016).

Together with auxin, we also observed cytokinin levels within root tip using a synthetic transcriptional reporter *TCSn::GFP* that reflects cytokinin presence by activation of two component signalling sensor causing binding to a DNA element that results in the expression of green fluorescent protein (Zürcher *et al.* 2013). We have excised root tips expressing *TCSn::GFP* at the median region of the root meristem and exposed them for 30 minutes to 2.5V/cm aligned electric field, 30 minutes after excision. We have also exposed *TCSn::GFP* expressing regenerating root tips to mock conditions. We have also exposed uncut *TCSn::GFP* expressing root tips to the same conditions. We have observed the pattern of cytokinin activity using confocal microscope imaging of regenerating root tips in a temporal manner once a day until the root tip has regenerated.

We can observe from the images shown in Figure 37 that the uncut root tips have highest cytokinin presence in the columella and in the lateral root cap. Once these are removed, some

cytokinin presence can be seen in the vasculature of the remaining root stump as well as some in some remaining cells of lateral root cap. By day 2 of regeneration process we can see cytokinin activity in the new columella cells. This was also observed by Efroni *et al.* 2016. However we did not observe any variation in the pattern of cytokinin activity in both uncut and cut roots as a result of treating the roots with a brief electric field treatment (Kral *et al.* 2016).

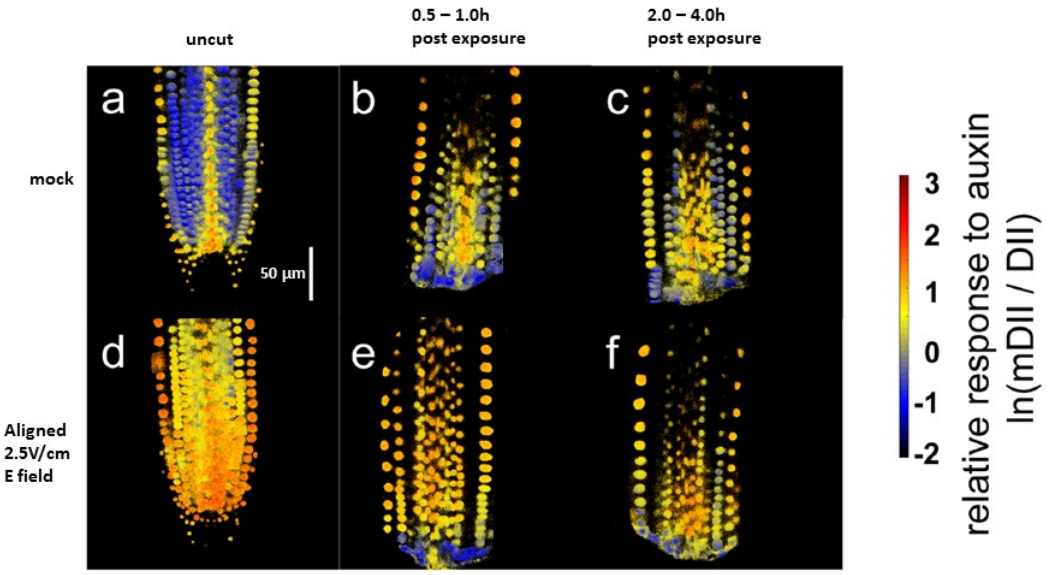

Figure 36: Roots expressing *pRPS5A::DII:nx3Venus pRPS5A::mDII:ntdTomato*, ratiometric reporter of auxin (*R2D2*) had their root tip removed at median position and were exposed to mock treatment or to aligned orientation 2.5V/cm electric field for 30 minutes, 30 minutes after root tip removal. Root tips were imaged when uncut within 1 hour of mock or E field exposure (a, d), imaged within 1 hour of removal the root tip and exposure to the electric field or mock treatment (b, e) or within 4 hours of root tip removal and exposure to treatment (c, f). Each image is representative of at least 9 roots imaged. The ratio was constructed by using natural logarithm on a fraction obtained by dividing signal from control over signal from auxin dependent fluorophore. Colour scale is used to show high or low auxin concentration with red being the highest and dark blue/black being the lowest. Scale bar stands for 50µm. Taken from (Kral *et al.* 2016), distributed under CC BY 4.0 open access license.

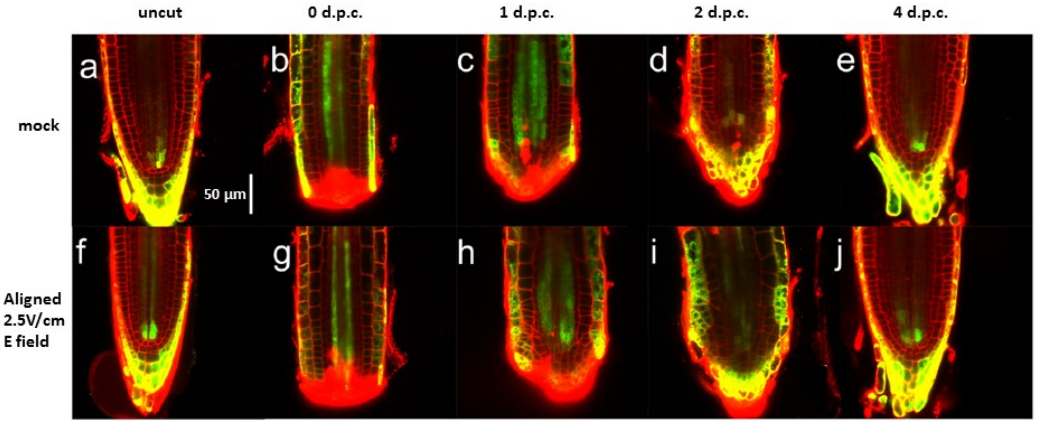

Figure 37: Roots expressing *TCSn::GFP* reporter, used to observe cytokinin presence, had their with root tip removed at median position and were exposed to mock treatment (A-E) or to aligned orientation 2.5V/cm electric field (F-J) for 30 minutes, 30 minutes after root tip removal. Root tips were stained with 10µg/ml propidium iodide to reveal morphology of the regenerating root tip. Root tips were imaged when uncut, 0 days post cut (d.p.c.), 1 d.p.c., 2 d.p.c. and 4 d.p.c. Each image is representative of at least 7 roots. Scale bar stands for 50µm. Taken from (Kral *et al.* 2016), distributed under CC BY 4.0 open access license.

4.3 Discussion

4.3.1 External electric field and tissue reorganisation

We have shown that *A. thaliana* regeneration of root apical meristem can be perturbed with a short exposure to 2.5V/cm external electric field. Calculating regeneration ratio with 95% confidence interval we have shown that under defined conditions (root tip excision at 200µm±10µm, electric field exposure 30 minutes after excision) the probability for a root to regenerate has increased two-fold. The magnitude of the increase of the regeneration frequency varies with different excision zone and with different time spent between excision and exposure to electric field.

It appears that the youngest most distal meristem tissue is the least affected by the electric field, the median region of the root meristem after excision gets affected by electric field for the longest period after cut. The most mature region of the meristem, when cut has been made at the proximal region can be affected by electric field and the field has the strongest effect in this region but it remains susceptible for 30 minutes and not longer than 80 minutes. The cells in the proximal region are most differentiated and overall in the early stages of the regeneration the cells are differentiating fast (Sena *et al.* 2009).

A possible hypothesis could be that the cells found in the root stump when excised in the median region are at similar differentiation stage at 80 minutes post excision as those found in the stump cut at the proximal region 30 minutes post excision. This suggests there is a small differentiation window when the cells are able to be affected by electric field. The last clue that was obtained from the regenerating root tip exposure was the ability to perturb regeneration with aligned electric field at 80 minutes, but with anti-aligned electric field at 160 minutes. This suggests that there may be a polarized distribution of molecular actors such as ions or proteins that allow electricity to perturb root regeneration in temporal and spatial manner (Kral *et al.* 2016) (Figure 38).

Other studies have shown that single cell identity changes occur within 3 hours of induction of regeneration process (Efroni *et al.* 2016). It is therefore likely that there are some early-acting cell

fate transition programs triggered in the case of regenerating root and somehow root stump exposure to weak external electric field early in the regeneration process is perturbing this process, increasing the likelihood of the root to regenerate.

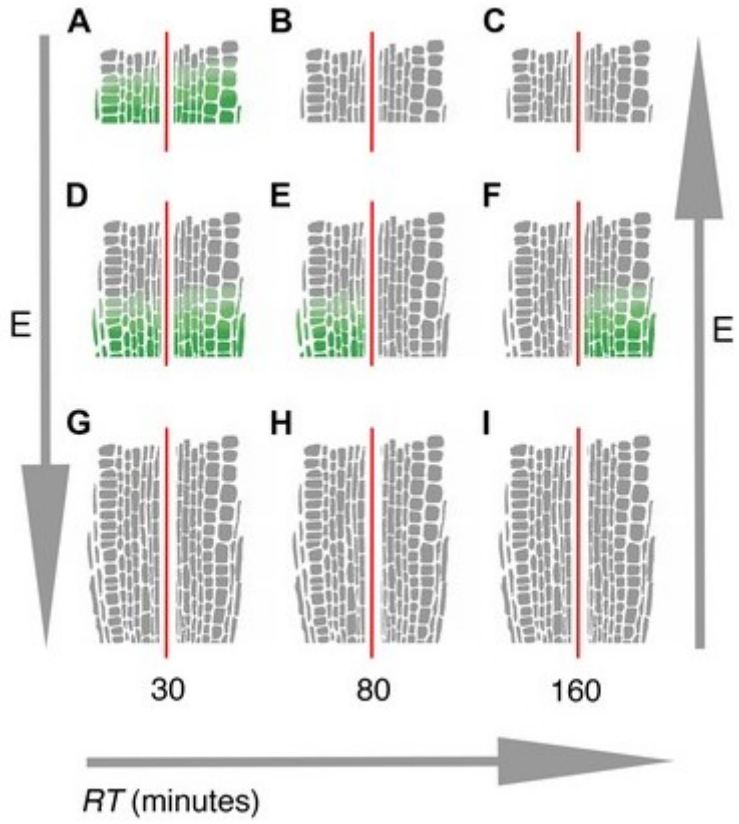

Figure 38: Outline of the competence of the root stump cells to respond to external electric field. Strong green colour highlights roots that react to electric field (E). The half-roots on left/right do not show any spatial significance; instead they stand for roots exposed to aligned/anti-aligned electric field. (A-C) Proximal excisions, (D-F) median excisions, (G-I) distal excisions are shown, with root cuts 30 min (A, D, G), 80 min (B, E, H) and 160 min (C, F, I) before exposure to electric field. Taken from (Kral *et al.* 2016), distributed under CC BY 4.0 open access license.

4.3.2 Auxin, external electric field and root regeneration

It is likely that stabilising feedback loops such as auxin-cytokinin driven transcription are disrupted with wounding. As an example of such stabilising feedback loop are stele cells where specific transcription activation leads to cytokinin synthesis (Dello Ioio *et al.* 2012), while SHR transcription factor triggers cytokinin degradation in endodermis next to stele (Kurakawa *et al.* 2007). It is therefore possible that in these situations transient temporal windows occur, when root development can be modulated by changed hormone concentrations, which leads to definition of new tissue borders and boundaries (Efroni *et al.* 2016).

We have shown that overall auxin distribution has changed in the root stump, following weak external electric field treatment, compared with untreated roots. The difference in the auxin concentration was observable only 1 hour after the root's exposure to electric field and this change in the auxin distribution have disappeared within 4 hours after exposure to electric field. This result correlates with the result of increased regeneration competence by using the same electricity treatment. Further experiments are necessary to show that the mechanism with which electric field perturbs root regeneration makes use of the changed auxin distribution.

In other studies it has been shown that application of exogenous auxin in the hours following root tip excision was able to change the tissue boundaries of newly forming organs (Efroni *et al.* 2016). We did not observe any change in the expression pattern of *pSCR::H2B:YFP* as a result of application of electric field. The activity of the SCARECROW transcription factor was reported to be more modulated by exogenous application of cytokinin analogue rather than by auxin analogue (Efroni *et al.* 2016). It is possible that there is a threshold auxin concentration necessary that changes SCR cell fate establishment that might not have been reached, even though auxin distribution was temporarily perturbed.

We have not studied the cytokinin distribution in the very first hours of root tip regeneration after electric field exposure. During daily observations throughout the whole regeneration process, cytokinin distribution did not appear to be changed by the brief treatment with electric field 30 minutes after root tip excision. It is possible that changes in the cytokinin distribution during electricity perturbation of root regeneration are very transient, only observable few hours after the electric exposure, similar to the perturbation of auxin distribution

It is possible that another tissue marker such as WIP4, transcription factor necessary for cell fate determination in the primary root tip (Crawford *et al.* 2015) may be a better marker to observe cell fate perturbation by electric field than SCR. The WIP4 expression is found early on after excision of the root tip in the most distal part of the regenerating root stump, and the expression pattern

appears to spread proximally with application of exogenous auxin (Efroni *et al.* 2016). It is unknown what is the threshold auxin concentration needed to achieve the effect of spreading the WIP4 expression pattern. We have observed increased auxin presence in the very distal area of the root stump early after electric field perturbation. We could examine the expression acitivity of WIP4 as a clue for electric field driven perturbation of cell fate re-establishment in regenerative root tips.

It is possible that the cells undergoing cell fate transitions are undergoing these transitions with some probability of success, which may be aided by hormone presence in the cells changing fates. Therefore, electric field causing redistribution of auxin in the regenerating root stump early after the onset of regeneration process could aid cell fate transitions. This could be one part of the mechanism with which electric field affects root tip regeneration.

4.3.3 Electric field, cell proliferation and root regeneration

We have observed cell division quantitatively and we measured marked decrease of cell division in the first hours of the root regeneration process. The decrease in cell division occurred even earlier in the root regeneration process than normally when the root stump was subjected to weak external electric field, which was shown to perturb root regeneration competence. This is a correlation between cell divisions, root regeneration and electric field that we currently don't have an explanation for.

Ectopic auxin presence has been previously observed to cause abnormal cell divisions in root tip (Sabatini *et al.* 1999), so it may be possible that the auxin increase caused by electric field temporarily causes a decrease in cell divisions. However, there is an overall decrease of cell divisions within 4 hours from root tip excision even in the regenerating root tips not exposed to electric field. It is possible that the temporary cell division decrease may be necessary component of the root regeneration process. One attempt to assess the necessity of temporary cell division decrease for root tip regeneration could be to quantify cell divisions in the root stumps that have been excised, however have not managed to regenerate root tip. If there are significant differences in the cell

division dynamics observed in the early stages of root regeneration process in the root stumps that regenerate root tips in comparison to those that won't regenerate the root tip, it could suggest the necessity for the temporary cell division decrease in root regeneration.

In several animal models for regeneration such as *Xenopus* or *Hydra*, the activity of apoptosis-related caspases are noted to be necessary for the regenerative tissue to successfully complete regenerative processes such as cell fate switching and increased proliferation (King and Newmark 2012). Without caspase activity both *Xenopus* does not regenerate its tail (Tseng *et al.* 2007), and *Hydra* does not recover its head (Fan and Bergmann 2008). It is possible that in *Arabidopsis* similar, seemingly contradictory action of proliferative tissue, such as temporary decrease in cell divisions, is necessary for successful regeneration as it may enable processes necessary for root tip regeneration such as cell fate switching.

5 Results III: Root electrotropism

5.1 Background

5.1.1 Observing growing roots in weak external electric field

Soil is a complex environment with a number of physical and biological factors affecting its state. Plants, in order to survive, while maintaining a sessile lifestyle have evolved to examine the cues found within soil and either exploit nutrients or avoid obstacles, toxins or pathogens. They do this with roots, specialised organs for soil exploration and nutrient uptake. One of the effects found in soil is the presence of transient electric fields. These electromagnetic fields in soil are generated with local non-uniformly distributed ion concentrations (Jouniaux *et al.* 2009). This often occurs based on the irregular surface of soil particles that prevent diffusion and homogenisation of ions, instead this leads to irregular presence of minerals that plant roots need to find, identify and absorb (Hodge 2006).

Roots explore soil by directional growth rather than movement. This is referred to as tropism, and tropic growth is based on asymmetric cell expansion in a given part of the root, causing the root to change direction of growth (Muday 2001). Root tropisms have been observed to many different physical stimuli, such as gravitropism based on the gravity vector, phototropism based on a light gradient, as well as thigmotropism based on touch or a plants' interaction with a solid object, or hydrotropism when root orients itself towards a water source (Gilroy 2008). It is possible that in addition to already mentioned inducements, electromagnetic field acts as a cue for directional growth of roots, the behaviour named electrotropism. This behaviour may provide advantage to roots within soil, when searching for nutrients or avoiding unwanted chemicals. Not surprisingly other organisms found in soil such as nematode *C. elegans* (Chrisman *et al.* 2016) and soil-dwelling amoeba *Dictyostelium* (Shanley *et al.* 2006) are adapted to respond to electric fields found in soil with electrotactic movement.

In laboratory conditions, root curvature towards anode, positive electrode, was first observed in the roots of *Lepidium*, *Synapsis* and *Raphanus* (Plowman, 1904), (Shrank, 1959) with strong electric field. Multiple reports have since explained the root turn towards positive electrode in plants such as *Zea mays* and *Vigna murgo* have been caused by strong electric field inducing damage to the root observed in a central part of the elongation zone of the root (Stenz and Weisenseel 1991), (Stenz and Weisenseel 1993), (Wolverton *et al.* 2000), (Wawrecki and Zagórska-Marek 2007). However using weaker external electric fields, typically 1V/cm with direct current, leads to root of *Zea mays* to curve towards cathode, negative electrode, with no notable damage to the root tip (Stenz and Weisenseel 1993), (Wawrecki and Zagórska-Marek 2007). This turn towards negative electrode is the true electrotropic turn observed in the laboratory conditions. The region for the turn responsible was identified as the distal elongation zone of the root tip in *Vigna murgo* (Wolverton *et al.* 2000).

Arabidopsis thaliana is a very useful model organism to observe, study and explain a range of plant phenomena. *Arabidopsis* was used to explain a mechanism behind a number of root tropisms, with one example being gravitropism (Kiss *et al.* 1989), (Abas *et al.* 2006), (Rahman *et al.* 2010). This is because in addition to diploid genome, short generation time and self-fertilisation, over the years a big collection of mutants and transgenic reporters have been established in *Arabidopsis*. In combination with real time imagining techniques at macro, micro and nano scales, as well as genotyping and the use of molecular biology techniques, *Arabidopsis* makes for a powerful investigation tool when examining novel phenomena. It is surprising that to our knowledge *A. thaliana* was never used to observe electrotropism and probe its underlying molecular mechanism.

Our aim is to use novel set-ups described in Results I chapter 3, V-box and V-slide, to expose growing *A. thaliana* roots to weak external electric fields to observe electrotropism. We are also aiming to use *A. thaliana* genetic mutants and molecular reporters to understand the underlying genetic and molecular factors that drive the electrotropic turn.

5.1.2 Gravitropism versus electrotropism, role for auxin?

The gravitropic turn has been studied more consistently than the electrotropic turn and therefore there is a lot more information known about the underlying mechanism of gravitropism. *Arabidopsis* roots sense gravity vector using statoliths, amyloplast starch filled granules found in statocytes, specialised cells in the root collumella (Kiss *et al.* 1989). The statoliths deposit to different parts of the cell, depending on the orientation of the root tip with respect to gravity and trigger a signalling cascade with the aim of reorienting the root tip (Band *et al.* 2012) (Figure 39).

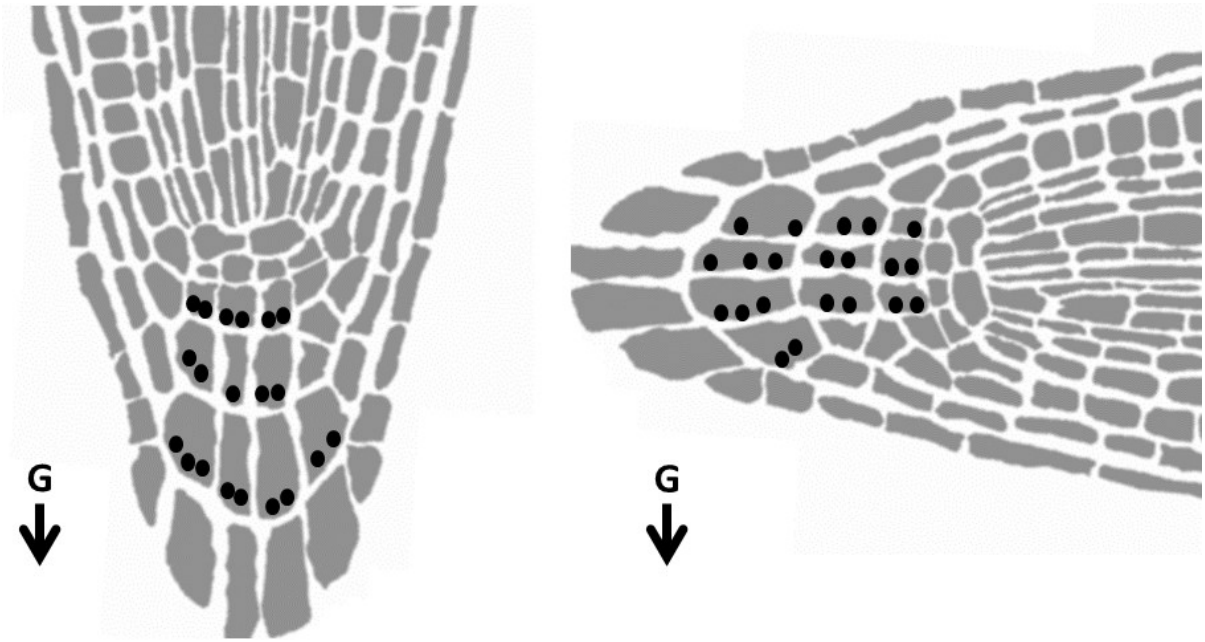

Figure 39: Diagram of statolith reorientation in response to gravity.

The immediate signal transduction pathway is not completely understood, however proton and Ca^{2+} ionic dynamic changes have been observed in root tips after statolith repositioning (Fasano *et al.* 2001), (Monshausen *et al.* 2011). After initial signalling, a considerable amount of research focused on explaining the mechanism behind asymmetric cell expansion that ultimately leads to the reorientation of root tip with the gravity vector. This is driven by hormone auxin, which is distributed in the root tip with a number of influx and efflux transporters, leading to 'reverse fountain' with the auxin maximum at the quiescent centre (Leyser 2006) (Figure 40).

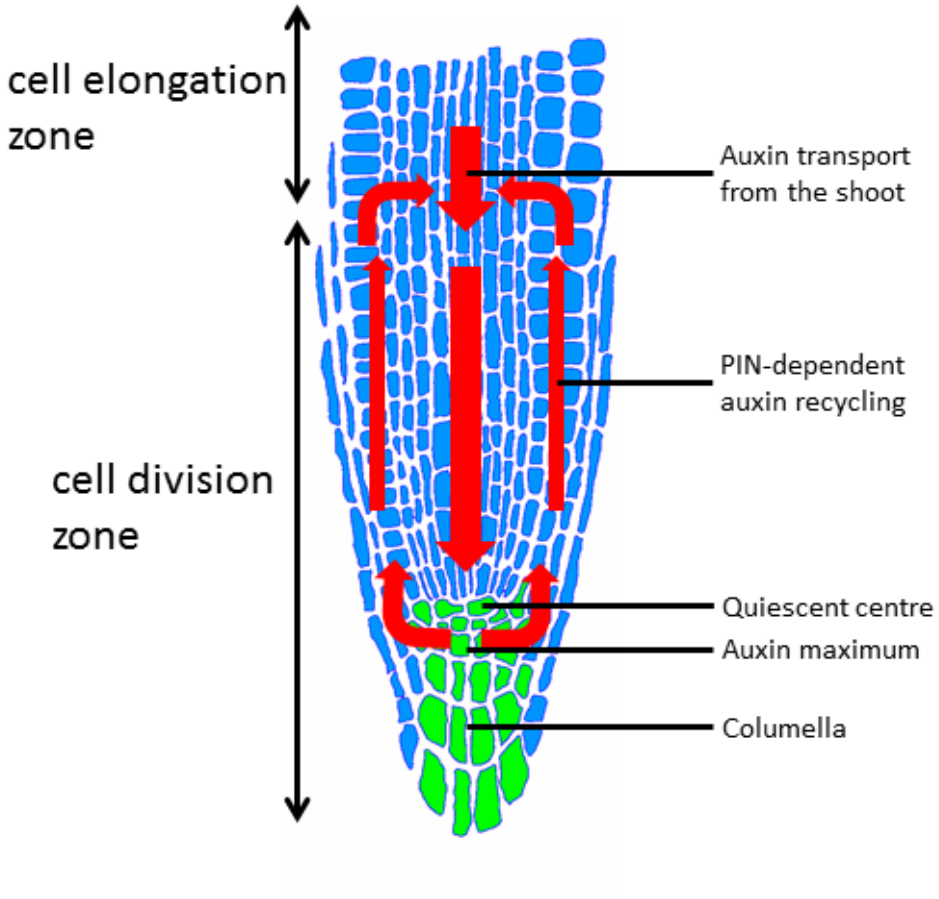

Figure 40: Description of auxin transport in the root tip. Green indicates cells with highest auxin concentration, red arrows indicate direction of auxin flow.

Related to gravitropism, two knock-out mutants have been identified to completely lose the ability to perceive gravity. These were identified to be missing functional genes of *pin2* and *aux1*. These two genes encode transporters of auxin located in the epidermis and cortex for PIN2 and epidermis and lateral root cap in the case of AUX1. The PIN2 transporter moves auxin away from the quiescent centre through outer cell files of root meristem, while AUX1 provides sufficient intracellular auxin in the outer cell files of the cell (Abas *et al.* 2006), (Marchant *et al.* 1999). Together these two proteins give rise to the 'reverse fountain' effect of auxin transport.

The reason why these two transporters are indispensable for gravitropic turn, is because they influence and change the flow of auxin through the outer cell files during change in perceived gravity (Abas *et al.* 2006), (Marchant *et al.* 1999). PIN2 protein in particular was observed to be more concentrated on the side of the root tip that was the lowest (Rahman *et al.* 2010). This results in

increased auxin flow on one side of root tip epidermis and cortex in comparison with the opposite side. Increased auxin concentration then leads to inhibition of cell expansion in those cells (Figure 41). This is controlled through H^+ ATP-ase pumps, changing the surrounding apoplast pH of the cells. With the altered pH, the cell wall expands more or less depending on the exact pH of the apoplast (Rayle and Cleland 1992), (Barbez *et al.* 2017). Water uptake of the cell is altered to aid cell expansion (Péret *et al.* 2012), (Dünser and Kleine-Vehn 2015) . The result is asymmetric cell expansion on both sides of the outer cell files of the root tip and results in root turn.

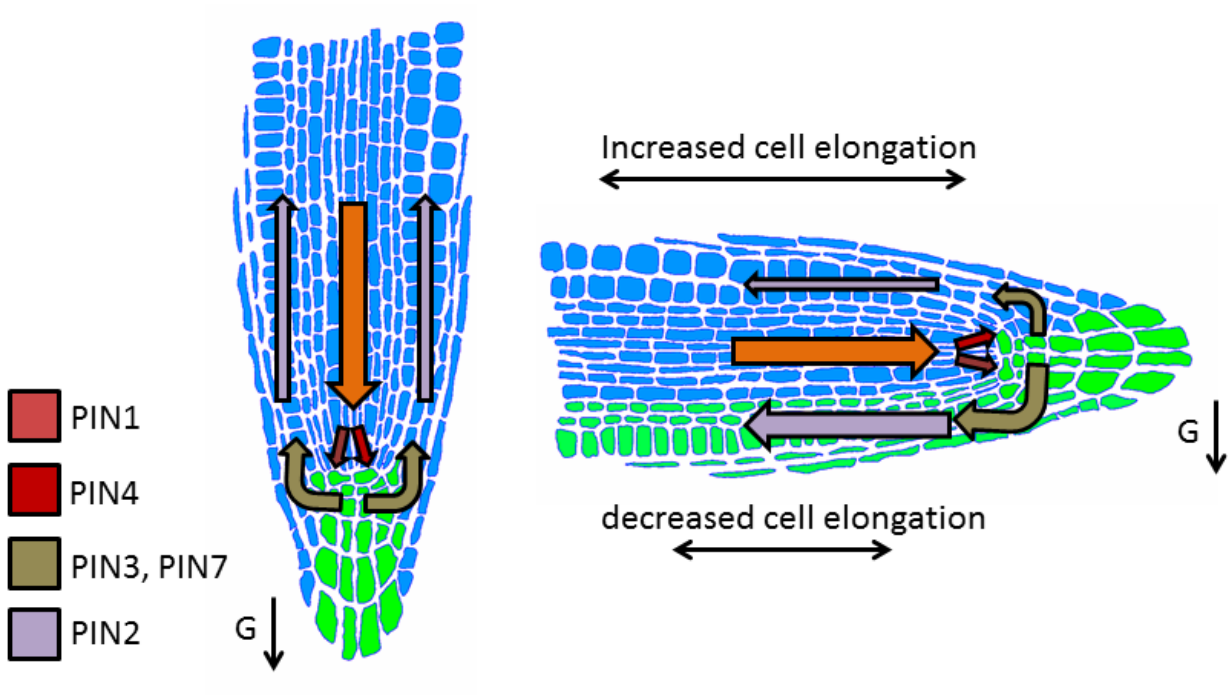

Figure 41: Differential auxin flow during gravitropism is caused by asymmetric accumulation of PINs in spatially distrinct zones on two sides of the root. Green cells have higher concentration of auxin than blue cells causing asymmetrical cell expansion.

There are a few reports of the use of auxin inhibitors on maize roots, during electrotropism. These showed that the use of auxin transport blockers pyrenoyl benzoic acid (PBA) and 2,3,5-triiodobenzoic acid (TIBA), have prevented the electrotropic turn, but they did not inhibit growth (Ishikawa and Evans 1990), (Moore *et al.* 1987). To what extent is auxin driving the electrotropic turn, however is largely unanswered.

Our motivation is to examine the similarities and the differences between electrotropism and gravitropism. We assume that electrotropism just like gravitropism is cell expansion based, so

we hope to examine how similar the two mechanisms are. Therefore we aim to quantitatively characterise possible electrotropism of agravitropic *Arabidopsis* mutants *pin2* and *aux1* to see if the auxin transporters responsible for the gravitropic turn are also essential for the electrotropic turn. We also would like to see auxin distribution during electrotropism, which is possible thanks to genetic auxin reporter R2D2 (Liao *et al.* 2015). The main aim is to observe if electrotropism and gravitropism share the same molecular mechanism or if separate mechanisms drive the two phenomena.

5.1.3 Necessity of ion transport in electrotropism, a role for ion dynamics and signalling?

Ions, such as H^+, K^+,Na^+, Ca^{2+}, Cl^- act as signalling molecules in most processes in plants. Specifically in tropisms, a number of ion based dynamic events have been predicted or observed. The role of H^+-ATPases have been linked to gravitropism and also as an action preceding auxin signaling in phototropism (Barbez *et al.* 2017), (Hohm *et al.* 2014).

Calcium signalling is crucial to many morphogenetic and developmental processes (Hepler 2005). In addition to observing Ca^{2+} increases on the lower side of the root during gravitropism in *Arabidopsis*, correlating with auxin concentration increase (Monshausen *et al.* 2011), dated evidence shows that after electrotropic turn, Ca^{2+} ions were measured in higher concentrations in the vicinity of one of the sides of the root tip of *Zea mays* (Moore *et al.* 1987).

K^+ ions have been shown to be important in water uptake, cell osmotic balance and cell expansion mechanisms (Osakabe *et al.* 2013), which raises possibility of K^+ ion dynamic changes occurring during the electrotropic turn. In addition to ion specific effects, in gravitropism, transient changes in membrane potential have been observed in quick temporal succession to the root receiving gravity stimulation in *Lepidium sativum* (Behrens *et al.* 1985), (Sievers *et al.* 1995). It is possible that specific ions, such as H^+, K^+ or $Ca2^+$ or non-specific membrane potential changes will be present during electrotropic turn in *Arabidopsis*.

Ion dynamics and rapid changes in the ion concentration are controlled by ion channels. Ion channels found in plants can be ion gated, ligand gated as well as voltage gated. The ion channel activity can be triggered by any number of physical, chemical or electric cues (Hedrich and Becker).

We have selected a number of *Arabidopsis thaliana* mutants missing a functioning ion channel (Table 10), the selection was done based on voltage dependent activation of the channel or previous implication of a channel with membrane voltage changes. We aim to expose these mutants to weak external electric field and quantitatively screen through the roots missing an ion channel, hoping to identify a non-electrotropic mutant. The ion channels were picked based on a hypothesis that ion distribution in the tissue is likely to be affected by external electric fields. If the ions influenced by the electric field play part in electrotropism, the presence or absence of channels that control the ion flow may prove crucial for the electrotropic mechanism.

Table 10: Here listed is selection of genes for reverse genetic screen. The goal of the screen is to link a gene from the selection with an electrotropic phenotype.

Gene	Function
aha1	H^+ ATP-ase (proton pump)
aha2	H^+ ATP-ase (proton pump)
ost2	H^+ ATP-ase (proton pump)
clcB	voltage dependent Cl^- channel
clcD	voltage dependent Cl^- channel
clcG	voltage dependent Cl^- channel
akt1	voltage dependent K^+ channel
kco4	Ca^{2+}, H^+ dependent K^+ channel
kat1	voltage dependent K^+ channel
kat3	Regulatory subunit for K^+ channels
skor	K^+ dependent K^+ channel
gork	K^+ dependent K^+ channel
tpc1	voltage dependent Ca^{2+} channel
vdac1	voltage dependent anion channel
vdac4	voltage dependent anion channel
glr1.1	glutamate triggered Ca^{2+} channel
glr1.2	glutamate triggered Ca^{2+} channel
glr1.4	glutamate triggered Ca^{2+} channel
glr2.3	glutamate triggered Ca^{2+} channel
glr2.4	glutamate triggered Ca^{2+} channel
glr3.2	glutamate triggered Ca^{2+} channel
glr3.3	glutamate triggered Ca^{2+} channel
glr3.4	glutamate triggered Ca^{2+} channel
glr3.6	glutamate triggered Ca^{2+} channel

Proton pumps

The channels selected for the screen include H^+ ATP-ase proton pumps AHA1 and AHA2, involved in apoplastic pH control (Gaxiola *et al.* 2007), as well as *Arabidopsis* plants expressing a constitutively active version of AHA2 dubbed OST2-1D (Merlot *et al.* 2007).

Potassium channels

K^+ ion channels present in the screen selection were Shaker-like voltage gated K^+ channels, such as KAT1, AKT1, SKOR and GORK as well as regulatory subunit associated with these proteins, KAT3. Functionally they are known to be interacting with H^+ ATPases and are involved in the regulation of stomatal opening in *Arabidopsis* (Inoue and Kinoshita 2017). Also included with the K^+ channels, is the KCO1 and KCO4 tandem pore vacuolar K^+ channels, controlled by Ca^{2+} and H^+ ions. KCO4 was shown to be involved in the membrane depolarisation of pollen tubes (Becker *et al.* 2004) and KCO1 is involved in osmoregulation and was shown to be strongly expressed in the mitotically active tissues such as root meristem(Lew 1991), (Czempinski *et al.* 2002).

Voltage dependent anion channels

We have selected for the screen five voltage dependent anion channels, CLC C, CLC D, CLC G that transport Cl^- and two NO_3^- transporters CLC A and CLC B. CLC A and CLC B channels are involved in the nitrate accumulation (De Angeli *et al.* 2006), (von der Fecht-Bartenbach *et al.* 2010), and CLC G & CLC C transporter is important in Cl^- and regulation of salt stress and are expressed in roots (Nguyen *et al.* 2016). CLC D channel is involved in the regulation of endosomal compartments, and does not have effect on plant ion homeostasis. However roots missing CLC D channel have been shown to have grown less than the wild-type roots (Fecht-Bartenbach *et al.* 2007).

We have also added five non-specific voltage dependent anion channels, VDAC1, VDAC2, VDAC3, VDAC4 & VDAC5. These have been shown to be localised on PM as well as mitochondrial

membrane of root cells and at least three of the channels VDAC1, VDAC2 and VDAC4 are necessary for normal root growth (Robert *et al.* 2012).

Calcium channels

Present in the screen is also a voltage gated calcium channel TPC1, which is controlling vacuolar uptake of Ca^{2+} as well as maintenance of vacuolar membrane potential. The channel seems to be important for the germination process as well as control of stomata movement (Peiter *et al.* 2005).

The last group of ion channels included in the search for a non-electrotropic mutant have been the ligand gated Ca^{2+} ion channels, known as GLRs. There have been twenty GLRs identified in *Arabidopsis* plants and a subgroup of those have been shown to be expressed in roots (Chiu *et al.* 2002). GLRs are homologous to iGLURs, glutamate receptors found in animal nervous system. In plants they have been shown to be linked with a number of processes such as pollen tube growth (Michard *et al.* 2011), as well as voltage based signalling of herbivore triggered stress (Mousavi *et al.* 2013).

The aim is to examine the potential role of the ion channels listed above during plant electrotropism. It is likely that some of these ion channels fill redundant roles, since ion dynamics are essential to plant growth, but we hope that we may be able to find a non-redundant action of an ion channel that will be necessary for the electrotropic turn of the root. In relation to this, we hope to examine Ca^{2+} ion dynamics in the roots directly at microscopic resolution, during the electrotropic turn, thanks to the gene encoded FRET-based calcium reporter YC3.6 (Krebs *et al.* 2012).

5.1.4 Aims

- Wild type root electrotropism

To observe *Arabidopsis thaliana* root electrotropism when root is exposed to weak external electric field, with electrodes parallel to the orientation of the root. We aim to collect live time lapse

videos of the phenomenon and quantitatively characterise the electrotropic turn with the measurement of deflection of the root tip through time. We also would like to observe *A. thaliana* root electrotropism in different media, with different conductance properties in order to further understand the relevance of current during the roots' exposure to electric field. We also want to see if we observe any side-effects or damage to the root tip as a result of being subject to electric field, as damage to root tip has caused confusion about the electrotropic effect in the past (Stenz and Weisenseel 1993).

- Auxin action in root electrotropism

To describe the action of hormone auxin during the root electrotropism. Particularly we aim to see if gravitropic and electrotropic effect share the same molecular process. We want to examine agravitropic mutants *pin2* and *aux1* and see if they are able to respond to electric field stimulation. We also want to observe the distribution of hormone auxin in *A. thaliana* roots subjected to electric field, and if it is similar to the asymmetric distribution of auxin during gravitropism.

- Search for non-electrotropic mutant

To use the ability of quantitative characterisation of the electrotropic turn to examine a number of *A. thaliana* ion channel mutants, effectively establishing a reverse genetic screen, to identify a non-electrotropic mutant. Once identified we examine possible presence of dose-dependence by testing electrotropic effect not-only in homozygous mutants of the gene and wild-type plants, but also heterozygous plants containing only one functioning copy of the ion channel in question.

- Calcium dynamics in electrotropic root

To observe live dynamics of Ca^{2+} ions during root electrotropism at micro spatial scale and second temporal scale. We aim to observe wild-type roots expressing *pUBQ10::YC3.6* using time-lapse microscopy, which a FRET-based genetic reporter of Ca^{2+} in V-slide, a microscopic chamber that allows for electric field exposure.

5.2 Results

5.2.1 Arabidopsis root electrotropism when exposed to 1V/cm E field

We have exposed *A. thaliana* roots to 1V/cm electric field in V-box set up (Results I, 3.2.2) in order to see the response of roots to electric field. We have used 1V/cm electric field exposure based on historic exposures of *Zea Mays* roots to electric field (Stenz and Weisenseel 1993). In agreement with the previous experiments, the root of *Arabidopsis* was observed to curve towards cathode, negative electrode. This process has occurred in a short time span within minutes of electric field exposure (Figure 42A).

The effect was recorded as time-lapse video using Raspberry Pi camera (Results I, 3.2.2), with each frame recorded at 10 minute intervals. This allowed for quantitation of the turn using FIJI (Schindelin *et al.* 2012a). The turn was calculated by counting deflection of the root at 10 minute intervals. The deflection at t_n was calculated by subtracting the degree angle of the root at t_0 from the degree angle of the root at t_n (Figure 42B). A population of wild type roots have been subjected to mock conditions using V-box set up, but without the electric field on or the roots were subject to 1V/cm electric field exposure. Root tip deflections were calculated for every 10 minutes recorded during two hours of E field exposure. The distributions of the deflections can be seen in box plot (Figure 42C).

At every time point measured, the root tips exposed to 1V/cm E field have a significantly different root tip deflection compared with the root tips exposed to mock conditions. Even in as little as 10 minutes of electric stimulation the average (±standard deviation) deflection exposed root tips was measured at 9.4^{o}±3.66^{o} in comparison with 1.1^{o}±2^{o} deflection of root tips subjected to mock exposure. It shows that 10 minutes is sufficient to cause an observable electrotropism in *Arabidopsis thaliana* roots. 10 minutes was a limit based on the time-lapse imaging, and therefore, it is likely that the difference of root tip deflection between E field exposed and non-exposed root tips may be detectable even earlier than 10 minutes, however this was not measured.

In addition, the average root tip deflection at 60 minutes of E field exposure was found to be 29.6°±13° and it was found to be 34°±15.1° at 120 minutes. Together with the observed linear increase (Figure 42C) of the root tip deflection between 10 and 60 minutes, this suggests that *Arabidopsis* roots subjected to E field perform most of the electrotropic turn within first hour of external electric field treatment. After the first hour, root tips remain bent towards cathode, however the electrotropic turn does not further increase.

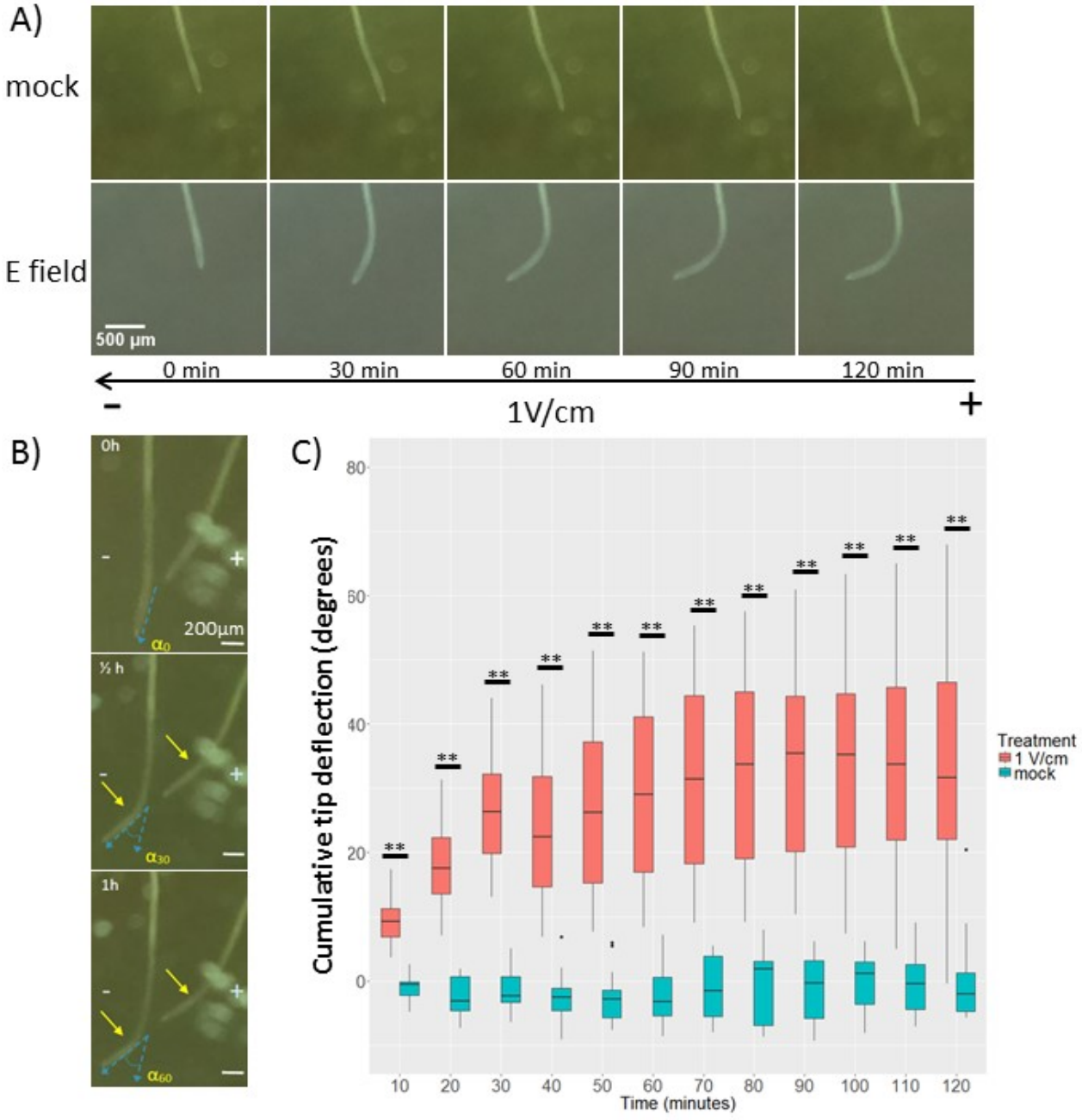

Figure 42: Electrotropism of wildtype (col-0) roots exposed to 1V/cm electric field. **A)** Images representing a timelapse of wt roots collected within V-box, in mock (N=14) and when exposed to 1V/cm E field (N=24). Each image represents a 30 minutes. Scalebar 500µm. **B)** Quantification of angles from the image data collected. Deflection was calculated as difference between angle at t=0, and an angle at t=n. **C)** Quantitative representation of the electrotropic behaviour. The deflection of each root tip was calculated as a difference between angle of the root tip at the t=0 and the angle of the root tip at the observed time point t=n. The box plot shows the distribution of root tip deflections over period of 2 hours in discreet 10 minute intervals. The box plot shows distribution median with a line in within the box, the box itself stands for 50% of the distribution closest to the median. The lines below and above the box stand for two quadrants containing data distributed 25% and more away from the median. The two distributions show roots exposed to mock condition (N≥14) and to 1V/cm E field (N≥24). The two distributions were tested for normality using Shapiro Wilk test. Variance of the distributions was tested using Fischer's test, and significant difference between the two distributions was tested using Welch T test. Any significant difference ($p<0.01$) is marked with **.

5.2.2 Arabidopsis root electrotropism when exposed to 1V/cm E field in media with different compositions

In addition to exposing root tips in medium B to 1V/cm electric field as it was previously reported by (Stenz and Weisenseel 1993), we wanted to see how the electrotropic response of the root tips changes with different media in comparison to the response observed when roots were submerged in medium B. *A. thaliana* roots were subjected to 1V/cm electric field in six common plant media at three different concentrations. The results were collected with the help of supervised MRes student, Philip Li. The media tested are listed in Table 11. The electric current was measured for each medium, while being pumped in the V-box set up (Results I, 3.2.2). With less concentrated media we observed predicted weaker current.

It can be observed in Figure 43A that the root tips submerged in 1/4X media turned less than those submerged in 1/10X media which turned less than the root tips submerged in 1/500X media. Variation in deflection of root tips can be observed also between individual media types, as a result of different media consistencies. The distributions of the root tip deflections in different media measured at 2 hour mark of 1V/cm E field exposure can be seen in box plot in Figure 43B.

The root tips submerged to 1/4X White's media performed statistically same root tip turn with an average of 34°±19° after two hours as those submerged to medium B, which showed 34°±15.1° deflection. DKW, Hoagland's No.2, Gamborg's B-5 and Chu (N6) media at 1/4X concentration caused a significant decrease in the distributions of root tip deflections of WT *Arabidopsis* roots in comparison to medium B. Also, root tips submerged in milliQ water and exposed to 1V/cm E field were observed to show a significant decrease in root tip deflection after 2 hours with respect to medium B and an average deflection of 4.28°±19.29°. The root tips submerged in 1/4X MS media and exposed to E field after 2 hours showed an average root tip deflection of 11.6°±18° and a distribution of deflections that is statistically same to all the other deflection distributions observed. This is most likely due to low number of roots used to construct the distribution.

When roots were submerged in 1/10X media concentrations and exposed to 1V/cm E field, after 2 hours all of the root deflection distributions were statistically same to the deflections measured when root tips were submerged in medium B during E field exposure. The deflections of root tips submerged to 1/10X Chu (N6), 1/10X Hoagland's No.2 and 1/10X MS have been also statistically same with the deflections of the root tips submerged to milliQ water. This may have resulted from low number of roots measured for each distribution.

When roots were submerged in 1/500X media concentration and exposed to 1V/cm E field, after two hours, the deflection distributions of the root tip submerged to DKW, Gamborg's B-5, Hoagland's No.2 and MS was statistically same to those root tip deflections collected by submerging roots in medium B and exposing them to E field. The roots submerged in Chu (N6) media for the E field exposure showed a significantly higher average of deflections at 76°±14°, in comparison with root tip deflections of roots submerged to medium B. The roots submerged in White's media for the E field exposure showed a significantly higher average of deflections at 51.25°±24°, in comparison with root tip deflections of roots submerged to medium B, but significantly lower average of deflections in comparison with roots submerged to Chu (N6) media.

Table 11: Six different plant media as well as two hypoionic media were tested to submerge roots during electrotropic experiments in V-box. The concentration, given amount and current measurement for each medium is shown here.

Name	Abbreviation	Concentration	Amount (g/L)	Current (mA)
Murashige and Skoog	MS	1/4X	1.075	8.19
		1/10X	0.430	1.27
		1/500X	0.008	0.55
DKW/Juglans	DKW	1/4X	1.300	9.28
		1/10X	0.520	1.18
		1/500X	0.010	0.54
Hoagland's No. 2	H2	1/4X	0.400	3.57
		1/10X	0.160	1.66
		1/500X	0.003	0.4
Gamborg's B-5	GB5	1/4X	0.780	12.11
		1/10X	0.310	3.41
		1/500X	0.006	0.55
White's	White's	1/4X	0.234	2.37
		1/10X	0.093	1.08
		1/500X	0.001	0.38
Chu (N6)	ChuN6	1/4X	1.000	10.56
		1/10X	0.400	3.41
		1/500X	0.008	0.43
Medium B		No salts		0.17
Water		No salts		0.06

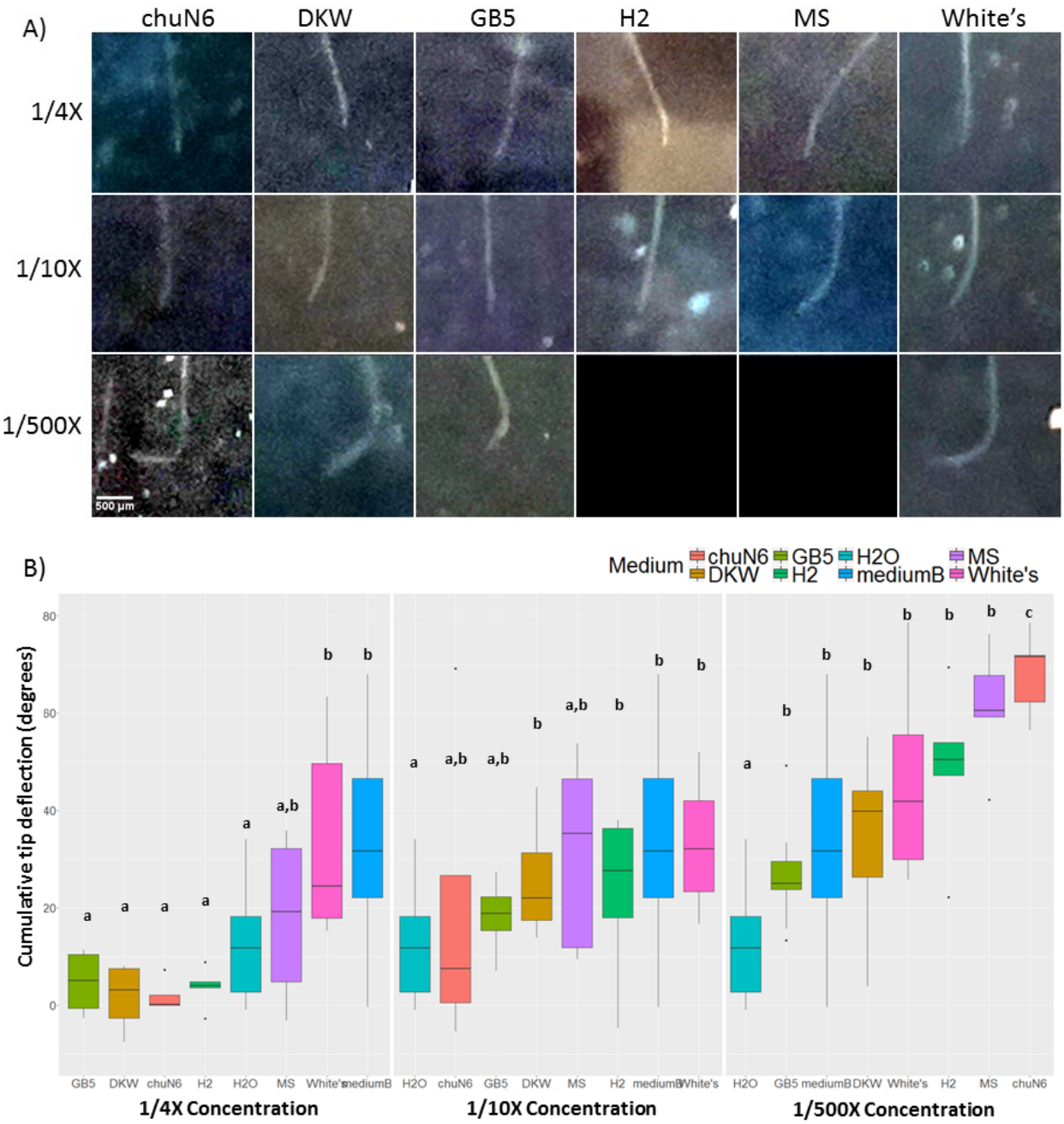

Figure 43: WT roots of A. thaliana were exposed to 1V/cm E field in different media at different concentrations (Table 11). Root deflections were observed after 2 hours of exposure. A) Images show a representative root for each different medium tested after 2 hours in 1V/cm E field. Each image represents at least N≥5 roots. Scalebar 500 µm. B) Quantitative representation of root tip electrotropism of WT (col-0) roots in 1/4X, 1/10X & 1/500X concentration of different plant salt media when exposed to 1V/cm E field. The deflection of each root tip was calculated as a difference between angle of the root tip at the t=0 and the angle of the root tip at t=120. The box plot shows the distribution of root tip deflections at the 2 hour timepoint. Six different plant media were tested, with medium B and water acting as a control. Number of roots measured in each medium that was used for each distribution was at least 4. The box plot shows distribution median with a line in within the box, the box itself stands for 50% of the distribution closest to the median. The lines below and above the box stand for two quadrants containing data distributed 25% and more away from the median. The distributions were tested for normality using Shapiro-Wilk test. The data was tested for variance within each concentration group using one way ANOVA test. Significant differences between individual distributions within a group were tested with post-hoc Tukey HSD test. Letters are used to point out significant differences, $p<0.05$.

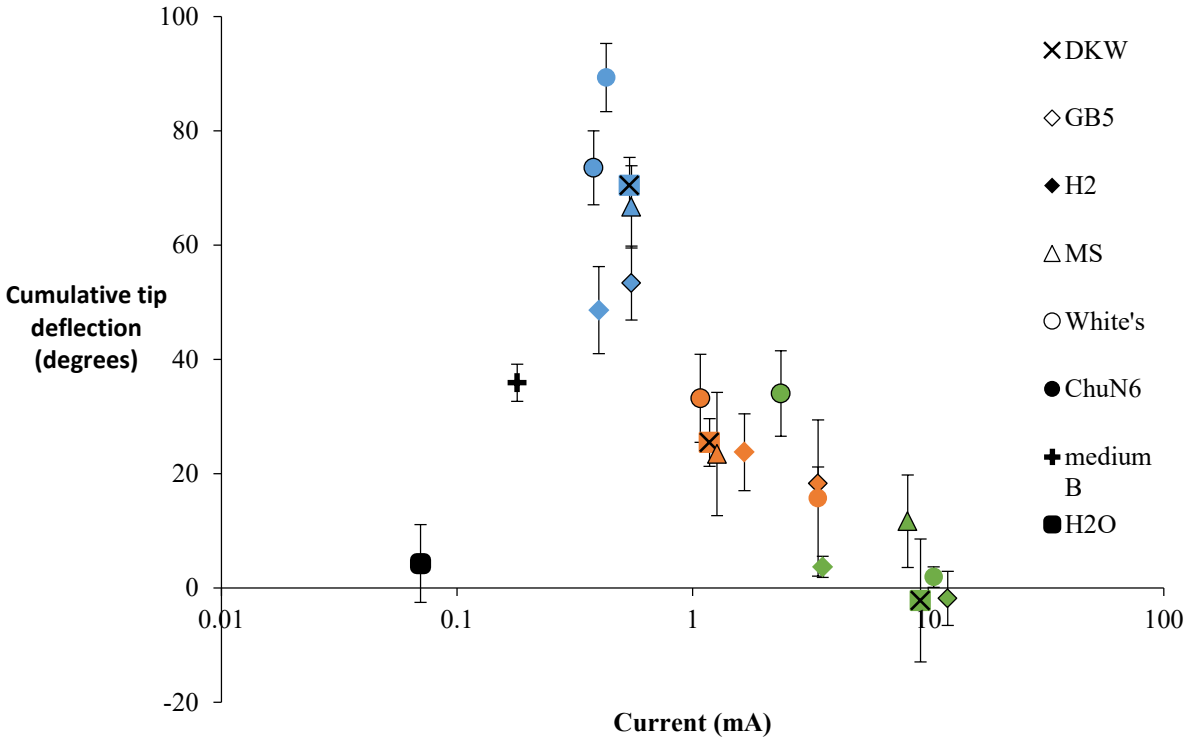

Figure 44: Deflections of root tip after exposure to 1V/cm E field for 2 hours in different media. Each point contains at least N≥4 root tip deflections. The root tips were exposed to five different salt media at 3 different concentrations (1/4X, green), (1/10X, orange) & (1/500X, blue) and two media without salts (medium B, water). The data is plotted against current (mA) that was measured during exposure within the V-box set up, for each different medium. The x-axis is shown in log scale to better fit the data onto the graph, the current values measured, were not subjected to any calculation post-measurement. Symbols indicate averages, error bars show SEM.

Since different media contain different components and different concentrations of same chemical components, our goal is not trying to figure out which component of the media may have been the result of the shown differences. Instead we wanted to understand how the overall conductance of all the different media may affect the ability of the *A. thaliana* to perform the electrotropic turn.

We have plotted the average ± (standard error of the mean) deflections of root tips when submerged to all of the tested media after 2 hour 1V/cm electric field exposure against the current measured in the media during the exposure (Figure 44). This shows that despite variation in the media, there is a zone of current between 0.18mA-2.37mA in the V-box set up that has to be generated when exposing roots to 1V/cm electric field in order to observe the electrotropic turn. This can also be thought of as the salinity of the media, which needs to be present. Any media that

contain salinity that leads to current being lower or higher than the 0.18mA-2.37mA will result in *Arabidopsis thaliana* roots turning significantly less, when exposed to 1V/cm E field.

5.2.3 A. thaliana root electrotropism is caused by asymmetric cell expansion

After macroscopic observations, the aim was to observe the electropic turn of *Arabidopsis* on microscopic scale. For this we have used the custom build V-slide (Results I, 3.2.3) that allowed for perfusion of medium and presence of electric field while being able to be mounted into the stage of confocal microscope. Wild type (col-0) *Arabidopsis thaliana* root tips expressing *pUBQ10::WAVE131:YFP* construct coding for a yellow fluorescent cell membrane marker (Geldner *et al.* 2009), were subjected to 1V/cm electric field in medium B while mounted in V-slide.

The electrotropic effect was recorded as time-lapse video using camera attached to confocal microscope with each frame recorded at 2 minute intervals for duration of 60 minutes. This allowed for high temporal and spatial resolution observation of the electrotropic turn (Figure 45A). Due to low throughput nature of the observation only 3 roots were observed. However using qualitative analysis, epidermal root cells found in the transition zone of root meristem can be seen to expand more on the side of the root facing positive electrode than those facing negative electrode, in 60 minutes of exposure to electric field (Figure 45B).

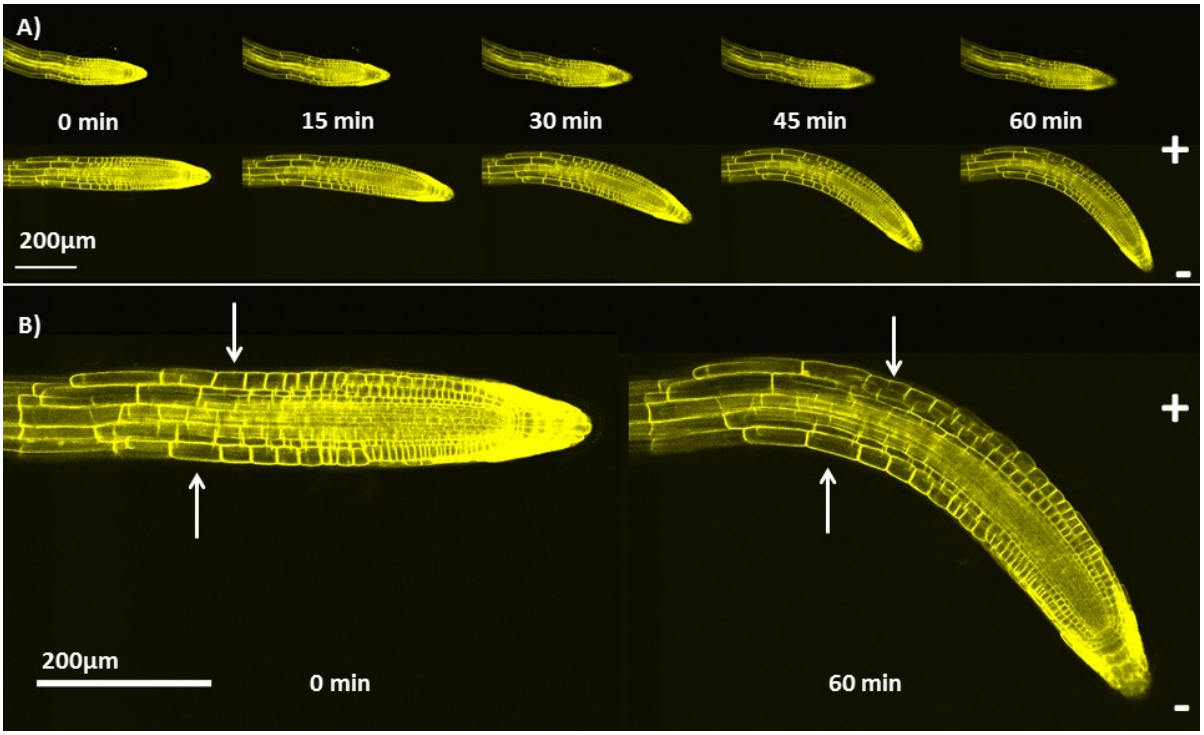

Figure 45: Here shown is the effect of the 1V/cm E field on a WT (col-0) root expressing WAVE131:YFP protein observed using V-slide. A) roots exposed to mock condition (top) and those exposed to E field (bottom) are shown in a panel depicting timelapsed images, with 15 minute intervals. The + and – depict the direction of the E field. The scalebar represents 200µm, images showing mock and E field condition stand for N≥3 roots. B) larger size images of a root exposed to E field at t=0 and t=60 min are shown. The + and – depict the direction of the E field. The arrows are highlighting the epidermal area of the root where asymmetrical expansion of cells on the side facing +ve electrode vs the side facing –ve electrode can be seen. The image stands for 3 roots.

5.2.4 Side effects of external electric field exposure on A. thaliana roots

According to previous reports a prolonged exposure of roots to electric field, with varying strengths can cause the roots to be damaged and also in some instances cause the root to turn towards the anode (Stenz and Weisenseel 1993), (Wawrecki and Zagórska-Marek 2007). We wanted to examine if there is any observable side effect on wild type *Arabidopsis* roots when exposed to 1V/cm electric field in medium B, for duration longer than 120 minutes.

Using V-box set up with Raspberry Pi camera we have examined any changes other than the described electropic turn on 24 roots exposed to long duration electric field exposure. With qualitative analysis we have observed all 24 root tips to 'whiten' and stop growing after more than 4 hours of constant 1V/cm electric field exposure (Figure 46A). This means that the electrotropic turn shown in Figure 42 is a temporary effect preceding irreversible damage caused by the electric field that results in the root to lose ability to grow.

It is important to note that a proportion (8/17, 47%) of wild type (col-0) *Arabidopsis* roots exposed to mock conditions of electric field treatment while still submerged in medium B, in V-box set up, but with no E field applied have also shown whitened root tips after several hours (image not shown).

In order to further examine whitening damage that was caused by the mixed contribution of medium B and electric field on *A. thaliana* roots, we have observed roots expressing *WAVE131:YFP* membrane marker, perfoming the electrotropic turn in medium B. This qualitative examination was done using the V-slide set up, confocal microscope and stronger 2.5V/cm electric field. Within 10-30 minutes of being subject to stronger 2.5V/cm electric field, the epidermal cells in the transition zone facing positive electrode have been observed to swell and burst (Figure 46B). Since we have observed only a small number of roots, we can only qualitatively compare the side of the root facing positive electrode with the root side facing negative electrode. In all the observations performed, epidermal cells found facing negative electrode were never observed to burst in comparison to epidermal cells found facing positive electrode, which burst every time.

In addition to cellular morphological changes, we wanted to see if there are any ion dynamic changes in the root tips during the same 2.5V/cm electric field treatment in medium B in V slide. We have used the *pUBQ10::YC3.6* (Krebs *et al.* 2012) FRET calcium ratiometric reporter to observe any changes in the Ca^{2+} concentration during the burst effect observed in epidermal cells when roots were subjected to electric field. The images in the Figure 47 show the result of ratiometric analyses of signals received from two fluorescent components of the YC3.6 reporter. It can be seen that within 10-30 minutes all of the roots that were observed exhibit an increased presence Ca^{2+} ions preceding the epidermal cell burst.

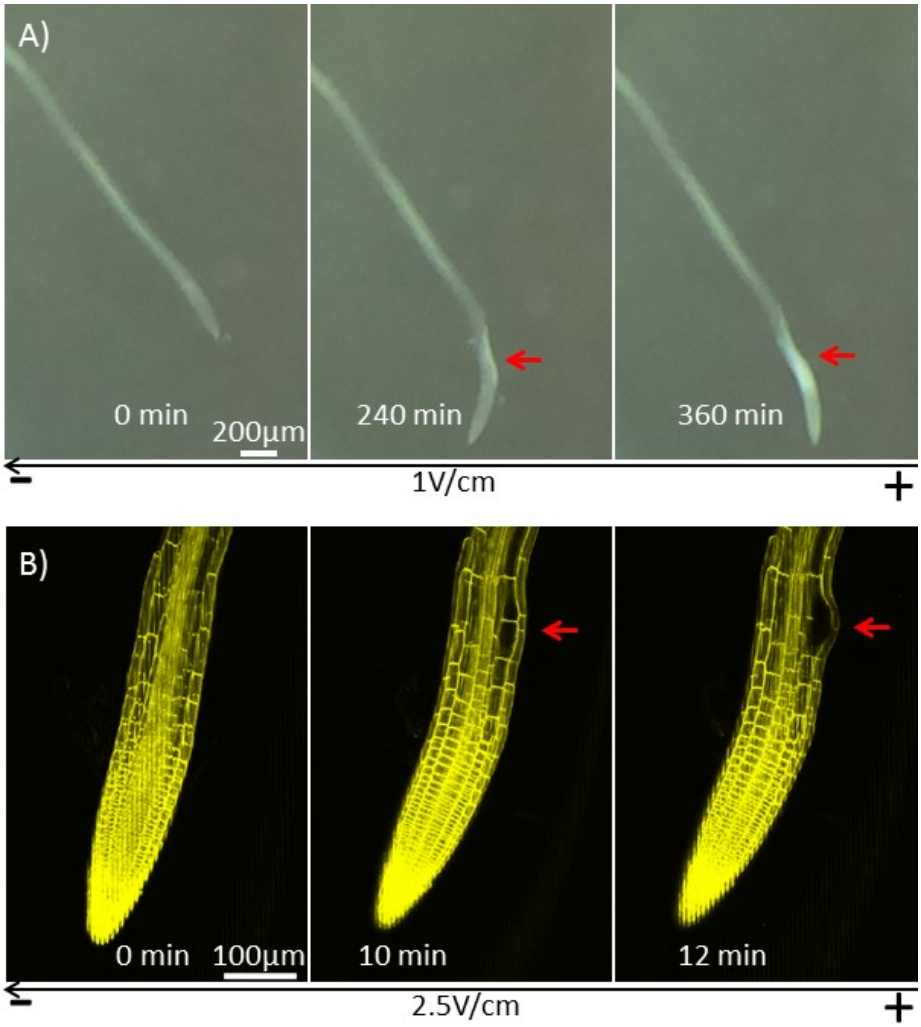

Figure 46: Damage caused to roots with E field under specific conditions in medium B. A) Exposure of WT (col-0) root tips to 1V/cm E field in medium B with live time-lapse. E field exposure for longer than 4 hours using V-box set up causes the root tip to whiten. After this event the roots were not seen growing or turning. The red arrow points to the site of the damage. The images represent effect observed in 24 roots. Scalebar 200 µm. B) WT root tips expressing WAVE131:YFP fluorescent membrane marker were subjected to 2.5V/cm E field in medium B using V-slide set up to induce damage in a live time-lapse. The red arrow points to cells that face +ve electrode and eventually burst. The images represent 3 observed roots. Scalebar 100 µm.

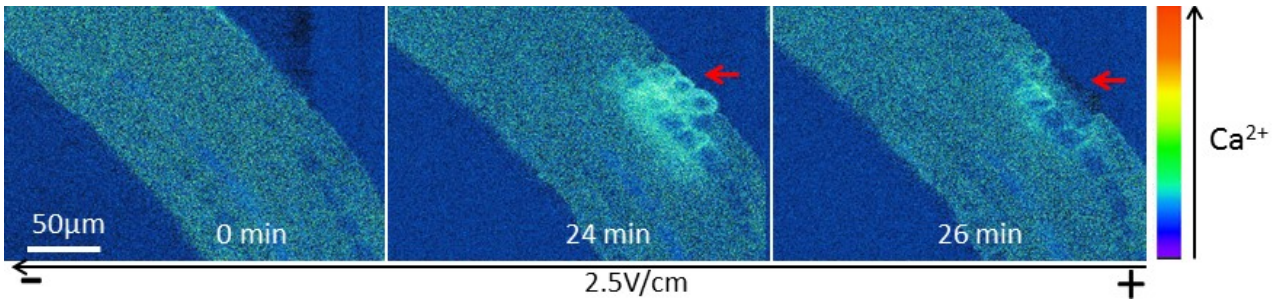

Figure 47: *A. thaliana* WT roots expressing YC3.6:NES calcium FRET reporter were exposed to 2.5V/cm E field in medium B using V-slide observed with live time-lapse. The images show ratiometric result made after processing raw images (Methods, 2.3.8). A given ratio is indicated with a colour from colour bar. Higher ratio indicates increased presence of Ca^{2+} free ions. Higher ratio is depicted by colours closer to red end of the colour bar and lower ratio is shown by colours closer to purple end of the colour bar. The red arrow points increased Ca^{2+} presence and cells that eventually burst. The images represent 2 roots. The scalebar 50 µm.

5.2.5 Agravitropic roots are capable of electrotropic turn

In order to examine if gravitropism and electrotropism share parts of a molecular mechanism, we have subjected *pin2* and *aux1* agravitropic roots submerged in medium B to 1V/cm electric field using V-box (Results I, 3.2.2). The results were collected as a timelapse video with Raspberry Pi camera throughout 2 hour E field exposure with 10 minute frame intervals. The collection of data for *pin2* mutant was helped by a supervised MRes student Philip Li, and for the *aux1* mutant the data collection was helped by a supervised undergraduate student Mara Sgroi.

We have confirmed that the populations of roots we use for the electrotropic experiment are indeed agravitropic (Figure 48A), (Figure 49A). We have observed that both *aux1* and *pin2* mutant populations of roots had a significantly different root tip deflection only 10 minutes after the start of the electric field exposure in comparison with the roots that were not subjected to E field (Figure 48B),(Figure 49B). It could be seen that E field exposed *pin2* root tips have gradually increased the root tip deflection until 110 minutes of exposure when the average (±standard deviation) deflection was found to be 74.4°±23.3°. This is in contrast to the roots exposed to mock conditions which showed the average deflection of 0.6°±3.4° (Figure 48B).

Population of *aux1* roots exposed to E field has behaved differently to *pin2* roots. *Aux1* root tips exposed to electric field have shown to be significantly different to roots exposed to mock conditions until 60 minutes of exposure with average deflection of 26.8°±15.1° in comparison to 5.77°±17.1°. However by 120 minutes, *aux1* roots that were subject to E field exposure were not significantly different to those subjected to mock conditions with an average deflection of 8.8°±28.9° for exposed roots versus 11.7°±25.3° average deflection of roots exposed to mock condition (Figure 49B).

As a next step we compared *pin2* and *aux1* electrotropism to the one of wild type col-0 roots. Qualitatively the electrotropic turn appears the same for agravitropic mutants as the one of WT roots until 60 minute mark. At 120 minute mark it can be seen that the *aux1* electrotropic turn is

less than that of wild type plants, while *pin2* electrotropic turn does not appear to decrease after 2 hours of E field exposure (Figure 48C), (Figure 49C). When we quantitatively compared root tip deflections of *pin2* roots to WT roots both exposed to 1V/cm electric field we observed significantly increased electrotropism of *pin2* roots in comparison with WT roots from 40 minutes of E field exposure onwards until 110 minutes. At this point the average deflection of *pin2* root tips was found to be $74.4^{o}\pm23.3^{o}$ in comparison to WT roots which showed an average deflection of $34.4^{o}\pm17^{o}$ (Figure 48D).

The distribution of aux1 root tip deflections, caused by the root tip being subject to 1V/cm E field appears to be statistically same as the distribution of wild type root tip deflections until 90 minutes. At this point the average deflection of aux1 root tips is $21.7^{o}\pm23.1^{o}$ and the average deflection of the wild type root tips is found to be $34.9^{o}\pm15.1^{o}$. At 120 minute mark the root tips of WT roots are significantly more deflected than that of the *aux1* root tips with the average deflection of WT roots at $34.4^{o}\pm17^{o}$ and $8.8^{o}\pm28.9^{o}$ that of *aux1* roots (Figure 49D). The results here show that even though root electrotropism of agravitropic roots is similar to that of wild type roots for the first hour of the electrotropic phenomenon, in the second hour of the electrotropic turn *pin2* roots continue increasing their electrotropic turn, while wild type roots stagnate their turn and the *aux1* root electrotropic turn is decreased. This suggests that AUX1 protein and therefore the influx transport of auxin in the lateral root cap cells as well as epidermal cells may be necessary for the maintenance of the root tip turn. The result also suggests that PIN2 is not necessary for the electrotropic turn.

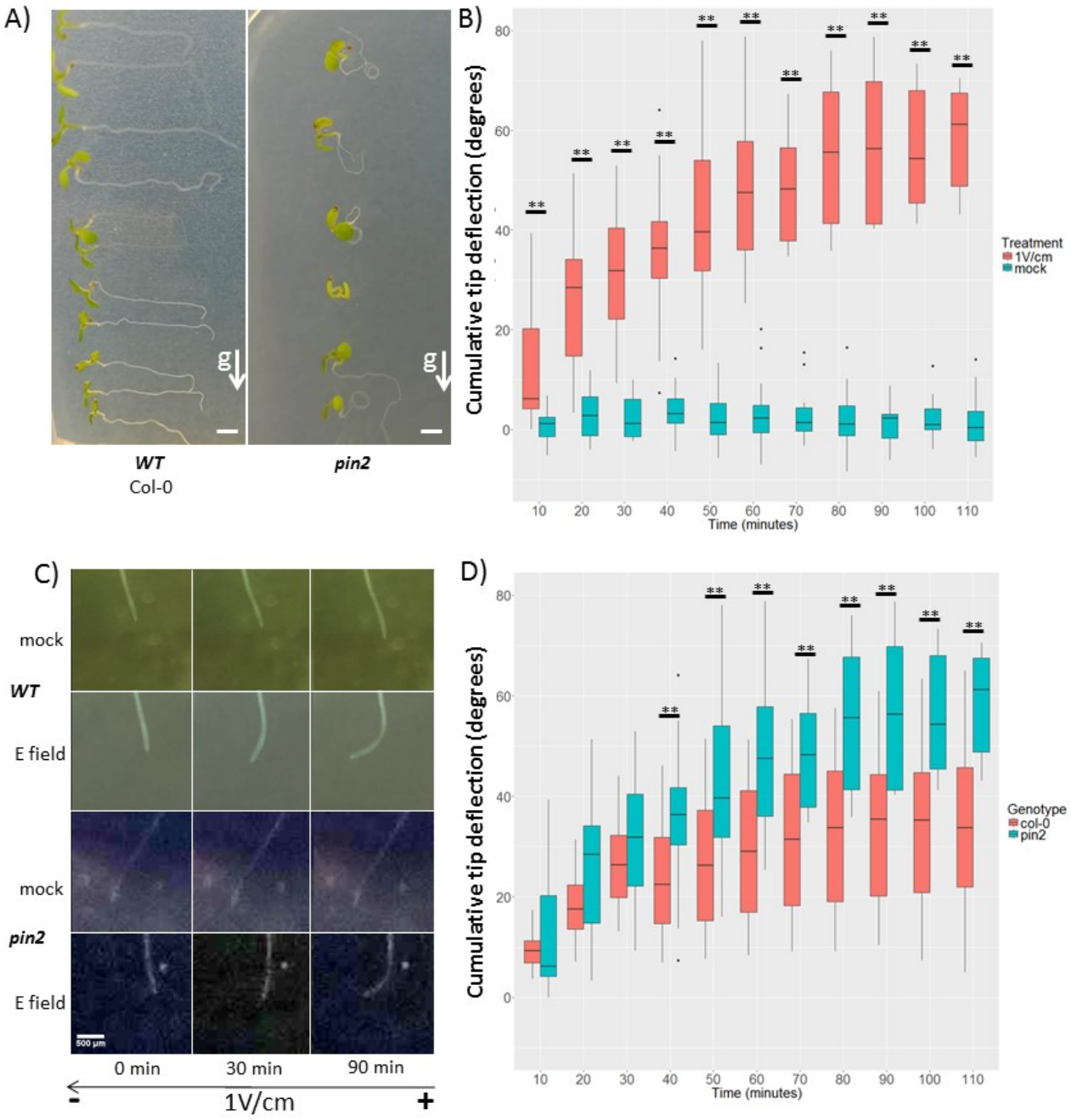

Figure 48: *A. thaliana* agravitropic *pin2 (-/-)* roots show electrotropic behaviour. **A)** WT (col-0) roots positioned perpendicularly to gravity vector (arrow) are able to reorient root tip, so that root growth is aligned with the gravity field. *pin2 (-/-)* roots are unable to respond to gravity field and grow any direction. Scalebar is 500µm **B)** Quantitative description of electrotropism of *pin2* (-/-)roots. The box plot show distributions of root deflections collected by measuring an angle of a root at t=0 and t=n and counting the difference. Total of N=18 roots were exposed to mock conditions and N=10 roots to 1V/cm E field in V-box, while submerged in medium B. **C)** Images showing time lapse of WT and *pin2 (-/-)* roots in V-box submerged in medium B, exposed either to mock condition or to 1V/cm E field. The scalebar stands for 500µm. **D)** Quantitative comparison of electrotropism of WT and *pin2* (-/-) roots. The box plot show distributions of root deflections collected by measuring an angle of a root at t=0 and t=n and counting the difference. Total of N=10 *pin2 (-/-)* and N=24 WT roots were exposed to 1V/cm E field in V-box, while submerged in medium B. The box plots in (B, D) show the distributions of root tip deflections over period of 110 minutes in discreet 10 minute intervals. The box plot shows distribution median with a line within the box, the box itself stands for 50% of the data closest to the median. The lines below and above the box stand for two quadrants containing data distributed 25% and more away from the median. The distributions were tested for normality using Shapiro Wilk test. Compared distributions were tested for equal variance using Fischer's test, and then tested for significant difference using Welch T test. Any significant difference ($p<0.01$) is marked with **.

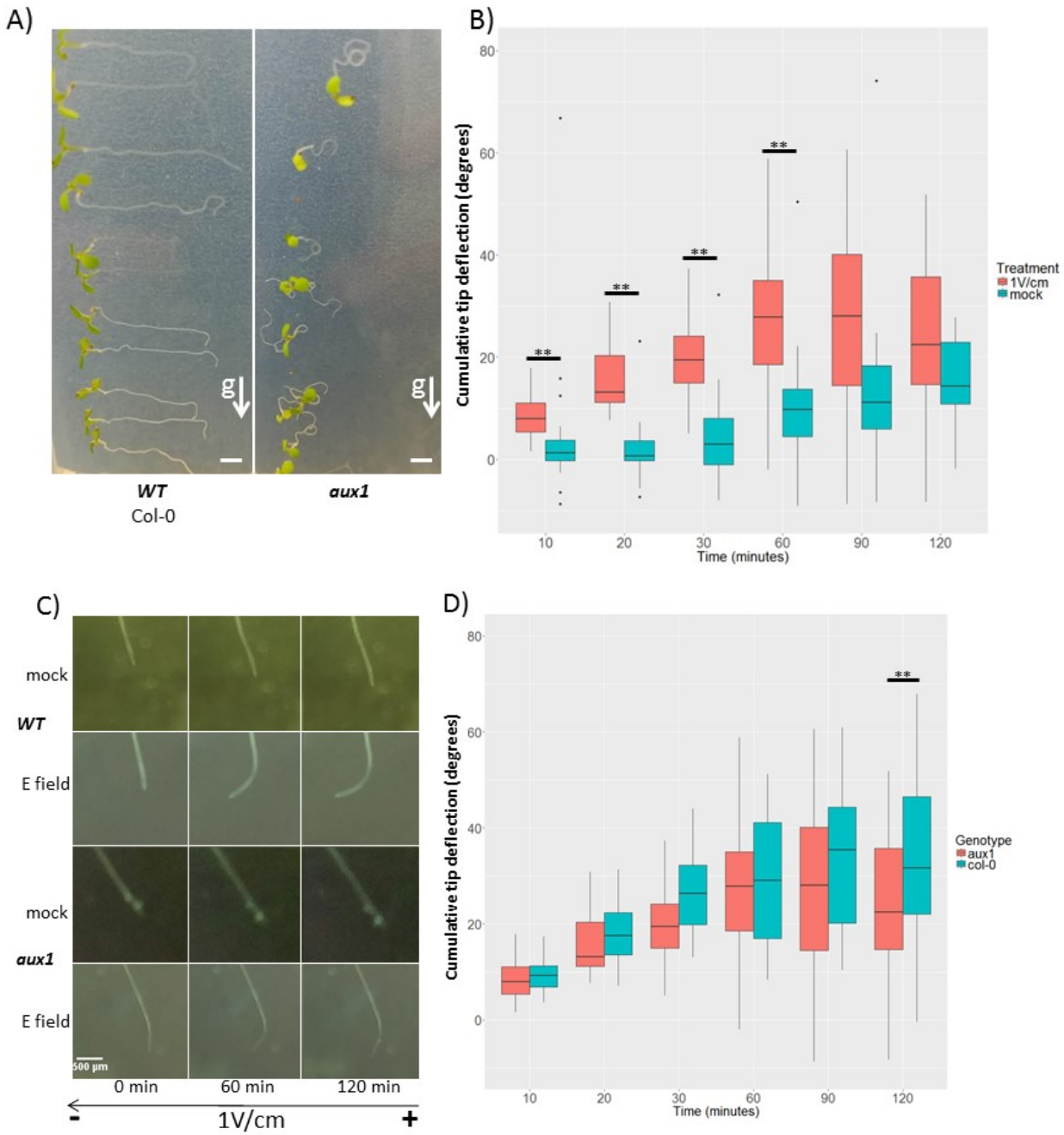

Figure 49: *A. thaliana* agravitropic *aux1 (-/-)* roots show electrotropic behaviour. **A)** WT (col-0) roots positioned perpendicularly to gravity vector (arrow) are able to reorient root tip, so that root growth is aligned with the gravity field. *aux1 (-/-)* roots are unable to respond to gravity field and grow any direction. Scalebar shows 500µm. **B)** Quantitative description of electrotropism of *aux1* (-/-) roots. The box plot show distributions of root deflections collected by measuring an angle of a root at t=0 and t=n and counting the difference. Total of N=23 roots were exposed to mock conditions and N=20 roots to 1V/cm E field in V-box, while submerged in medium B. **C)** Images showing time lapse of WT and *pin2 (-/-)* roots in V-box submerged in medium B, exposed either to mock condition or to 1V/cm E field. The scalebar stands for 500µm. **D)** Quantitative comparison of electrotropism of WT and *aux1* (-/-) roots. The box plot show distributions of root deflections collected by measuring an angle of a root at t=0 and t=n. Total of N=20 *aux1 (-/-)* and N=24 WT roots were exposed to 1V/cm E field in V-box, while submerged in medium B. The box plots in (B, D) show the distributions of root tip deflections over period of 120 minutes in discreet 10 minute intervals for first 30 minutes and 30 minute intervals then on. The box plot shows distribution median with a line within the box, the box itself stands for 50% of the data closest to the median. The lines below and above the box stand for two quadrants containing data distributed 25% and more away from the median. The distributions were tested for normality using Shapiro Wilk test. Compared distributions were tested for equal variance using Fischer's test, and then tested for significant difference using Welch T test. Any significant difference ($p<0.01$) is marked with **.

5.2.6 PIN2 protein membrane distribution during electrotropism

In order to identify a potential PIN2 protein asymmetric distribution after roots have been exposed to 1V/cm electric field using V-box set up, so we have exposed *PIN2::PIN2:GFP* reporter roots to E field for 40 minutes and imaged the root meristem using confocal microscope after the exposure. We wanted to measure the relative concentration of PIN2 proteins in epidermal and cortex cell files found on two sides of the root meristem, when mid-cross section of the root is considered (Figure 50). In order to do this, with the support of a post-doc in the lab, Paolo Baesso, we developed a semi-automatic MATLAB script for identification of membranes and measurement of fluorescence intensity for individual membranes.

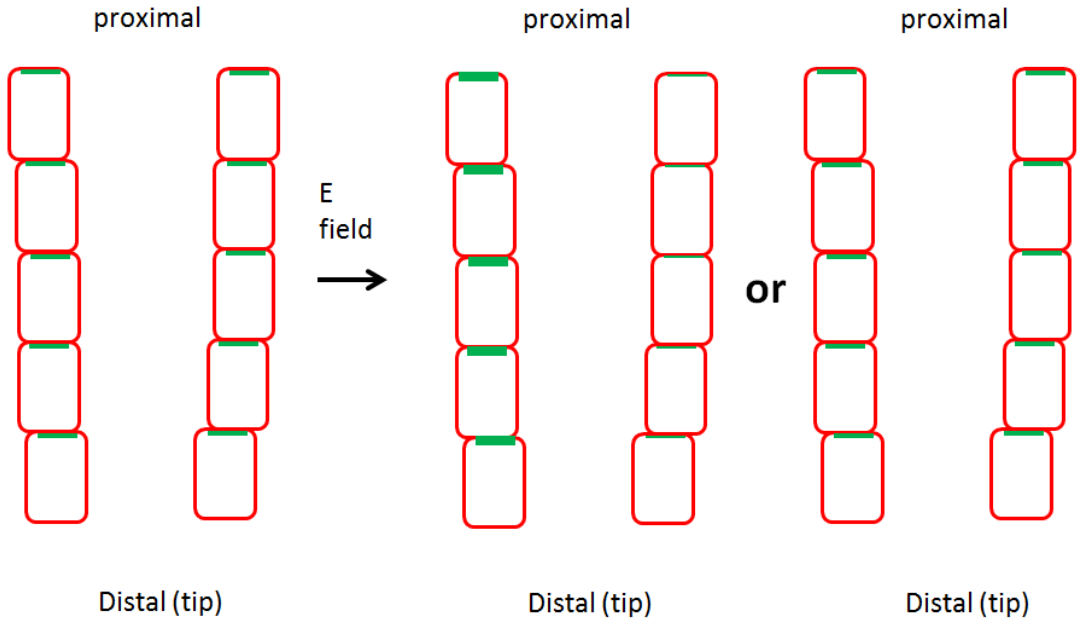

Figure 50: Graphical representation of the hypothesis. The two files represent epidermal cell files at the median section of the root, green lines represent PIN2 protein and its localisation.

The script relies on an operator to input start and end to each membrane, afterwards MATLAB algorithm connects the start end points and generates 17 pixel width rectangle, in which the membrane is found (Figure 51A), (Figure 51B). The width of membrane is less than 17 pixels, so algorithm considers for each point in x, only a centre of mass pixel in y with +/- 4 pixels, calculated using centre of mass algorithm, resulting in 9 pixel membrane widths for each point in x. This is calculated along the length of the whole extracted rectangle (Figure 51C), also described in the

equation below (Methods, 2.3.5). The value for an individual membrane is then generated by averaging individual centre of mass distributions, to get a single value for a membrane with standard deviation. The distributions of fluorescence intensities of individual membranes that were found in root tips in mock condition or the condition where the cell files were facing negative or positive electrode was plotted using box plots (Figure 51D).

$$\forall x_j (1 \leq j \leq L): y_j^{CM} = \frac{\sum_{i=1}^{17} y_i \cdot I(x_j, y_i)}{\sum I(x_j, y_i)}$$

Regardless of the treatment, it appears that there were a small number of membranes that had much higher pixel intensity than all the other counted membranes. This suggests that there are few membranes in epidermis and cortex with much higher PIN2 concentration than all the other membranes in root meristem. When comparing the three distributions, non-parametric statistical test showed difference between the distribution accounting for the membranes of cells facing positive electrode and the other two distributions, those of cells facing no E field and those of cells facing negative electrode. There was no other significant difference observed. The results suggest that the mechanism of PIN2 induced auxin accumulation in the outer cell files of one side of the root meristem is not the cause of electrotropic turn.

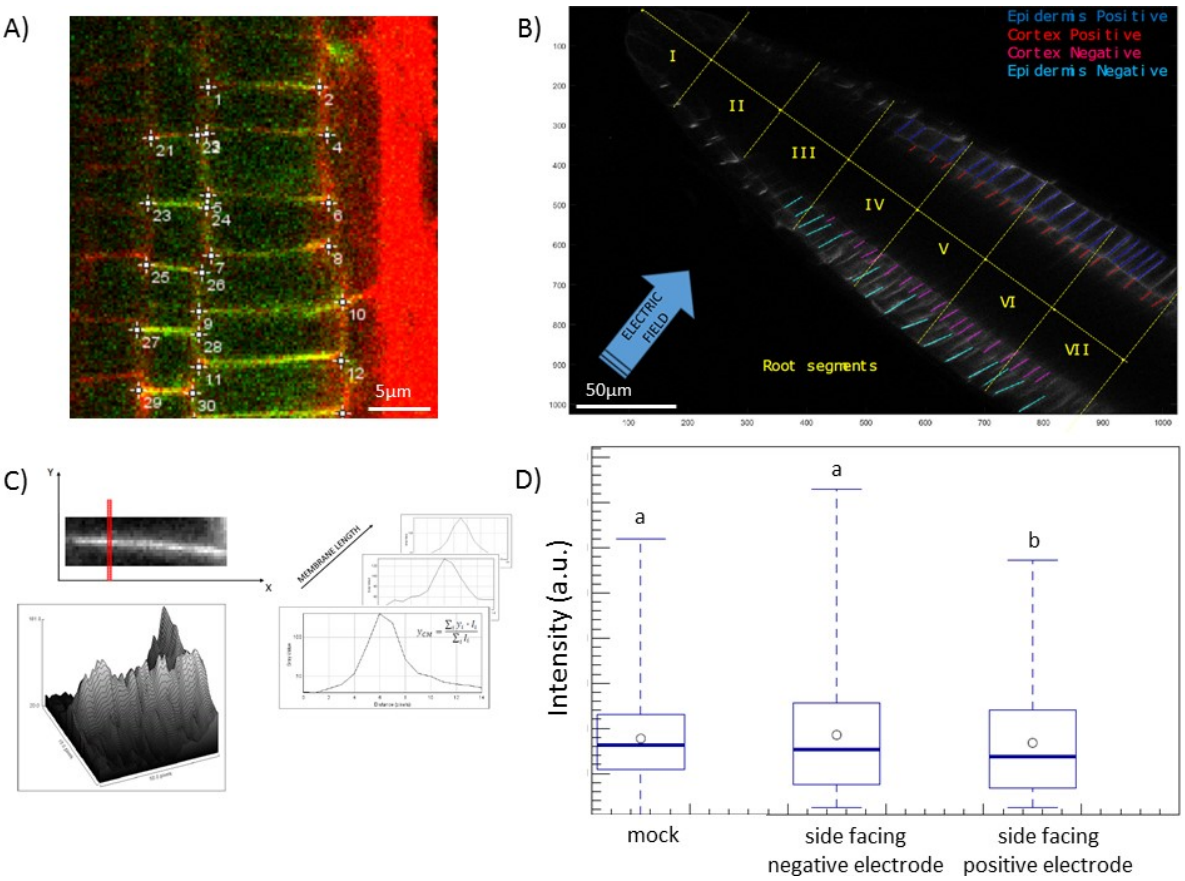

Figure 51: Semi-automatic quantitative analysis of membrane fluorescence of WT roots expressing PIN2:GFP protein exposed to 1V/cm E field in V-box for 30 minutes and submerged in medium B. **A)** Image depicts a WT root expressing PIN2:GFP located on the membranes of epidermal and cortex cells. Image also show marks placed by operator to describe 'start' and 'end' of individual membranes. The root cell wall was stained with 10µg/ml propidium iodide for easier visualisation. Scalebar stands for 10µm. **B)** Location of lines by MATLAB script using 'start ' and 'end' points from operator. Scalebar stands for 50µm. **C)** The algorithm considers 17 pixels next to the highest intensity pixel and makes a hard cut off of 9 pixels closest to centre of mass. The value of these 9 pixels is then averaged to generate an intensity value for an individual point along the membrane line. This is repeated all along the line marking a membrane. Once all the points along an individual membrane have their intensity value generated, an average of these is calculated to give an average intensity value for a single membrane. **D)** Distribution of membrane fluorescence intensities is plotted for roots that was exposed to mock conditions in V-box and submerged in medium B (N=1080 membranes from N=16 roots), and sides of roots that were facing positive electrode (N=531 membranes from N=17 roots) and negative electrode (N=533 membranes from N=17 roots) during exposure to 1V/cm E field in V-box when submerged in medium B. The distributions are shown using boxplots, where line indicates distribution median and circle the average. The box stand for 50% of the distribution closest to the median, and the dotted lines stand for parts of data that are 25% or more away from median. The three distributions were tested for normality using Shapiro-Wilk test and all follow non-normal distribution. Wilcoxon paired signed rank test checked for significant difference, marked with **a** & **b** ($p<0.05$).

5.2.7 Auxin distribution during root electrotropism

We wanted to see if the pattern of auxin distribution was perturbed in roots that subjected to 1V/cm electric field in V-box, in order to assess auxin involvement in the electrotropic turn. Historical evidence showing that in presence of auxin transport inhibitors roots have failed to perform electrotropism (Ishikawa and Evans 1990), (Moore *et al.* 1987).

In order to achieve this we have used ratiometric reporter of auxin dubbed R2D2, with a *RPS5A-mDII-ntdTomato RPS5A-DII-n3xVenus* transgene (Liao *et al.* 2015). This gene expresses two forms of protein that forms a complex with auxin. DII-n3xVENUS, which is degraded within minutes upon binding with auxin, this protein fluoresces yellow and an area within root can be observed to indicate increase of auxin presence with a decrease in fluorescence and mDII-ntdTOMATO, is the second protein, which contains an engineered auxin non-degradable form of DII protein and fluoresces red. Both of the proteins are localised in the nucleus for easy spatial recognition and calculation of auxin presence can be done by generating a ratio between the two fluorescences observed at each imaged nucleus.

We have imaged R2D2 roots using a confocal microscope after 40 minutes of E field exposure. We can observe that qualitatively the distribution of auxin both in root meristem and in the transition zone of roots exposed to mock or 1V/cm E field conditions appear the same (Figure 52A). In order to quantitatively measure the amount of auxin on the sides of the root facing negative and positive electrode as well as mock, the nuclei found in the images of root meristem (distal) and transition zone (proximal) were segmented and the fluorescence ratio was measured in each nucleus (Methods, 2.3.6).

We found that both in the root meristem and at the transition zone there was no significant difference between the epidermal cells subjected to mock exposure versus those that faced positive or negative electrode during 1V/cm electric field exposure (Figure 52B). The results suggest that the auxin distribution in the root tip does not change during root electrotropism. As with any negative

result, it is also likely that we did not detect observable change only because we used our experimental assay together with our tools, R2D2 expressing root and confocal microscope, but for now we cannot confirm any change of auxin distribution as a result of root electrotropism.

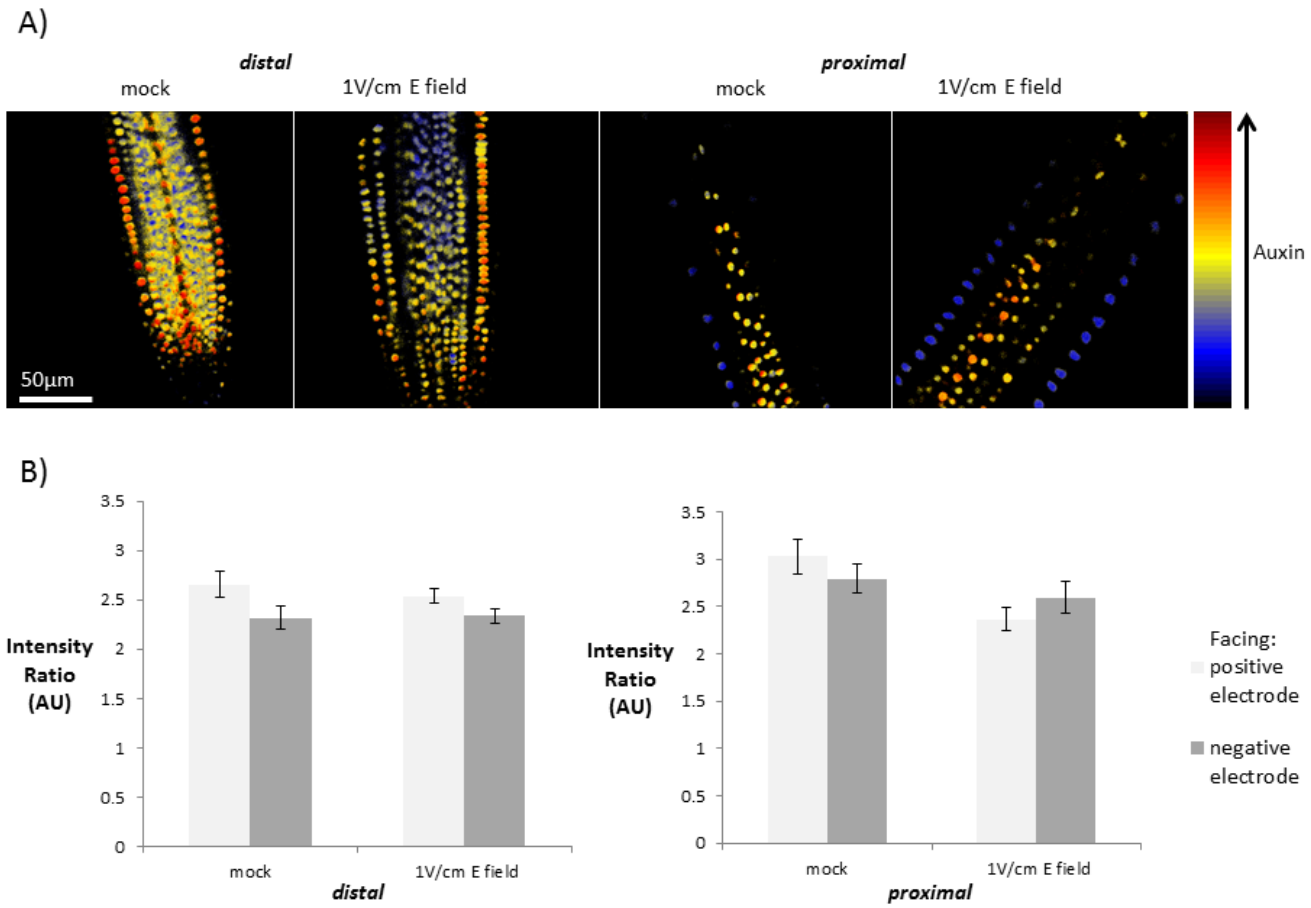

Figure 52: *A. thaliana* roots expressing a transgene *RPS5A-mDII-ntdTomato RPS5A-DII-n3xVenus* ratiometric reporter of auxin dubbed *R2D2* were subjected to 1V/cm E field for 30 minutes in V-box and submerged in medium B. A) Images show the ratiometric nucleus localised response of the reporter within the root to auxin presence in mock (N=12) condition and E field treated (N=16) condition in the distal end of the root tip in the meristem, as well as the response of the reporter in the proximal part of the root, when subjected to mock (N=11) or E field (N=13) treatment. The colour bar indicates the level of auxin in each nucleus with black being the lowest amount of auxin and red being the highest. The Scalebar stands for 50µm. B) Graph shows fluorescence intensity ratio for two sides of the root (facing negative and positive electrode) in two, distal and proximal, regions of the root tip. The mean (±Standard Error of the Mean) showed by a barplot has been constructed by measuring fluorescence intensity ratio in the nuclei of epidermal cells of the tested roots, with at least N=124 nuclei manually segmented per sample. The fluorescence intensity ratio was calculated by using ln(CTRL intensity/ SIGNAL intensity). The control intensity is the fluorescence intensity collected using confocal microscope from the mDII-ntdTomato fluorophore and signal intensity is the fluorescence intensity collected from the DII-n3xVenus. The distributions were tested for normality using Shapiro-Wilk test. The data distributions have been tested for equal variance using Fisher's test and tested for significant difference using Welch T-test.

5.2.8 Searching for non-electrotropic mutant using reverse genetic screen

We wanted to find a genetic link to the electropic phenomenon. One way of searching for a genetic link is to examine *Arabidopsis* mutants with non-functional genes and assess them for a phenotype, in our case electrotropism. Any mutants that do not have the same electrotropic turn as wild type *Arabidopsis*, particularly if they show decreased or non-existent turn, shows indication of necessity for a functional gene.

In order to find a non-electrotropic mutant, a number of genes were selected to be screened quantitatively for a decrease in root tip deflection for 2 hours of 1V/cm electric field exposure in the V-box set up (Results I, 3.2.2). Timelapse images of all the roots with selected mutations were collected with Raspberry Pi camera. The list of genes screened is shown in Table 12. The genes for ion channels were picked since we hypothesised many ions in the root are affected by electric field and cell ion transport may be necessary for electrotropism. We have also included three more PIN auxin transporters, *pin1*, *pin3*, *pin7* in order to assess more auxin transporters than just *pin2* and *aux1*.

In order to increase throughput and speed of the screen, the individuals screened were not genotyped. The seeds were obtained from Nottingham Seed Stock Centre, whenever possible of homozygous genotype. To mitigate this uncertainty we used at least two alleles for each gene, in some cases three alleles. The root deflection data of different alleles were afterwards combined to provide a distribution of deflections for roots with a mutation in a single gene. The data were collected with the help of supervised undergraduate student Shayna Lin, and supervised MSc student Nicolas Oliver.

The distributions of deflections of all mutants exposed to 1V/cm electric field for 2 hours as well as those of two different wild-type ecotypes (col-0 and Ler) are plotted as box plots in Figure 53. From the individual distributions, we can see only mutants with non-functional gene *glr1.2* and *glr3.4* to have significantly decreased cumulative root tip deflection in all of the time points. In

addition, mutants with non-functional genes *clcD*, *kat1*, *skor* and *tpc1* have decreased cumulative root tip deflection in the first 30 minutes, and mutant *gork* has decreased deflection in the first 50 minutes. Also mutant *ost2-1D* with constantly active proton pump has a decreased root tip deflection at 120 minutes, but not before. *pin1,* auxin transport mutant had an increased root tip deflection after 90 minutes and *pin3,* auxin transport mutant had increased root tip deflection after 60 minutes, but not before. Last *glr2.4* mutant had decreased root tip deflection the first 30 minutes and the last 30 minutes, but not in between (Figure 53).

Overall the results suggest that genes related to metal ion transport are necessary for the root tip electrotropism earlier than the genes involved in proton transport. Additionally at least two of the GLRs, GLR 1.2 and GLR3.4 are necessary for all stages of electrotropism. PIN mutants, PIN3 and PIN1 follow similar pattern to that of PIN2, when absent, root electrotropism increases.

In order to simplify the comparison of all the root tip deflections collected and be able to draw conclusion from such a big dataset we compared all of the distributions together at 60 minute mark of 1V/cm electric field exposure. This time was chosen as it was visually observed to be an inflection point after which wildtype electrotropism changes less than before this point. Some of the distributions had incomplete data sets not spanning the whole 120 minute duration, but all of them were measured at least up to an hour. Also higher variability of some of the data produced from the screen after 2 hours of electric field exposure was observed than after 60 minutes. The data is shown in Figure 54.

Table 12: The table shows a collection of genes which were tested for their role in *A. thaliana* electrotropism. *A. thaliana* roots with knock-out alleles for selected genes, were subjected to 1V/cm E field in V-box when submerged in medium B for 2 hours. The table lists the average deflection (±standard deviation) after 1 hour of exposure for a given number of roots when subjected to E field. The table also shows ecotype background of each of the mutants, as well as mutant line (when known), type of knock-out mutation, and an allele name(s). When the allele is previously unpublished, the Nottingham Arabidopsis Seed Centre number is used instead. The function of a protein that the gene codes for is also mentioned.

Gene	Function	Allele	Mutation type	Line	Background	Average deflection	N° of roots
WT					Col-0	29.6±13.13	24
WT					Ler	32.77±18.01	14
pin1	Auxin efflux transporter	*pin1-1*	NA (Ethyl Methane Sulfonate)		En-2	40.16±12.76	23
pin3	Auxin efflux transporter	*pin3-4*	T-DNA Insertion	SALK	Col-0	52±18.28	25
pin7	Auxin efflux transporter	*pin7-1*	T-DNA Insertion		Ler	31.32±20.1	24
aha1	H^+ ATP-ase (proton pump)	*aha1-6*	T-DNA Insertion	SALK	Col-0	53.18±12.3	3
aha2	H^+ ATP-ase (proton pump)	*aha2-5*	T-DNA Insertion	SALK	Col-0	30.88±11.84	12
aha1	H^+ ATP-ase (proton pump)	*ost2-1D*	NA (Ethyl Methane Sulfonate)		Ler	47.4±28.91	8
clcB	voltage dependent Cl^- channel	*N852518* *N667718*	T-DNA Insertion	SALK	Col-2 Col-0	27.62±11.86	8
clcD	voltage dependent Cl^- channel	*N855430* *N542895* *N680982*	T-DNA Insertion	WiscDsLox SALK SALK	Col-2 Col-0 Col-0	13.95±3.61	5
clcG	voltage dependent Cl^- channel	*N686466*	T-DNA Insertion	SALK	Col-0	26.97±16.1	8
akt1	voltage dependent K^+ channel	*akt1-1*	T-DNA Insertion		Ws	29.35±12.07	4
kco4	Ca^{2+}, H^+ dependent K^+ channel	*N666058*	T-DNA Insertion	SALK	Col-0	30.61±6.27	7
kat1	voltage dependent K^+ channel	*N681711* *N678836*	T-DNA Insertion	SALK SALK	Col-0 Col-0	15.34±13.88	7
kat3	Regulatory subunit for K^+ channels	*N667113* *N664173* *N633047*	T-DNA Insertion	SALK SALK	Col-0 Col-0	31.27±5.82	6
skor	K^+ dependent K^+ channel	*N655760* *N658036*	T-DNA Insertion	SALK SALK	Col-0 Col-0	15.87±7.07	8
gork	K^+ dependent K^+ channel	*N654279* *N655190*	T-DNA Insertion	SALK SALK	Col-0 Col-0	15.42±12.05	7
tpc1	voltage	*N645413*	T-DNA	SALK	Col-0	13.92±5.05	3

	dependent Ca^{2+} channel		Insertion				
vdac1	voltage dependent anion channel	*N653635*	T-DNA Insertion	SALK	Col-0	30±2.9	5
vdac4	voltage dependent anion channel	*N656391*	T-DNA Insertion	SALK	Col-0	23.84±5.15	3
glr1.1	glutamate receptor-like, Ca^{2+} channel	*N654208*	T-DNA Insertion	SALK	Col-0	29.01±10.64	4
glr1.2	glutamate receptor-like, Ca^{2+} channel	*N664922* *N664609*	T-DNA Insertion	SALK SALK	Col-0 Col-0	10.92±11.39	12
glr1.4	glutamate receptor-like, Ca^{2+} channel	*N663986* *N665506*	T-DNA Insertion	SALK SALK	Col-0 Col-0	21.95±9.32	2
glr2.3	glutamate receptor-like, Ca^{2+} channel	*N613206*	T-DNA Insertion	SALK	Col-0	32.1±13.3	8
glr2.4	glutamate receptor-like, Ca^{2+} channel	*N681712* *N654061*	T-DNA Insertion	SALK SALK	Col-0 Col-0	17.02±2.87	5
glr3.2	glutamate receptor-like, Ca^{2+} channel	*N676991*	T-DNA Insertion	SALK	Col-0	41.54±1.89	2
glr3.3	glutamate receptor-like, Ca^{2+} channel	*N672760* *N663463*	T-DNA Insertion	SALK SALK	Col-0 Col-0	27.80±5.42	5
glr3.4	glutamate receptor-like, Ca^{2+} channel	*glr3.4-1* *N853381*	T-DNA Insertion	SALK WiscDsLOX	Col-0 Col-2	12.06±7.47	55
glr3.6	glutamate receptor-like, Ca^{2+} channel	*N663316*	T-DNA Insertion	SALK	Col-0	27.30±4.97	4

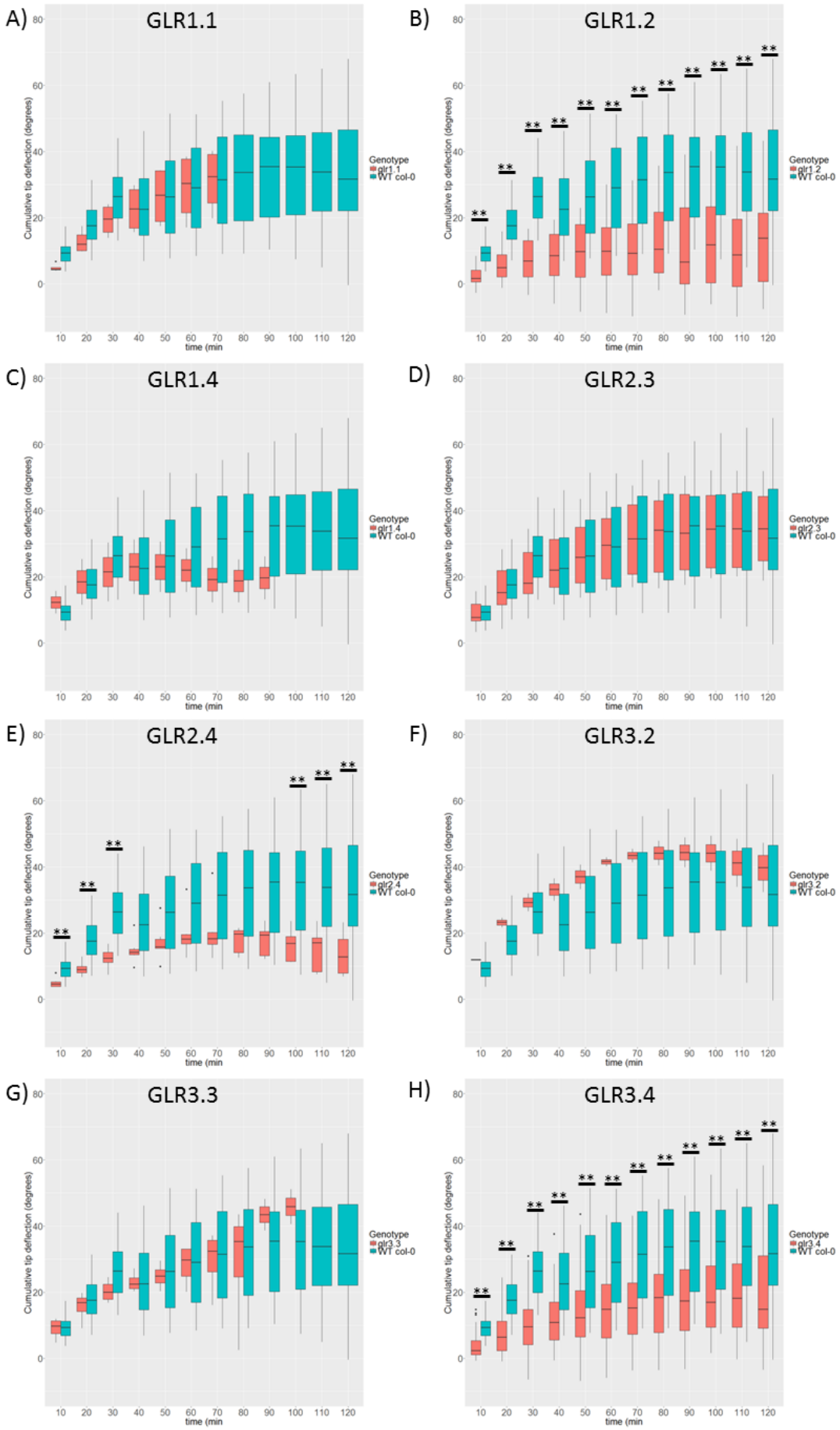
A)
GLR1.1
B)
GLR1.2
C)
GLR1.4
D)
GLR2.3
E)
GLR2.4
F)
GLR3.2
G)
GLR3.3
H)
GLR3.4
Cumulative tip deflection (degrees)
time (min
Genotype
WT col-0
**

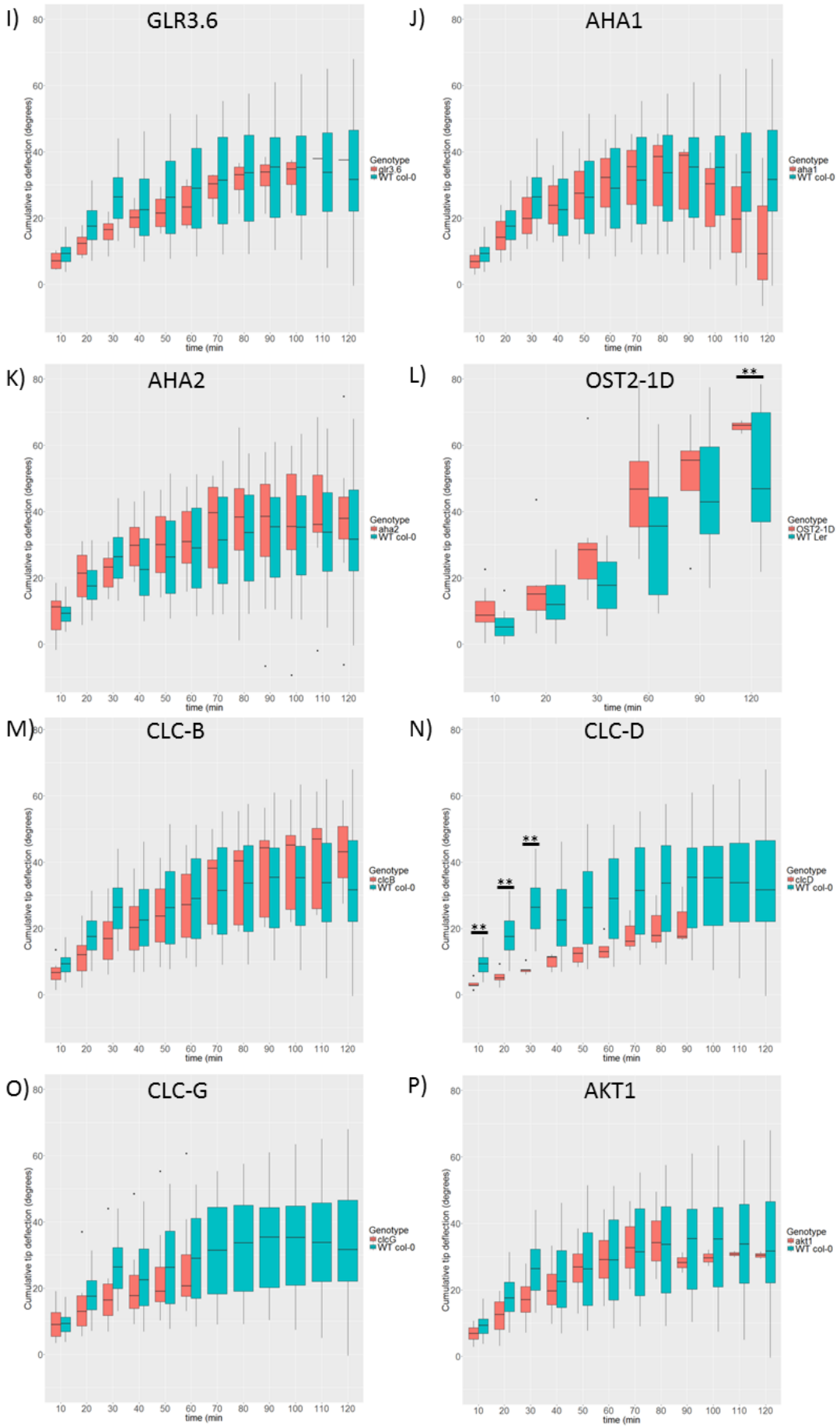
I)
GLR3.6
J)
AHA1
K)
AHA2
L)
OST2-1D
M)
CLC-B
N)
CLC-D
O)
CLC-G
P)
AKT1
Cumulative tip deflection (degrees)
time (min
Genotype
glr3.6
aha1
aha2
OST2-1D
clcB
clcD
clcG
akt1
WT col-0
WT Ler
**

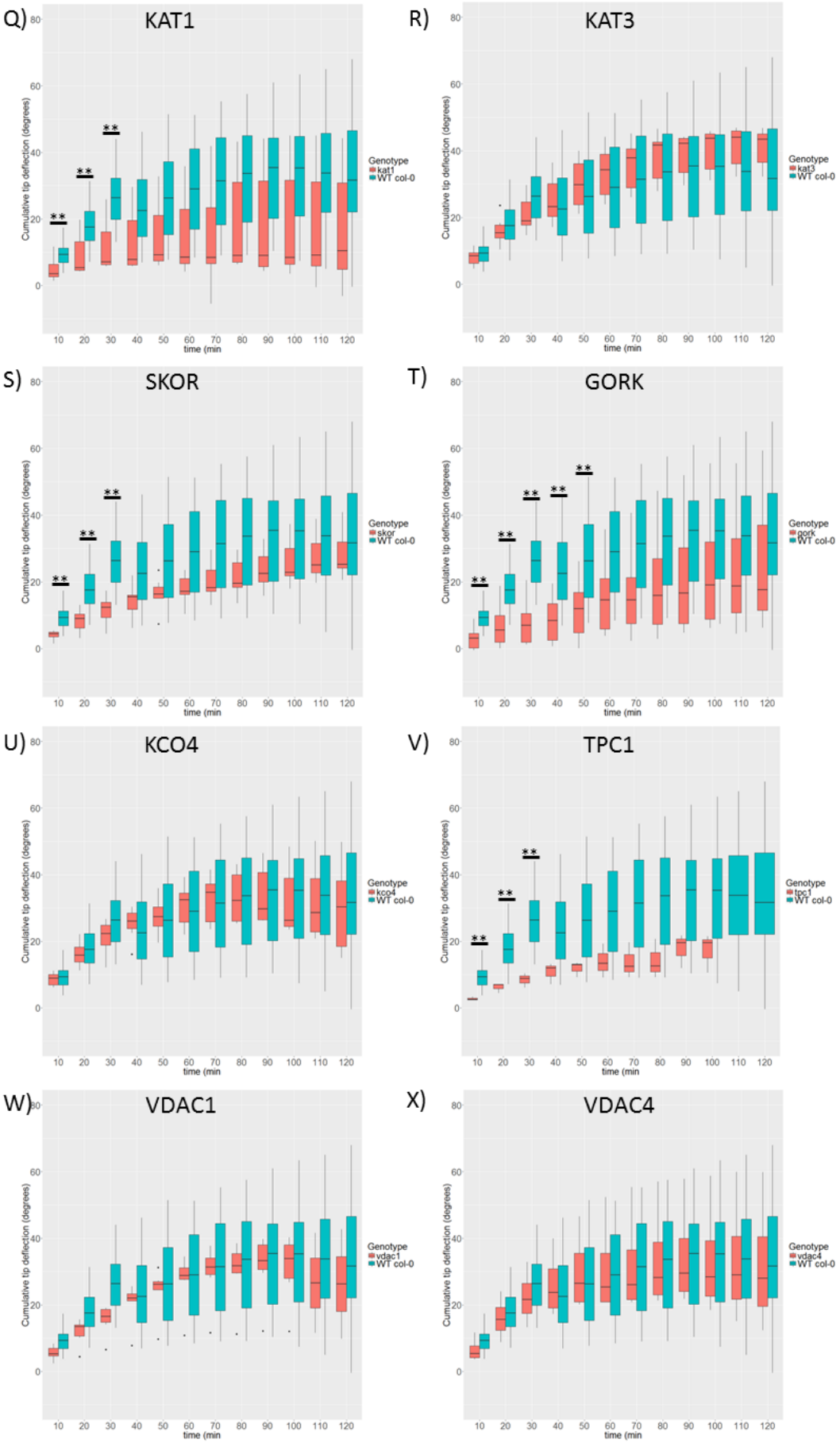
Q)
KAT1
R)
KAT3
S)
SKOR
T)
GORK
U)
KCO4
V)
TPC1
W)
VDAC1
X)
VDAC4
Cumulative tip deflection (degrees)
time (min
Genotype
kat1
kat3
skor
gork
kco4
tpc1
vdac1
vdac4
WT col-0
**

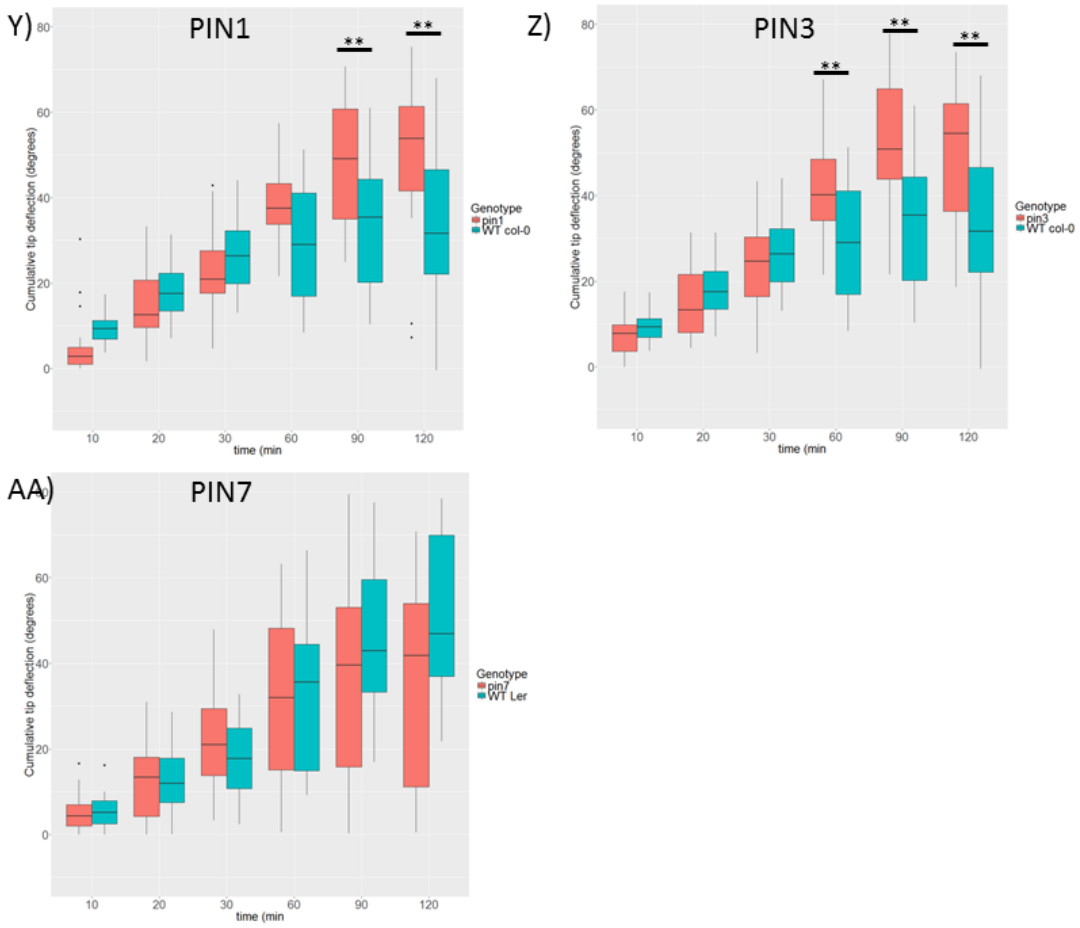

Figure 53: Quantitative comparison of electrotropism of roots with a mutation in a stated gene when exposed to 1V/cm electric field for duration of 2 hours in the V-box with wild type root tip deflections. The data combines deflections from multiple alleles mentioned in **Table 12**. The box plot show distributions of root deflections collected by measuring an angle of a root at t=0 and t=n. The box plot shows distribution median with a line within the box, the box itself stands for 50% of the data closest to the median. The lines below and above the box stand for two quadrants containing data distributed 25% and more away from the median. The mutants tested were A) *glr1.1* B) *glr1.2* C) *glr1.4* D)*glr2.3* E) *glr2.4* F) *glr3.2* G) *glr3.3* H) *glr3.4* I) *glr3.6* J) *aha1* K) *aha2* L) *ost2-1D* M) *clcB* N) *clcD* O) *clcG* P) *akt1* Q) *kat1* R) *kat3* S) *skor* T) *gork* U) *kco4* V) *tpc1* W) *vdac1* X) *vdac4* Y) *pin1* Z) *pin3* AA) *pin7*. The number of roots in each distribution set is mentioned in **Table 12**. The distributions were tested for normality using Shapiro-Wilk test. Non-parametric Mann-Whitney U test was used to determine significant difference between mutant and wildtype distributions. Significant difference between any distribution and WT col-0 & WT Ler distributions is marked with ** for p-value<0.01.

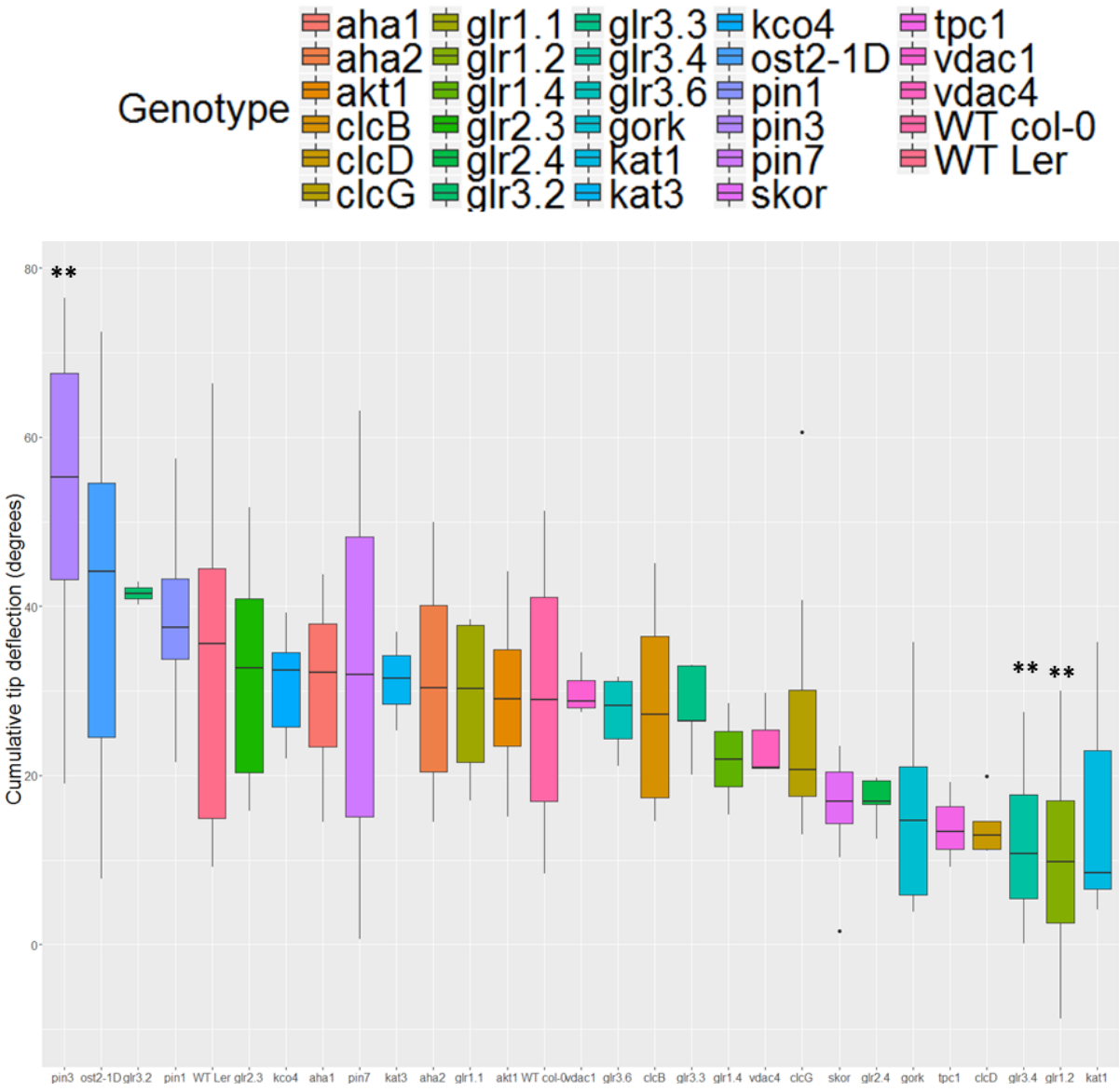

Figure 54: Quantitative description of electrotropism of a number of roots with an assumed knock-out mutation in listed genes (**Table 12**). Roots were subjected to 1V/cm E field while submerged in medium B in V box. Root angle deflections after 1 hour of exposure were measured. The box plot show distributions of root deflections collected by measuring an angle of a root at t=0 and t=60min and counting the difference. Total number of roots tested as well as average and standard deviation for each distribution is presented in **Table 12.**Error! Reference source not found. The box plot shows istribution median with a line within the box, the box itself stands for 50% of the data closest to the median. The lines below and above the box stand for two quadrants containing data distributed 25% and more away from the median. The distributions were tested for normality using Shapiro-Wilk test. Non-parametric Mann-Whitney U test was used to determine significant difference between mutant and wildtype distributions. Significant difference between any distribution and WT col-0 & WT Ler distributions is marked with ** for p-value<0.01.

5.2.9 Arabidopsis knock-out mutant glr3.4 shows reduced electrotropism

Once we have identified the ion channels that are likely to be necessary for wild type electrotropism, we wanted to confirm their necessity by comparing mutant roots and wild type roots originating from the same segregating population. In particular, the ion transporter GLR 3.4 is a crucial Ca^{2+} channel, triggered by a number of small amino acids such as Glu, Ser, Ala, Asn, Gly and less so Cys (Qi *et al.* 2006). GLR3.4 has been documented to be expressed mainly in the root tip, in the phloem (Vincill *et al.* 2013), and it forms a heterotetramer on the membranes of organelles such as plastids as well as on the plasma membrane (Teardo *et al.* 2011).

In order to fully confirm if the absence of GLR3.4 protein results in decreased electrotropism, we wanted to compare plants with recessive homozygous mutant *glr3.4* genotype with homozygous wild-type *glr3.4* genotype obtained from the segregating of the heterozygous *glr3.4* genotype plants that have one functional and one non-functional *glr3.4* allele. This allowed us a more direct comparison of the effect of missing a *glr3.4* on electrotropism since homozygous *glr3.4* recessive genotype and homozygous wildtype segregated genotype are expected to have very similar genetic make-up apart from the mutation in *glr3.4* gene, much more so than homozygous recessive *glr3.4* and standard lab propagated col-0 wild type. We identified wild type homozygous plants and recessive homozygous *glr3.4* mutant plants from seeds originating from a plant heterozygous for a described *glr3.4-1* allele with a T-DNA insertion mutation (Vincill *et al.* 2012) and we quantified the response of the roots of the plants with segregated genotypes to the electric field.

In order to identify the presence or absence of the *glr3.4-1* allele and homozygosity or heterozygosity of individual plants we performed PCR reactions with primers designed to distinguish wild type allele and *glr3.4-1 allele* (Figure 55B) (Methods, 2.3.9). Altogether 54 roots were genotyped from same population of segregating individuals and 23 were shown to be wild type, 21 were shown to be homozygous recessive and 10 were found to be heterozygous for *glr3.4-1* allele.

We have also tested the gravitropic response of the confirmed homozygous *glr3.4* mutants in order to see if this gene is necessary for wild type gravitropism. We wanted to further examine to which extent electrotropism and gravitropism shares the same molecular mechanism. From qualitative observation we can conclude that roots with missing GLR3.4 protein are as gravitropic as wild type roots (Figure 55A). The result suggests that if there is a point in molecular pathways of gravitropism and electrotropism that is shared between the two, the involvement of GLR3.4 channel comes downstream of it and its presence and functionality is only relevant for electrotropism.

We have exposed confirmed homozygous recessive *glr3.4* mutants and segregated wild type roots to 1V/cm electric field for duration of 2 hours in V-box. The electrotropic phenomenon was recorded using Raspberry Pi camera with frame rate 10 minutes. The root deflections were measured at each time point to obtain a distribution of deflections for the two genotypes. The quantitative distributions of wild type and mutant electrotropism response were compared and tested for significant difference. From Figure 55C we can see a trend of decreased root electrotropism in the case of roots homozygous for *glr3.4-1* mutated allele in comparison to wild type. This decrease was not significantly different across the whole time series, but from 20 minutes to 70 minutes the roots of homozygous recessive mutant have turned significantly less than those with homozygous wild type *glr3.4* gene.

Overall the results suggest that the *glr3.4* gene is necessary for electrotropism. In addition the *glr 3.4* mutants showed wild type-like gravitropic response, further strengthening the argument that gravitropism and electrotropism are governed through separate mechanisms.

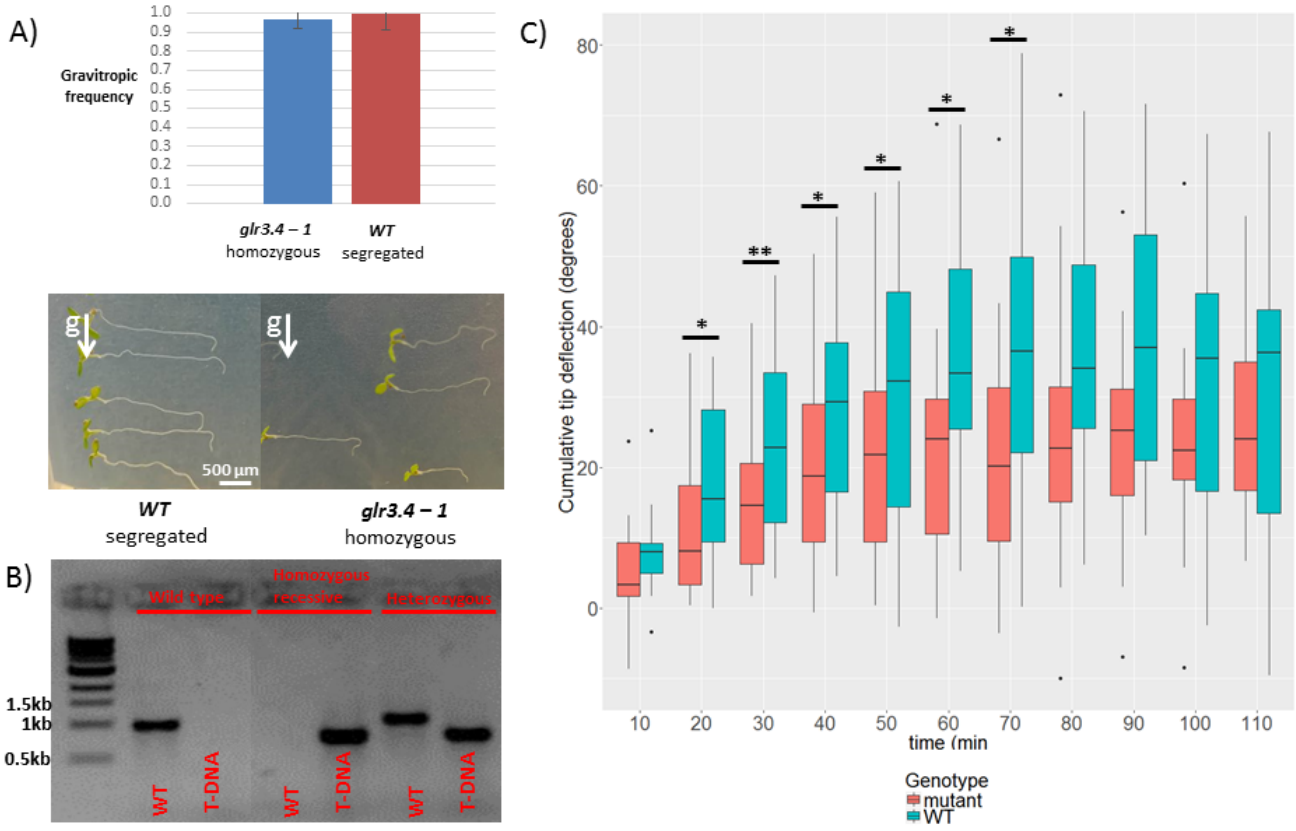

Figure 55: Roots of confirmed *glr3.4-1* homozygous mutants and roots of wild type segregated from a heterozygous *glr3.4-1* population have been tested for gravitropism, genotype and electrotropism. A) Wild type roots and *glr3.4-1* homozygous roots qualitative response to gravity, and fraction of roots of both genotypes that respond to gravity vector. N=22 WT roots and N=32 homozygous recessive *glr3.4* roots were used to construct the fractions. B) Three possible genotyping outcomes: WT, homozygous recessive and heterozygous for *glr3.4-1* allele per individual plant tested. 54 individuals were genotyped. DNA band confirming presence of wild type allele is 1kb long, whereas DNA band confirming presence of *glr3.4-1* allele is 700bp long. C) Roots with *glr3.4-1* homozygous genotype and roots with wild type homozygous genotype segregated from the same with *glr3.4-1* heterozygous population have been subjected to 1V/cm electric field in V-box submerged in medium B. The box plot show distributions of root deflections collected by measuring an angle of a root at t=0 and t=n and counting the difference. All of the roots were exposed to 1V/cm electric field, total of N=23 wild type homozygous and N=21 *glr3.4-1* homozygous roots. The box plots show the distributions of root tip deflections over period of 110 minutes in discreet 10 minute intervals. The box plot shows distribution median with a line within the box, the box itself stands for 50% of the data closest to the median. The lines below and above the box stand for two quadrants containing data distributed 25% and more away from the median. The distributions were tested for normality using Shapiro-Wilk test. Compared distributions were tested for equal variance using Fischer's test, and then tested for significant difference using Welch T-test. Any significant difference ($p<0.05$) is marked with * and ($p<0.01$) with **.

5.2.10 Rescue mutant of glr3.4 expressing GLR3.4:GFP shows wild type electrotropism

In order to further confirm that GLR3.4 is necessary for wild type like response of roots to 1V/cm electric field, we have obtained *glr3.4-1* rescue mutants that express *pGLR3.4::GLR3.4:GFP* transgene (Vincill *et al.* 2013). Roots expressing GLR3.4:GFP protein were first genotyped to confirm the T-DNA insertion and presence of *glr3.4-1* allele. The roots were also genotyped the presence of non-disrupted *glr3.4* gene (Methods, 2.3.9). Seven genotyped roots have shown to contain both mutated *glr3.4-1* allele as well as non-disrupted allele of *glr3.4* (Figure 56A). We have also checked for the presence of GFP in the roots, by observing roots using confocal microscope. We can confirm observation of green fluorescence in the roots of plants expressing *proGLR3.4::GLR3.4:GFP* (Figure 56B).

Once confirmed that the plants are indeed transgenic rescue mutants of *glr3.4* gene, we have subjected the roots of these plants to the exposure of 1V/cm electric field using V-box set up. The images of the electrotropic process were collected as a time lapse video using Raspberry Pi camera, with duration of 2 hours and frame rate of 10 minutes. The root tip deflection of roots expressing *pGLR3.4::GLR3.4:GFP* were compared to WT col-0 and *glr 3.4* mutant in order to quantitatively compare the electrotropism of the rescue mutant with that of wild type and mutant. We have observed that the root tips of the rescue mutants have performed statistically same electrotropic turn towards cathode just like wild type roots (Figure 56C). We have also observed that the root tips of the rescue mutants have performed significantly different electrotropic turn towards cathode in comparison to double homozygous *glr3.4-1* mutant in first 80 minutes of the observation (Figure 56D). This shows that insertion of *proGLR3.4::GLR3.4:GFP* gene construct into plants homozygous for *glr3.4-1* allele allows the roots to perform wild type-like electrotropic turn. This turn is different to the one performed by plants homozygous for *glr 3.4-1*, further suggesting GLR 3.4 is necessary for wild type electrotropism.

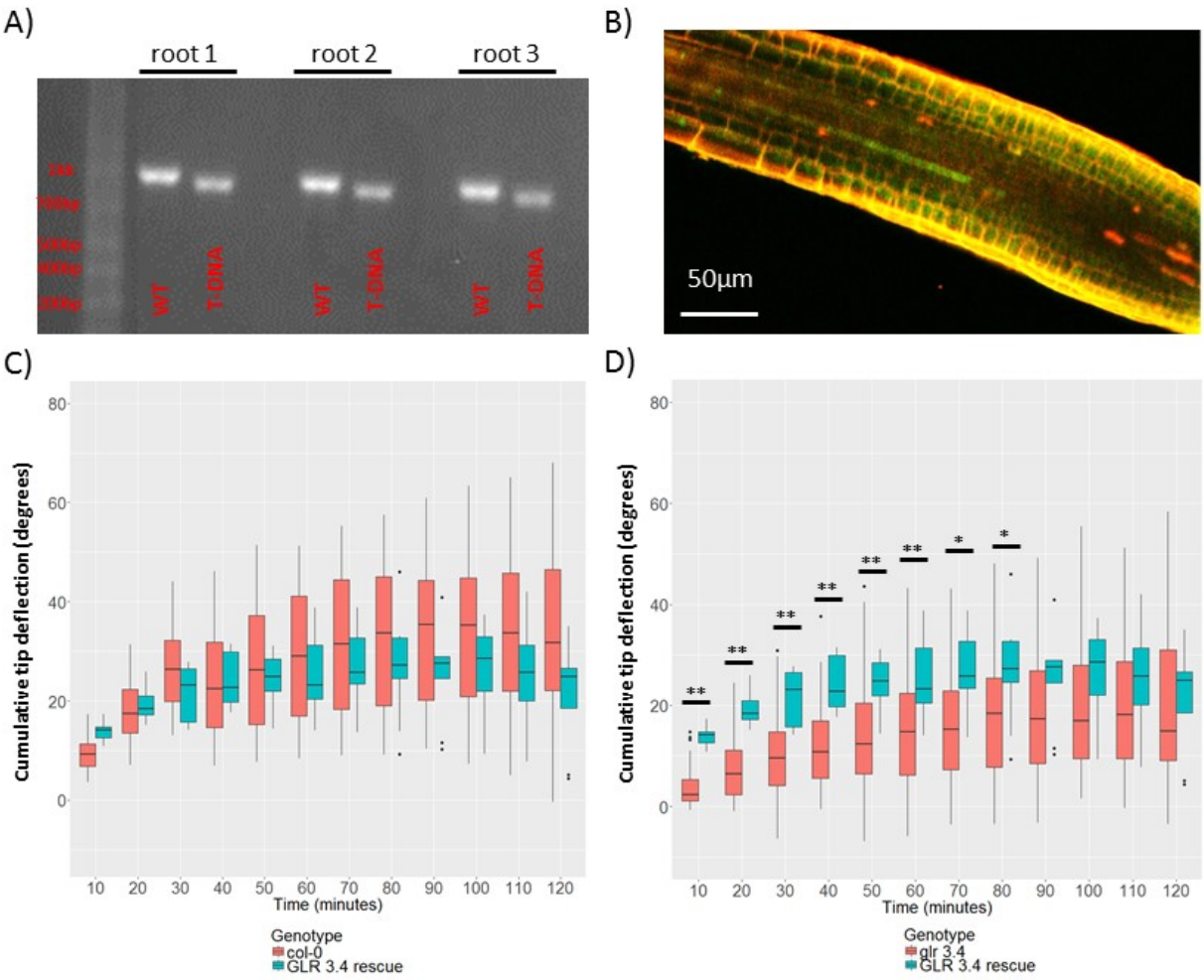

Figure 56: Roots expressing *proGLR3.4::GLR3.4:GFP* in *glr3.4 (-/-)* background have been genotyped, imaged and subjected to 1V/cm E field in V-box while submerged in medium B for 2 hours. **A)** Seven roots with assumed *proGLR3.4::GLR3.4:GFP* construct present in the genome were genotyped (Methods, 2.3.9) for the presence of SALK based T-DNA insert (LBb1.3) and the wild type allele. **B)** Root expressing *proGLR3.4::GLR3.4:GFP* in *glr3.4 (-/-).* Red colour shows the propidium iodide and the green colour indicates the presence of the GLR:GFP protein within the root. The image represents 2 roots. Scalebar 50µm. **C)** Quantitative comparison of electrotropism of WT and *proGLR3.4::GLR3.4:GFP glr3.4 (-/-)* roots. The box plot show distributions of root deflections collected by measuring an angle of a root at t=0 and t=n and counting the difference. Total of N=9 *proGLR3.4::GLR3.4:GFP glr3.4 (-/-)* and N=24 WT roots were exposed to 1V/cm E field in V-box, while submerged in medium B. **D)** Quantitative comparison of root electrotropism of *glr 3.4 (-/-)* mutant and rescue *proGLR3.4::GLR3.4:GFP* in *glr3.4 (-/-)* background. The box plot show distributions of root deflections collected by measuring an angle of a root at t=0 and t=n and counting the difference. Total of N=55 roots with *glr 3.4 (-/-)* genotype and N=9 roots with *proGLR3.4::GLR3.4:GFP glr3.4 (-/-)* genotype to were exposed to 1V/cm E field in V-box, while submerged in medium B. The box plots show the distributions of root tip deflections over period of 120 minutes in discreet 10 minute intervals. The box plot shows distribution median with a line within the box, the box itself stands for 50% of the data closest to the median. The lines below and above the box stand for two quadrants containing data distributed 25% and more away from the median. The distributions were tested for normality with Shapiro-Wilk test. Compared distributions were tested for equal variance using Fischer's test, and then tested for significant difference using Welch T test. $p<0.05$ * $p<0.01$ **.

5.2.11 Calcium (Ca^{2+}) dynamics in electrotropic roots

In order to further question the role of GLRs and ion dynamics in the root electrotropism, we have used roots expressing Ca^{2+} ion reporter and observed them live while subjected to 1V/cm electric field. For this we have used *UBQ10::YC3.6:NES* transgene expressing roots (Krebs *et al.* 2012), and observed them using inverted light wide field microscope, while placed in the V-slide and submerged in medium B (Methods, 2.3.7). The images were collected using camera mounted on the wide field microscope, and the data was collected as a time-lapse video with 10 second frame rate. The data was collected as two channel images which were processed and divided to obtain ratio images (Methods, 2.3.8). Together this set-up allowed for real time observation of Ca^{2+} fluctuations during electrotropic phenomenon.

We have observed that the roots do not have the same ratio baseline and there is a high variation among all the roots, even without the electric field treatment. This can be seen at 4.50min in the images in the Figure 57. All the roots observed also show decrease in the FRET ratio across time (Figure 57). It is possible that the decrease is related to the bleaching of fluorophores. Therefore thanks to high variation among roots and high fluctuation of Ca^{2+} signal, we cautiously analysed images of roots expressing YC3.6 subjected to electric field.

We can observe a variation among the roots and gradual decrease in the FRET ratio, in the roots exposed to electric field, similar to those exposed to mock conditions (Figure 58). When we observe proximal meristem zone and transition zone, at 3.30 minutes after turning on the 1V/cm electric field, we can detect a temporary increase in the FRET ratio only on the side of the root facing positive electrode (Figure 58). This temporary increase is seen up to 7 minutes after turning on the electric field. The observed increase is asymmetric, suggesting a temporary rise in Ca^{2+} ions in the epidermis and cortex of the root meristem and transition zone facing the anode while electrotropic turn is taking place.

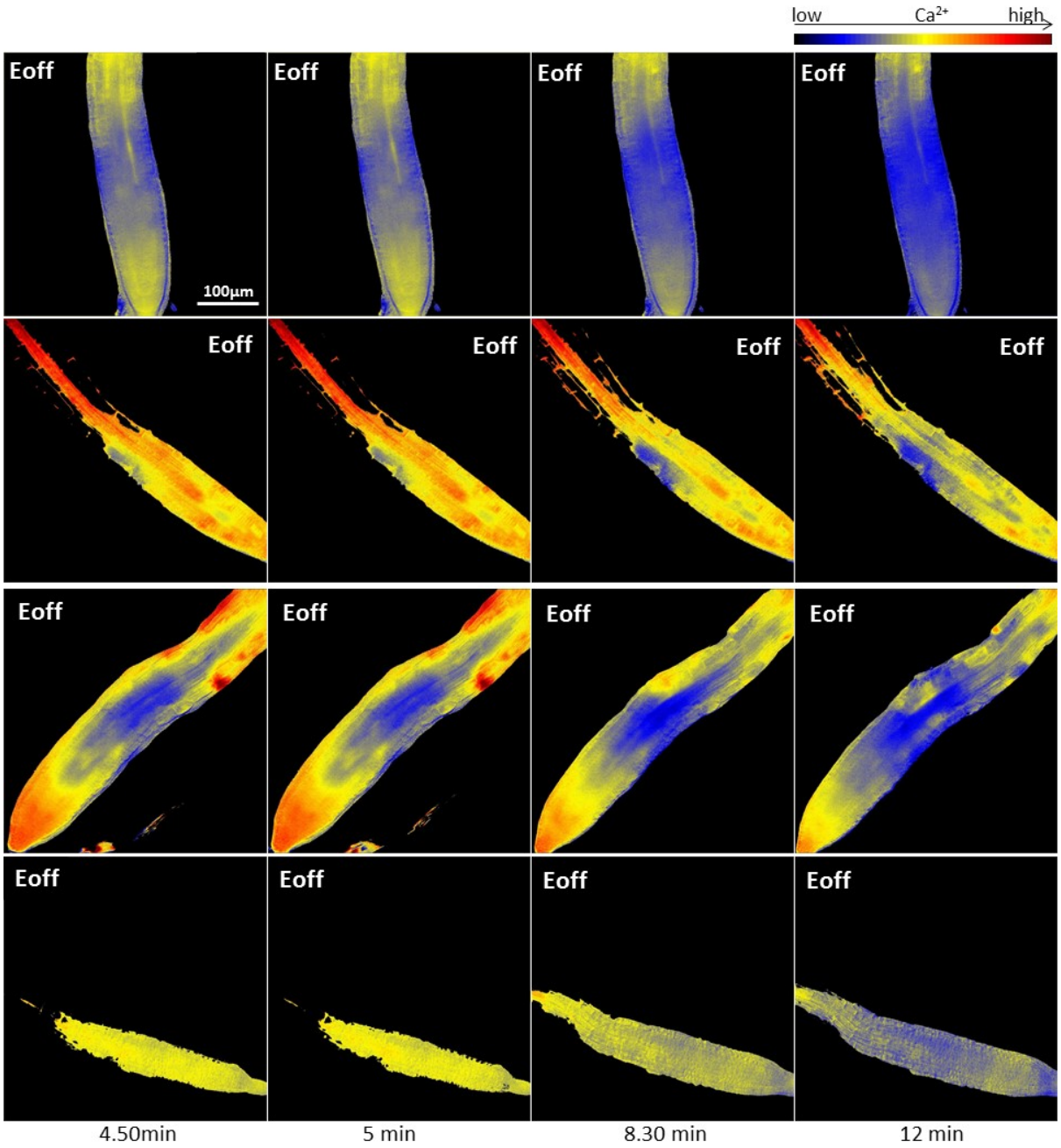

Figure 57: Roots expressing *UBQ10::YC3.6:NES* FRET reporter have been subjected to mock conditions in V-slide to allow for real-time observation of Ca^{2+} ion dynamics. Eoff indicates that the external electric field was not applied. Snapshots of the live observation are shown here, taken at 4.50min, 5min, 8.30min and 12min. FRET ratio of the intensities collected is shown as a ratiometric image. The colour bar indicates concentration of Ca^{2+} ions, with dark blue being the lowest amount and dark red being the highest amount. All 4 observed roots are presented. Scalebar 100µm.

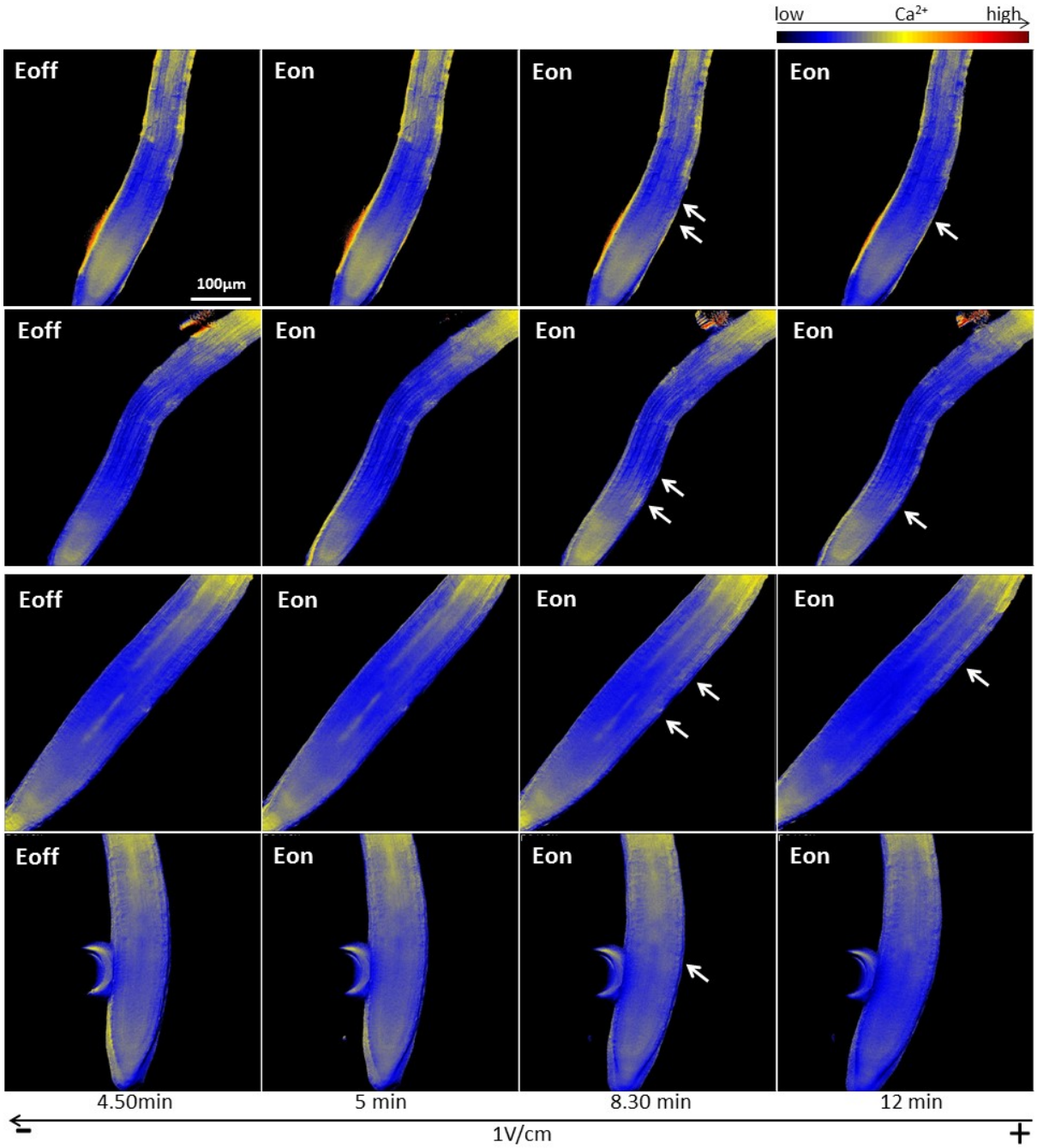

Figure 58: Roots expressing *UBQ10::YC3.6:NES* FRET reporter have been subjected to 1V/cm external electric field in V-slide to allow for real-time observation of Ca^{2+} ion dynamics. Eoff indicates that the external electric field was not being applied and Eon stands for external electric field being applied. Snapshots of the live observation are shown here, taken at 4.50min, 5min, 8.30min and 12min. FRET ratio of the intensities collected is shown as a ratiometric image. The colour bar indicates concentration of Ca^{2+} ions, with dark blue being the lowest amount and dark red being the highest amount. The arrows indicate asymmetric temporary Ca^{2+} increase. All 4 observed roots are presented. Scalebar 100µm.

5.3 Discussion

5.3.1 Electrotropism is conserved among species and is likely driven by osmotically controlled cell expansion

We can confirm that *Arabidopsis thaliana* is another plant species, together with *Zea Mays, Lepidium sativum* and *Vigna Murgo* (Stenz and Weisenseel 1991), (Stenz and Weisenseel 1993), (Wolverton *et al.* 2000) that is capable of root tip curvature in presence of weak external field. Overall this suggests that the electrotropism towards cathode is a response shared by many species. The question, however remains if the electrotropic phenomenon is an evolved response to electromagnetic fields found in soil or it is a result of a hijack of another root mechanism forced out of equilibrium by electric field.

There are many types of soil with different electro conductive properties (Manna and Chowdhuri 2007). This means rather than correlating the strengths of the electric field in experimental condition with those found in soil, the next step can be to attempt to observe electrotropism in soil. However electric fields also influence water retention and water movement in soil (Yu *et al.* 2016), so it is likely that a wild type root navigating soil uses cues that stimulate hydrotropism as well as electrotropism. The two behaviours can be dissected with the use of non-hydrotropic mutant *miz1*(Kobayashi *et al.* 2007) and non-electrotropic mutant *glr3.4*. Finally a growth competition study between wild type and plants having a *glr3.4* mutation grown in soil with as equally distributed water content as possible, but generating an electric field through unequal ion distribution can be established to see if electrotropic plants do indeed have a growth/size/flowering advantage.

Our results suggest that the electrotropic curvature is not observed in all situations when 1V/cm electric field is present. Instead a medium within which the root is growing has to meet a given conductance criteria, and by extension a certain salt/mineral content. With non-existent salt and mineral content roots do not turn in response to electric field. Also these root tips show damage early on after the beginning of exposure to electric field (data not shown). The closest to non-salt,

non-mineral medium in which the root electrotropism can be observed is medium B (Stenz and Weisenseel 1993), which contains MES and TRIS buffers. On the other hand media with high salt content, such as routinely used 1/4X MS medium, also do not provide the correct environment in which electrotropism can be observed. This evidence, together with the fact that macro electrotropism can be observed within 10 minutes of beginning of electric field treatment, makes it likely that simple turgor pressure drives cell expansion that appears to occur during electrotropism.

Water movement in and out of the cell is a crucial component that counteracts hyper and hypo osmotic stress. One of the most important ions involved in the regulation of cell expansion through turgor driven pressure is the flux of K^+ ions (Lebaudy *et al.* 2007). It is possible that the action of electric field causes the movement of ions found in the apoplastic space across the root tip and generates the first ionic asymmetry. Roots that were exposed to excess K^+ ions (100mM) for two hours prior exposure to electric field, but not during the electric field exposure did not show the electrotropic turn (Preliminary Results IV, 6.2.3). This suggests that excess K^+ in and around cells, may be enough to counteract initiation of electrotropism. It is possible that differential amount of ions on the outside of the epidermal cells facing positive electrode than those facing negative electrode, may have been enough to cause membrane depolarisation on one epidermal side but not the other. This could result in difference in osmotic pressure, in hypoionic medium, but not in isoionic or hyperionic medium, in the two epidermal layers facing negative and positive electrode. This would then lead to initiation of the cell expansion asymmetry (Figure 59).

Another line of evidence in favour of osmotic pressure being the driver of cell expansion can be the damage caused by application of stronger (2.5V/cm) electric field. When cells on the two sides of the root, facing negative and positive electrode, were subjected to electric field the cells facing positive electrode were seen to expand until they burst. This may have been simply the result quicker accumulation of positive ions on the epidermal side of the root facing negative electrode, causing an even quicker increase in water build up inside the cell. The observed Ca^{2+} temporary spike

in the cell area about to burst may have been the result of MCA1 & MCA2 mechanosensitive protein channels (Kamano *et al.* 2015), that detect cell stretching and respond to hypo-osmotic stress(Nakagawa *et al.* 2007). However, as a first step towards confirming this hypothesis, membrane voltage in the distal elongation zone of the root will have to be monitored.

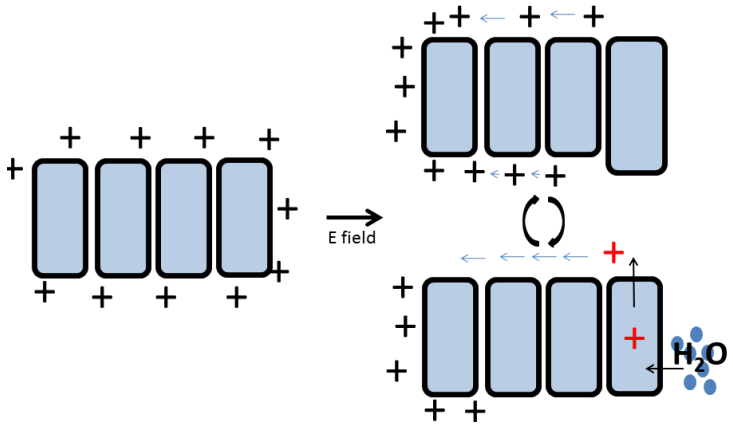

Figure 59: Schematic suggests how electric field driven ion displacement could cause water uptake in one cell on the side of the root but not the other. This differential water uptake could underlie the beginning of the mechanism for root tip electrotropism.

5.3.2 Auxin is likely not necessary for initiation of root electrotropism, but may be needed for the maintenance of the electrotropic curvature

Agravitropic mutants *pin2* and *aux1* which are missing genes crucial for auxin driven asymmetric cell expansion in response to gravity still performed root tip curvature triggered by electric field. In addition, no change in auxin distribution was observed in the root meristem as well as in the transition and early elongation zone, the zone of the root tip where the electrotropic turn occurs. There are other tropisms such as hydrotropism, where the asymmetric cell expansion is driven by asymmetric expansion of cortex cell layer, independently to that of auxin (Dietrich *et al.* 2017). Electrotropic mechanism is based on the expansion of cell epidermal layer and possibly also cortex.

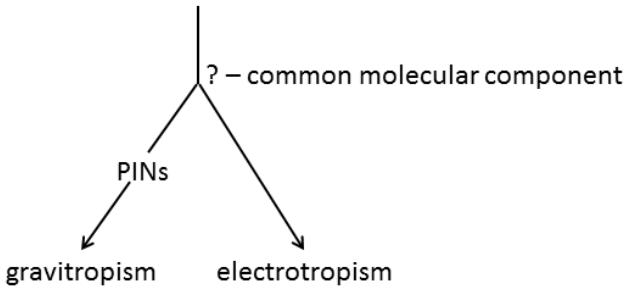

Figure 60: Summary of results obtained by studying gravitropism and electrotropism of roots missing functional *pin* genes.

Historic reports claim necessity of auxin for electrotropic turn, shown with the use of auxin transport inhibitors PBA and TIBA (Moore *et al.* 1987), (Ishikawa and Evans 1990). We have attempted to block auxin transport with the NPA (N-(1-Naphthyl) phthalamidic acid), which is also an auxin transport inhibitor. The results showed us that every time we inhibited gravitropism, we also inhibited growth (data not shown). Another way of enquiry could be to subject auxin resistant mutant *axr1* (Leyser *et al.* 1993), to electric field and observe its root curvature. Overall it appears that gravitropism and electrotropism are governed through two completely separate mechanisms (Figure 60), and that having a non-functional PIN2 protein enhances the electrotropic response. This is possibly because gravitropism based epidermal cell elongation may compete with the electrotropic turn. This can be further supported by the stronger electropic response by *pin3* mutants, which are also reported to be partially agravitropic (Friml *et al.* 2002b).

However, electrotropic turn was weaker 2 hours after roots containing *aux1* mutation were subjected to electric field in comparison with wild type roots. It is important to note that even though PIN2 and AUX1 proteins are expressed in the same epidermal cell file, they do not have redundant functions. While PIN2 shows cell polarity in the epidermal cells and moves auxin away from the quiescent centre, AUX1 protein expression does not show cell polarity and instead controls the overall concentration of auxin present in the epidermal cells (Swarup *et al.* 2001). This may suggest that there is a certain auxin concentration threshold that needs to be present in the epidermal cells of the root tip, in order to be able to maintain the root turning towards cathode in

presence of electric field. This can be tested with the addition of membrane permaeble synthetic auxin NAA (1-naphthaleneacetic acid) into media of the roots containing *aux1* mutation when exposed to electric field. If it is simply the need of a given concentration of auxin in the epidermal cells and not lack of assymetric distribution of auxin that causes *aux1* roots to lose the ability to maintain electrotropic turn, then application of NAA should allow *aux1* to show wild type electrotropism. Overall, this could suggest that even though auxin does not establish asymetry and is not directly responsible for the control of electricity induced cell expansion, it still needs to be present in the distal elongation zone in order to maintain electrotropic curvature.

5.3.3 Calcium channel GLR3.4 is likely to supply Ca^{2+} needed for the electrotropic turn

We have shown that roots missing a functional *glr3.4* gene have reduced electrotropic turn in comparison with wild type coming from the same segregating population. Glutamate-Like Receptor proteins found in plants are a unique set of 20 calcium channels, which are homologous to iGLURs found in animal brains, where they are responsible for synaptic function (Lam *et al.* 1998).

In plants, GLR3.4 function is not very well known in the primary root tip, however it had been shown to control Ca^{2+} signalling in the phloem to regulate initiation of lateral root primordia (Vincill *et al.* 2013). Its subcellular localisation is not exactly defined, since multiple localisation points have been identified with the GLR3.4 protein, both to plastids and plasma membrane (Teardo *et al.* 2011). We can hypothesise that the GLR3.4 protein acts as a gate keeper of Ca^{2+} ions, and the release of Ca^{2+} ions, either from their subcellular compartment into the cell cytoplasm, or from the apoplastic space into cytoplasm is necessary for root electrotropism. This shows that electrotropism is most likely guided by a Ca^{2+} dependent mechanism. We have observed possible temporary Ca^{2+} increase in the outer cell files of the root facing positive electrode, when root tip was subjected to electric field. We would like to repeat this observation using YC3.6 reporter in the roots with non-functional *glr3.4*, to see if the Ca^{2+} increase is dependent on GLR3.4.

Also, roots missing functional *glr3.4* gene were still capable of gravitropism. This is important when considering molecular mechanisms of gravitropism and electrotropism and if the two mechanisms share at least one molecular component. If they do, GLR3.4 action is downstream of this shared common signalling component (Figure 61). It is also likely that gravitropism and electrotropism do not share any common molecular component, apart from auxin involvement, which however may serve different cellular purposes in both phenomena.

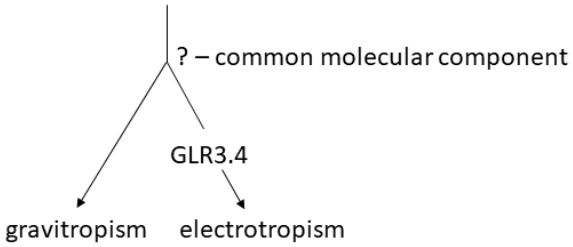

Figure 61: Summary of results obtained by studying gravitropism and electrotropism of roots missing a functional *glr3.4* gene.

In addition we have identified another GLR gene *glr1.2*, in the reverse genetic screen, as a candidate necessary for wild type electrotropism. The next step would be to use segregating population containing *glr1.2* knock-out allele, to quantitatively compare homozygous, heterozygous and wild type plants in their response to electric field. In addition we would also like to see the presence or absence of temporary Ca^{2+} increase in the roots missing functional *glr1.2* subjected to electric field. What exactly is the role of the Ca^{2+} dynamic during electrotropism is for now unknown. It could be in an attempt to maintain membrane voltage or even as an attempt to regulate flow of specific ions, such as K^{+} (Shabala *et al.* 2006).

5.3.4 Hypothesis of molecular mechanism of electrotropism

Our hypothesis for the mechanism behind the electrotropic turn proposes that osmosis driven asymmetric cell expansion is responsible for electrotropism (Figure 62). This is partly facilitated by GLR3.4 a component of a calcium channel, which with an unexplained mechanism may contribute towards positive ion efflux from cells.

Specific ion concentration in the cell apoplast, which is maintained by cell to ensure correct membrane voltage as well as specific concentration of ions, is disrupted as a result of ion displacement by electric field. Positive ions head towards the negative electrode and negative ions head towards positive electrode. This causes changed apoplast of cells facing cathode as well as anode. Overall cells are more negative within cytoplasm than in the apoplast. Therefore cells receiving negative ions into their apoplast may have depolarised membrane. This may prompt, through an unknown mechanism possibly involving GLR3.4, to release positive ions into the apoplast in an attempt to maintain membrane voltage or to maintain specific concentration of a given ion, such as Ca^{2+} or K^{+}. The cells facing negative electrode do not have to release positive ions into the apoplast, because the transmembrane potential did not decrease. Cells attempting to counteract this depolarisation event by releasing ions into the apoplast may dilute, if present in hypo-ionic environment, leading to increased cell turgor.

Released Ca^{2+} or other positive ions do not remain in the apoplast of the cell, which released the ions, but are displaced with the electric field towards negative electrode. This leads to positive feedback loop, where more positive ions that are moved away by electric field, results to more positive ions released from the cell, ending up with ever expanding cell. This results in asymmetric cell expansion and eventually cell bursting of the cells facing positive electrode. The mechanism does not work in iso-osmotic or hyperosmotic conditions since water uptake into the cell is essential for the electrotropic cell expansion.

We could ask why is the specific region of the root, the distal elongation zone, responsible for the electrotropic turn. It is possible that specific ion channels such as GLR3.4 and others have to be expressed in this region, localised to correct membrane and be functional in maintenance of membrane voltage in order for cell to enter the electric field driven cell expansion. But every plant cell is capable of membrane voltage maintenance, even if it is done by different ion channels than

the ones found in the root tip. Unique feature of the distal elongation zone is the rapid elongation of the cells caused by auxin concentration dependant cell wall loosening (Barbez *et al.* 2017).

Distal elongation zone specific cell wall loosening is likely allowing asymmetric electric field driven cell expansion. Under the conditions with rigid cell wall, cells expanding thanks to water uptake reach full turgor and their expansion is limited by the rigidity of the wall. However in the distal elongation zone, the cell wall is not as rigid and therefore cells, which are about to expand as a result of electric field, apply pressure on the loosened wall and cause cell expansion. This is a possible reason why AUX1 auxin transporter is necessary for maintenance of root electrotropism, since it supplies auxin concentration into the distal elongation zone, allowing cell wall loosening.

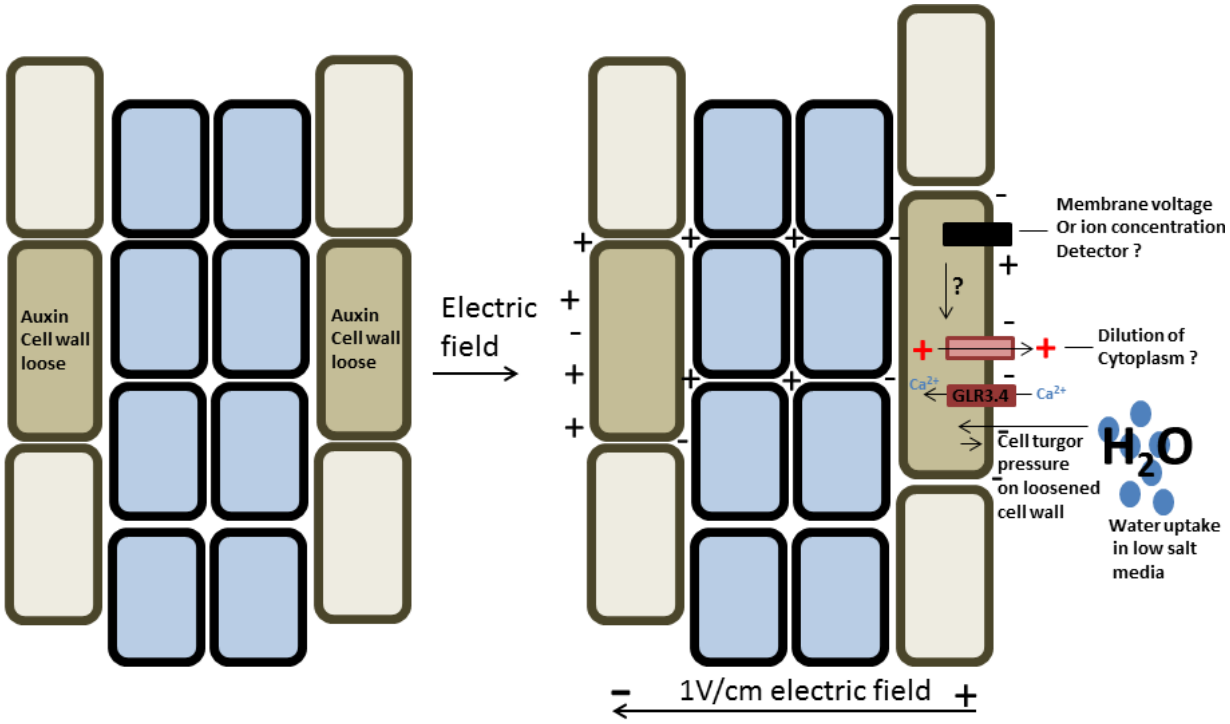

Figure 62: Proposed mechanism of the root electrotropic turn. The panel on the left shows root without exposure to electric field, root on the right shows mechanisms that may be undertaking place when root is subjected to electric field. Blue cells show the inner cell files of the root and two shades of brown show outer cell files of the root. The dark brown indicates cells that are rapidly elongating in the distal elongation zone, caused by auxin driven cell wall relaxation. + and – indicate positively and negatively charged ions, two rectangles black and dark red indicate unknown detection and response components, one of which may be GLR3.4.

An unanswered question remains what is the first asymmetric signal across distal elongation zone, possibly transmembrane potential change or change of specific ion concentration such as H^+,

K^+ or even Ca^{2+}. Second question ties onto the first, what mechanism, receptor, membrane protein or signal protein conveys to the cell that it has to balance out the changed membrane voltage potential or a changed concentration of ions.

5.3.5 Ion transport through plasmodesmata

Apoplast does not have to be the only transport route of ions through the root. Plasmodesmata are long known to act as cell to cell transporters allowing for direct communication between cells (Maule 2008). These are small up to 40-60 nm wide channels that connect symplastic space. Cells in different tissues are not all connected with the same amount of plasmodesmata between each other. This gives rise to possible passive control of molecular flow where tissues that are connected with more plasmodesmata than others may allow a more frequent molecular exchange than those cells with fewer plasmodesmata connections (Zhu *et al.* 1998). As an example the vascular cells have a lower amount of plasmodesmata per μm^2 than epidermal and cortex cells (Zhu *et al.* 1998).

Plasmodesmata mediated flow of molecules may also be controlled actively by β-1,3 glucan callose deposition in the cell wall, which results in constriction of the plasmodesmata channels (Zavaliev *et al.* 2011). Intercellular transport through plasmodesmata is important for a number of developmental phenomena such as embryonic development, post-embryonic development as well as lateral root formation (Xu *et al.* 2011), (Nakajima *et al.* 2001), (Benitez-Alfonso *et al.* 2013).

Plasmodesmata may be involved in regulating electrotropism of roots, particularly allowing ion flow through different cell files. A way to test this hypothesis could be to use mutants missing β-1,3 glucan callose degrading enzymes and expose these to weak external electric field. Double mutant *pdbg1*, *pdbg2* is missing two 1,3-β-D-glucanase enzymes and has been shown to have reduced number of symplastic connections (Benitez-Alfonso *et al.* 2013). This mutant could be tested for electrotropic phenotype.

6 Preliminary Results IV: Plant Membrane Voltage Dynamics

6.1 Background

6.1.1 Electric signals in Arabidopsis roots

Many of the signals used for intercellular communication are based on electrical signals. Neurons are well known for the use of membrane voltage in signal propagation, but closer to the topic of this PhD, numerous regenerative phenomena mainly in animals as well as cell migration and developmental patterning were documented to be controlled by electric signals rather than by specific chemical or physical input (Chang and Minc 2014). As an example, endogenous voltage changes in the membranes of cells in the severed limbs in *Xenopus* guide their regeneration (Adams, Masi and Levin 2007). Also muscle pattern in *Xenopus* can be altered by changing transmembrane voltage in specific stages of *Xenopus* development (Lobikin *et al.* 2015). It is becoming clearer that at least in animals, cellular membrane voltage acts as an important component during developmental processes.

Even though the effects of endogenous bioelectricity in plants are very sparsely documented, plants as well as animals are capable of using electric signals to influence the physiological state of cells in a given tissue (Baluska *et al* (eds.), 2006). There are a number of different depolarization events and different types of electric waves along cellular membranes that were observed in plants, with a few of them also given physiological meaning.

Short event of electric membrane depolarisation and repolarisation with defined path, known as Action Potential (AP) has been found in some plants such as *Mimosa pudica* and others such as algae *Chara* (Homann and Thiel). APs are triggered with the activation of Ca^{2+} ion channels leading to the increased intracellular Ca^{2+} levels. Other ion channels particularly those involved in the transport of Cl^- and K^+ are also involved (Hedrich and Becker). The generation of action potentials

follows all or nothing rule and it is slower in plants than in animals also with a longer refractory period (Fromm and Lautner 2007).

Table 13: Summary of the electric waves observed in plants. Table adapted from Zimmermann et al. 2009, copyright by the American Society of Plant Biologists.

	Action Potentials	**Variable Potentials**	**System Potentials**
Trigger	Voltage Threshold	Rapid Turgor Increase	Plasma membrane depolarisation
Propagation	Self-propagating	Non self-propagating	Self-propagating
Speed	20-400cm/min, limited to tissue organ	10s to several minutes, can affect the whole plant	5-10cm/min, can affect the whole plant
Mechanism	Activation of ion channels (Ca^{2+}, Cl^-, K^+)	Inactivation of the H^+ pump	Activation of the H^+ pump
Ion movement and change in membrane voltage	Ca^{2+} triggers Cl^- efflux and voltage change	Causalities unclear	Ion movements follow voltage change
Polarisation	Depolarisation	Depolarisation	Hyperpolarisation
Time of initial voltage change	<20s	10s to several minutes	8 – 12 minutes
Signal Type	All or nothing	Graded signals of variable size	Signals depend on stimulus

There are other different mechanisms that pass electric signals in plant organs and also in the whole plants, which do not behave like AP. One type is known as Variation Potential (VP) or Slow Wave Potential (SWP) due to the long lasting repolarisation step. VP unlike AP is dependent on the intensity of stimulus that triggered it and does not self-perpetuate (Fromm and Lautner 2007). It is usually triggered by wounding or organ removal or exposure to fire and it was observed in a number of species such as pea or cucumber (Stahlberg and Cosgrove 1995). The intensity of VP is also dependent on the distance from the wound site and shows variation, and it appears that it is reliant on the tension of xylem for it to be functional. The ions involved in the propagation of VP do not

seem to be the same as AP, instead it seems that a temporary switch-off of H^+ ATPases can be responsible (Stahlberg et al. 2006).

There is a third type of electric wave propagation found in the plants referred to as System Potential or SP (Zimmermann et al. 2009). This type has a trigger based on wounding with the intensity translated into strength of the signal, but the stimulus comes from depolarisation of membranes. This signal can be self-perpetuating and has been observed in a number of species such as *H. vulgare* and *V. faba*. The functionality of SP relies on activation of H^+ ATPases, and does not need hydraulic pressure (Zimmermann et al. 2009).

More recently multiple types of electrical depolarisations along veins of leaves were observed in response to biotic stress of herbivore attack. It was shown by Mousavi et al. 2013, that variable wound induced electric waves that were observed from the leaf attacked by herbivore to distal leaves in *Arabidopsis*. It was further shown that the resulting effect of the electric signal was accumulation of jasmonoyl-isoleucine, a defence hormone, in the distal leaves. The effect was diminished in mutants of multiple Glutamate-like calcium channels (Mousavi et al. 2013).

The electric patterns found in plants are important signalling messengers, but there is a lack of described physiological and developmental consequences from these electric signals. In comparison, the already mentioned effects of electric field in animals act as a morphogen-like signal allowing for patterning specification in tissues. We would like to examine if the membrane voltage dynamics play a role in controlling root regeneration or tropism.

6.1.2 Potassium and membrane depolarisations

Plant roots rely heavily on ions in their surroundings for nutrients and signalling. The most abundant micronutrient for plants is the K^+ which has roles in multitude of physiological processes. The response of plant cells to stresses, pathogens, environmental conditions as well as oxidants and heavy metals relies on movement of K^+ across plant cell membrane. This process is controlled by specific and non-specific ion channels (Results III, 5.1.3), which have to be activated for the K^+ influx

or efflux to occur (Demidchik 2014). The result of this controlled flow of potassium across the membrane is change in membrane voltage. This can result in membrane depolarisation or hyperpolarisation. One of the simplest ways to induce membrane depolarisations is to flood the external root environment with excess amount of K^+ ions. Root cells attempt to respond to the stress by controlled K^+ uptake, reducing the difference in concentration between cytoplasm and apoplast localised ions, resulting in decreased voltage difference (Krebs *et al.* 2012). This method can be used as a controlled way to induce membrane depolarisations, and may be particularly useful when characterising novel methods of membrane voltage measurement.

6.1.3 Observing membrane voltage using voltage sensitive dyes

One of the reasons, why there isn't much data found in plants linking cell membrane voltage changes to physiological and developmental occurrences is the lack of tools for observation of electric fields within plant tissue. Almost all of the electric patterns observed in plants have been done with single surface electrodes (Mousavi et al. 2013), or with a multi-electrode array (Masi *et al.* 2009), which allow for very sensitive measurement, but are limited in spatial use to the surface of plant tissues. In addition, this equipment is often bulky, which does not allow for microscopic observation of tissues at the same time as taking voltage measurement.

Microscopic observation of transmembrane voltage changes can be achieved with two methods. It can be done using genetic reporters that code for designed sensors of voltage and report voltage using fluorescence, or with the use of voltage sensitive fluorescent dyes. There are pros and cons for both approaches. Transgenic reporters allow for specific localisation within tissue or cell, and using FRET-fluorescence they report voltage changes ratiometrically in real time. Example of such sensor is the Voltage Sensitive Fluorescent Protein (Akemann *et al.* 2012), which was also transformed into *Arabidopsis* (Matzke and Matzke 2013). However to develop them, an error prone cloning and transformation process has to be used. Every time a new mutant could be examined a long cross-breeding procedure has to take place and the genetic sensors often do not work as

expected once *in vivo* due to mis-expression or other post-transcriptional uncertainties associated with expressing a protein biosensor. This is the case with VSFP in *Arabidopsis* (data not shown).

Voltage sensitive dyes do not suffer from the same problems as those associated with genetic reporters. They can be deployed into any plant organ thanks to easy dissolvability and instantly be visible in any tissue. There are drawbacks too such as uncontrolled diffusion of the dyes, which may counteract any biological effects that the dye is reporting. Nevertheless voltage sensitive dyes are easily used and can provide valuable information about membrane potential. To our knowledge, they were used to report changes in the membrane potential in plant tissues only a handful of times.

The best example is DiBAC4(3) (Bis (1,3-dibutylbarbuturic acid) trimethine oxonol), one of the fluorescent dyes used for membrane potential sensing (Figure 63). It embeds itself into the membrane when the cell membrane becomes depolarised and aggregates at the plasma membrane. It is also able to aggregate within cells upon cell membrane depolarisation and can be found aggregating also on the membranes of organelles. It is a single colour dye, it does not report in a ratiometric manner, but it can be seen to increase or decrease fluorescence in a particular cell as a direct relation to transmembrane potential (Yamada *et al.* 2001). Many of the electro-dynamics described in animal cells have been done using DiBAC4(3) (Oviedo *et al.* 2008) and it is considered the gold standard voltage sensitive dye. It is an anionic dye, and it readily dissolves in H_2O and DMSO. In the absence of depolarisation in cell membranes the dye does not aggregate, providing low or decreased fluorescence signal from the cell membranes with resting potential or at hyperpolarised state.

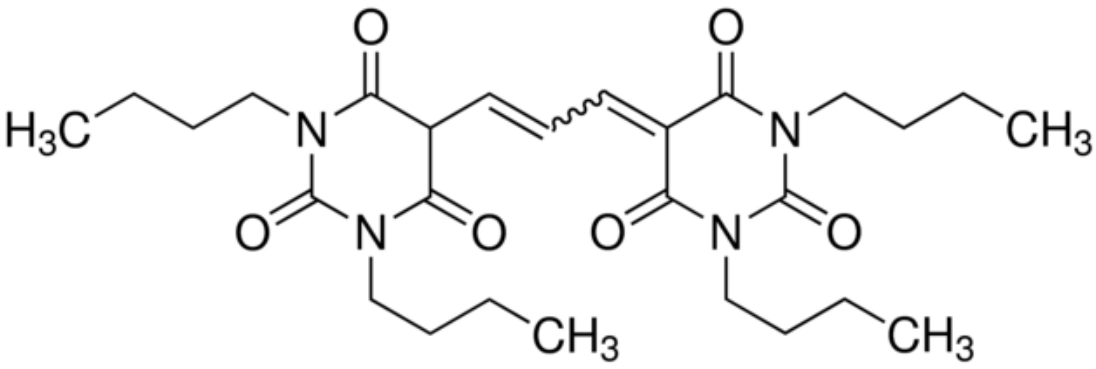

Figure 63: Molecular structure of Bis(1,3-dibutylbarbituric acid) trimethine oxonol (diBAC4(3)) voltage sensitive dye.

DiBAC4(3) was used only a handful of times to observe cell voltage potential in plants. The fluorescence measurements of DiBAC4(3) were calibrated with patch clamp technique on guard cell protoplasts of *Arabidopsis* as well as *Vicia faba* (Konrad and Hedrich 2008). It was shown that DiBAC4(3) allows for semi-quantitative measurements of voltage in plant protoplasts. In intact plants DiBAC4(3) was used to observe action potentials in the phloem of *Helianthus annuus*, while calibrated with surface electrode (Zhao *et al.* 2015).

Table 14: Summary of voltage sensitive dyes tested in thesis.

Voltage sensitive dyes	**DiBAC4(3)**	**Rhodamine 6G**	**SS44-DC**
Charge	anionic	cationic	cationic
Cell penetration	Embedding in cell membrane, as well as entering/exiting cells	Entering/exiting cells	unknown
Expectation when membrane in depolarised state	Increased fluorescence	Decreased fluorescence	unknown
Used in Plants to Report Membrane Potential	Yes	No	No
Fluorescence	Excitation with 488nm, emission in green spectrum	Excitation with 507nm, emission in yellow spectrum	Excitation with 628nm, emission in red spectrum
Reference	Use in plants (Konrad and Hedrich 2008) Use in animals (Oviedo *et al.* 2008)	Use in animals (Ehrenberg *et al.* 1988)	Unpublished

In addition to DiBAC4(3), there are other voltage sensitive dyes that have been used in the past to observe cell voltage. One of these is Rhodamine 6G, which was used before to observe membrane potential in animal cells (Ehrenberg *et al.* 1988), but not in plant cells. Rhodamine 6G is a cationic dye, which can easily penetrate cell membrane and was observed to decrease fluorescence in animal cells with depolarised membranes and cause an increase in fluorescence in cells with hyperpolarised membranes (Mandala *et al.* 1999). Since the observations of membrane voltage potential both in animals and in plants require always more sensitive and specific probes, commercial research is continually developing these tools. One of the dyes in pre-commercial testing is SS44, provided as a gift from Akita Innovations (Billerica MA, USA). This is a novel voltage sensitive dye, promised to be a superior to DiBAC4(3). Since SS44 is a completely new dye, it requires characterisation in animal cells as well as plant cells and therefore we don't assume any expected behaviour of the dye when cells membranes are at resting, hyperpolarised or depolarised state.

We want to characterise voltage sensitive dyes, DiBAC4(3), Rhodamine 6G and SS44 in the root tip, observe membrane depolarisation and establish protocols for the use of voltage sensitive dyes in the *Arabidopsis* root. In addition, in order to induce changes in the membrane voltage in a controlled manner, we will use K^+ ion a commonly used depolarisation approach membranes (Konrad and Hedrich 2008), (Krebs *et al.* 2012).

6.1.4 Aims

- The optimisation of protocols for the use of voltage sensitive dyes in the *Arabidopsis* root

We want to observe the interaction of root tip with three voltage sensitive dyes, DiBAC4(3), Rhodamine 6G and SS44. We want to see if the dye is able to report on the changes in membrane potential by perturbing the transmembrane potential with depolarising buffers. We also want to at least qualitatively assess which of the dyes is the best suited for membrane potential reporting in the root.

- Test the hypothesis of correlations between transmembrane potential changes and electrotropism

Given that the electrotropic mutant is an ion channel mutant, and that charged ions such as Ca^{2+} are most likely crucial elements in electrotropic turn, we want to examine the connection between electrotropism and transmembrane voltage changes. In the first instance we want to observe electrotropism in roots with depolarised cell membranes.

6.2 Results

6.2.1 Characterisation of voltage sensitive dyes in Arabidopsis roots

In order to observe cellular voltage changes, we have to be able to manipulate transmembrane potential. We decided to use 100mM KCl as a trigger for depolarisation of cells, as it was also previously used (Krebs *et al.* 2012). In addition we wanted to ensure that Cl^- does not counteract the depolarisation effect, since it is also readily transported through cell membrane to maintain cell homeostasis, so we also used 100mM potassium gluconate. Gluconate is a sugar that does not get easily transported across plant cell membrane and overall is considered as an inert agent, during cell depolarisation.

We used 45minute pre-treatment with depolarisation buffer to depolarise cells in the roots of *Arabidopsis* and stained them in depolarisation buffer with DiBAC4(3), Rhodamine 6G or SS44 for 15 minutes. Afterwards we mounted the roots on the slides and observed them with the confocal microscope. DiBAC4(3) is expected to enter cells that were depolarised, resulting in the increase of fluorescence observed within the cells, and Rhodamine 6G is expected to behave in the opposite manner, it exits the cell during depolarisation, resulting in a decrease of fluorescence. The observed roots that were treated with depolarising buffer and stained with DiBAC4(3) indeed showed increased fluorescence, especially within cells (Figure 64). The roots that were treated with depolarising buffer and stained with Rhodamine 6G showed decreased overall fluorescence than the roots with cells that were not depolarised.

Since the SS44 dye is a new tool, we did not exactly know if it will be exiting or entering the cell upon membrane depolarisation. We treated WT (col-0) roots expressing *pUBQ10::WAVE131:YFP* cell membrane marker (Geldner *et al.* 2009) to depolarising buffer, stained with SS44 and observed qualitative differences between roots with depolarised and non-depolarised cell membranes using confocal microscope. We can see that the surrounding of the epidermal cells gives a high SS44 fluorescence output in the roots that were not depolarised, but this fluorescence completely disappeared when the root cells were depolarised. Instead in the depolarised cells we can observe

increased accumulation of fluorescent aggregates within cortex cells, which is not observed in the cortex cells of untreated roots (Figure 65).

Even though there wasn't an independent measurement tool used to confirm root cell depolarisation, we can confirm with these preliminary experiments that the dyes show qualitative changes in the root, when root cells are depolarised. When comparing between the three dyes, DiBAC4(3) signal is the most obvious thanks to an increase in fluorescence, whereas Rhodamine 6G and SS44 difference in fluorescence is harder to note due to decrease in fluorescence.

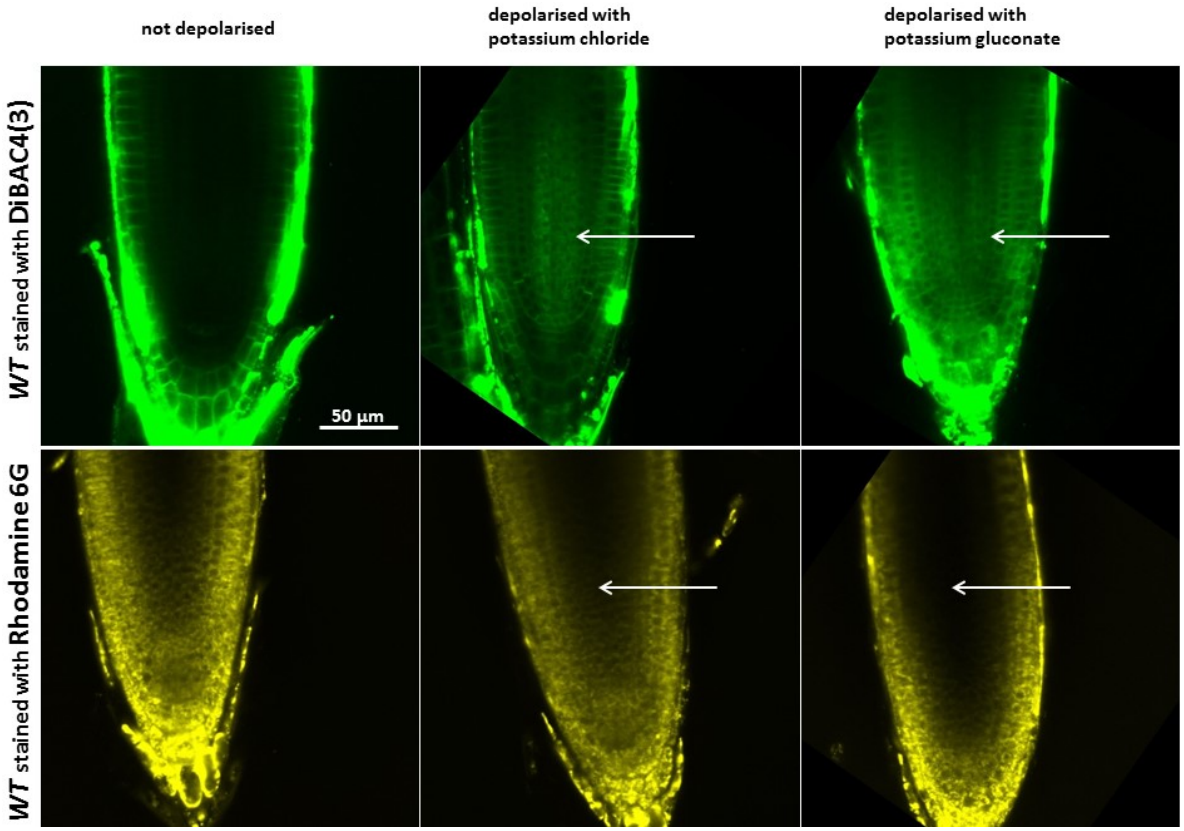

Figure 64: Wild type (col-0) roots have been stained with dyes that are used to report membrane and cell voltage. 5µg/ml DiBAC4(3) or 1µM Rhodamine 6G was applied to the roots for 1 hour (Methods, 2.4.1). Some of the roots were exposed to the dye and depolarising chemical, 100mM KCl or 100mM Kgluconate. Pictures represent at least 3 roots. Scalebar 50 µm.

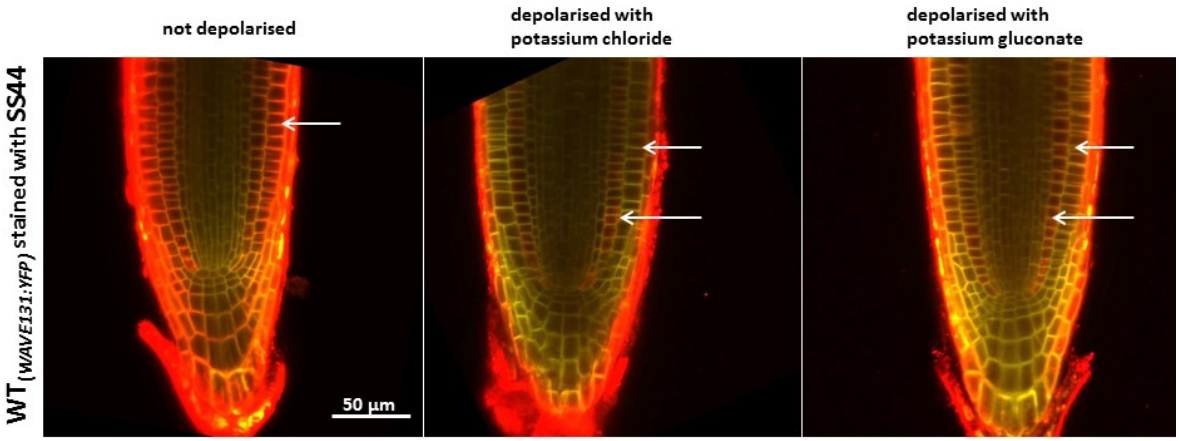

Figure 65: Roots expressing *UBQ10::WAVE131:YFP* in col-0 background, have been stained with new voltage sensitive dye SS44 (100nM) for 15 minutes. Some of the roots exposed to the dye were also exposed to the depolarising chemical, 100mM KCl or 100mM Kgluconate for 1 hour. Pictures represent at least 3 roots. Scalebar 50 µm.

6.2.2 Time course observations with membrane voltage dyes

In order to test whether repolarisation of root cells occurs and if it is observable with the voltage sensitive dyes, we observed roots subjected to depolarisation buffer and then transferred back to non-depolarisation buffer while stained with DiBAC4(3). We also attempted to observe continuous depolarisation while roots were subject to depolarising buffer while stained in Rhodamine 6G.

We have treated *Arabidopsis* roots for 1 hour to a buffer with potassium chloride, after which the roots were stained with DiBAC4(3) and placed into a buffer without potassium chloride and mounted on the confocal microscope for time-lapse observation. We have observed that the fluorescence within cells, which is a sign of cell depolarisation, was still present 5 minutes after roots were placed into a buffer without potassium chloride, but within 20 minutes we can observe a qualitative decrease in overall fluorescence and almost complete absence of fluorescence within cells (Figure 66). The result suggest that whole root depolarisation and repolarisation events are possible to be observed with DiBAC4(3) with a minute temporal scale.

We have kept *Arabidopsis* roots in a buffer without potassium chloride, but with added Rhodamine 6G to stain the root. We then moved the root to a depolarising buffer and observed it using time-lapse confocal microscopy. We observed an increase in fluorescence originating from Rhodamine 6G for the duration of 60 minutes (Figure 67). Marked increase was first obvious 30

minutes into the observation. This is a bizarre result since we expect a decrease of Rhodamine 6G fluorescence upon depolarisation of cells in the root. The difference between roots observed in Figure 64 treated with depolarising buffer and Figure 67 at 60 minutes is the time-lapse element, when roots were exposed to the depolarising buffer within a slide rather than in a petri dish. We cannot explain the difference between the two observations, but overall the result suggests that Rhodamine 6G is not a reliable dye to be used for membrane voltage reporting.

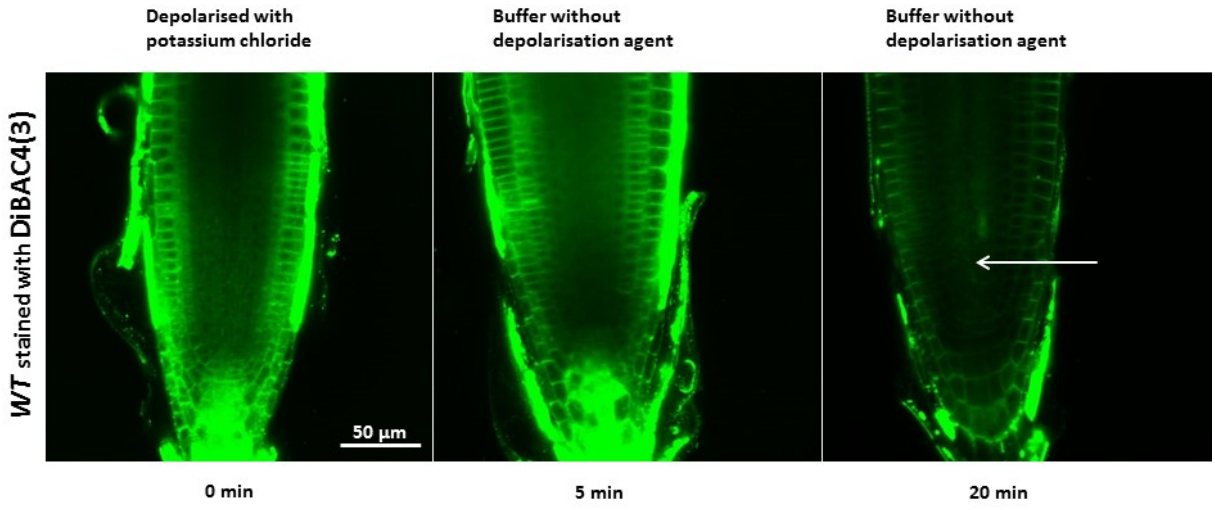

Figure 66: WT (col-0) roots were exposed to a buffer with DiBAC4(3) voltage sensitive dye and 100mM KCl (depolarising chemical) for 1 hour. After 1 hour, roots were moved to a buffer containing the dye, but no depolarisation chemical and were observed using time-lapse microscopy. Frames of the observation at 5 and 20 minutes are shown. Pictures represent at least 3 roots. Scalebar 50µm.

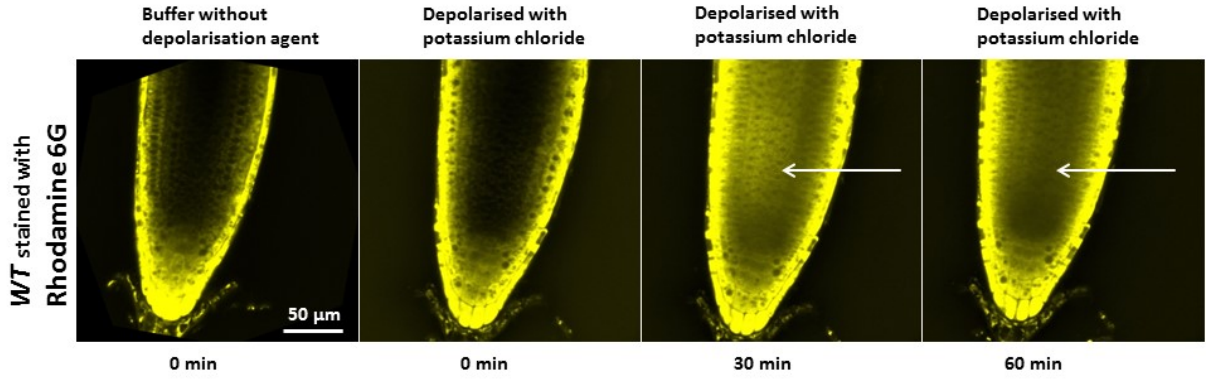

Figure 67: WT (col-0) roots were exposed to a buffer with Rhodamine 6G (1µM) voltage sensitive for 30 minutes. Afterwards, roots were moved to a buffer containing the dye, as well as the depolarisation chemical (100mM KCl) and were observed using time-lapse microscopy. Frames of the observation at 0, 30 and 60 minutes are shown. Pictures represent at least 3 roots. Scalebar 50µm.

6.2.3 Root electrotropism is lost by pre-treatment with depolarising buffer

In the root, membrane potential is found across each membrane separating symplast and apoplast, which is a result of difference in charge of symplast and apoplast. When studying electrotropism (Results III, chapter 5) a question arises, whether membrane potentials are changed during the root electrotropism and what is the spatial and temporal pattern of the hypothesised changes. With the voltage sensitive dyes we have observed changes in membrane potentials within the root, when exposing the root to the depolarisation buffer. To identify whether membrane potential changes into hyperpolarised or depolarised state from resting potential are a necessary component for electrotropism, we perturbed the resting potential of cells within the root prior electric field treatment. By exposing roots to depolarising buffer and then subjecting them to electric field treatment, we were able to observe and quantify the electrotropic turn while membrane potentials of the cells were already in depolarised state. This allowed us to assess whether the perturbation of the membrane potential prior electrotropism has any effect on the electrotropic turn.

We triggered depolarisation of the membrane potential by adding 100mM KCl into the root growth buffer 1 hour before exposure to the electric field. After the depolarisation pre-treatment, we have removed the roots from the growth buffer, placed them in medium B and exposed them to 1V/cm electric field using V-box set up (Results I, 3.2.2). We have observed their response using time-lapse imaging with Raspberry Pi camera, and the results were collected as a series of images taken in 10 minute intervals throughout 2 hour electric exposure.

We observed that roots pre-treated with depolarising buffer did not respond to electric field in the same way as roots that were not pre-treated. As a result of pre-treatment with 100mM KCl, the roots did not perform the electrotropic turn and instead remained showing gravitropic behaviour, aligning with the gravity vector (Figure 68A). We have also quantified the cumulative root tip deflections for roots that were or weren't pre-treated with 100mM KCl. We have plotted the distributions of deflections at each time point and we observed roots that were not pre-treated with

depolarisation buffer turn significantly more at all-time points in comparison with pre-treated roots (Figure 68B). The result shows that roots containing depolarised membranes prior electric field treatment are unable to perform the electrotropic turn suggesting that the change of the membrane potential from resting to depolarised state may be necessary for electrotropism.

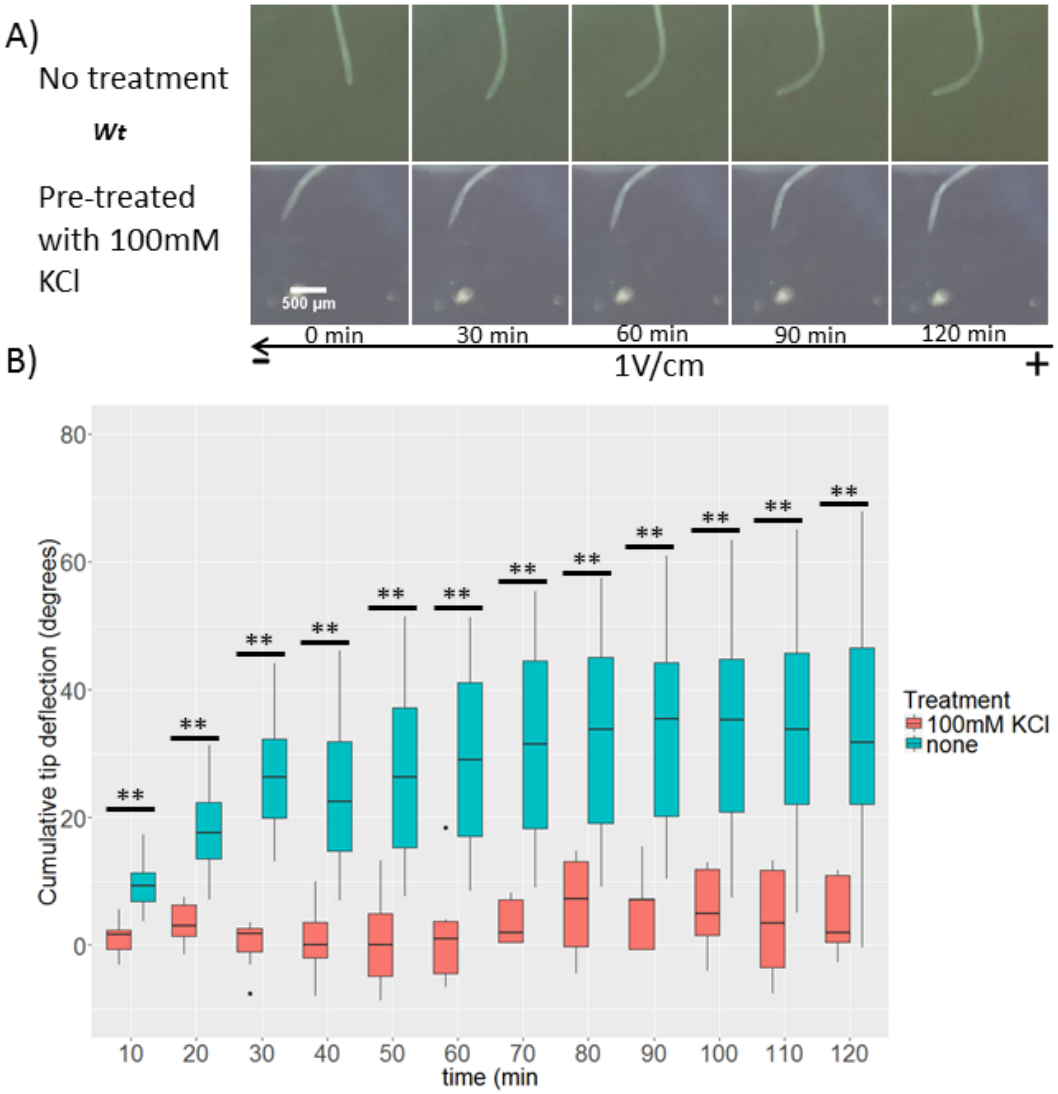

Figure 68: Electrotropism of wildtype (col-0) roots exposed to 1V/cm electric field with 1 hour pre-treatment with 100mM KCl. **A)** Images representing a timelapse of wt roots collected within V-box, exposed to 1V/cm E field, with no pre-treatment (N=24) and with 100mM KCl 1 hour pre-treatment (N=7). Images show 120 minute progression in 30 minute steps. Scalebar 500µm. **C)** Quantitative representation of the electrotropic behaviour. The deflection of each root tip was calculated as a difference between angle of the root tip at the t=0 and the angle of the root tip at the observed time point t=n. The box plot shows the distribution of root tip deflections over period of 2 hours in discreet 10 minute intervals. The box plot shows distribution median with a line in within the box, the box itself stands for 50% of the distribution closest to the median. The lines below and above the box stand for two quadrants containing data distributed 25% and more away from the median. The two distributions show roots exposed to E field without pre-treatment (N≥24) and with 100mM KCl pre-treatment (N≥7). The two distributions were tested for normality using Shapiro Wilk test. Variance of the distributions was tested using Fischer's test, and significant difference between the two distributions was tested using Welch T test. Any significant difference ($p<0.01$) is marked with **.

6.3 Discussion

6.3.1 Microscopic observation of plant cell voltage dynamics

We have shown that out of the three tested dyes at least DiBAC4(3), shows reliable change of fluorescence as a result of depolarisation buffer-triggered cell uptake. In other studies, where DiBAC4(3) has been used to monitor *Arabidopsis* protoplast membrane potential as well as cellular action potentials in *Helianthus annuus*, an independent measurement was used. In the case of protoplast membrane voltage, patch-clamp technique was utilised to confirm that DiBAC4(3) indeed reported a change in voltage (Konrad and Hedrich 2008) and in the case of a stem, a surface electrode was used (Zhao *et al.* 2015).

It may be technically challenging to fully independently confirm that the cells within root, especially those within the vasculature cell files, have changed membrane potential. It is possible to collect root cell protoplasts and use microelectrode measurement of membrane potential patch clamp at the same time as imaging the DiBAC4(3) derived fluorescence, but the spatial element of the root organisation will be lost. It is also possible to position micro electrodes on the epidermal surface of the *Arabidopsis* root and image DiBAC4(3) derived fluorescence, assuming that *in vivo* validation of the epidermal cell membrane voltage potential measurements together with DiBAC4(3) imaging may be enough to extrapolate for other tissues. Regardless the technical difficulties, in order to more fully confirm that changes in DiBAC4(3) fluorescence indeed report changes in membrane potential, an independent measurement may be necessary.

From our observations and trials with voltage sensitive dyes, it appears that similar to preference of using DiBAC4(3) for reporting membrane potential in animal cells (Adams and Levin 2012), may be established in plant cells. From our results it appeared that Rhodamine 6G is not a reliable dye. SS44 may prove to be a useful tool for membrane voltage measurement, new versions of the dye are being developed by Akita Innovations and all of these will be tested for reporting of plant membrane voltage in Dr Sena's laboratory. However SS44 is new and it requires further tests that have already been done with DiBAC4(3), such as independent

measurements and clear understanding of the conditions under which the SS44 and its derivatives enter and exit cells.

One dye that was used to report voltage in the plants that we did not test is the RH414 (N-(3-Triethylammoniumpropyl)-4-(4-(4-(Diethylamino)phenyl)Butadienyl)Pyridinium Dibromide). It was used to report membrane voltage of the sieve elements during wound response of *Vicia faba* (Furch *et al.* 2007), and it may be worth observing the reporting qualities of this voltage sensitive dye in the *Arabidopsis* roots.

An important point moving forward with the voltage sensitive dyes, monitoring the electric changes in the root as well as differences in resting membrane potential is the detection and analysis of the signal obtained from fluorescence images. Our results showed that when using a common, concentrated depolarisation stimulant (potassium chloride, potassium gluconate), the fluorescence intensity change within cells caused by DiBAC4(3) uptake was strong enough to be noticed qualitatively. It is possible that the differences in fluorescence of DiBAC4(3) may be smaller when reporting on membrane voltage changes during physiological phenomena. This means that post-image acquisition, image processing may be necessary to unravel some of the cell depolarisation events when observing the root in other physiological phenomena such as electrotropism or root regeneration. Especially other results that reported short lived bursts of cell depolarisation were only observed after computational analysis (Qin *et al.* 2013), (Zhao *et al.* 2015).

6.3.2 Electrotropism and membrane potential

The aim of testing new tools for observation of cell membrane voltage is that they may be used to report in living tissue on previously unknown components of physiological mechanisms. This is also the intention with the voltage sensitive dyes presented in the results. Once validated with independent measurement, DiBAC4(3) as well as other dyes may be used to examine if there are specific transmembrane potential patterns in the regenerating root tip, as well as during

electrotropism. Even though we did not yet complete direct observation of membrane potential dynamics during electrotropism, we have showed that membrane depolarisation with KCl before electric treatment may be enough to stop roots from performing electrotropism. We are yet unsure if it is the specific excess of potassium ions that caused the non-electrotropic response or the membrane depolarisation prior electric field treatment. An easy way to test if the cell depolarisation prior to electric exposure inhibits electrotropism, is to use another depolarising agent, such as hormone abscisic acid (Konrad and Hedrich 2008). When the non-electrotropic response is not related to potassium, but to depolarisation of cells, roots that had cell membranes depolarised with abscisic acid should still not turn as a response to electric field. These results are a first step towards showing that transmembrane potential of cells is changed during electrotropism and this change is necessary for electrotropic turn to occur.

7 Concluding Remarks

7.1 New experimental tools

To be able to study the effect of external electric field on root regeneration and root tropism, we had to modify existing experimental tools and come up with completely new ones (Results I, 3) to allow us the study of biological phenomena described in this thesis (Results II, 4; Results III, 5; Prelimary Results IV, 6). We have used approaches common in hardware design such as prototyping and 3D printing, and as a result we have constructed one-off devices that were able to serve their intended purpose. These tools, not only worked well for distinctive experiments of root exposure to electricity, but also are an example of specification driven assay development.

It was challenging to fulfil the desired criteria for V-tank, V-box and V-slide and it may have been easier to compromise on some design needs to have the assay development done faster or to avoid the difficult parts of building such tools altogether. However, this would have an undesired effect of collecting unreliable observations when exposing roots to external electric field, a situation which has been revealed previously (Stenz and Weisenseel 1993). This means that the quality of the biological data comes from the design of the tools that have been built to collect them. This may be a trivial point to mention, but it is especially relevant for biologists wanting to study completely new phenomena.

Since there are already multitudes of proven tools designed to observe, examine and measure biological samples built by engineers with no specific experiment in mind, the tools themselves can set a limit on what biological phenomena can be reliably measured. However, when design principles and positive attitude to building new assay tools is adopted by an examiner of new biological occurrences, reliable data and new facts ignored by others can be uncovered. The hope is that this thesis can serve as an example of one such instance, when new experimental tools with a design purpose to collect reliable data custom built by a biologist, have uncovered new phenomena in plants.

7.2 External electric field affects root development and growth

We have observed two unique phenotypes when we exposed regenerating (Results II, 4) and growing roots (Results III, 5) to weak external electric field.

When regenerating roots have been exposed to electric field, it was observed that the frequency of root regeneration has increased. Even though the precise mechanism of the electric field action has not yet been elucidated, we can speculate that the mechanism may involve change in the distribution of auxin in the remaining root tissue and has an inter-cellular component since temporarily decreased cell divisions in the root stump were observed. However it would be very difficult to perform any genetic or pharmacological screen to further elucidate the molecular mechanism behind the electricity perturbed root regeneration frequency phenotype, since the experiment relies on a high number of individual root replicates to measure root regeneration frequency, which takes long time to obtain.

We have also measured a previously described phenotype of root electrotropism, quantitated and observed for the first time in *Arabidopsis*. Unlike electric perturbation of root tip regeneration, root electrotropism can be observed on single roots and this has allowed us to unravel multiple findings. The action of gravitropism and electrotropism appears to be controlled by a different molecular mechanism, even though there is still a level of auxin transport provided by AUX1 transporter that has to be present for wild type electrotropism. In addition we have managed to identify a mutant with reduced electrotropic response, *glr3.4* and identify multiple GLRs and other ion channels that can be examined further for their role in electrotropism. GLRs are unique proteins that show high homology with iGLURs animal ion channels expressed in neurons with an important role in memory and learning. It is possible that these channels have a role in the roots' mechanism of electric field perception and response, either through Ca^{2+} signalling or other unobserved dynamic event that can be further studied.

For future work we can also suggest the examination of mutants with decreased electrotropism phenotype, for their electricity perturbed root regeneration frequency phenotype. The outcome of this experiment could potentially unravel if individual phenomena observed when roots are exposed to weak external electric field share common molecular features and components or if electric field affects different mechanisms when stimulating roots in different developmental states.

7.3 Cell membrane potentials and role for bioelectricity in root development

We have used novel voltage sensitive dyes to report on membrane potentials in root meristem, and we have perturbed electrotropic response by depolarisation of cell membranes (Preliminary Results IV, 6).

The topic of membrane potentials in plants and their function in physiological and developmental processes is still controversial due to small amount of evidence. This is because there is no validated method to observe membrane potentials in all of the tissues of the root. The current tools have been limited to surface electrodes that are not able to measure individual cell membrane potentials. There is a need for new tools to observe cell membrane potentials within tissue and with micro resolution. Further membrane potential observations using fluorescent voltage sensitive dyes will have to be conducted and independent method such as micro electrode measurement will be necessary to validate the reporting of the membrane potentials with VSDs. Once validated, the dyes will enable reliable observation of membrane potentials and their fluctuations in the root.

It is possible that using voltage sensitive dyes to observe membrane potentials within root will allow for completely new discoveries. In animals it was observed that even the difference among resting membrane potentials in different tissues have developmental consequences (Adams *et al.* 2007). It is worth using new voltage sensitive dyes to examine known phenomena in root development such as specification of quiescent centre or lateral root formation. It may be possible

to correlate possible spatial and temporal pattern of membrane potentials with developmental processes in the root. We may further speculate that perturbation of such membrane potential patterns may lead to perturbation of developmental processes in the root. These experiments will be crucial when describing the potential role of endogenously generated bioelectricity in root development.

8 Bibliography

Abas, L., Benjamins, R., Malenica, N., Paciorek, T., Wisniewska, J., Moulinier-Anzola, J.C., Sieberer, T., Friml, J. and Luschnig, C. (2006) Intracellular trafficking and proteolysis of the Arabidopsis auxin-efflux facilitator PIN2 are involved in root gravitropism. *Nat Cell Biol*, **8**, 249-256.

Adams, D.S. and Levin, M. (2012) Measuring Resting Membrane Potential Using the Fluorescent Voltage Reporters DiBAC(4)(3) and CC2-DMPE. *Cold Spring Harbor protocols*, **2012**, 459-464.

Adams, D.S., Masi, A. and Levin, M. (2007) H+ pump-dependent changes in membrane voltage are an early mechanism necessary and sufficient to induce Xenopus tail regeneration. *Development*, **134**, 1323-1335.

Aida, M., Beis, D., Heidstra, R., Willemsen, V., Blilou, I., Galinha, C., Nussaume, L., Noh, Y.-S., Amasino, R. and Scheres, B. (2004) The PLETHORA Genes Mediate Patterning of the Arabidopsis Root Stem Cell Niche. *Cell*, **119**, 109-120.

Akemann, W., Mutoh, H., Perron, A., Park, Y.K., Iwamoto, Y. and Knöpfel, T. (2012) Imaging neural circuit dynamics with a voltage-sensitive fluorescent protein. *Journal of Neurophysiology*, **108**, 2323-2337.

Alonso, J.M., Stepanova, A.N., Leisse, T.J., Kim, C.J., Chen, H., Shinn, P., Stevenson, D.K., Zimmerman, J., Barajas, P., Cheuk, R., Gadrinab, C., Heller, C., Jeske, A., Koesema, E., Meyers, C.C., Parker, H., Prednis, L., Ansari, Y., Choy, N., Deen, H., Geralt, M., Hazari, N., Hom, E., Karnes, M., Mulholland, C., Ndubaku, R., Schmidt, I., Guzman, P., Aguilar-Henonin, L., Schmid, M., Weigel, D., Carter, D.E., Marchand, T., Risseeuw, E., Brogden, D., Zeko, A., Crosby, W.L., Berry, C.C. and Ecker, J.R. (2003) Genome-wide insertional mutagenesis of Arabidopsis thaliana. *Science*, **301**, 653-657.

Arnaud, C., Bonnot, C., Desnos, T. and Nussaume, L. (2010) The root cap at the forefront. *Comptes Rendus Biologies*, **333**, 335-343.

Bai, L., Zhang, G., Zhou, Y., Zhang, Z., Wang, W., Du, Y., Wu, Z. and Song, C.P. (2009) Plasma membrane-associated proline-rich extensin-like receptor kinase 4, a novel regulator of Ca signalling, is required for abscisic acid responses in Arabidopsis thaliana. *Plant J*, **60**, 314-327.

Baluška, F. and Mancuso, S. (2013) Ion channels in plants: From bioelectricity, via signaling, to behavioral actions. *Plant Signaling & Behavior*, **8**, e23009.

Baluška, F., Mancuso, S., Volkmann, D. and Barlow, P.W. (2009) The 'root-brain' hypothesis of Charles and Francis Darwin: Revival after more than 125 years. *Plant Signaling & Behavior*, **4**, 1121-1127.

Band, L.R., Wells, D.M., Larrieu, A., Sun, J., Middleton, A.M., French, A.P., Brunoud, G., Sato, E.M., Wilson, M.H., Péret, B., Oliva, M., Swarup, R., Sairanen, I., Parry, G., Ljung, K., Beeckman, T., Garibaldi, J.M., Estelle, M., Owen, M.R., Vissenberg, K., Hodgman, T.C., Pridmore, T.P., King, J.R., Vernoux, T. and Bennett, M.J. (2012) Root gravitropism is regulated by a transient lateral auxin gradient controlled by a tipping-point mechanism. *Proceedings of the National Academy of Sciences*, **109**, 4668-4673.

Barbez, E., Dünser, K., Gaidora, A., Lendl, T. and Busch, W. (2017) Auxin steers root cell expansion via apoplastic pH regulation in Arabidopsis thaliana. *Proceedings of the National Academy of Sciences*, **114**, E4884-E4893.

Beane, W.S., Morokuma, J., Lemire, J.M. and Levin, M. (2012) Bioelectric signaling regulates head and organ size during planarian regeneration. *Development*, **140**, 313.

Becker, D., Geiger, D., Dunkel, M., Roller, A., Bertl, A., Latz, A., Carpaneto, A., Dietrich, P., Roelfsema, M.R.G., Voelker, C., Schmidt, D., Mueller-Roeber, B., Czempinski, K. and Hedrich, R. (2004) AtTPK4, an Arabidopsis tandem-pore K+ channel, poised to control the pollen membrane voltage in a pH- and Ca2+-dependent manner. *Proceedings of the National Academy of Sciences of the United States of America*, **101**, 15621-15626.

Beemster, G.T.S. and Baskin, T.I. (2000) STUNTED PLANT 1 Mediates Effects of Cytokinin, But Not of Auxin, on Cell Division and Expansion in the Root of Arabidopsis. *Plant Physiology*, **124**, 1718.

Behrens, H.M., Gradmann, D. and Sievers, A. (1985) Membrane-potential responses following gravistimulation in roots of Lepidium sativum L. *Planta*, **163**, 463-472.

Benfey, P.N., Linstead, P.J., Roberts, K., Schiefelbein, J.W., Hauser, M.T. and Aeschbacher, R.A. (1993) Root development in Arabidopsis: four mutants with dramatically altered root morphogenesis. *Development*, **119**, 57-70.

Benitez-Alfonso, Y., Faulkner, C., Pendle, A., Miyashima, S., Helariutta, Y. and Maule, A. (2013) Symplastic Intercellular Connectivity Regulates Lateral Root Patterning. *Developmental Cell*, **26**, 136-147.

Bennett, M.J., Marchant, A., Green, H.G., May, S.T., Ward, S.P., Millner, P.A., Walker, A.R., Schulz, B. and Feldmann, K.A. (1996) Arabidopsis AUX1 Gene: A Permease-Like Regulator of Root Gravitropism. *Science*, **273**, 948-950.

Birnbaum, K., Shasha, D.E., Wang, J.Y., Jung, J.W., Lambert, G.M., Galbraith, D.W. and Benfey, P.N. (2003) A Gene Expression Map of the Arabidopsis Root. *Science*, **302**, 1956-1960.

Blilou, I., Xu, J., Wildwater, M., Willemsen, V., Paponov, I., Friml, J., Heidstra, R., Aida, M., Palme, K. and Scheres, B. (2005) The PIN auxin efflux facilitator network controls growth and patterning in Arabidopsis roots. *Nature*, **433**, 39-44.

Boonsirichai, K., Sedbrook, J.C., Chen, R., Gilroy, S. and Masson, P.H. (2003) ALTERED RESPONSE TO GRAVITY Is a Peripheral Membrane Protein That Modulates Gravity-Induced Cytoplasmic Alkalinization and Lateral Auxin Transport in Plant Statocytes. *The Plant Cell*, **15**, 2612.

Brower, D.L. and McIntosh, J.R. (1980) The effects of applied electric fields on Micrasterias. I. Morphogenesis and the pattern of cell wall deposition. *Journal of Cell Science*, **42**, 261.

Carlsbecker, A., Lee, J.-Y., Roberts, C.J., Dettmer, J., Lehesranta, S., Zhou, J., Lindgren, O., Moreno-Risueno, M.A., Vatén, A., Thitamadee, S., Campilho, A., Sebastian, J., Bowman, J.L., Helariutta, Y. and Benfey, P.N. (2010) Cell signalling by microRNA165/6 directs gene dose-dependent root cell fate. *Nature*, **465**, 316-321.

Chang, F. and Minc, N. (2014) Electrochemical Control of Cell and Tissue Polarity. *Annual Review of Cell and Developmental Biology*, **30**, 317-336.

Chapman, E.J. and Estelle, M. (2009) Mechanism of Auxin-Regulated Gene Expression in Plants. *Annual Review of Genetics*, **43**, 265-285.

Chiu, J.C., Brenner, E.D., DeSalle, R., Nitabach, M.N., Holmes, T.C. and Coruzzi, G.M. (2002) Phylogenetic and Expression Analysis of the Glutamate-Receptor–Like Gene Family in Arabidopsis thaliana. *Molecular Biology and Evolution*, **19**, 1066-1082.

Chrisman, S.D., Waite, C.B., Scoville, A.G. and Carnell, L. (2016) C. elegans Demonstrates Distinct Behaviors within a Fixed and Uniform Electric Field. *PLOS ONE*, **11**, e0151320.

Cogalniceanu, G., Radu, M., Fologea, D., Moisoi, N. and Aurelia, B. (1998) Stimulation of tobacco shoot regeneration by alternating weak electric field. *Bioelectrochemistry and Bioenergetics*, **44**, 257-260.

Colón-Carmona, A., You, R., Haimovitch-Gal, T. and Doerner, P. (1999) Spatio-temporal analysis of mitotic activity with a labile cyclin–GUS fusion protein. *The Plant Journal*, **20**, 503-508.

Crawford, B.C.W., Sewell, J., Golembeski, G., Roshan, C., Long, J.A. and Yanofsky, M.F. (2015) Genetic control of distal stem cell fate within root and embryonic meristems. *Science*, **347**, 655.

Cruz-Ramirez, A., Diaz-Trivino, S., Blilou, I., Grieneisen, V.A., Sozzani, R., Zamioudis, C., Miskolczi, P., Nieuwland, J., Benjamins, R., Dhonukshe, P., Caballero-Perez, J., Horvath, B., Long, Y., Mahonen, A.P., Zhang, H., Xu, J., Murray, J.A., Benfey, P.N., Bako, L., Maree, A.F. and Scheres, B. (2012) A bistable circuit involving SCARECROW-RETINOBLASTOMA integrates cues to inform asymmetric stem cell division. *Cell*, **150**, 1002-1015.

Cui, H., Levesque, M.P., Vernoux, T., Jung, J.W., Paquette, A.J., Gallagher, K.L., Wang, J.Y., Blilou, I., Scheres, B. and Benfey, P.N. (2007) An Evolutionarily Conserved Mechanism Delimiting SHR Movement Defines a Single Layer of Endodermis in Plants. *Science*, **316**, 421.

Czempinski, K., Frachisse, J.-M., Maurel, C., Barbier-Brygoo, H. and Mueller-Roeber, B. (2002) Vacuolar membrane localization of the Arabidopsis'two-pore' K+ channel KCO1. *The Plant Journal*, **29**, 809-820.

De Angeli, A., Monachello, D., Ephritikhine, G., Frachisse, J.M., Thomine, S., Gambale, F. and Barbier-Brygoo, H. (2006) The nitrate/proton antiporter AtCLCa mediates nitrate accumulation in plant vacuoles. *Nature*, **442**, 939-942.

De Rybel, B., Adibi, M., Breda, A.S., Wendrich, J.R., Smit, M.E., Novák, O., Yamaguchi, N., Yoshida, S., Van Isterdael, G., Palovaara, J., Nijsse, B., Boekschoten, M.V., Hooiveld, G., Beeckman, T., Wagner, D., Ljung, K., Fleck, C. and Weijers, D. (2014) Integration of growth and patterning during vascular tissue formation in <em>Arabidopsis</em&gt. *Science*, **345**.

Dello Ioio, R., Linhares, F.S., Scacchi, E., Casamitjana-Martinez, E., Heidstra, R., Costantino, P. and Sabatini, S. (2007) Cytokinins Determine Arabidopsis Root-Meristem Size by Controlling Cell Differentiation. *Current Biology*, **17**, 678-682.

Dello Ioio, R., Nakamura, K., Moubayidin, L., Perilli, S., Taniguchi, M., Morita, M.T., Aoyama, T., Costantino, P. and Sabatini, S. (2008) A genetic framework for the control of cell division and differentiation in the root meristem. *Science*, **322**, 1380-1384.

Dello Ioio, R., Galinha, C., Fletcher, Alexander G., Grigg, Stephen P., Molnar, A., Willemsen, V., Scheres, B., Sabatini, S., Baulcombe, D., Maini, Philip K. and Tsiantis, M. (2012) A PHABULOSA/Cytokinin Feedback Loop Controls Root Growth in Arabidopsis. *Current Biology*, **22**, 1699-1704.

Demidchik, V. (2014) Mechanisms and physiological roles of K+ efflux from root cells. *J Plant Physiol*, **171**, 696-707.

Demidchik, V., Essah, P.A. and Tester, M. (2004) Glutamate activates cation currents in the plasma membrane of Arabidopsis root cells. *Planta*, **219**, 167-175.

Dietrich, D., Pang, L., Kobayashi, A., Fozard, J.A., Boudolf, V., Bhosale, R., Antoni, R., Nguyen, T., Hiratsuka, S., Fujii, N., Miyazawa, Y., Bae, T.-W., Wells, D.M., Owen, M.R., Band, L.R., Dyson, R.J., Jensen, O.E., King, J.R., Tracy, S.R., Sturrock, C.J., Mooney, S.J., Roberts, J.A., Bhalerao, R.P., Dinneny, J.R., Rodriguez, P.L., Nagatani, A., Hosokawa, Y., Baskin, T.I., Pridmore, T.P., De Veylder, L., Takahashi, H. and Bennett, M.J. (2017) Root hydrotropism is controlled via a cortex-specific growth mechanism. **3**, 17057.

Dolan, L. and Davies, J. (2004) Cell expansion in roots. *Curr Opin Plant Biol*, **7**, 33-39.

Dolan, L., Janmaat, K., Willemsen, V., Linstead, P., Poethig, S., Roberts, K. and Scheres, B. (1993) Cellular organisation of the Arabidopsis thaliana root. *Development*, **119**, 71.

Dünser, K. and Kleine-Vehn, J. (2015) Differential growth regulation in plants—the acid growth balloon theory. *Current Opinion in Plant Biology*, **28**, 55-59.

Eapen, D., Barroso, M.L., Ponce, G., Campos, M.E. and Cassab, G.I. (2005) Hydrotropism: root growth responses to water. *Trends in Plant Science*, **10**, 44-50.

Efroni, I., Mello, A., Nawy, T., Ip, P.-L., Rahni, R., DelRose, N., Powers, A., Satija, R. and Birnbaum, K.D. (2016) Root Regeneration Triggers an Embryo-like Sequence Guided by Hormonal Interactions. *Cell*, **165**, 1721-1733.

Ehrenberg, B., Montana, V., Wei, M.D., Wuskell, J.P. and Loew, L.M. (1988) Membrane potential can be determined in individual cells from the nernstian distribution of cationic dyes. *Biophys J*, **53**, 785-794.

Fan, Y. and Bergmann, A. (2008) Apoptosis-induced compensatory proliferation. The Cell is dead. Long live the Cell! *Trends in Cell Biology*, **18**, 467-473.

Fasano, J.M., Swanson, S.J., Blancaflor, E.B., Dowd, P.E., Kao, T.-h. and Gilroy, S. (2001) Changes in Root Cap pH Are Required for the Gravity Response of the Arabidopsis Root. *The Plant Cell*, **13**, 907-922.

Fecht-Bartenbach, J.v.d., Bogner, M., Krebs, M., Stierhof, Y.-D., Schumacher, K. and Ludewig, U. (2007) Function of the anion transporter AtCLC-d in the trans-Golgi network. *The Plant Journal*, **50**, 466-474.

Feldman, L.J. (1976) The de Novo Origin of the Quiescent Center Regenerating Root Apices of Zea mays. *Planta*, **128**, 207-212.

Ferreira, P.C., Hemerly, A.S., Engler, J.D., van Montagu, M., Engler, G. and Inze, D. (1994) Developmental expression of the arabidopsis cyclin gene cyc1At. *Plant Cell*, **6**, 1763-1774.

FONDREN, W.M. and MOORE, R. (1987) Collection of Gravitropic Effectors from Mucilage of Electrotropically-stimulated Roots of Zea mays L. *Annals of Botany*, **59**, 657-659.

Forzani, C., Aichinger, E., Sornay, E., Willemsen, V., Laux, T., Dewitte, W. and Murray, J.A. (2014) WOX5 suppresses CYCLIN D activity to establish quiescence at the center of the root stem cell niche. *Curr Biol*, **24**, 1939-1944.

Friml, J., Benkova, E., Blilou, I., Wisniewska, J., Hamann, T., Ljung, K., Woody, S., Sandberg, G., Scheres, B., Jurgens, G. and Palme, K. (2002a) AtPIN4 mediates sink-driven auxin gradients and root patterning in Arabidopsis. *Cell*, **108**, 661-673.

Friml, J., Vieten, A., Sauer, M., Weijers, D., Schwarz, H., Hamann, T., Offringa, R. and Jurgens, G. (2003) Efflux-dependent auxin gradients establish the apical-basal axis of Arabidopsis. *Nature*, **426**, 147-153.

Friml, J., Wisniewska, J., Benkova, E., Mendgen, K. and Palme, K. (2002b) Lateral relocation of auxin efflux regulator PIN3 mediates tropism in Arabidopsis. *Nature*, **415**, 806-809.

Friml, J., Yang, X., Michniewicz, M., Weijers, D., Quint, A., Tietz, O., Benjamins, R., Ouwerkerk, P.B.F., Ljung, K., Sandberg, G., Hooykaas, P.J.J., Palme, K. and Offringa, R. (2004) A PINOID-Dependent Binary Switch in Apical-Basal PIN Polar Targeting Directs Auxin Efflux. *Science*, **306**, 862.

Fromm, J. and Lautner, S. (2007) Electrical signals and their physiological significance in plants. *Plant, Cell & Environment*, **30**, 249-257.

Furch, A.C.U., Hafke, J.B., Schulz, A. and van Bel, A.J.E. (2007) Ca2+-mediated remote control of reversible sieve tube occlusion in Vicia faba. *Journal of Experimental Botany*, **58**, 2827-2838.

Galinha, C., Hofhuis, H., Luijten, M., Willemsen, V., Blilou, I., Heidstra, R. and Scheres, B. (2007) PLETHORA proteins as dose-dependent master regulators of Arabidopsis root development. *Nature*, **449**, 1053-1057.

Gallagher, K.L., Paquette, A.J., Nakajima, K. and Benfey, P.N. (2004) Mechanisms Regulating SHORT-ROOT Intercellular Movement. *Current Biology*, **14**, 1847-1851.

Galvan-Ampudia, C.S., Julkowska, M.M., Darwish, E., Gandullo, J., Korver, R.A., Brunoud, G., Haring, M.A., Munnik, T., Vernoux, T. and Testerink, C. (2013) Halotropism is a response of plant roots to avoid a saline environment. *Curr Biol*, **23**, 2044-2050.

Galweiler, L., Guan, C., Muller, A., Wisman, E., Mendgen, K., Yephremov, A. and Palme, K. (1998) Regulation of polar auxin transport by AtPIN1 in Arabidopsis vascular tissue. *Science*, **282**, 2226-2230.

Gao, R., Zhao, S., Jiang, X., Sun, Y., Zhao, S., Gao, J., Borleis, J., Willard, S., Tang, M., Cai, H., Kamimura, Y., Huang, Y., Jiang, J., Huang, Z., Mogilner, A., Pan, T., Devreotes, P.N. and Zhao, M. (2015) A large-scale screen reveals genes that mediate electrotaxis in Dictyostelium discoideum. *Science signaling*, **8**, ra50.

Gaxiola, R.A., Palmgren, M.G. and Schumacher, K. (2007) Plant proton pumps. *FEBS Letters*, **581**, 2204-2214.

Geldner, N., Dénervaud-Tendon, V., Hyman, D.L., Mayer, U., Stierhof, Y.-D. and Chory, J. (2009) Rapid, combinatorial analysis of membrane compartments in intact plants with a multicolor marker set. *The Plant Journal*, **59**, 169-178.

Gilroy, S. (2008) Plant tropisms. *Current Biology*, **18**, R275-R277.
Grieneisen, V.A., Xu, J., Maree, A.F., Hogeweg, P. and Scheres, B. (2007) Auxin transport is sufficient to generate a maximum and gradient guiding root growth. *Nature*, **449**, 1008-1013.
Hangarter, R.P. (1997) Gravity, light and plant form. *Plant Cell Environ*, **20**, 796-800.
Hartig, K. and Beck, E. (2006) Crosstalk between auxin, cytokinins, and sugars in the plant cell cycle. *Plant biology (Stuttgart, Germany)*, **8**, 389-396.
Haruta, M., Burch, H.L., Nelson, R.B., Barrett-Wilt, G., Kline, K.G., Mohsin, S.B., Young, J.C., Otegui, M.S. and Sussman, M.R. (2010) Molecular characterization of mutant Arabidopsis plants with reduced plasma membrane proton pump activity. *The Journal of biological chemistry*, **285**, 17918-17929.
Hedrich, R. and Becker, D. Green circuits — The potential of plant specific ion channels. *Plant Molecular Biology*, **26**, 1637-1650.
Heidstra, R., Welch, D. and Scheres, B. (2004) Mosaic analyses using marked activation and deletion clones dissect Arabidopsis SCARECROW action in asymmetric cell division. *Genes & Development*, **18**, 1964-1969.
Helariutta, Y., Fukaki, H., Wysocka-Diller, J., Nakajima, K., Jung, J., Sena, G., Hauser, M.-T. and Benfey, P.N. (2000) The SHORT-ROOT Gene Controls Radial Patterning of the Arabidopsis Root through Radial Signaling. *Cell*, **101**, 555-567.
Hepler, P.K. (2005) Calcium: A Central Regulator of Plant Growth and Development. *The Plant Cell*, **17**, 2142.
Himanen, K., Boucheron, E., Vanneste, S., de Almeida Engler, J., Inze, D. and Beeckman, T. (2002) Auxin-mediated cell cycle activation during early lateral root initiation. *Plant Cell*, **14**, 2339-2351.
Hirose, N., Takei, K., Kuroha, T., Kamada-Nobusada, T., Hayashi, H. and Sakakibara, H. (2008) Regulation of cytokinin biosynthesis, compartmentalization and translocation. *J Exp Bot*, **59**, 75-83.
Hirsch, R.E., Lewis, B.D., Spalding, E.P. and Sussman, M.R. (1998) A role for the AKT1 potassium channel in plant nutrition. *Science*, **280**, 918-921.
Hodge, A. (2006) Plastic plants and patchy soils. *Journal of Experimental Botany*, **57**, 401-411.
Hohm, T., Demarsy, E., Quan, C., Allenbach Petrolati, L., Preuten, T., Vernoux, T., Bergmann, S. and Fankhauser, C. (2014) Plasma membrane H(+)-ATPase regulation is required for auxin gradient formation preceding phototropic growth. *Molecular Systems Biology*, **10**, 751.
Homann, U. and Thiel, G. Cl− and K+ channel currents during the action potential in Chara. simultaneous recording of membrane voltage and patch currents. *The Journal of Membrane Biology*, **141**, 297-309.
Hou, G., Kramer, V.L., Wang, Y.S., Chen, R., Perbal, G., Gilroy, S. and Blancaflor, E.B. (2004) The promotion of gravitropism in Arabidopsis roots upon actin disruption is coupled with the extended alkalinization of the columella cytoplasm and a persistent lateral auxin gradient. *Plant J*, **39**, 113-125.
Hu, Y., Xie, Q. and Chua, N.-H. (2003) The Arabidopsis Auxin-Inducible Gene ARGOS Controls Lateral Organ Size. *The Plant Cell*, **15**, 1951-1961.
Hwang, I. and Sheen, J. (2001) Two-component circuitry in Arabidopsis cytokinin signal transduction. *Nature*, **413**, 383-389.
Inoue, S.-i. and Kinoshita, T. (2017) Blue Light Regulation of Stomatal Opening and the Plasma Membrane H(+)-ATPase. *Plant Physiology*, **174**, 531-538.
Inoue, T., Higuchi, M., Hashimoto, Y., Seki, M., Kobayashi, M., Kato, T., Tabata, S., Shinozaki, K. and Kakimoto, T. (2001) Identification of CRE1 as a cytokinin receptor from Arabidopsis. *Nature*, **409**, 1060-1063.
Ishikawa, H. and Evans, M.L. (1990) Electrotropism of Maize Roots : Role of the Root Cap and Relationship to Gravitropism. *Plant Physiology*, **94**, 913-918.

Joubes, J. and Chevalier, C. (2000) Endoreduplication in higher plants. *Plant Mol Biol*, **43**, 735-745.
Jouniaux, L., Maineult, A., Naudet, V., Pessel, M. and Sailhac, P. (2009) Review of self-potential methods in hydrogeophysics. *Comptes Rendus Geoscience*, **341**, 928-936.
Judelson, H.S. and Blanco, F.A. (2005) The spores of Phytophthora: weapons of the plant destroyer. *Nat Rev Micro*, **3**, 47-58.
Kamano, S., Kume, S., Iida, K., Lei, K.-J., Nakano, M., Nakayama, Y. and Iida, H. (2015) Transmembrane Topologies of Ca2+-permeable Mechanosensitive Channels MCA1 and MCA2 in Arabidopsis thaliana. *Journal of Biological Chemistry*, **290**, 30901-30909.
King, R.S. and Newmark, P.A. (2012) The cell biology of regeneration. *The Journal of Cell Biology*, **196**, 553.
Kiss, J.Z., Correll, M.J., Mullen, J.L., Hangarter, R.P. and Edelmann, R.E. (2003) Root phototropism: how light and gravity interact in shaping plant form. *Gravitational and space biology bulletin : publication of the American Society for Gravitational and Space Biology*, **16**, 55-60.
Kiss, J.Z., Hertel, R. and Sack, F.D. (1989) Amyloplasts are necessary for full gravitropic sensitivity in roots of Arabidopsis thaliana. *Planta*, **177**, 198-206.
Kiss, J.Z., Miller, K.M., Ogden, L.A. and Roth, K.K. (2002) Phototropism and gravitropism in lateral roots of Arabidopsis. *Plant Cell Physiol*, **43**, 35-43.
Kleine-Vehn, J., Ding, Z., Jones, A.R., Tasaka, M., Morita, M.T. and Friml, J. (2010) Gravity-induced PIN transcytosis for polarization of auxin fluxes in gravity-sensing root cells. *Proceedings of the National Academy of Sciences*, **107**, 22344-22349.
Kleine-Vehn, J., Leitner, J., Zwiewka, M., Sauer, M., Abas, L., Luschnig, C. and Friml, J. (2008) Differential degradation of PIN2 auxin efflux carrier by retromer-dependent vacuolar targeting. *Proceedings of the National Academy of Sciences*, **105**, 17812-17817.
Kobayashi, A., Takahashi, A., Kakimoto, Y., Miyazawa, Y., Fujii, N., Higashitani, A. and Takahashi, H. (2007) A gene essential for hydrotropism in roots. *Proceedings of the National Academy of Sciences*, **104**, 4724-4729.
Konrad, K.R. and Hedrich, R. (2008) The use of voltage-sensitive dyes to monitor signal-induced changes in membrane potential–ABA triggered membrane depolarization in guard cells†. *The Plant Journal*, **55**, 161-173.
Kral, N., Hanna Ougolnikova, A. and Sena, G. (2016) Externally imposed electric field enhances plant root tip regeneration. *Regeneration*, **3**, 156-167.
Krebs, M., Held, K., Binder, A., Hashimoto, K., Den Herder, G., Parniske, M., Kudla, J. and Schumacher, K. (2012) FRET-based genetically encoded sensors allow high-resolution live cell imaging of Ca2+ dynamics. *The Plant Journal*, **69**, 181-192.
Křeček, P., Skůpa, P., Libus, J., Naramoto, S., Tejos, R., Friml, J. and Zažímalová, E. (2009) The PIN-FORMED (PIN) protein family of auxin transporters. *Genome Biology*, **10**, 1-11.
Kurakawa, T., Ueda, N., Maekawa, M., Kobayashi, K., Kojima, M., Nagato, Y., Sakakibara, H. and Kyozuka, J. (2007) Direct control of shoot meristem activity by a cytokinin-activating enzyme. *Nature*, **445**, 652-655.
Lam, H.-M., Chiu, J., Hsieh, M.-H., Meisel, L., Oliveira, I.C., Shin, M. and Coruzzi, G. (1998) Glutamate-receptor genes in plants. *Nature*, **396**, 125-126.
Lebaudy, A., Véry, A.-A. and Sentenac, H. (2007) K+ channel activity in plants: Genes, regulations and functions. *FEBS Letters*, **581**, 2357-2366.
Lee, Y., Lee, W.S. and Kim, S.H. (2013) Hormonal regulation of stem cell maintenance in roots. *J Exp Bot*, **64**, 1153-1165.
Leitz, G., Kang, B.-H., Schoenwaelder, M.E.A. and Staehelin, L.A. (2009) Statolith Sedimentation Kinetics and Force Transduction to the Cortical Endoplasmic Reticulum in Gravity-Sensing Arabidopsis Columella Cells. *The Plant Cell*, **21**, 843-860.
Levesque, M.P., Vernoux, T., Busch, W., Cui, H., Wang, J.Y., Blilou, I., Hassan, H., Nakajima, K., Matsumoto, N., Lohmann, J.U., Scheres, B. and Benfey, P.N. (2006) Whole-Genome Analysis of the SHORT-ROOT Developmental Pathway in Arabidopsis. *PLOS Biology*, **4**, e143.

Lew, R.R. (1991) Electrogenic Transport Properties of Growing Arabidopsis Root Hairs : The Plasma Membrane Proton Pump and Potassium Channels. *Plant Physiology*, **97**, 1527-1534.

Leyser, H.M.O., Lincoln, C.A., Timpte, C., Lammer, D., Turner, J. and Estelle, M. (1993) Arabidopsis auxin-resistance gene AXR1 encodes a protein related to ubiquitin-activating enzyme E1. *Nature*, **364**, 161-164.

Leyser, O. (2006) Dynamic Integration of Auxin Transport and Signalling. *Current Biology*, **16**, R424-R433.

Li, J., Zhu, S., Song, X., Shen, Y., Chen, H., Yu, J., Yi, K., Liu, Y., Karplus, V.J., Wu, P. and Deng, X.W. (2006) A Rice Glutamate Receptor–Like Gene Is Critical for the Division and Survival of Individual Cells in the Root Apical Meristem. *The Plant Cell*, **18**, 340.

Liao, C.-Y., Smet, W., Brunoud, G., Yoshida, S., Vernoux, T. and Weijers, D. (2015) Reporters for sensitive and quantitative measurement of auxin response. *Nat Meth*, **12**, 207-210.

Liu, J., Sheng, L., Xu, Y., Li, J., Yang, Z., Huang, H. and Xu, L. (2014) WOX11 and 12 are involved in the first-step cell fate transition during de novo root organogenesis in Arabidopsis. *Plant Cell*, **26**, 1081-1093.

Lobikin, M., Pare, J.F., Kaplan, D.L. and Levin, M. (2015) Selective depolarization of transmembrane potential alters muscle patterning and muscle cell localization in Xenopus laevis embryos. *The International journal of developmental biology*, **59**, 303-311.

Lucas, M., Swarup, R., Paponov, I.A., Swarup, K., Casimiro, I., Lake, D., Peret, B., Zappala, S., Mairhofer, S., Whitworth, M., Wang, J., Ljung, K., Marchant, A., Sandberg, G., Holdsworth, M.J., Palme, K., Pridmore, T., Mooney, S. and Bennett, M.J. (2011) SHORT-ROOT Regulates Primary, Lateral, and Adventitious Root Development in Arabidopsis. *Plant Physiology*, **155**, 384.

Luschnig, C., Gaxiola, R.A., Grisafi, P. and Fink, G.R. (1998) EIR1, a root-specific protein involved in auxin transport, is required for gravitropism in Arabidopsis thaliana. *Genes & Development*, **12**, 2175-2187.

Mandala, M., Serck-Hanssen, G., Martino, G. and Helle, K.B. (1999) The fluorescent cationic dye rhodamine 6G as a probe for membrane potential in bovine aortic endothelial cells. *Analytical biochemistry*, **274**, 1-6.

Manna, T.K. and Chowdhuri, P. (2007) Generalised equation of soil critical electric field EC based on impulse tests and measured soil electrical parameters. *IET Generation, Transmission & Distribution*, **1**, 811-817.

Marchant, A., Kargul, J., May, S.T., Muller, P., Delbarre, A., Perrot-Rechenmann, C. and Bennett, M.J. (1999) AUX1 regulates root gravitropism in Arabidopsis by facilitating auxin uptake within root apical tissues. *The EMBO Journal*, **18**, 2066-2073.

Maren, S. and Baudry, M. (1995) Properties and mechanisms of long-term synaptic plasticity in the mammalian brain: relationships to learning and memory. *Neurobiology of learning and memory*, **63**, 1-18.

Masi, E., Ciszak, M., Stefano, G., Renna, L., Azzarello, E., Pandolfi, C., Mugnai, S., Baluška, F., Arecchi, F.T. and Mancuso, S. (2009) Spatiotemporal dynamics of the electrical network activity in the root apex. *Proceedings of the National Academy of Sciences*, **106**, 4048-4053.

Massa, G.D. and Gilroy, S. (2003) Touch modulates gravity sensing to regulate the growth of primary roots of Arabidopsis thaliana. *Plant J*, **33**, 435-445.

Matsuzaki, Y., Ogawa-Ohnishi, M., Mori, A. and Matsubayashi, Y. (2010) Secreted Peptide Signals Required for Maintenance of Root Stem Cell Niche in <em>Arabidopsis</em&gt. *Science*, **329**, 1065.

Matzke, M. and Matzke, A. (2013) Membrane “potential-omics”: toward voltage imaging at the cell population level in roots of living plants. *Frontiers in Plant Science*, **4**.

Maule, A.J. (2008) Plasmodesmata: structure, function and biogenesis. *Current Opinion in Plant Biology*, **11**, 680-686.

Merlot, S., Leonhardt, N., Fenzi, F., Valon, C., Costa, M., Piette, L., Vavasseur, A., Genty, B., Boivin, K., Müller, A., Giraudat, J. and Leung, J. (2007) Constitutive activation of a plasma membrane H(+)-ATPase prevents abscisic acid-mediated stomatal closure. *The EMBO Journal*, **26**, 3216-3226.

Michard, E., Lima, P.T., Borges, F., Silva, A.C., Portes, M.T., Carvalho, J.E., Gilliham, M., Liu, L.-H., Obermeyer, G. and Feijó, J.A. (2011) Glutamate Receptor–Like Genes Form Ca²⁺ Channels in Pollen Tubes and Are Regulated by Pistil d-Serine. *Science*, **332**, 434.

Miller, N.D., Durham Brooks, T.L., Assadi, A.H. and Spalding, E.P. (2010) Detection of a gravitropism phenotype in glutamate receptor-like 3.3 mutants of Arabidopsis thaliana using machine vision and computation. *Genetics*, **186**, 585-593.

Minc, N. and Chang, F. (2010) ELECTRICAL CONTROL OF CELL POLARIZATION IN THE FISSION YEAST SCHIZOSACCHAROMYCES POMBE. *Current biology : CB*, **20**, 710-716.

Monshausen, G.B., Miller, N.D., Murphy, A.S. and Gilroy, S. (2011) Dynamics of auxin-dependent Ca2+ and pH signaling in root growth revealed by integrating high-resolution imaging with automated computer vision-based analysis. *The Plant Journal*, **65**, 309-318.

Moore, R., Fondren, W.M. and Marcum, H. (1987) Characterization of Root Agravitropism induced by Genetic, Chemical, and Developmental Constraints. *American Journal of Botany*, **74**, 329-336.

Morris, D.A. (1980) The influence of small direct electric currents on the transport of auxin in intact plants. *Planta*, **150**, 431-434.

Moubayidin, L., Di Mambro, R., Sozzani, R., Pacifici, E., Salvi, E., Terpstra, I., Bao, D., van Dijken, A., Dello Ioio, R., Perilli, S., Ljung, K., Benfey, P.N., Heidstra, R., Costantino, P. and Sabatini, S. (2013) Spatial coordination between stem cell activity and cell differentiation in the root meristem. *Dev Cell*, **26**, 405-415.

Mousavi, S.A.R., Chauvin, A., Pascaud, F., Kellenberger, S. and Farmer, E.E. (2013) GLUTAMATE RECEPTOR-LIKE genes mediate leaf-to-leaf wound signalling. *Nature*, **500**, 422-+.

Mousavi, S.A.R., Nguyen, C.T., Farmer, E.E. and Kellenberger, S. (2014) Measuring surface potential changes on leaves. *Nat. Protocols*, **9**, 1997-2004.

Muday, G.K. (2001) Auxins and Tropisms. *Journal of Plant Growth Regulation*, **20**, 226-243.

Mullen, J.L., Ishikawa, H. and Evans, M.L. (1998) Analysis of changes in relative elemental growth rate patterns in the elongation zone of Arabidopsis roots upon gravistimulation. *Planta*, **206**, 598-603.

Nakagawa, Y., Katagiri, T., Shinozaki, K., Qi, Z., Tatsumi, H., Furuichi, T., Kishigami, A., Sokabe, M., Kojima, I., Sato, S., Kato, T., Tabata, S., Iida, K., Terashima, A., Nakano, M., Ikeda, M., Yamanaka, T. and Iida, H. (2007) Arabidopsis plasma membrane protein crucial for Ca2+ influx and touch sensing in roots. *Proceedings of the National Academy of Sciences*, **104**, 3639-3644.

Nakajima, K., Sena, G., Nawy, T. and Benfey, P.N. (2001) Intercellular movement of the putative transcription factor SHR in root patterning. *Nature*, **413**, 307-311.

Nguyen, C.T., Agorio, A., Jossier, M., Depré, S., Thomine, S. and Filleur, S. (2016) Characterization of the Chloride Channel-Like, AtCLCg, Involved in Chloride Tolerance in Arabidopsis thaliana. *Plant and Cell Physiology*, **57**, 764-775.

Nishimura, K.Y., Isseroff, R.R. and Nuccitelli, R. (1996) Human keratinocytes migrate to the negative pole in direct current electric fields comparable to those measured in mammalian wounds. *J Cell Sci*, **109 (Pt 1)**, 199-207.

Osakabe, Y., Arinaga, N., Umezawa, T., Katsura, S., Nagamachi, K., Tanaka, H., Ohiraki, H., Yamada, K., Seo, S.-U., Abo, M., Yoshimura, E., Shinozaki, K. and Yamaguchi-Shinozaki, K. (2013) Osmotic Stress Responses and Plant Growth Controlled by Potassium Transporters in Arabidopsis. *The Plant Cell*, **25**, 609-624.

Oviedo, N.J., Nicolas, C.L., Adams, D.S. and Levin, M. (2008) Live Imaging of Planarian Membrane Potential Using DiBAC4(3). *Cold Spring Harbor Protocols*, **2008**, pdb.prot5055.

Pacifici, E., Polverari, L. and Sabatini, S. (2015) Plant hormone cross-talk: the pivot of root growth. *Journal of Experimental Botany*, **66**, 1113-1121.

Patel, N. and Poo, M.M. (1982) Orientation of neurite growth by extracellular electric fields. *The Journal of Neuroscience*, **2**, 483.

Peiter, E., Maathuis, F.J.M., Mills, L.N., Knight, H., Pelloux, J., Hetherington, A.M. and Sanders, D. (2005) The vacuolar Ca2+-activated channel TPC1 regulates germination and stomatal movement. *Nature*, **434**, 404-408.

Peng, H.B. and Jaffe, L.F. (1976) Polarization of fucoid eggs by steady electrical fields. *Developmental Biology*, **53**, 277-284.

Péret, B., Li, G., Zhao, J., Band, L.R., Voß, U., Postaire, O., Luu, D.-T., Da Ines, O., Casimiro, I., Lucas, M., Wells, D.M., Lazzerini, L., Nacry, P., King, J.R., Jensen, O.E., Schäffner, A.R., Maurel, C. and Bennett, M.J. (2012) Auxin regulates aquaporin function to facilitate lateral root emergence. *Nat Cell Biol*, **14**, 991-998.

Perilli, S., Di Mambro, R. and Sabatini, S. (2012) Growth and development of the root apical meristem. *Current Opinion in Plant Biology*, **15**, 17-23.

Petersson, S.V., Johansson, A.I., Kowalczyk, M., Makoveychuk, A., Wang, J.Y., Moritz, T., Grebe, M., Benfey, P.N., Sandberg, G. and Ljung, K. (2009) An Auxin Gradient and Maximum in the Arabidopsis Root Apex Shown by High-Resolution Cell-Specific Analysis of IAA Distribution and Synthesis. *The Plant Cell*, **21**, 1659-1668.

Pi, L., Aichinger, E., van der Graaff, E., Llavata-Peris, C.I., Weijers, D., Hennig, L., Groot, E. and Laux, T. (2015) Organizer-Derived WOX5 Signal Maintains Root Columella Stem Cells through Chromatin-Mediated Repression of CDF4 Expression. *Dev Cell*, **33**, 576-588.

Pickett, F.B., Wilson, A.K. and Estelle, M. (1990) The aux1 Mutation of Arabidopsis Confers Both Auxin and Ethylene Resistance. *Plant Physiology*, **94**, 1462-1466.

Qi, Z., Stephens, N.R. and Spalding, E.P. (2006) Calcium Entry Mediated by GLR3.3, an Arabidopsis Glutamate Receptor with a Broad Agonist Profile. *Plant Physiology*, **142**, 963.

Qin, Y., Huang, L., Liu, A., Zhao, D.-j., Wang, Z.-y., Liu, Y.-m. and Mao, T.-l. (2013) Visualization of synchronous propagation of plant electrical signals using an optical recording method. *Mathematical and Computer Modelling*, **58**, 661-669.

Rahman, A., Takahashi, M., Shibasaki, K., Wu, S., Inaba, T., Tsurumi, S. and Baskin, T.I. (2010) Gravitropism of Arabidopsis thaliana Roots Requires the Polarization of PIN2 toward the Root Tip in Meristematic Cortical Cells. *The Plant Cell*, **22**, 1762-1776.

Rathore, K.S. and Goldsworthy, A. (1985) Electrical Control of Shoot Regeneration in Plant Tissue Cultures. *Nat Biotech*, **3**, 1107-1109.

Rayle, D.L. and Cleland, R.E. (1992) The Acid Growth Theory of auxin-induced cell elongation is alive and well. *Plant Physiology*, **99**, 1271-1274.

Reddy, G.V., Heisler, M.G., Ehrhardt, D.W. and Meyerowitz, E.M. (2004) Real-time lineage analysis reveals oriented cell divisions associated with morphogenesis at the shoot apex of <em>Arabidopsis thaliana</em&gt. *Development*, **131**, 4225.

Robert, N., d'Erfurth, I., Marmagne, A., Erhardt, M., Allot, M., Boivin, K., Gissot, L., Monachello, D., Michaud, M., Duchêne, A.-M., Barbier-Brygoo, H., Maréchal-Drouard, L., Ephritikhine, G. and Filleur, S. (2012) Voltage-dependent-anion-channels (VDACs) in Arabidopsis have a dual localization in the cell but show a distinct role in mitochondria. *Plant Molecular Biology*, **78**, 431-446.

Roman, G., Lubarsky, B., Kieber, J.J., Rothenberg, M. and Ecker, J.R. (1995) Genetic Analysis of Ethylene Signal Transduction in Arabidopsis Thaliana: Five Novel Mutant Loci Integrated into a Stress Response Pathway. *Genetics*, **139**, 1393-1409.

Rost, T.L. and Jones, T.J. (1988) Pea Root Regeneration After Tip Excisions at Different Levels: Polarity of New Growth. *Annals of Botany*, **61**, 513-523.

Sabatini, S., Beis, D., Wolkenfelt, H., Murfett, J., Guilfoyle, T., Malamy, J., Benfey, P., Leyser, O., Bechtold, N., Weisbeek, P. and Scheres, B. (1999) An Auxin-Dependent Distal Organizer of Pattern and Polarity in the Arabidopsis Root. *Cell*, **99**, 463-472.

Sabatini, S., Heidstra, R., Wildwater, M. and Scheres, B. (2003) SCARECROW is involved in positioning the stem cell niche in the Arabidopsis root meristem. *Genes & Development*, **17**, 354-358.

Santuari, L., Sanchez-Perez, G.F., Luijten, M., Rutjens, B., Terpstra, I., Berke, L., Gorte, M., Prasad, K., Bao, D., Timmermans-Hereijgers, J.L.P.M., Maeo, K., Nakamura, K., Shimotohno, A., Pencik, A., Novak, O., Ljung, K., van Heesch, S., de Bruijn, E., Cuppen, E., Willemsen, V., Mähönen, A.P., Lukowitz, W., Snel, B., de Ridder, D., Scheres, B. and Heidstra, R. (2016) The PLETHORA Gene Regulatory Network Guides Growth and Cell Differentiation in Arabidopsis Roots. *The Plant Cell*, **28**, 2937.

Sanz, L., Dewitte, W., Forzani, C., Patell, F., Nieuwland, J., Wen, B., Quelhas, P., De Jager, S., Titmus, C., Campilho, A., Ren, H., Estelle, M., Wang, H. and Murray, J.A. (2011) The Arabidopsis D-type cyclin CYCD2;1 and the inhibitor ICK2/KRP2 modulate auxin-induced lateral root formation. *Plant Cell*, **23**, 641-660.

Sarkar, A.K., Luijten, M., Miyashima, S., Lenhard, M., Hashimoto, T., Nakajima, K., Scheres, B., Heidstra, R. and Laux, T. (2007) Conserved factors regulate signalling in Arabidopsis thaliana shoot and root stem cell organizers. *Nature*, **446**, 811-814.

Schaller, G.E., Bishopp, A. and Kieber, J.J. (2015) The Yin-Yang of Hormones: Cytokinin and Auxin Interactions in Plant Development. *The Plant Cell*, **27**, 44.

Scheres, B. (2007) Stem-cell niches: nursery rhymes across kingdoms. *Nat Rev Mol Cell Biol*, **8**, 345-354.

Schindelin, J., Arganda-Carreras, I., Frise, E., Kaynig, V., Longair, M., Pietzsch, T., Preibisch, S., Rueden, C., Saalfeld, S., Schmid, B., Tinevez, J.-Y., White, D.J., Hartenstein, V., Eliceiri, K., Tomancak, P. and Cardona, A. (2012a) Fiji: an open-source platform for biological-image analysis. *Nat Meth*, **9**, 676-682.

Schindelin, J., Arganda-Carreras, I., Frise, E., Kaynig, V., Longair, M., Pietzsch, T., Preibisch, S., Rueden, C., Saalfeld, S., Schmid, B., Tinevez, J.Y., White, D.J., Hartenstein, V., Eliceiri, K., Tomancak, P. and Cardona, A. (2012b) Fiji: an open-source platform for biological-image analysis. *Nat Methods*, **9**, 676-682.

Sena, G., Wang, X., Liu, H.-Y., Hofhuis, H. and Birnbaum, K.D. (2009) Organ regeneration does not require a functional stem cell niche in plants. *Nature*, **457**, 1150-1153.

Shabala, S., Demidchik, V., Shabala, L., Cuin, T.A., Smith, S.J., Miller, A.J., Davies, J.M. and Newman, I.A. (2006) Extracellular Ca²⁺ Ameliorates NaCl-Induced K⁺ Loss from Arabidopsis Root and Leaf Cells by Controlling Plasma Membrane K⁺-Permeable Channels. *Plant Physiology*, **141**, 1653.

Shani, E., Weinstain, R., Zhang, Y., Castillejo, C., Kaiserli, E., Chory, J., Tsien, R.Y. and Estelle, M. (2013) Gibberellins accumulate in the elongating endodermal cells of Arabidopsis root. *Proceedings of the National Academy of Sciences*, **110**, 4834-4839.

Shanley, L.J., Walczysko, P., Bain, M., MacEwan, D.J. and Zhao, M. (2006) Influx of extracellular Ca²⁺ is necessary for electrotaxis in <em>Dictyostelium</em&gt. *Journal of Cell Science*, **119**, 4741.

Sievers, A., Sondag, C., Trebacz, K. and Hejnowicz, Z. (1995) Gravity induced changes in intracellular potentials in statocytes of cress roots. *Planta*, **197**, 392-398.

Smith, S.D. (1974) EFFECTS OF ELECTRODE PLACEMENT ON STIMULATION OF ADULT FROG LIMB REGENERATION*. *Annals of the New York Academy of Sciences*, **238**, 500-507.

Sozzani, R., Cui, H., Moreno-Risueno, M.A., Busch, W., Van Norman, J.M., Vernoux, T., Brady, S.M., Dewitte, W., Murray, J.A.H. and Benfey, P.N. (2010) Spatiotemporal regulation of cell-cycle genes by SHORTROOT links patterning and growth. *Nature*, **466**, 128-132.

Sozzani, R. and Iyer-Pascuzzi, A. (2014) Postembryonic control of root meristem growth and development. *Current Opinion in Plant Biology*, **17**, 7-12.

Stahlberg, R., Cleland, R.E. and Volkenburgh, E. (2006) Slow Wave Potentials — a Propagating Electrical Signal Unique to Higher Plants. In *Communication in Plants: Neuronal Aspects of Plant Life* (Baluška, F., Mancuso, S. and Volkmann, D. eds). Berlin, Heidelberg: Springer Berlin Heidelberg, pp. 291-308.

Stahlberg, R. and Cosgrove, D.J. (1995) Comparison of electric and growth responses to excision in cucumber and pea seedlings. II. Long-distance effects are caused by the release of xylem pressure. *Plant, Cell & Environment*, **18**, 33-41.

Stenz, H.G. and Weisenseel, M.H. (1991) DC-Electric Fields Affect the Growth Direction and StatocytePolarity of Root Tips (Lepidium sativum). *Journal of Plant Physiology*, **138**, 335-344.

Stenz, H.G. and Weisenseel, M.H. (1993) Electrotropism of Maize (Zea mays L.) Roots (Facts and Artifacts). *Plant Physiology*, **101**, 1107-1111.

Stephens, N.R., Qi, Z. and Spalding, E.P. (2008) Glutamate Receptor Subtypes Evidenced by Differences in Desensitization and Dependence on the GLR3.3 and GLR3.4 Genes. *Plant Physiology*, **146**, 529-538.

Swarup, R., Friml, J., Marchant, A., Ljung, K., Sandberg, G., Palme, K. and Bennett, M. (2001) Localization of the auxin permease AUX1 suggests two functionally distinct hormone transport pathways operate in the Arabidopsis root apex. *Genes & Development*, **15**, 2648-2653.

Swarup, R., Kramer, E.M., Perry, P., Knox, K., Leyser, H.M., Haseloff, J., Beemster, G.T., Bhalerao, R. and Bennett, M.J. (2005) Root gravitropism requires lateral root cap and epidermal cells for transport and response to a mobile auxin signal. *Nat Cell Biol*, **7**, 1057-1065.

Swarup, R., Perry, P., Hagenbeek, D., Van Der Straeten, D., Beemster, G.T.S., Sandberg, G., Bhalerao, R., Ljung, K. and Bennett, M.J. (2007) Ethylene Upregulates Auxin Biosynthesis in Arabidopsis Seedlings to Enhance Inhibition of Root Cell Elongation. *The Plant Cell*, **19**, 2186.

Teardo, E., Formentin, E., Segalla, A., Giacometti, G.M., Marin, O., Zanetti, M., Lo Schiavo, F., Zoratti, M. and Szabò, I. (2011) Dual localization of plant glutamate receptor AtGLR3.4 to plastids and plasmamembrane. *Biochimica et Biophysica Acta (BBA) - Bioenergetics*, **1807**, 359-367.

Tseng, A.-S., Adams, D.S., Qiu, D., Koustubhan, P. and Levin, M. (2007) Apoptosis is required during early stages of tail regeneration in Xenopus laevis. *Developmental Biology*, **301**, 62-69.

Ubeda-Tomas, S., Federici, F., Casimiro, I., Beemster, G.T., Bhalerao, R., Swarup, R., Doerner, P., Haseloff, J. and Bennett, M.J. (2009) Gibberellin signaling in the endodermis controls Arabidopsis root meristem size. *Curr Biol*, **19**, 1194-1199.

van den Berg, C., Willemsen, V., Hage, W., Weisbeek, P. and Scheres, B. (1995) Cell fate in the Arabidopsis root meristem determined by directional signalling. *Nature*, **378**, 62-65.

van den Berg, C., Willemsen, V., Hendriks, G., Weisbeek, P. and Scheres, B. (1997) Short-range control of cell differentiation in the Arabidopsis root meristem. *Nature*, **390**, 287-289.

Vincill, E.D., Bieck, A.M. and Spalding, E.P. (2012) Ca(2+) Conduction by an Amino Acid-Gated Ion Channel Related to Glutamate Receptors. *Plant Physiology*, **159**, 40-46.

Vincill, E.D., Clarin, A.E., Molenda, J.N. and Spalding, E.P. (2013) Interacting Glutamate Receptor-Like Proteins in Phloem Regulate Lateral Root Initiation in Arabidopsis. *The Plant Cell*, **25**, 1304-1313.

von der Fecht-Bartenbach, J., Bogner, M., Dynowski, M. and Ludewig, U. (2010) CLC-b-Mediated NO−3/H+ Exchange Across the Tonoplast of Arabidopsis Vacuoles. *Plant and Cell Physiology*, **51**, 960-968.

Ward, J.M., Mäser, P. and Schroeder, J.I. (2009) Plant Ion Channels: Gene Families, Physiology, and Functional Genomics Analyses. *Annual review of physiology*, **71**, 59-82.

Wawrecki, W. and Zagórska-Marek, B. (2007) Influence of a Weak DC Electric Field on Root Meristem Architecture. *Annals of Botany*, **100**, 791-796.

Weiland, M., Mancuso, S. and Baluska, F. (2015) Signalling via glutamate and GLRs in Arabidopsis thaliana. *Functional Plant Biology*, **43**, 1-25.

Welch, D., Hassan, H., Blilou, I., Immink, R., Heidstra, R. and Scheres, B. (2007) Arabidopsis JACKDAW and MAGPIE zinc finger proteins delimit asymmetric cell division and stabilize tissue boundaries by restricting SHORT-ROOT action. *Genes Dev*, **21**, 2196-2204.

Wendrich, J.R., Moller, B.K., Uddin, B., Radoeva, T., Lokerse, A.S., De Rybel, B. and Weijers, D. (2015) A set of domain-specific markers in the Arabidopsis embryo. *Plant reproduction*, **28**, 153-160.

Wiśniewska, J., Xu, J., Seifertová, D., Brewer, P.B., Růžička, K., Blilou, I., Rouquié, D., Benková, E., Scheres, B. and Friml, J. (2006) Polar PIN Localization Directs Auxin Flow in Plants. *Science*, **312**, 883-883.

Wolverton, C., Mullen, J.L., Ishikawam, H. and Evans, M.L. (2000) Two distinct regions of response drive differential growth in Vigna root electrotropism. *Plant, Cell & Environment*, **23**, 1275-1280.

Xu, X.M., Wang, J., Xuan, Z., Goldshmidt, A., Borrill, P.G.M., Hariharan, N., Kim, J.Y. and Jackson, D. (2011) Chaperonins Facilitate KNOTTED1 Cell-to-Cell Trafficking and Stem Cell Function. *Science*, **333**, 1141.

Yamada, A., Gaja, N., Ohya, S., Muraki, K., Narita, H., Ohwada, T. and Imaizumi, Y. (2001) Usefulness and Limitation of DiBAC₄(3), a Voltage-Sensitive Fluorescent Dye, for the Measurement of Membrane Potentials Regulated by Recombinant Large Conductance Ca²⁺-Activated K⁺ Channels in HEK293 Cells. *The Japanese Journal of Pharmacology*, **86**, 342-350.

Yu, Z., Li, H., Liu, X., Xu, C. and Xiong, H. (2016) Influence of soil electric field on water movement in soil. *Soil and Tillage Research*, **155**, 263-270.

Zavaliev, R., Ueki, S., Epel, B.L. and Citovsky, V. (2011) Biology of callose (beta-1,3-glucan) turnover at plasmodesmata. *Protoplasma*, **248**, 117-130.

Zhao, D.-J., Chen, Y., Wang, Z.-Y., Xue, L., Mao, T.-L., Liu, Y.-M., Wang, Z.-Y. and Huang, L. (2015) High-resolution non-contact measurement of the electrical activity of plants in situ using optical recording. **5**, 13425.

Zhao, M., Song, B., Pu, J., Wada, T., Reid, B., Tai, G., Wang, F., Guo, A., Walczysko, P., Gu, Y., Sasaki, T., Suzuki, A., Forrester, J.V., Bourne, H.R., Devreotes, P.N., McCaig, C.D. and Penninger, J.M. (2006) Electrical signals control wound healing through phosphatidylinositol-3-OH kinase-[gamma] and PTEN. *Nature*, **442**, 457-460.

Zhu, T., O'Quinn, R.L., Lucas, W.J. and Rost, T.L. (1998) Directional cell-to-cell communication in theArabidopsis root apical meristem II. Dynamics of plasmodesmatal formation. *Protoplasma*, **204**, 84-93.

Zimmermann, M.R., Maischak, H., Mithöfer, A., Boland, W. and Felle, H.H. (2009) System Potentials, a Novel Electrical Long-Distance Apoplastic Signal in Plants, Induced by Wounding. *Plant Physiology*, **149**, 1593-1600.

Zürcher, E., Tavor-Deslex, D., Lituiev, D., Enkerli, K., Tarr, P.T. and Müller, B. (2013) A Robust and Sensitive Synthetic Sensor to Monitor the Transcriptional Output of the Cytokinin Signaling Network in Planta. *Plant Physiology*, **161**, 1066.

9 Appendix

9.1 MATLAB script for R2D2 ratiometric image generation

```
function [ output_args ] = RD2D_allFiles( input_args )
     myMapLog = [    0         0         0
          0         0    0.1111
          0         0    0.2222
          0         0    0.3333
          0         0    0.4444
          0         0    0.5556
          0         0    0.6667
          0         0    0.7778
          0         0    0.8889
          0         0    1.0000
     0.0625    0.0625    0.9375
     0.1250    0.1250    0.8750
     0.1875    0.1875    0.8125
     0.2500    0.2500    0.7500
     0.3125    0.3125    0.6875
     0.3750    0.3750    0.6250
     0.4375    0.4375    0.5625
     0.5000    0.5000    0.5000
     0.5625    0.5625    0.4375
     0.6250    0.6250    0.3750
     0.6875    0.6875    0.3125
     0.7500    0.7500    0.2500
     0.8125    0.8125    0.1875
     0.8750    0.8750    0.1250
     0.9375    0.9375    0.0625
     1.0000    1.0000         0
     1.0000    0.9375         0
     1.0000    0.8750         0
     1.0000    0.8125         0
     1.0000    0.7500         0
     1.0000    0.6875         0
     1.0000    0.6250         0
     1.0000    0.5625         0
     1.0000    0.5000         0
     1.0000    0.4375         0
     1.0000    0.3750         0
     1.0000    0.3125         0
     1.0000    0.2500         0
     1.0000    0.1875         0
     1.0000    0.1250         0
     1.0000    0.0625         0
     1.0000         0         0
     0.9375         0         0
     0.8750         0         0
     0.8125         0         0
     0.7500         0         0
     0.6875         0         0
     0.6250         0         0
     0.5625         0         0
     0.5000         0         0];

     myFolders= { 'E:\PhD\R2D2images\tiff files\root 3\images\',
                                                              };
     [nFolders, ~]=size(myFolders);
```

```
    myFigure= figure('Position',[1 1 1600 1400], 'Color',[1.0 1.0 1.0]);
    set(myFigure, 'Renderer', 'painters');
    outFolder= 'E:\PhD\R2D2images\tiff files\root 3\results v2\';

    for iFolder=1:nFolders
    myFolder= char(myFolders(iFolder));
    ctrlFileList=listCtrlFiles(myFolder);

    [nFiles, ~]=size(ctrlFileList);


    for iFile= 1: nFiles
        ctrlFileName= ctrlFileList(iFile,:);
        sgnlFileName= strrep(ctrlFileList(iFile,:), 'ch00.tif',
'ch01.tif');

        % LOAD IMAGES
        fprintf('LOADING FILES %s AND %s\n', ctrlFileName, sgnlFileName);
        ctrlImg= uint16(imread([myFolder ctrlFileName]));
        sgnlImg= uint16(imread([myFolder sgnlFileName]));

        % GET NOISE FOR CONTROL IMAGE
        [ySize, xSize]=size(ctrlImg);
        yNoise= ySize - 41;
        xNoise= xSize - 41;
        [meanNoiseCtrl, stdNoiseCtrl]= getNoise(ctrlImg, xNoise, yNoise,
80);
        % REMOVE PEDESTAL FROM CONTROL IMAGE
        ctrlImg= ctrlImg - meanNoiseCtrl;
        ctrlImg= double(ctrlImg);
        threshold= 30*stdNoiseCtrl;

        % DECODE FILE NAME
        [Root, Type, Day, Field] = decodeFileName(ctrlFileName);

        % REMOVE PEDESTAL FOR SIGNAL IMAGE
        [meanNoiseSgnl, stdNoiseSgnl]= getNoise(sgnlImg, xNoise, yNoise,
80);
        sgnlImg= sgnlImg - uint16(meanNoiseSgnl);
        sgnlImg= double(sgnlImg);

        % CALCULATE RATIO
        ratioImg= ratioImages(ctrlImg, sgnlImg, threshold);

        % PLOT RATIO IMAGE
        imagesc(ratioImg);
        axis equal;
        set(gca,'position',[0 0 1 1],'units','normalized');
        caxis([-0.2, 0.2]);
        myCmap= colormap(myMapLog);

        % DISPLAY COLOR BAR
        myCol= colorbar;
        myCol.Label.String = 'Ln(CTRL/SIGNAL)';

        % WRITE TITLE
        myTitle= ['ROOT ' num2str(Root) '-' num2str(Type) '; DAY '
num2str(Day) '; ' Field];
        title(myTitle);
```

```
        axis off

        % EXPORT IMAGE
export_fig(sprintf('%s %s_root%d-%d_Day%d', outFolder, Field, Root, Type,
Day), '-a1', '-tiff');

    end

    % PRINT PDF
    set(myFigure,'PaperOrientation','landscape');
    set(myFigure,'PaperUnits','normalized');
    set(myFigure,'PaperPosition', [0 0 1 1]);

        end
    close(myFigure);
end


function [ outImage ] = ratioImages( ctrlImage, signalImage, threshold )

    [ySize, xSize] = size( ctrlImage );
    outImage= zeros(ySize, xSize);

    for y= 1: ySize
        for x= 1: xSize
            if( ctrlImage(y, x) > threshold)
                outImage(y, x) =  (ctrlImage(y, x)/ signalImage(y, x));
                            else
                            end
        end
    end
    outImage= log(outImage);
end


function [ Root, Type, Day, Field ] = decodeFileName( fileName )

    % REMOVE CH and FILE EXTENSION
    expression = '_ch(\w+).tif';
    replace = '';

    fileName = regexprep(fileName,expression,replace);

    C = strsplit(fileName,'_');

    % DECODE FIELD
    if ( strcmp(C(1), 'noE'))
        Field= 'CTRL';
    else
        Field= 'E';
    end



    % DECODE DAY
    Day=   sscanf( char(C(2)) , 'day%d');

    % DECODE ROOT AND TYPE
    [RootType]=  sscanf( char(C(3)) , '%d%1c');
```

```
    Root= RootType(1);
    Type= RootType(2);
    if Type==97
        Type=0;
    else
        Type=1;
    end
end

function [ myFolderInfo ] = listCtrlFiles( myFolder )
 %% LISTCTRLFILES List all control images in folder

    myFolderInfo = ls([myFolder '*ch00.tif']);

end
```

9.2 Script for timelapse imaging using Raspberry Pi

Crontab function in shell of Raspberry Pi NOOBS set to repeat script:

```
#!/bin/bash
DATE=$(date +"%Y-%m-%d_%H%M")
raspistill -o /home/pi/Desktop/picturefile1/$DATE.jpg
```

9.3 MATLAB script for PIN membrane extraction and centre of mass calculation

```
function [ m, y0 ] = findLine( inputImage )
 %% FINDLINE Finds the best line that fits the 3D data form inputImage once
projected on the XY plane

    inputImage = imadjust(inputImage);
    level= 0.6;
    thrImage = im2bw(inputImage, level);

    [row, col]= find(thrImage);

    p = polyfit(col, row, 1);
    m=p(1);
    y0=p(2);
end


function [ ] = findMembranes(imageName  )

 % DEFINE FOLDERS
    resultsFolder= '\\icnas1.cc.ic.ac.uk\nk2909\MATLAB\MATLAB
NIKO\ForNick\AnalysisResults\';
    imageFolder= '\\icnas1.cc.ic.ac.uk\nk2909\MATLAB\MATLAB
NIKO\ForNick\ImageRepository\';

% CREATE FIGURES
    mainFigure= figure();
    mainAxes= axes('Parent', mainFigure);
    membraneFigure= figure();
    membraneAxes= axes('Parent', membraneFigure);
```

```
% READ INPUT IMAGE

 imageName= 'r2z1_ch00.tif';
 inputImage= [imageFolder imageName];
 myImage= TIFF_read(inputImage);

 % READ POINTS FROM TXT FILE
 pointFile = strrep(imageName, '.tif', '.txt');
 pointFile = [imageFolder pointFile];
 points= readBeadFile_imgj(pointFile);
 [inputPoints, ~]= size(points);
 membraneN= inputPoints/2; % N membranes= half number of points

image(myImage, 'Parent', mainAxes);
hold (mainAxes, 'on');
 %LOOP OVER EACH MEMBRANE
    for memb= 1: membraneN
        xPoint_i= points(2*memb-1, 1);
        yPoint_i= points(2*memb-1, 2);
        xPoint_f= points(2*memb, 1);
        yPoint_f= points(2*memb, 2);
        disp(' ' );
        disp(['MEMBRANE N ' num2str(memb)]);
        disp(['OPERATOR POINTS (' num2str(xPoint_i) ', ' num2str(yPoint_i)
'); (' num2str(xPoint_f) ', ' num2str(yPoint_f) ')']);

     % MAKE SURE THE FIRST COORDINATE IS LOWER THAN SECOND
        if (xPoint_i > xPoint_f)
            tmp= xPoint_i;
            xPoint_i= xPoint_f;
            xPoint_f= tmp;
        end
        if (yPoint_i > yPoint_f)
            tmp= yPoint_i;
            yPoint_i= yPoint_f;
            yPoint_f= tmp;
        end


     % FOR EACH MEMBRANE EXTRACT SUB IMAGE (just a membrane)
        subImage= myImage(xPoint_i: xPoint_f, yPoint_i: yPoint_f );
        [sizeY, sizeX]=size(subImage);

        [maxInt, maxPosX]= max(subImage);
        maxPosX= maxPosX+ xPoint_i;

     % FIT LINE TO MEMBRANE
        [m, y0]= findLine(subImage);
        theta= atan(m);

        real_y0= y0 +  xPoint_i - 1;
        Lpixel= round(sqrt( power((yPoint_i- yPoint_f),2) +
power((xPoint_i- xPoint_f),2) )); %Length of membrane in pixels

     % CREATE A VECTOR CONTAINING N POINTS
        disp(['MEMBRANE LENGTH= ' num2str(Lpixel) ' PIXELS']);
        nPoints= 30; %segmentation of membrane
        memX=[];
        memY=[];
```

```
        fakeZ=[];
        amplitudes=[];

        if nPoints > Lpixel
            nPoints= Lpixel;
        end
        step= Lpixel/nPoints;
        for t= 1:step:Lpixel
            newX= yPoint_i + cos(theta)*t;
            memX= [memX, newX];

            newY= real_y0  + sin(theta)*t;
            memY= [memY, newY];

            fakeZ= [fakeZ, 200];

% FILL A VECTOR WITH INTENSITY VALUES TAKEN ALONG LINE ORTHOGONAL TO
MEMBRANE
            vInt= fillHistoAtPoint(myImage, newX, newY, m);
         % NOW FIT THE DATA EXTRACT RESULTS WITH "fitResult.AMPL"
            fitResult= fitHistoNick(vInt);
            if fitResult.AMPL < 4092
                amplitudes= [amplitudes, fitResult.AMPL];
            end

        end
        makeAmpPlot(membraneAxes, amplitudes );
        saveAmpsToFile(resultsFolder, imageName, ampl_vec);
        disp(['FITTING FROM (' num2str(round(memY(end))) ', '
num2str(round(memX(end))) ') TO (' num2str(round(memY(1))) ', '
num2str(round(memX(1))) ')']);
        disp('');

     % DISPLAY DATA AND LINE
        tx= [round(min(memY)): round(max(memY))];
        ty= [round(min(memX)): round(max(memX))];
        subImage= myImage(round(min(memY)): round(max(memY)),
round(min(memX)): round(max(memX)) );

        plot(mainAxes, memX, memY, 'Color', 'red', 'Linewidth', 0.75);
    end


end

 function [ vInt ] = fillHistoAtPoint( inputImage, x0, y0, m )


    q= 51;
    theta= atan(-1/m);

    vInt=zeros(q,1);
    t= -floor(q/2);

    [sizeY, sizeX, ~]= size(inputImage);

    for i= 1:q
        newX= round(x0 + cos(theta)*t);
```

```
        newY= round(y0  + sin(theta)*t);

        if newX <1 || newX>sizeX || newY<1 || newY> sizeY
            vInt(i)= 0;
        else
            vInt(i)= inputImage(newY, newX);
        end
        t= t+1;
    end


end


function [ f1 ] = fitHistoNick( vInt )
 %% FITHISTO Fit input data with Gaussian
 %
    t= [-floor(size(vInt)/2):floor(size(vInt)/2)];

    gaussEqn = 'AMPL*exp(-((x-MEAN)/SIGMA)^2)+PEDESTAL';
    startPoints = [100 0 50 3];
    f1 = fit(t', vInt, gaussEqn, 'Start', startPoints);

end


function [ output_args ] = makeAmpPlot(membraneAxes, ampl_vec )

    hold(membraneAxes, 'on');
    plot(ampl_vec, 'Parent', membraneAxes);

end


function [  ] = minTest(  )


    inputFile= ['\\icnas1.cc.ic.ac.uk\nk2909\MATLAB\MATLAB NIKO\ForNick\'
'r2z1_ch00.tif'];
    myTiff = Tiff(inputFile, 'r');
    myTiff.setDirectory(1);

    myImage= myTiff.read();
    myTiff.close();

    subImage= myImage( 795:860, 940 :1020);
    image(subImage)


end

function [ output_args ] = saveAmpsToFile(resultsFolder, imageName,
ampl_vec )

    outFile= [resultsFolder imageName]

end
```

9.4 MATLAB script for YC3.6 ratiometric image generation

```
function [ output_args ] = RD2D_allFiles( input_args )
     myMapLog = [    0         0         0
          0         0    0.1111
          0         0    0.2222
          0         0    0.3333
          0         0    0.4444
          0         0    0.5556
          0         0    0.6667
          0         0    0.7778
          0         0    0.8889
          0         0    1.0000
     0.0625    0.0625    0.9375
     0.1250    0.1250    0.8750
     0.1875    0.1875    0.8125
     0.2500    0.2500    0.7500
     0.3125    0.3125    0.6875
     0.3750    0.3750    0.6250
     0.4375    0.4375    0.5625
     0.5000    0.5000    0.5000
     0.5625    0.5625    0.4375
     0.6250    0.6250    0.3750
     0.6875    0.6875    0.3125
     0.7500    0.7500    0.2500
     0.8125    0.8125    0.1875
     0.8750    0.8750    0.1250
     0.9375    0.9375    0.0625
     1.0000    1.0000         0
     1.0000    0.9375         0
     1.0000    0.8750         0
     1.0000    0.8125         0
     1.0000    0.7500         0
     1.0000    0.6875         0
     1.0000    0.6250         0
     1.0000    0.5625         0
     1.0000    0.5000         0
     1.0000    0.4375         0
     1.0000    0.3750         0
     1.0000    0.3125         0
     1.0000    0.2500         0
     1.0000    0.1875         0
     1.0000    0.1250         0
     1.0000    0.0625         0
     1.0000         0         0
     0.9375         0         0
     0.8750         0         0
     0.8125         0         0
     0.7500         0         0
     0.6875         0         0
     0.6250         0         0
     0.5625         0         0
     0.5000         0         0];

     myFolders= { 'E:\PhD\YC36NESimages\tiff files\root 3\images\',
                                                              };
     [nFolders, ~]=size(myFolders);

     myFigure= figure('Position',[1 1 1600 1400], 'Color',[1.0 1.0 1.0]);
     set(myFigure, 'Renderer', 'painters');
     outFolder= 'E:\PhD\YC36NESimages\tiff files\root 3\results v2\';
```

```
    for iFolder=1:nFolders
    myFolder= char(myFolders(iFolder));
    ctrlFileList=listCtrlFiles(myFolder);

    [nFiles, ~]=size(ctrlFileList);


    for iFile= 1: nFiles
        ctrlFileName= ctrlFileList(iFile,:);
        sgnlFileName= strrep(ctrlFileList(iFile,:), 'ch00.tif',
'ch01.tif');

        % LOAD IMAGES
        fprintf('LOADING FILES %s AND %s\n', ctrlFileName, sgnlFileName);
        ctrlImg= uint16(imread([myFolder ctrlFileName]));
        sgnlImg= uint16(imread([myFolder sgnlFileName]));

        % GET NOISE FOR CONTROL IMAGE
        [ySize, xSize]=size(ctrlImg);
        yNoise= ySize - 41;
        xNoise= xSize - 41;
        [meanNoiseCtrl, stdNoiseCtrl]= getNoise(ctrlImg, xNoise, yNoise,
80);
        % REMOVE PEDESTAL FROM CONTROL IMAGE
        ctrlImg= ctrlImg - meanNoiseCtrl;
        ctrlImg= double(ctrlImg);
        threshold= 30*stdNoiseCtrl;

        % DECODE FILE NAME
        [Root, Type, Day, Field] = decodeFileName(ctrlFileName);

        % REMOVE PEDESTAL FOR SIGNAL IMAGE
        [meanNoiseSgnl, stdNoiseSgnl]= getNoise(sgnlImg, xNoise, yNoise,
80);
        sgnlImg= sgnlImg - uint16(meanNoiseSgnl);
        sgnlImg= double(sgnlImg);

        % CALCULATE RATIO
        ratioImg= ratioImages(ctrlImg, sgnlImg, threshold);

        % PLOT RATIO IMAGE
        imagesc(ratioImg);
        axis equal;
        set(gca,'position',[0 0 1 1],'units','normalized');
        caxis([-0.2, 0.2]);
        myCmap= colormap(myMapLog);

        % DISPLAY COLOR BAR?
        myCol= colorbar;
        myCol.Label.String = 'Ln(CTRL/SIGNAL)';

        % WRITE TITLE
        myTitle= ['ROOT ' num2str(Root) '-' num2str(Type) '; DAY '
num2str(Day) '; ' Field];
        title(myTitle);
        axis off
```

```
        % EXPORT IMAGE
export_fig(sprintf('%s %s_root%d-%d_Day%d', outFolder, Field, Root, Type,
Day), '-a1', '-tiff');

    end

    % PRINT PDF
    set(myFigure,'PaperOrientation','landscape');
    set(myFigure,'PaperUnits','normalized');
    set(myFigure,'PaperPosition', [0 0 1 1]);

    end
    close(myFigure);
end


function [ outImage ] = ratioImages( ctrlImage, signalImage, threshold )

    [ySize, xSize] = size( ctrlImage );
    outImage= zeros(ySize, xSize);

    for y= 1: ySize
        for x= 1: xSize
            if( ctrlImage(y, x) > threshold)
                outImage(y, x) =  signalImage(y, x) / ctrlImage(y, x);
            else
            end
        end
    end
    outImage= log(outImage);
end


function [ Root, Type, Day, Field ] = decodeFileName( fileName )
    expression = '_ch(\w+).tif';
    replace = '';

    fileName = regexprep(fileName,expression,replace);

    C = strsplit(fileName,'_');

    % DECODE FIELD
    if ( strcmp(C(1), 'noE'))
        Field= 'CTRL';
    else
        Field= 'E';
    end


    % DECODE DAY
    Day=   sscanf( char(C(2)) , 'day%d');

    % DECODE ROOT AND TYPE
    [RootType]=  sscanf( char(C(3)) , '%d%1c');
    Root= RootType(1);
    Type= RootType(2);
    if Type==97
        Type=0;
```

```
    else
        Type=1;
    end
end


function [ myFolderInfo ] = listCtrlFiles( myFolder )

    myFolderInfo = ls([myFolder '*ch00.tif']);

end
```

9.5 Permissions to use previously published figures

OXFORD UNIVERSITY PRESS LICENSE
TERMS AND CONDITIONS

Nov 21, 2017

This Agreement between Mr. Nicolas Kral ("You") and Oxford University Press ("Oxford University Press") consists of your license details and the terms and conditions provided by Oxford University Press and Copyright Clearance Center.

License Number	4212460121112
License date	Oct 19, 2017
Licensed content publisher	Oxford University Press
Licensed content publication	Journal of Experimental Botany
Licensed content title	Hormonal regulation of stem cell maintenance in roots
Licensed content author	Lee, Yew; Lee, Woo Sung
Licensed content date	Nov 25, 2012
Type of Use	Thesis/Dissertation
Institution name	
Title of your work	Quantitative Characterisation of Root Tip Regeneration and Tropism in External Electric Field
Publisher of your work	n/a
Expected publication date	Nov 2017
Permissions cost	0.00 USD
Value added tax	0.00 USD
Total	0.00 USD
Requestor Location	Mr. Nicolas Kral 7A fernhead road London, W93EU United Kingdom Attn: Mr. Nicolas Kral

Publisher Tax ID	GB125506730
Billing Type	Invoice
Billing Address	Mr. Nicolas Kral 7A fernhead road London, United Kingdom W93EU Attn: Mr. Nicolas Kral
Total	0.00 USD

Terms and Conditions

STANDARD TERMS AND CONDITIONS FOR REPRODUCTION OF MATERIAL FROM AN OXFORD UNIVERSITY PRESS JOURNAL

1. Use of the material is restricted to the type of use specified in your order details.
2. This permission covers the use of the material in the English language in the following territory: world. If you have requested additional permission to translate this material, the terms and conditions of this reuse will be set out in clause 12.
3. This permission is limited to the particular use authorized in (1) above and does not allow you to sanction its use elsewhere in any other format other than specified above, nor does it apply to quotations, images, artistic works etc that have been reproduced from other sources which may be part of the material to be used.
4. No alteration, omission or addition is made to the material without our written consent. Permission must be re-cleared with Oxford University Press if/when you decide to reprint.
5. The following credit line appears wherever the material is used: author, title, journal, year, volume, issue number, pagination, by permission of Oxford University Press or the sponsoring society if the journal is a society journal. Where a journal is being published on behalf of a learned society, the details of that society must be included in the credit line.
6. For the reproduction of a full article from an Oxford University Press journal for whatever purpose, the corresponding author of the material concerned should be informed of the proposed use. Contact details for the corresponding authors of all Oxford University Press journal contact can be found alongside either the abstract or full text of the article concerned, accessible from www.oxfordjournals.org Should there be a problem clearing these rights, please contact journals.permissions@oup.com
7. If the credit line or acknowledgement in our publication indicates that any of the figures, images or photos was reproduced, drawn or modified from an earlier source it will be necessary for you to clear this permission with the original publisher as well. If this permission has not been obtained, please note that this material cannot be included in your publication/photocopies.
8. While you may exercise the rights licensed immediately upon issuance of the license at the end of the licensing process for the transaction, provided that you have disclosed complete and accurate details of your proposed use, no license is finally effective unless and until full payment is received from you (either by Oxford University Press or by Copyright Clearance Center (CCC)) as provided in CCC's Billing and Payment terms and conditions. If full payment is not received on a timely basis, then any license preliminarily granted shall be deemed automatically revoked and shall be void as if never granted. Further, in the event that you breach any of these terms and conditions or any of CCC's Billing and Payment terms and conditions, the license is automatically revoked and shall be void as if never granted. Use of materials as described in a revoked license, as well as any use of the materials beyond the scope of an unrevoked license, may constitute copyright

infringement and Oxford University Press reserves the right to take any and all action to protect its copyright in the materials.
9. This license is personal to you and may not be sublicensed, assigned or transferred by you to any other person without Oxford University Press's written permission.
10. Oxford University Press reserves all rights not specifically granted in the combination of (i) the license details provided by you and accepted in the course of this licensing transaction, (ii) these terms and conditions and (iii) CCC's Billing and Payment terms and conditions.
11. You hereby indemnify and agree to hold harmless Oxford University Press and CCC, and their respective officers, directors, employs and agents, from and against any and all claims arising out of your use of the licensed material other than as specifically authorized pursuant to this license.
12. Other Terms and Conditions:
v1.4

Questions? customercare@copyright.com or +1-855-239-3415 (toll free in the US) or +1-978-646-2777.

ELSEVIER LICENSE
TERMS AND CONDITIONS

Nov 21, 2017

This Agreement between Mr. Nicolas Kral ("You") and Elsevier ("Elsevier") consists of your license details and the terms and conditions provided by Elsevier and Copyright Clearance Center.

License Number	4212490664805
License date	Oct 19, 2017
Licensed Content Publisher	Elsevier
Licensed Content Publication	Current Biology
Licensed Content Title	Plant tropisms
Licensed Content Author	Simon Gilroy
Licensed Content Date	Apr 8, 2008
Licensed Content Volume	18
Licensed Content Issue	7
Licensed Content Pages	3
Start Page	R275
End Page	R277
Type of Use	reuse in a thesis/dissertation
Intended publisher of new work	other

Portion	figures/tables/illustrations
Number of figures/tables/illustrations	1
Format	both print and electronic
Are you the author of this Elsevier article?	No
Will you be translating?	No
Original figure numbers	Figure 1
Title of your thesis/dissertation	Quantitative Characterisation of Root Tip Regeneration and Tropism in External Electric Field
Expected completion date	Nov 2017
Estimated size (number of pages)	160
Requestor Location	Mr. Nicolas Kral 7A fernhead road London, W93EU United Kingdom Attn: Mr. Nicolas Kral
Publisher Tax ID	GB 494 6272 12
Total	0.00 USD
Terms and Conditions	

INTRODUCTION

1. The publisher for this copyrighted material is Elsevier. By clicking "accept" in connection with completing this licensing transaction, you agree that the following terms and conditions apply to this transaction (along with the Billing and Payment terms and conditions established by Copyright Clearance Center, Inc. ("CCC"), at the time that you opened your Rightslink account and that are available at any time at http://myaccount.copyright.com).

GENERAL TERMS

2. Elsevier hereby grants you permission to reproduce the aforementioned material subject to the terms and conditions indicated.
3. Acknowledgement: If any part of the material to be used (for example, figures) has appeared in our publication with credit or acknowledgement to another source, permission must also be sought from that source. If such permission is not obtained then that material may not be included in your publication/copies. Suitable acknowledgement to the source must be made, either as a footnote or in a reference list at the end of your publication, as follows:
"Reprinted from Publication title, Vol /edition number, Author(s), Title of article / title of chapter, Pages No., Copyright (Year), with permission from Elsevier [OR APPLICABLE SOCIETY COPYRIGHT OWNER]." Also Lancet special credit - "Reprinted from The Lancet, Vol. number, Author(s), Title of article, Pages No., Copyright (Year), with permission from Elsevier."
4. Reproduction of this material is confined to the purpose and/or media for which permission is hereby given.
5. Altering/Modifying Material: Not Permitted. However figures and illustrations may be altered/adapted minimally to serve your work. Any other abbreviations, additions, deletions and/or any other alterations shall be made only with prior written authorization

of Elsevier Ltd. (Please contact Elsevier at permissions@elsevier.com). No modifications can be made to any Lancet figures/tables and they must be reproduced in full.
6. If the permission fee for the requested use of our material is waived in this instance, please be advised that your future requests for Elsevier materials may attract a fee.
7. Reservation of Rights: Publisher reserves all rights not specifically granted in the combination of (i) the license details provided by you and accepted in the course of this licensing transaction, (ii) these terms and conditions and (iii) CCC's Billing and Payment terms and conditions.
8. License Contingent Upon Payment: While you may exercise the rights licensed immediately upon issuance of the license at the end of the licensing process for the transaction, provided that you have disclosed complete and accurate details of your proposed use, no license is finally effective unless and until full payment is received from you (either by publisher or by CCC) as provided in CCC's Billing and Payment terms and conditions. If full payment is not received on a timely basis, then any license preliminarily granted shall be deemed automatically revoked and shall be void as if never granted. Further, in the event that you breach any of these terms and conditions or any of CCC's Billing and Payment terms and conditions, the license is automatically revoked and shall be void as if never granted. Use of materials as described in a revoked license, as well as any use of the materials beyond the scope of an unrevoked license, may constitute copyright infringement and publisher reserves the right to take any and all action to protect its copyright in the materials.
9. Warranties: Publisher makes no representations or warranties with respect to the licensed material.
10. Indemnity: You hereby indemnify and agree to hold harmless publisher and CCC, and their respective officers, directors, employees and agents, from and against any and all claims arising out of your use of the licensed material other than as specifically authorized pursuant to this license.
11. No Transfer of License: This license is personal to you and may not be sublicensed, assigned, or transferred by you to any other person without publisher's written permission.
12. No Amendment Except in Writing: This license may not be amended except in a writing signed by both parties (or, in the case of publisher, by CCC on publisher's behalf).
13. Objection to Contrary Terms: Publisher hereby objects to any terms contained in any purchase order, acknowledgment, check endorsement or other writing prepared by you, which terms are inconsistent with these terms and conditions or CCC's Billing and Payment terms and conditions. These terms and conditions, together with CCC's Billing and Payment terms and conditions (which are incorporated herein), comprise the entire agreement between you and publisher (and CCC) concerning this licensing transaction. In the event of any conflict between your obligations established by these terms and conditions and those established by CCC's Billing and Payment terms and conditions, these terms and conditions shall control.
14. Revocation: Elsevier or Copyright Clearance Center may deny the permissions described in this License at their sole discretion, for any reason or no reason, with a full refund payable to you. Notice of such denial will be made using the contact information provided by you. Failure to receive such notice will not alter or invalidate the denial. In no event will Elsevier or Copyright Clearance Center be responsible or liable for any costs, expenses or damage incurred by you as a result of a denial of your permission request, other than a refund of the amount(s) paid by you to Elsevier and/or Copyright Clearance Center for denied permissions.

LIMITED LICENSE

The following terms and conditions apply only to specific license types:

15. **Translation**: This permission is granted for non-exclusive world **English** rights only unless your license was granted for translation rights. If you licensed translation rights you may only translate this content into the languages you requested. A professional translator must perform all translations and reproduce the content word for word preserving the integrity of the article.
16. **Posting licensed content on any Website**: The following terms and conditions apply as follows: Licensing material from an Elsevier journal: All content posted to the web site must maintain the copyright information line on the bottom of each image; A hyper-text must be included to the Homepage of the journal from which you are licensing at http://www.sciencedirect.com/science/journal/xxxxx or the Elsevier homepage for books at http://www.elsevier.com; Central Storage: This license does not include permission for a scanned version of the material to be stored in a central repository such as that provided by Heron/XanEdu.
Licensing material from an Elsevier book: A hyper-text link must be included to the Elsevier homepage at http://www.elsevier.com . All content posted to the web site must maintain the copyright information line on the bottom of each image.

Posting licensed content on Electronic reserve: In addition to the above the following clauses are applicable: The web site must be password-protected and made available only to bona fide students registered on a relevant course. This permission is granted for 1 year only. You may obtain a new license for future website posting.
17. **For journal authors:** the following clauses are applicable in addition to the above:
Preprints:
A preprint is an author's own write-up of research results and analysis, it has not been peer-reviewed, nor has it had any other value added to it by a publisher (such as formatting, copyright, technical enhancement etc.).
Authors can share their preprints anywhere at any time. Preprints should not be added to or enhanced in any way in order to appear more like, or to substitute for, the final versions of articles however authors can update their preprints on arXiv or RePEc with their Accepted Author Manuscript (see below).
If accepted for publication, we encourage authors to link from the preprint to their formal publication via its DOI. Millions of researchers have access to the formal publications on ScienceDirect, and so links will help users to find, access, cite and use the best available version. Please note that Cell Press, The Lancet and some society-owned have different preprint policies. Information on these policies is available on the journal homepage.
Accepted Author Manuscripts: An accepted author manuscript is the manuscript of an article that has been accepted for publication and which typically includes author-incorporated changes suggested during submission, peer review and editor-author communications.
Authors can share their accepted author manuscript:

- immediately
    - via their non-commercial person homepage or blog
    - by updating a preprint in arXiv or RePEc with the accepted manuscript
    - via their research institute or institutional repository for internal institutional uses or as part of an invitation-only research collaboration work-group
    - directly by providing copies to their students or to research collaborators for their personal use
    - for private scholarly sharing as part of an invitation-only work group on

commercial sites with which Elsevier has an agreement

- After the embargo period
  - via non-commercial hosting platforms such as their institutional repository
  - via commercial sites with which Elsevier has an agreement

In all cases accepted manuscripts should:

- link to the formal publication via its DOI
- bear a CC-BY-NC-ND license - this is easy to do
- if aggregated with other manuscripts, for example in a repository or other site, be shared in alignment with our hosting policy not be added to or enhanced in any way to appear more like, or to substitute for, the published journal article.

Published journal article (JPA): A published journal article (PJA) is the definitive final record of published research that appears or will appear in the journal and embodies all value-adding publishing activities including peer review co-ordination, copy-editing, formatting, (if relevant) pagination and online enrichment.
Policies for sharing publishing journal articles differ for subscription and gold open access articles:
Subscription Articles: If you are an author, please share a link to your article rather than the full-text. Millions of researchers have access to the formal publications on ScienceDirect, and so links will help your users to find, access, cite, and use the best available version.
Theses and dissertations which contain embedded PJAs as part of the formal submission can be posted publicly by the awarding institution with DOI links back to the formal publications on ScienceDirect.
If you are affiliated with a library that subscribes to ScienceDirect you have additional private sharing rights for others' research accessed under that agreement. This includes use for classroom teaching and internal training at the institution (including use in course packs and courseware programs), and inclusion of the article for grant funding purposes.
Gold Open Access Articles: May be shared according to the author-selected end-user license and should contain a CrossMark logo, the end user license, and a DOI link to the formal publication on ScienceDirect.
Please refer to Elsevier's posting policy for further information.
18. **For book authors** the following clauses are applicable in addition to the above: Authors are permitted to place a brief summary of their work online only. You are not allowed to download and post the published electronic version of your chapter, nor may you scan the printed edition to create an electronic version. **Posting to a repository:** Authors are permitted to post a summary of their chapter only in their institution's repository.
19. **Thesis/Dissertation**: If your license is for use in a thesis/dissertation your thesis may be submitted to your institution in either print or electronic form. Should your thesis be published commercially, please reapply for permission. These requirements include permission for the Library and Archives of Canada to supply single copies, on demand, of the complete thesis and include permission for Proquest/UMI to supply single copies, on demand, of the complete thesis. Should your thesis be published commercially, please reapply for permission. Theses and dissertations which contain embedded PJAs as part of the formal submission can be posted publicly by the awarding institution with DOI links back to the formal publications on ScienceDirect.

20. **Other Conditions**:

v1.9

Questions? customercare@copyright.com or +1-855-239-3415 (toll free in the US) or +1-978-646-2777.

ELSEVIER LICENSE
TERMS AND CONDITIONS

Nov 21, 2017

This Agreement between Mr. Nicolas Kral ("You") and Elsevier ("Elsevier") consists of your license details and the terms and conditions provided by Elsevier and Copyright Clearance Center.

License Number	4212491101047
License date	Oct 19, 2017
Licensed Content Publisher	Elsevier
Licensed Content Publication	Cell
Licensed Content Title	Root Regeneration Triggers an Embryo-like Sequence Guided by Hormonal Interactions
Licensed Content Author	Idan Efroni,Alison Mello,Tal Nawy,Pui-Leng Ip,Ramin Rahni,Nicholas DelRose,Ashley Powers,Rahul Satija,Kenneth D. Birnbaum
Licensed Content Date	Jun 16, 2016
Licensed Content Volume	165
Licensed Content Issue	7
Licensed Content Pages	13
Start Page	1721
End Page	1733
Type of Use	reuse in a thesis/dissertation
Intended publisher of new work	other
Portion	figures/tables/illustrations
Number of figures/tables/illustrations	1
Format	both print and electronic
Are you the author of this Elsevier article?	No
Will you be translating?	No

Original figure numbers	Figure 7
Title of your thesis/dissertation	Quantitative Characterisation of Root Tip Regeneration and Tropism in External Electric Field
Expected completion date	Nov 2017
Estimated size (number of pages)	160
Requestor Location	Mr. Nicolas Kral 7A fernhead road London, W93EU United Kingdom Attn: Mr. Nicolas Kral
Publisher Tax ID	GB 494 6272 12
Total	0.00 USD
Terms and Conditions	

INTRODUCTION

1. The publisher for this copyrighted material is Elsevier. By clicking "accept" in connection with completing this licensing transaction, you agree that the following terms and conditions apply to this transaction (along with the Billing and Payment terms and conditions established by Copyright Clearance Center, Inc. ("CCC"), at the time that you opened your Rightslink account and that are available at any time at http://myaccount.copyright.com).

GENERAL TERMS

2. Elsevier hereby grants you permission to reproduce the aforementioned material subject to the terms and conditions indicated.
3. Acknowledgement: If any part of the material to be used (for example, figures) has appeared in our publication with credit or acknowledgement to another source, permission must also be sought from that source. If such permission is not obtained then that material may not be included in your publication/copies. Suitable acknowledgement to the source must be made, either as a footnote or in a reference list at the end of your publication, as follows:
"Reprinted from Publication title, Vol /edition number, Author(s), Title of article / title of chapter, Pages No., Copyright (Year), with permission from Elsevier [OR APPLICABLE SOCIETY COPYRIGHT OWNER]." Also Lancet special credit - "Reprinted from The Lancet, Vol. number, Author(s), Title of article, Pages No., Copyright (Year), with permission from Elsevier."
4. Reproduction of this material is confined to the purpose and/or media for which permission is hereby given.
5. Altering/Modifying Material: Not Permitted. However figures and illustrations may be altered/adapted minimally to serve your work. Any other abbreviations, additions, deletions and/or any other alterations shall be made only with prior written authorization of Elsevier Ltd. (Please contact Elsevier at permissions@elsevier.com). No modifications can be made to any Lancet figures/tables and they must be reproduced in full.
6. If the permission fee for the requested use of our material is waived in this instance, please be advised that your future requests for Elsevier materials may attract a fee.
7. Reservation of Rights: Publisher reserves all rights not specifically granted in the combination of (i) the license details provided by you and accepted in the course of this licensing transaction, (ii) these terms and conditions and (iii) CCC's Billing and Payment terms and conditions.

8. License Contingent Upon Payment: While you may exercise the rights licensed immediately upon issuance of the license at the end of the licensing process for the transaction, provided that you have disclosed complete and accurate details of your proposed use, no license is finally effective unless and until full payment is received from you (either by publisher or by CCC) as provided in CCC's Billing and Payment terms and conditions. If full payment is not received on a timely basis, then any license preliminarily granted shall be deemed automatically revoked and shall be void as if never granted. Further, in the event that you breach any of these terms and conditions or any of CCC's Billing and Payment terms and conditions, the license is automatically revoked and shall be void as if never granted. Use of materials as described in a revoked license, as well as any use of the materials beyond the scope of an unrevoked license, may constitute copyright infringement and publisher reserves the right to take any and all action to protect its copyright in the materials.
9. Warranties: Publisher makes no representations or warranties with respect to the licensed material.
10. Indemnity: You hereby indemnify and agree to hold harmless publisher and CCC, and their respective officers, directors, employees and agents, from and against any and all claims arising out of your use of the licensed material other than as specifically authorized pursuant to this license.
11. No Transfer of License: This license is personal to you and may not be sublicensed, assigned, or transferred by you to any other person without publisher's written permission.
12. No Amendment Except in Writing: This license may not be amended except in a writing signed by both parties (or, in the case of publisher, by CCC on publisher's behalf).
13. Objection to Contrary Terms: Publisher hereby objects to any terms contained in any purchase order, acknowledgment, check endorsement or other writing prepared by you, which terms are inconsistent with these terms and conditions or CCC's Billing and Payment terms and conditions. These terms and conditions, together with CCC's Billing and Payment terms and conditions (which are incorporated herein), comprise the entire agreement between you and publisher (and CCC) concerning this licensing transaction. In the event of any conflict between your obligations established by these terms and conditions and those established by CCC's Billing and Payment terms and conditions, these terms and conditions shall control.
14. Revocation: Elsevier or Copyright Clearance Center may deny the permissions described in this License at their sole discretion, for any reason or no reason, with a full refund payable to you. Notice of such denial will be made using the contact information provided by you. Failure to receive such notice will not alter or invalidate the denial. In no event will Elsevier or Copyright Clearance Center be responsible or liable for any costs, expenses or damage incurred by you as a result of a denial of your permission request, other than a refund of the amount(s) paid by you to Elsevier and/or Copyright Clearance Center for denied permissions.

LIMITED LICENSE

The following terms and conditions apply only to specific license types:
15. **Translation**: This permission is granted for non-exclusive world **English** rights only unless your license was granted for translation rights. If you licensed translation rights you may only translate this content into the languages you requested. A professional translator must perform all translations and reproduce the content word for word preserving the integrity of the article.
16. **Posting licensed content on any Website**: The following terms and conditions apply as follows: Licensing material from an Elsevier journal: All content posted to the web site must maintain the copyright information line on the bottom of each image; A hyper-text

must be included to the Homepage of the journal from which you are licensing at http://www.sciencedirect.com/science/journal/xxxxx or the Elsevier homepage for books at http://www.elsevier.com; Central Storage: This license does not include permission for a scanned version of the material to be stored in a central repository such as that provided by Heron/XanEdu.
Licensing material from an Elsevier book: A hyper-text link must be included to the Elsevier homepage at http://www.elsevier.com . All content posted to the web site must maintain the copyright information line on the bottom of each image.

Posting licensed content on Electronic reserve: In addition to the above the following clauses are applicable: The web site must be password-protected and made available only to bona fide students registered on a relevant course. This permission is granted for 1 year only. You may obtain a new license for future website posting.
17. **For journal authors:** the following clauses are applicable in addition to the above:
Preprints:
A preprint is an author's own write-up of research results and analysis, it has not been peer-reviewed, nor has it had any other value added to it by a publisher (such as formatting, copyright, technical enhancement etc.).
Authors can share their preprints anywhere at any time. Preprints should not be added to or enhanced in any way in order to appear more like, or to substitute for, the final versions of articles however authors can update their preprints on arXiv or RePEc with their Accepted Author Manuscript (see below).
If accepted for publication, we encourage authors to link from the preprint to their formal publication via its DOI. Millions of researchers have access to the formal publications on ScienceDirect, and so links will help users to find, access, cite and use the best available version. Please note that Cell Press, The Lancet and some society-owned have different preprint policies. Information on these policies is available on the journal homepage.
Accepted Author Manuscripts: An accepted author manuscript is the manuscript of an article that has been accepted for publication and which typically includes author-incorporated changes suggested during submission, peer review and editor-author communications.
Authors can share their accepted author manuscript:

- immediately
    - via their non-commercial person homepage or blog
    - by updating a preprint in arXiv or RePEc with the accepted manuscript
    - via their research institute or institutional repository for internal institutional uses or as part of an invitation-only research collaboration work-group
    - directly by providing copies to their students or to research collaborators for their personal use
    - for private scholarly sharing as part of an invitation-only work group on commercial sites with which Elsevier has an agreement
- After the embargo period
    - via non-commercial hosting platforms such as their institutional repository
    - via commercial sites with which Elsevier has an agreement

In all cases accepted manuscripts should:

- link to the formal publication via its DOI
- bear a CC-BY-NC-ND license - this is easy to do
- if aggregated with other manuscripts, for example in a repository or other site, be shared in alignment with our hosting policy not be added to or enhanced in any way to appear more like, or to substitute for, the published journal article.

Published journal article (JPA): A published journal article (PJA) is the definitive final record of published research that appears or will appear in the journal and embodies all value-adding publishing activities including peer review co-ordination, copy-editing, formatting, (if relevant) pagination and online enrichment.
Policies for sharing publishing journal articles differ for subscription and gold open access articles:
Subscription Articles: If you are an author, please share a link to your article rather than the full-text. Millions of researchers have access to the formal publications on ScienceDirect, and so links will help your users to find, access, cite, and use the best available version.
Theses and dissertations which contain embedded PJAs as part of the formal submission can be posted publicly by the awarding institution with DOI links back to the formal publications on ScienceDirect.
If you are affiliated with a library that subscribes to ScienceDirect you have additional private sharing rights for others' research accessed under that agreement. This includes use for classroom teaching and internal training at the institution (including use in course packs and courseware programs), and inclusion of the article for grant funding purposes.
Gold Open Access Articles: May be shared according to the author-selected end-user license and should contain a CrossMark logo, the end user license, and a DOI link to the formal publication on ScienceDirect.
Please refer to Elsevier's posting policy for further information.
18. **For book authors** the following clauses are applicable in addition to the above: Authors are permitted to place a brief summary of their work online only. You are not allowed to download and post the published electronic version of your chapter, nor may you scan the printed edition to create an electronic version. **Posting to a repository:** Authors are permitted to post a summary of their chapter only in their institution's repository.
19. **Thesis/Dissertation**: If your license is for use in a thesis/dissertation your thesis may be submitted to your institution in either print or electronic form. Should your thesis be published commercially, please reapply for permission. These requirements include permission for the Library and Archives of Canada to supply single copies, on demand, of the complete thesis and include permission for Proquest/UMI to supply single copies, on demand, of the complete thesis. Should your thesis be published commercially, please reapply for permission. Theses and dissertations which contain embedded PJAs as part of the formal submission can be posted publicly by the awarding institution with DOI links back to the formal publications on ScienceDirect.

Elsevier Open Access Terms and Conditions
You can publish open access with Elsevier in hundreds of open access journals or in nearly 2000 established subscription journals that support open access publishing. Permitted third party re-use of these open access articles is defined by the author's choice of Creative Commons user license. See our open access license policy for more information.

ELSEVIER LICENSE
TERMS AND CONDITIONS

Nov 21, 2017

This Agreement between Mr. Nicolas Kral ("You") and Elsevier ("Elsevier") consists of your license details and the terms and conditions provided by Elsevier and Copyright Clearance Center.

License Number	4223590064114
License date	Nov 07, 2017
Licensed Content Publisher	Elsevier
Licensed Content Publication	Cell
Licensed Content Title	A Bistable Circuit Involving SCARECROW-RETINOBLASTOMA Integrates Cues to Inform Asymmetric Stem Cell Division
Licensed Content Author	Alfredo Cruz-Ramírez,Sara Díaz-Triviño,Ikram Blilou,Verônica A. Grieneisen,Rosangela Sozzani,Christos Zamioudis,Pál Miskolczi,Jeroen Nieuwland,René Benjamins,Pankaj Dhonukshe,Juan Caballero-Pérez,Beatrix Horvath,Yuchen Long,Ari Pekka Mähönen et al.
Licensed Content Date	Aug 31, 2012
Licensed Content Volume	150
Licensed Content Issue	5
Licensed Content Pages	14
Start Page	1002
End Page	1015
Type of Use	reuse in a thesis/dissertation
Portion	figures/tables/illustrations
Number of figures/tables/illustrations	1
Format	both print and electronic
Are you the author of this Elsevier article?	No
Will you be translating?	No
Original figure numbers	1
Title of your thesis/dissertation	Quantitative Characterisation of Root Tip Regeneration and Tropism in External Electric Field
Expected completion date	Nov 2017

Estimated size (number of pages)	160
Requestor Location	Mr. Nicolas Kral 7A fernhead road London, W93EU United Kingdom Attn: Mr. Nicolas Kral
Publisher Tax ID	GB 494 6272 12
Total	0.00 USD
Terms and Conditions	

INTRODUCTION

1. The publisher for this copyrighted material is Elsevier. By clicking "accept" in connection with completing this licensing transaction, you agree that the following terms and conditions apply to this transaction (along with the Billing and Payment terms and conditions established by Copyright Clearance Center, Inc. ("CCC"), at the time that you opened your Rightslink account and that are available at any time at http://myaccount.copyright.com).

GENERAL TERMS

2. Elsevier hereby grants you permission to reproduce the aforementioned material subject to the terms and conditions indicated.
3. Acknowledgement: If any part of the material to be used (for example, figures) has appeared in our publication with credit or acknowledgement to another source, permission must also be sought from that source. If such permission is not obtained then that material may not be included in your publication/copies. Suitable acknowledgement to the source must be made, either as a footnote or in a reference list at the end of your publication, as follows:
"Reprinted from Publication title, Vol /edition number, Author(s), Title of article / title of chapter, Pages No., Copyright (Year), with permission from Elsevier [OR APPLICABLE SOCIETY COPYRIGHT OWNER]." Also Lancet special credit - "Reprinted from The Lancet, Vol. number, Author(s), Title of article, Pages No., Copyright (Year), with permission from Elsevier."
4. Reproduction of this material is confined to the purpose and/or media for which permission is hereby given.
5. Altering/Modifying Material: Not Permitted. However figures and illustrations may be altered/adapted minimally to serve your work. Any other abbreviations, additions, deletions and/or any other alterations shall be made only with prior written authorization of Elsevier Ltd. (Please contact Elsevier at permissions@elsevier.com). No modifications can be made to any Lancet figures/tables and they must be reproduced in full.
6. If the permission fee for the requested use of our material is waived in this instance, please be advised that your future requests for Elsevier materials may attract a fee.
7. Reservation of Rights: Publisher reserves all rights not specifically granted in the combination of (i) the license details provided by you and accepted in the course of this licensing transaction, (ii) these terms and conditions and (iii) CCC's Billing and Payment terms and conditions.
8. License Contingent Upon Payment: While you may exercise the rights licensed immediately upon issuance of the license at the end of the licensing process for the transaction, provided that you have disclosed complete and accurate details of your proposed use, no license is finally effective unless and until full payment is received from

you (either by publisher or by CCC) as provided in CCC's Billing and Payment terms and conditions. If full payment is not received on a timely basis, then any license preliminarily granted shall be deemed automatically revoked and shall be void as if never granted. Further, in the event that you breach any of these terms and conditions or any of CCC's Billing and Payment terms and conditions, the license is automatically revoked and shall be void as if never granted. Use of materials as described in a revoked license, as well as any use of the materials beyond the scope of an unrevoked license, may constitute copyright infringement and publisher reserves the right to take any and all action to protect its copyright in the materials.
9. Warranties: Publisher makes no representations or warranties with respect to the licensed material.
10. Indemnity: You hereby indemnify and agree to hold harmless publisher and CCC, and their respective officers, directors, employees and agents, from and against any and all claims arising out of your use of the licensed material other than as specifically authorized pursuant to this license.
11. No Transfer of License: This license is personal to you and may not be sublicensed, assigned, or transferred by you to any other person without publisher's written permission.
12. No Amendment Except in Writing: This license may not be amended except in a writing signed by both parties (or, in the case of publisher, by CCC on publisher's behalf).
13. Objection to Contrary Terms: Publisher hereby objects to any terms contained in any purchase order, acknowledgment, check endorsement or other writing prepared by you, which terms are inconsistent with these terms and conditions or CCC's Billing and Payment terms and conditions. These terms and conditions, together with CCC's Billing and Payment terms and conditions (which are incorporated herein), comprise the entire agreement between you and publisher (and CCC) concerning this licensing transaction. In the event of any conflict between your obligations established by these terms and conditions and those established by CCC's Billing and Payment terms and conditions, these terms and conditions shall control.
14. Revocation: Elsevier or Copyright Clearance Center may deny the permissions described in this License at their sole discretion, for any reason or no reason, with a full refund payable to you. Notice of such denial will be made using the contact information provided by you. Failure to receive such notice will not alter or invalidate the denial. In no event will Elsevier or Copyright Clearance Center be responsible or liable for any costs, expenses or damage incurred by you as a result of a denial of your permission request, other than a refund of the amount(s) paid by you to Elsevier and/or Copyright Clearance Center for denied permissions.

LIMITED LICENSE

The following terms and conditions apply only to specific license types:
15. **Translation**: This permission is granted for non-exclusive world **English** rights only unless your license was granted for translation rights. If you licensed translation rights you may only translate this content into the languages you requested. A professional translator must perform all translations and reproduce the content word for word preserving the integrity of the article.
16. **Posting licensed content on any Website**: The following terms and conditions apply as follows: Licensing material from an Elsevier journal: All content posted to the web site must maintain the copyright information line on the bottom of each image; A hyper-text must be included to the Homepage of the journal from which you are licensing at http://www.sciencedirect.com/science/journal/xxxxx or the Elsevier homepage for books at http://www.elsevier.com; Central Storage: This license does not include permission for a scanned version of the material to be stored in a central repository such

as that provided by Heron/XanEdu.
Licensing material from an Elsevier book: A hyper-text link must be included to the Elsevier homepage at http://www.elsevier.com . All content posted to the web site must maintain the copyright information line on the bottom of each image.

Posting licensed content on Electronic reserve: In addition to the above the following clauses are applicable: The web site must be password-protected and made available only to bona fide students registered on a relevant course. This permission is granted for 1 year only. You may obtain a new license for future website posting.
17. **For journal authors:** the following clauses are applicable in addition to the above:
Preprints:
A preprint is an author's own write-up of research results and analysis, it has not been peer-reviewed, nor has it had any other value added to it by a publisher (such as formatting, copyright, technical enhancement etc.).
Authors can share their preprints anywhere at any time. Preprints should not be added to or enhanced in any way in order to appear more like, or to substitute for, the final versions of articles however authors can update their preprints on arXiv or RePEc with their Accepted Author Manuscript (see below).
If accepted for publication, we encourage authors to link from the preprint to their formal publication via its DOI. Millions of researchers have access to the formal publications on ScienceDirect, and so links will help users to find, access, cite and use the best available version. Please note that Cell Press, The Lancet and some society-owned have different preprint policies. Information on these policies is available on the journal homepage.
Accepted Author Manuscripts: An accepted author manuscript is the manuscript of an article that has been accepted for publication and which typically includes author-incorporated changes suggested during submission, peer review and editor-author communications.
Authors can share their accepted author manuscript:

- immediately
    - via their non-commercial person homepage or blog
    - by updating a preprint in arXiv or RePEc with the accepted manuscript
    - via their research institute or institutional repository for internal institutional uses or as part of an invitation-only research collaboration work-group
    - directly by providing copies to their students or to research collaborators for their personal use
    - for private scholarly sharing as part of an invitation-only work group on commercial sites with which Elsevier has an agreement
- After the embargo period
    - via non-commercial hosting platforms such as their institutional repository
    - via commercial sites with which Elsevier has an agreement

In all cases accepted manuscripts should:

- link to the formal publication via its DOI
- bear a CC-BY-NC-ND license - this is easy to do
- if aggregated with other manuscripts, for example in a repository or other site, be shared in alignment with our hosting policy not be added to or enhanced in any

way to appear more like, or to substitute for, the published journal article.

Published journal article (JPA): A published journal article (PJA) is the definitive final record of published research that appears or will appear in the journal and embodies all value-adding publishing activities including peer review co-ordination, copy-editing, formatting, (if relevant) pagination and online enrichment.
Policies for sharing publishing journal articles differ for subscription and gold open access articles:
Subscription Articles: If you are an author, please share a link to your article rather than the full-text. Millions of researchers have access to the formal publications on ScienceDirect, and so links will help your users to find, access, cite, and use the best available version.
Theses and dissertations which contain embedded PJAs as part of the formal submission can be posted publicly by the awarding institution with DOI links back to the formal publications on ScienceDirect.
If you are affiliated with a library that subscribes to ScienceDirect you have additional private sharing rights for others' research accessed under that agreement. This includes use for classroom teaching and internal training at the institution (including use in course packs and courseware programs), and inclusion of the article for grant funding purposes.
Gold Open Access Articles: May be shared according to the author-selected end-user license and should contain a CrossMark logo, the end user license, and a DOI link to the formal publication on ScienceDirect.
Please refer to Elsevier's posting policy for further information.
18. **For book authors** the following clauses are applicable in addition to the above: Authors are permitted to place a brief summary of their work online only. You are not allowed to download and post the published electronic version of your chapter, nor may you scan the printed edition to create an electronic version. **Posting to a repository:** Authors are permitted to post a summary of their chapter only in their institution's repository.
19. **Thesis/Dissertation**: If your license is for use in a thesis/dissertation your thesis may be submitted to your institution in either print or electronic form. Should your thesis be published commercially, please reapply for permission. These requirements include permission for the Library and Archives of Canada to supply single copies, on demand, of the complete thesis and include permission for Proquest/UMI to supply single copies, on demand, of the complete thesis. Should your thesis be published commercially, please reapply for permission. Theses and dissertations which contain embedded PJAs as part of the formal submission can be posted publicly by the awarding institution with DOI links back to the formal publications on ScienceDirect.

Elsevier Open Access Terms and Conditions
You can publish open access with Elsevier in hundreds of open access journals or in nearly 2000 established subscription journals that support open access publishing. Permitted third party re-use of these open access articles is defined by the author's choice of Creative Commons user license. See our open access license policy for more information.
Terms & Conditions applicable to all Open Access articles published with Elsevier:
Any reuse of the article must not represent the author as endorsing the adaptation of the article nor should the article be modified in such a way as to damage the author's honour or reputation. If any changes have been made, such changes must be clearly indicated.
The author(s) must be appropriately credited and we ask that you include the end user